

**SPECTRAL, STRUCTURAL AND BIOLOGICAL STUDIES  
OF SOME METAL COMPLEXES OF <sup>4</sup>N-SUBSTITUTED  
2-BENZOYLPYRIDINE THIOSEMICARBAZONES**

**Thesis submitted to the Cochin University of Science and  
Technology in partial fulfillment of the requirements for the degree of**

**DOCTOR OF PHILOSOPHY**

**in**

**CHEMISTRY**

**by**

**MARTHAKUTTY JOSEPH**

**Department of Applied Chemistry  
Cochin University of Science and Technology**

**Kochi-682022**

**July 2004**

**The Lord is my shepherd. There is nothing I shall want.**  
(Psalms 23. 1.)

---

Dr. M.R.Prathapachandra Kurup  
Head, Department of Applied Chemistry

**CERTIFICATE**

This is to certify that the thesis entitled **SPECTRAL, STRUCTURAL AND BIOLOGICAL STUDIES OF SOME METAL COMPLEXES OF 4-N-SUBSTITUTED 2-BENZOYLPYRIDINE THIOSEMICARBAZONES**, submitted to the Cochin University of Science and Technology, Kochi, by **Ms. MARTHAKUTTY JOSEPH**, in partial fulfillment of the requirements for the Degree of Doctor of Philosophy, is an authentic record of the original research work carried out by her, under my guidance and supervision, in the Department of Applied Chemistry and has not been included in any other thesis or submitted previously for the award of any other degree.



M.R. Prathapachandra Kurup  
(Supervising Guide)

Kochi-22  
19<sup>th</sup> July 2004

---

E-mail: [mrp@cusat.ac.in](mailto:mrp@cusat.ac.in), phone: 91-484-2575804

## DECLARATION

I hereby declare that the present work entitled "SPECTRAL, STRUCTURAL AND BIOLOGICAL STUDIES OF SOME METAL COMPLEXES OF <sup>4</sup>N-SUBSTITUTED 2-BENZOYLPIRIDINE THIOSEMICARBAZONES" is an original work done by me under the guidance of **Dr. M.R. Prathapachandra Kurup**, Professor and Head of the Department of Applied Chemistry, Cochin University of Science and Technology and has not been included in any other thesis or submitted previously for the award of any other degree.



Marthakutty Joseph

Kochi-22

19<sup>th</sup> July 2004

*To my*

*Beloved father and my late mother*

## *Acknowledgements*

*I would like to place on record my sincere gratitude to Dr. M.R. Prathapachandra Kurup, Professor and Head of the Department of Applied Chemistry, Cochin University of Science and Technology, for his valuable guidance and unremitting support throughout my research work. But for his constant encouragement and dedicated follow up I believe this work should not have been realized. I appreciate and acknowledge his dedication and stand beholden to him for his selfless support.*

*I sincerely thank Prof. Dr. S. Sugunan, former Head of the Department, Prof. Dr. K. K. Mohammed Yusuff, and all the other members of the faculty, Department of Applied Chemistry, Cochin University, for their help and encouragement. I thank Dr. H. K. Fun, School of Physics, Universiti Sains Malaysia and Dr. M. Nethaji, Principal Research Scientist, Indian Institute of Science, Bangalore for Single Crystal X-ray diffraction studies.*

*I remember with gratitude the service provided by the Regional Sophisticated Instrumentation Centre, at the Central Drug Research Institute, Lucknow, IIT Bombay, and Sophisticated instrumentation centre, IISc, Bangalore.*

*I thank A. Sreekanth, K. Anas. and T.R. John for recording the various spectra for me. I am grateful to Ms Archana Kishore, Dept. of Biotechnology, for helping me with the biological studies. I acknowledge in a special way the help and cooperation extended to me by my lab mates, Mr. Varghese Philip, V. Sumi. and all the others*

*I am grateful to the Principal, Nirmala College, Muvattupuzha, for his support and encouragement. A word of thanks to Ms. Ceenamamma Jacob and all my other colleagues in the Dept. of Chemistry and to the lab assistants for their support and help.*

*I cannot leave out my nephew, Jeson Dominic, who did the computer graphics for me, from the list of people I have to specially thank. My husband, Mr. Vincent Aerathu and my children Mathews and Anu have always been behind me to spur me on. My sister Ms. Mary Sojan also has contributed her share to my studies.*

*Above all I kneel down before God Almighty for having given me His strength and grace to carry this work to completion.*

*Marthakutty*

## PREFACE

Aqua complex ions of metals must have existed since the appearance of water on the earth, and the subsequent appearance of life depended on, and may even have resulted from the interaction of metal ions with organic molecules. Studies on the coordinating ability of metal ions with other molecules and anions culminated in the theories of Alfred Werner. Thereon the progress in the studies of metal complex chemistry was rapid. Many factors, like the utility and economic importance of metal chemistry, the intrinsic interest in many of the compounds and the intellectual challenge of the structural problems to be solved, have contributed to this rapid progress. X-ray diffraction studies further accelerated the progress.

The work cited in this thesis was carried out by the author in the Department of Applied Chemistry during 2001-2004. The primary aim of these investigations was to synthesise and characterize some transition metal complexes of 2-benzoylpyridine *N*(4)-substituted thiosemicarbazones and to study the antimicrobial activities of the ligands and their metal complexes. The work is divided into eight chapters.

Chapter 1 involves a brief introduction of the metal complexes of thiosemicarbazones including their stereochemistry and biological activities. The different analytical and spectroscopic techniques employed for the analysis of the ligands and their complexes are discussed in this chapter.

Chapter 2 deals with the synthesis and spectral characterization of the ligands, 2-benzoylpyridine *N*(4)-cyclohexylthiosemicarbazone (HL<sup>1</sup>) and 2-benzoylpyridine *N*(4)- phenylthiosemicarbazone (HL<sup>2</sup>). Single crystal X-ray diffraction studies of HL<sup>1</sup> also are given in this Chapter.

Chapter 3 contains the synthesis, spectral characterization, single crystal X-ray diffraction studies and antimicrobial activities of copper(II) complexes of 2-benzoylpyridine *N*(4)-cyclohexylthiosemicarbazone. Chapter 4 deals with the

synthesis, spectral characterization and antimicrobial activities of copper(II) complexes of 2-benzoylpyridine *N*(4)-phenylthiosemicarbazone

Chapters 5 and 6 contain the synthesis, spectral characterization and biological studies of iron(III) and manganese(II) complexes respectively. Chapter 7 describes the synthesis and spectral characterization of the nickel(II) complexes. And Chapter 8 describes the synthesis and spectral characterization of zinc(II), cadmium(II) and mercury(II) complexes.



# CONTENTS

## Chapter I

### THIOSEMICARBAZONES AND THEIR METAL COMPLEXES

1.1	Introduction	1
1.2	Bonding and stereochemistry	2
1.3	Biological activity of thiosemicarbazones and their metal complexes	4
1.4	Objective and scope of the present work	6
1.5	Analytical methods	7
1.5.1	Estimation of carbon, hydrogen and nitrogen	7
1.5.2	Magnetic susceptibility measurements	7
1.5.3	Conductance measurements	7
1.5.4	Electronic spectra	8
1.5.5	Infrared spectra	8
1.5.6	NMR spectra	8
1.5.7	EPR spectra	9
1.5.8	X-ray diffraction studies	9
1.5.9	Biological studies	10
	References	11

## Chapter 2

### SYNTHESIS AND CHARACTERIZATION OF THIOSEMICARBAZONE LIGANDS

2.1	Introduction	15
2.2	Synthesis of thiosemicarbazones	16
2.2.1	Synthesis of 2-benzoylpyridine <i>N</i> (4)-cyclohexylthiosemicarbazone (HL <sup>1</sup> )	17
2.2.2	Synthesis of 2-benzoylpyridine <i>N</i> (4)-phenylthiosemicarbazone (HL <sup>2</sup> )	18
2.3.	Physical measurements	19
2.3.1	X-ray crystallography	19
2.4	Results and discussion	20
2.4.1	Synthesis	20
2.4.2	Crystal structure of HL <sup>1</sup>	21
2.4.3	Infrared spectra	28
2.4.4	Electronic spectra	28
2.4.5	NMR spectrum of HL <sup>1</sup>	30
2.4.6	NMR spectrum of HL <sup>2</sup>	37
	References	39

## Chapter 3

### SYNTHESIS, SPECTRAL CHARACTERIZATION AND ANTIMICROBIAL ACTIVITIES OF COPPER(II) COMPLEXES OF 2-BENZOYLPYRIDINE N(4)-CYCLOHEXYLTHIOSEMICARBAZONE

3.1.	Introduction	42
3.2.	Experimental	43
3.2.1	Materials	43
3.2.2	Synthesis of complexes	43
3.2.3	Analytical methods	45
3.2.4	X-ray Crystallography	45
3.2.5	Antimicrobial activity	46
3.3.	Results and discussion	46
3.3.1	Analytical measurements	46
3.3.2	Crystal structures of [CuL <sup>1</sup> Cl], [{CuL <sup>1</sup> Br} <sub>2</sub> ] and [CuL <sup>1</sup> NCS]	48
3.3.3	Infrared spectra	61
3.3.4	Electronic spectra	71
3.3.5	EPR spectra	74
3.4.	Antimicrobial studies	82
3.4.1	Disc diffusion method	83
3.4.2	Minimum inhibitory concentration	85
	References	87

## **Chapter 4**

### **SYNTHESIS AND SPECTRAL CHARACTERIZATION OF COPPER(II) COMPLEXES OF 2- BENZOYLPYRIDINE N(4)-PHENYLTHIOSEMICARBAZONE**

4.1	Introduction	91
4.2	Experimental	92
4.2.1	Materials	92
4.2.2	Synthesis of complexes	92
4.2.3	Analytical methods	94
4.3	Results and discussion	94
4.3.1	Analytical measurements	94
4.3.2	Infrared spectra	95
4.3.3	Electronic spectra	102
4.3.4	EPR spectra	105
4.4	Antimicrobial activity	112
	References	115

## **Chapter 5**

### **SYNTHESIS, SPECTRAL AND BIOLOGICAL STUDIES OF IRON(III) COMPLEXES**

5.1	Introduction	118
5.2	Experimental	119

5.2.1	Materials	119
5.2.2	Synthesis of complexes	119
5.2.3	Analytical methods	119
5.3	Results and discussion	120
5.3.1	Analytical measurements	120
5.3.2	Magnetic susceptibility	121
5.3.3	Infrared spectra	121
5.3.4	Electronic spectra	126
5.3.5	EPR spectra	127
5.4	Antimicrobial activity	133
	References	134

## **Chapter 6**

### **SPECTRAL CHARACTERIZATION OF MANGANESE(II) COMPLEXES**

6.1	Introduction	136
6.2	Experimental	136
6.2.1	Materials	136
6.2.2	Synthesis of complexes	137
6.3	Results and discussion	137
6.3.1	Physical measurements	137
6.3.2	Magnetic moments	138
6.3.3	Infrared spectra	138
6.3.4	Electronic spectra	141
6.3.5	EPR spectra	142
	References	147

## **Chapter 7**

### **SYNTHESIS AND SPECTRAL CHARACTERIZATION OF NICKEL(II) COMPLEXES**

7.1	Introduction	148
7.2	Experimental	149
	7.2.1 Materials	149
	7.2.2 Synthesis of complexes	149
7.3	Results and discussion	150
	7.3.1 Physical measurements	150
	7.3.2 Magnetic susceptibilities	150
	7.3.3 Infrared spectra	152
	7.3.4 Electronic spectra	157
	7.3.5 <sup>1</sup> H NMR spectrum of [NiL <sub>2</sub> Cl]	158
	References	159

## **Chapter 8**

### **SYNTHESIS, SPECTRAL AND BIOLOGICAL STUDIES OF COMPLEXES OF ZINC(II), CADMIUM(II) AND MERCURY(II)**

8.1	Introduction	162
8.2	Experimental	163
	8.2.1 Materials	163
	8.2.2 Synthesis of complexes	164
8.3	Results and discussion	165

8.3.1	Physical measurements	165
8.3.2	Infrared spectra	165
8.3.3	Electronic spectra	172
8.3.4	<sup>1</sup> H NMR spectra	174
8.4	Antimicrobial activity	176
	References	177
	<b>SUMMARY AND CONCLUSION</b>	<b>178</b>
	<b>Abbreviations</b>	<b>182</b>

# CHAPTER 1



## THIOSEMICARBAZONES AND THEIR METAL COMPLEXES

### 1.1. Introduction

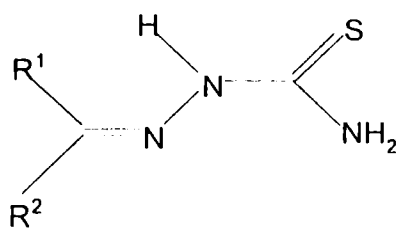
Thiosemicarbazones and their metal complexes exhibit a wide range of biological applications. Owing to the interest they generate in pharmacology, thiosemicarbazones and their metal complexes have been extensively studied. The biological activity of thiosemicarbazones results from their ability to form chelates with metal ions. Thiosemicarbazones have also been used in the analysis of metals [1, 2].

According to the IUPAC recommendations for the nomenclature of organic compounds [3], the derivatives of semicarbazides of the type,  $\text{RCH=N-NH-CX-NH}_2$  and  $\text{R}^1\text{R}^2\text{C=N-NH-CX-NH}_2$ , which are usually obtained by condensation of semicarbazide or thiosemicarbazide with suitable aldehydes and ketones, may be named by adding the class name 'semicarbazone' ( $\text{X=O}$ ) or 'thiosemicarbazone' ( $\text{X=S}$ ) after the name of the condensed aldehyde  $\text{RCHO}$  or ketone  $\text{R}^1\text{R}^2\text{C=O}$ . It is also usual to include in this class derivatives with substituents [4] on the amide or thioamide nitrogen,  $\text{R}^1\text{R}^2\text{C=N-NH-CX-NR}^3\text{R}^4$ , on the X atom,  $\text{R}^1\text{R}^2\text{C=N-N=CXR}^3\text{-NH}_2$  or on the hydrazinic nitrogen,  $\text{R}^1\text{R}^2\text{C=N-NR}^3\text{-CX-NH}_2$ .

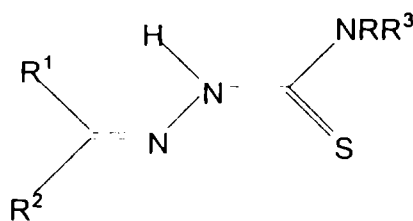
These classes of compounds usually react with metallic cations giving complexes in which the semicarbazones and thiosemicarbazones behave as chelate ligands. Research on the coordination chemistry [5], analytical applications [6], and biological activities [7] of these complexes has been increasing steadily for many years.

## 1.2. Bonding and stereochemistry

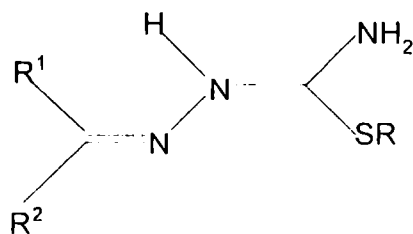
A review of the thiosemicarbazone structures included in the Cambridge structural database (CSD) [8] shows that in the free unsubstituted thiosemicarbazones in the solid state, the C=N-NH-CX-NH<sub>2</sub> backbone is usually almost planar, with the sulfur atom trans to the azomethine nitrogen {configuration *E*; Scheme 1.1(a)}. Although there are several electronic and steric factors that may contribute to the adoption of this arrangement, the most important is probably that the trans arrangement places the amine and azomethine nitrogen atoms in relative positions suitable for intramolecular hydrogen bonding [9]. In fact thiosemicarbazones in which the amine group is fully substituted crystallizes with the sulfur atom cis to the azomethine nitrogen {*Z* configuration; Scheme 1.1(b)}. Substitution of the hydrazinic hydrogen seems not to change the usual *E* configuration of the unsubstituted thiosemicarbazone, however, *S*-substituted thiosemicarbazones adopt the *Z* form {(Scheme 1.1(c))}.



Scheme 1.1(a)



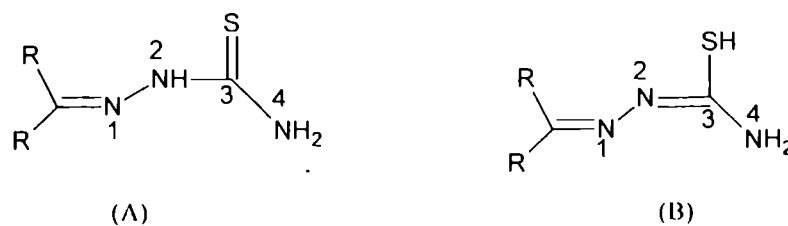
Scheme 1.1(b)



Scheme 1.1(c)

When forming complexes, while in *E* configuration, bonding occurs *via* the sulfur atom as a monodentate ligand. However, in most complexes [10], the thiosemicarbazones coordinate as bidentate ligands *via* the azomethine nitrogen and the thione/thiol sulfur. When an additional coordinating functionality is present in the proximity of the donating centres (eg. 2- heterocyclic thiosemicarbazones), the ligands bond in a tridentate manner. This can be done by either the neutral molecule [11,12] or by the monobasic anion upon the loss of the hydrogen from  $^2N$ . There are instances reported, where the heterocyclic atom and the azomethine nitrogen are involved in bidentate coordination [13].

Allocation of the charge distribution is complicated in thiosemicarbazones due to the existence of thione ( $\Lambda$ ) and thiol ( $B$ ) tautomers. Although the thione form predominates in the solid state, solutions of thiosemicarbazone show a mixture of both tautomers (Scheme 1.2). The IUPAC system for numbering the thiosemicarbazones is given in Scheme 1.2.



Scheme 1.2

There were reports of metal complexes containing thiosemicarbazones in the uncharged thione form and also complexes in which thiosemicarbazone moiety is closer to that of the thiol form in which the <sup>2</sup>N-hydrogen is lost. There were also reports of complexes containing both the neutral and the anionic forms of the ligand bonded to the same metal [14, 15].

### 1.3. Biological activity of thiosemicarbazones and their metal complexes

Thiosemicarbazones have been extensively studied as they show a variety of biological applications: antitumoral, antiviral, antibacterial, antimalarial and antifungal [16, 17]. Heterocyclic thiosemicarbazones exert their therapeutic properties in mammalian cells by inhibiting ribonucleotide reductase, a key enzyme in the synthesis of DNA precursors [18, 19]. The interaction of thiosemicarbazones with various biochemical systems has been studied to understand the potential antitumor behavior of this agent *in vivo*. For example, the 1:1 Cu(II) complex of 2-formylpyridine thiosemicarbazone has been shown to inhibit the RNA-dependent DNA polymerases [20].

Thiosemicarbazones react as bidentate ligands by bonding through the sulfur and azomethine nitrogen atoms. The additional coordination should take place when another coordinating group is present in the vicinity of the thiosemicarbazone moiety, behaving as a tridentate ligand.

Most thiosemicarbazones and their complexes are highly hydrophobic and their low solubility in water induces experimental limitations in biological studies [21]. The introduction of a hydrophilic group such as -NH<sub>2</sub> or -OH in heterocyclic ring systems should permit a soluble acid or sodium salt to be obtained with the goal of increasing the solubility in water [22]. Therefore, since the medicinal activity of thiosemicarbazones, may in part be related to their chelating ability, the

metal complexes are proved to be more biologically active than the thiosemicarbazones. A large number of these complexes involve biologically essential metal ions such as copper, iron and zinc.

It has been revealed that only certain substituted benzaldehyde and heterocyclic thiosemicarbazones possess antitubercular activity [23, 24]. In addition to their antibacterial activities, thiosemicarbazones inhibit growth of both fungi and protozoa. Wiles and Supunchuk [25] reported that heterocyclic derivatives of thiosemicarbazide are active against the growth of *Aspergillus niger* and *Chaetomium globosum* in very low concentrations. Thiosemicarbazones have been tested against a variety of viral infections including herpes virus, adnovirus, polio virus, and RNA tumor virus with mixed results.

An extensive series of thiosemicarbazones obtained from 2-acetylpyridine were tested by Klayman et al [26, 27] for antimalarial activity against *Plasmodium berghei*. The molecular features essential for this activity were found to be a 2-pyridylethylidene moiety, the presence of the thiocarbonyl sulfur and certain cyclic substituents at the terminal <sup>4</sup>N-atom. For example, the 2-acetylpyridine <sup>4</sup>N-dialkylthiosemicarbazones were the most active against *Neisseria gonorrhoeae*.

Cancerostatic properties have been reported for Au(III) complexes with bi- and tridentate thiosemicarbazones as well as with chelating phosphine thiol ligands [28]. A systematic study of the formyl thiosemicarbazones of different heterocyclic ring systems carried out by French and Blanz revealed that the thiosemicarbazone side chain must be adjacent to the heterocyclic nitrogen and a conjugated NNS tridentate ligand system is essential for anticancer activity [29]. As a result, pyridine and isoquinoline ring systems have been most extensively investigated for structure-activity relationships among the antitumor compounds of this series.

#### 1.4. Objective and scope of the present work

Thiosemicarbazones and their metal complexes present a wide range of biological applications [5, 30]. Thiosemicarbazones derived from 2-formyl and 2-acetylpyridine have been extensively investigated by several authors [31-39]. There are also some reports of thiosemicarbazones derived from 2-benzoylpyridine [40-43]. There is another report in the literature on the 4-benzoylpyridine derived analogues [44].

Thiosemicarbazones having a third potential bonding site are found to possess considerable biological activity [45, 46]. In some cases changing the point of attachment of the thiosemicarbazones chain from the 2-position in the pyridine ring to the 3- or 4- position causes a decrease in activity, presumably due to a lower coordination ability but the presence of a bulky group at the terminal nitrogen considerably increases the activity. Earlier works on <sup>4</sup>N-substituted thiosemicarbazones have concluded that, the presence of bulky groups at the <sup>4</sup>N position of the thiosemicarbazones moiety greatly enhances biological activity [47, 48, 49]. Consequent upon these findings, we have undertaken the work with the following objectives:

- To synthesise two ligands:  
<sup>4</sup>N-cyclohexyl-2-benzoylpyridine thiosemicarbazone III.<sup>1</sup> and  
<sup>4</sup>N-phenyl-2-benzoylpyridine thiosemicarbazone III.<sup>2</sup>; henceforth referred to as 2-benzoylpyridine *N*(4)-cyclohexylthiosemicarbazone and 2-benzoylpyridine *N*(4)- phenyl thiosemicarbazone respectively.
- To characterize the ligands using elemental analysis, IR, electronic, <sup>1</sup>H NMR, <sup>13</sup>C NMR, COSY and HMQC spectral studies.
- To synthesise Cu(II), Fe(III), Mn(II), Ni(II), Zn(II), Cd(II) and Hg(II) complexes and characterize these complexes using magnetic susceptibility

measurements, molar conductivity measurements, electronic, infrared, EPR and  $^1\text{H}$  NMR spectral studies.

- To carry out single crystal X-ray diffraction studies of the ligand III.1 and some copper(II) complexes.
- To study the antimicrobial activities of the two ligands and metal complexes.
- To find out the structure activity relationship based on the EPR parameters of the complexes.

## 1.5. Analytical methods

### 1.5.1. Estimation of carbon, hydrogen and nitrogen

The analyses of carbon, hydrogen and nitrogen were done on a Heracus elemental analyzer at Central Drug Research Institute, Lucknow.

### 1.5.2. Magnetic susceptibility measurements

The magnetic susceptibility measurements were carried out at Indian Institute of Technology, Roorkee, in the polycrystalline state at room temperature on a Par model 155 Vibrating Sample Magnetometer at 5 K Oersted field strength. Diamagnetic corrections were made using Pascal's constants.

### 1.5.3. Conductance measurements

The molar conductances of the complexes in dimethylformamide ( $10^{-3}$  M) at room temperature were measured on a Century CC-601 digital conductivity meter, at the Centre for research in Chemistry, Nirmala College, Muvattupuzha.

Kerala. A dip type conductivity cell with platinised platinum electrodes (cell constant  $0.999 \text{ cm}^{-1}$ ) was used.

#### ***1.5.4. Electronic spectra***

The diffuse reflectance spectra at room temperature in magnesium oxide diluents were recorded with Ocean Optics DRS Spectrophotometer. The Electronic spectra in solutions were recorded on a Shimadzu model UV-visible 160 A Spectrophotometer in 200-800 nm range.

#### ***1.5.5. Infrared spectra***

The IR spectra were recorded on a Shimadzu DR 8001 series FT-IR instrument using KBr pellets, in  $4000\text{-}400 \text{ cm}^{-1}$  range at CDRI, Lucknow. The far IR spectra were recorded on a NICOLET MAGNA 550 FT-IR spectrometer using polyethylene pellets in the range  $500\text{-}50 \text{ cm}^{-1}$  at RSIC, IIT, Bombay.

#### ***1.5.6. Nuclear magnetic resonance (NMR) spectra***

The  $^1\text{H}$  and  $^{13}\text{C}$  NMR spectra were recorded in a Bruker DRX 500 instrument using  $\text{CDCl}_3$  as the solvent and TMS as the internal reference at Sophisticated Instruments Facility, Indian Institute of Science, Bangalore. COSY homonuclear and HMQC heteronuclear spectra were also recorded with AMX 400 at the same centre.



### 1.5.7. Electron paramagnetic resonance (EPR) spectra

The EPR spectra were recorded on Varian E-112 X-band spectrometer operating with 100 KHz modulation frequency using tetracyanoethylene (TCNE) as a standard at RSIC, IIT, Bombay. The EPR spectra of the polycrystalline sample at 298 K and those of the solutions at 298 and 77 K were recorded in the X band; the  $g$  factors were quoted relative to the standard marker ( $g = 2.00277$ ). The EPR spectra of the iron(III) complexes were recorded in a Bruker ESP300, X-band CW spectrometer operating at 9.52 GHz equipped with a liquid nitrogen cryostat at the Physical chemistry Lab., ETH-Honggerderg, Zurich, Switzerland. The spectra were measured with modulation amplitude of 0.05 (0.01) mT and 100 kHz modulation frequency, and the field was calibrated by using 2,2-diphenyl-1-picrylhydrazyl (DPPH) with a  $g$  value of 2.0036.

### 1.5.8. X-ray diffraction studies

Single crystal X-ray crystallographic analysis of the compounds were carried out using a Siemens SMART CCD area-detector diffractometer at School of Physics, Universiti Sains Malaysia, and at the Department of Inorganic and Physical Chemistry, Indian Institute of Science, Bangalore. The intensity data were collected by  $\omega$ -scan mode for hkl. Empirical absorptions were employed by using  $\psi$ -scan technique. The structures were solved by direct methods and refined by least-square on  $F_o^2$  using the SHELXTL software package [50]. The collected data were reduced using SAINT program [51] and the empirical absorption was carried out using the SADABS program. Graphics quality plots were made by using the packages ORTEP and PLATON [52].

### ***1.5.9. Biological studies***

Antimicrobial studies of the ligands and the complexes were done at the Department of Biotechnology, Cochin University of Science and Technology. Disc diffusion method was used for studying the antimicrobial property and determining the MIC (minimum inhibitory concentration) of the compounds. The ligands and the complexes were screened against two Gram positive and three Gram negative bacteria.

**References**

1. J.M. Cano, M.E. Urena, A.Garcia, *Anal. Chem.* 58 (1986) 1449.
2. H. Nishioka, T. Kumagai, T. Nagahiro, *Microchem. J.* 50 (1994) 88.
3. R. Panico, W.H. Powel, J.C. Richer (Eds.), *IUPAC Nomenclature of Organic Compounds*, Blackwell, London, (1993) 105.
4. J.S. Casas, M.S. Garcia-Tasende, J.Sordo, *Coord. Chem. Rev.* 209 (2000) 197.
5. D.X. West, S.B. Padhye, P.B. Sonawane, *Struct. Bond.* 76 (1991) 1 and references therein.
6. R.B. Singh, H. Ishii, *Crit. rev. Anal. Chem.* 22 (1991) 381 and references therein.
7. S.N. Pandeya, J.R. Dimmock, *Pharmazie* 48 (1993) 659 and references therein.
8. F.H. Allen, O.Kennard, R.Taylor, *Acc. Chem. Res.* 16 (1983) 146.
9. D. Chattopadhyay, S.K. Mazumdar, T. Banerjee, W.S. Sheldrick, *Acta Crystallogr., Sect. C.* 45 (1989) 314.
10. F. Tui, K.I. Turta, N.V. Gerbeleu, *Russ. J. Inorg. Chem.* 22 (1977) 1497.
11. D.X. West, D.L. Huffman, *Transition Met. Chem.* 14 (1989) 190.
12. D.X. West, P.M. Ahrweiler, G. Ertem, J.P. Scovill, D.L. Klayman, J.L. Anderson, R. Gilardi, L.K. Pannel, *Transition Met. Chem.* 10 (1985) 264.
13. H.K. Parwana, G. Singh, *Indian J. Chem.* 26A (1987) 581.
14. D.X. West, R.M. Makeever, J.P. Scovill, D.L. Klayman, *Polyhedron* 3 (1984) 947.
15. A.V. Ablov, N.V. Gerbeleu, *Russ. J Inorg. Chem.* 9 (1964) 1260.
16. D.X. West, A.E. Liberta, S.B. Padhye, R.C. Chikate, P.B. Sonawane, A.S. Kumbhar, R.G. Yerande, *Coord. Chem. Rev.* 123 (1993) 49 and references therein.

17. P. Bindu, M.R.P. Kurup, T.R. Satyakeerty, *Polyhedron* 18 (1998) 321.
18. F.A. French, E.J. Blanz Jr, J.R. Do Amaral, D.A. French, *J. Med. Chem.* 13 (1970) 1117.
19. L.A. Saryan, E. Ankel, C. Krishnamurti, D.H. Petering, *J. Med. Chem.* 22 (1979) 1218.
20. W. Antholine, J. Knight, H. Whelan, D.H. Petering, *Mol. Pharmacol.* 13 (1977) 89.
21. A. Diaz, R. Pogni, R. Cao, H. Beraldo, M.M. Salberg, D.X. West, L. Gonzalez, E. Ochoa, *Polyhedron* 16 (1997) 3549.
22. K.C. Agarwal, A.C. Sartorelli, *J. Pharm. Sci.* 57 (1968) 1948.
23. E. Hoggarth, A. Martin, M. Storey, E. Young, *J. Pharmacol.* 4 (1949) 248.
24. R. Donovan, F. Pansy, G. Stryker, J. Bernstein, *J. Bacterio.* 59 (1950) 667.
25. D.M. Wiles, T. Supruchunk, *J. Med. Chem.* 12 (1969) 526.
26. D.L. Klayman, J.E. Bartosevich, T.S. Griffin, C.J. Mason, J.P. Scovill, *J. Med. Chem.* 22 (1979) 855.
27. D.L. Klayman, J.P. Scovil, J.F. Bartosevich, *J. Med. Chem.* 26 (1983) 1367.
28. K. Abram, U. Hilditch, L. Zheng, Y. Dilworth, IUPAC-Congress, Berlin, 1999.
29. D.H. Petering, W.E. Antholine, L.A. Saryan, *Metal Complexes as Antitumour agents in Anticancer and Interferron Agents*, Marcel Dekker, Ny (1984) 203.
30. C.A. Brown, W. Kaminsky, K.A. Clayborn, K.I. Goldberg, D.X. West, *J. Braz. Chem. Soc.* 13 (2002) 10.
31. J.P. Scovill, D.L. Klayman, C.F. Franchino, *J. Med. Chem.* 25 (1982) 1261.
32. D.X. West, C.S. Carlson, A.C. Whyte, A.E. Liberta, *Transition Met. Chem.* 15 (1990) 43.
33. D.X. West, S.L. Dietrich, I. Thientanavanich, C.A. Brown, *Transition Met. Chem.* 19 (1994) 195.

34. D.X. West, J.S. Saleda, A.E. Liberta, *Transition Met. Chem.* 17 (1992) 568.
35. D.X. West, H. Gebremedhin, T.J. Romack, *Transition Met. Chem.* 19 (1994) 426.
36. D.X. West, A.M. Stark, G.A. Bain, A.E. Liberta, *Transition Met. Chem.* 21 (1996) 289.
37. B.S. Garg, M.R.P. Kurup, S.K. Jain, Y.K. Bhoon, *Transition Met. Chem.* 16 (1991) 111.
38. D.X. West, L.K. Pannell, *Transition Met. Chem.* 14 (1989) 457.
39. A. Sreekanth, S. Sivakumar, M. R. P. Kurup, *J. Mol. Struct.* 655 (2003) 47.
40. D.X. West, I.S. Billeh, J.P. Jasinski, J.M. Jasinski, R.J. Butcher, *Transition Met. Chem.* 23 (1998) 209.
41. A. Sreekanth, M.R.P. Kurup, *Polyhedron* 22 (2003) 3321.
42. D.X. West, J.S. Ives, J. Krejct, M.M. Salberg, T.L. Zumbahlen, G.A. Bain, A.E. Liberta, *Polyhedron* 14 (1995) 2189.
43. H. Beraldo, W. Nacif, A. Rebolledo, R. Costa, J.D. Ardisson, XI<sup>th</sup> Brazilian Meeting on Inorganic Chemistry, 2002.
44. H. Beraldo, A.M. Barreto, R.P. Vicira, A.P. Rebolledo, N.L. Speziali, C.B. Pinheiro, G. Chapuis, *J. Mol. Struct.* 645 (2003) 213.
45. A.S. Dobeck, D.L. Klayman, E.J. Dickson, J.P. Scovil, E.C. Tramont, *Antimicrob Agents Chemother.* 18 (1980) 27.
46. R.W. Brockman, R.W. Sidwell, G. Arnett, S. Shaddix, *Proc Soc. Expt. Biol. Med.* 133 (1970) 609.
47. A.E. Liberta, D.X. West, *Biometals* 5 (1992) 121.
48. S.K. Jain, B.S. Garg, Y.K. Bhoon, *Spectrochim. Acta.* 42A (1986) 959.
49. M.E. Hossain, M.N. Alam, J. Begum, M. Akbar Ali, M. Nazimudhin, F.E. Smith, R.C. Hynes, *Inorg. Chim. Acta* 249 (1996) 207.
50. G.M. Sheldrick, *SHELXTL Version 5.1, Software Reference Manual*, Bruker AXS Inc., Madison, Wisconsin, USA, 1997.

51. Siemens, SMART and SAINT, Area Detector Control and Integration Software, Siemens Analytical X-ray Instruments Inc., Madison, Wisconsin, USA, 1996.
52. A.L. Speck, PLATON, A multipurpose Crystallographic Tool, Utrecht University, Utrecht, The Netherlands, 1999.

## SYNTHESIS AND CHARACTERIZATION OF THIOSEMICARBAZONE LIGANDS

### 2.1 Introduction

Heterocyclic thiosemicarbazones and their metal complexes are of considerable interest due to their significant biological activity [1-4] and medicinal properties. Thiosemicarbazones are compounds with versatile structural features [5, 6] and they can coordinate to the metal either as a neutral ligand or as a deprotonated anion through the N, N, S or O, N, S donor atoms [7]. The two NNS donors used for the preparation of the metal complexes are:

1. 2-Benzoylpyridine *N*(4)-cyclohexylthiosemicarbazone (HL<sup>1</sup>) {Phenyl (pyridine-2-yl) methanone *N*-cyclohexylthiosemicarbazone}
2. 2-Benzoylpyridine *N*(4)-phenylthiosemicarbazone (HL<sup>2</sup>) {Phenyl (pyridine-2-yl) methanone *N*-phenylthiosemicarbazone}

This Chapter deals with the synthesis and spectral characterization of ligands. It also deals with X-ray diffraction studies of HL<sup>1</sup>. The general structure and the numbering scheme of the two thiosemicarbazones are given in Fig. 2.1. This numbering scheme, according to the IUPAC system, is used throughout the entire work, except in sections 2.4.2., 2.4.5. and 2.4.6.

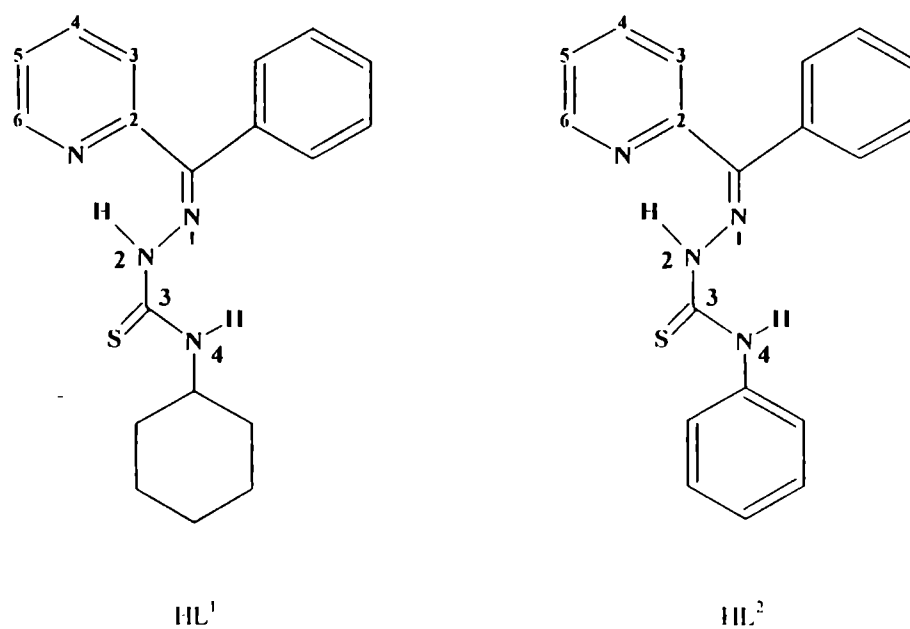


Fig.2.1. Structural formulas of thiosemicarbazones HL<sup>1</sup> and HL<sup>2</sup>

## 2. 2. Synthesis of thiosemicarbazones

Some general methods used for the synthesis of thiosemicarbazones are given below.

*Method 1:* By the condensation of a thiosemicarbazide, prepared from an aryl, aralkyl, or alkyl isothiocyanate and hydrazine, with an aldehyde or ketone.

*Method 2:* By the condensation of an aldehyde or ketone with methyl hydrazine carbodithioate to form an intermediate. The *S*-methyl group of the latter compound, upon displacement by an amine, forms the desired thiosemicarbazone.



*Method 3:* By the condensation of an isothiocyanate with the hydrazone of an aldehyde or ketone.

### **2.2.1. Synthesis of 2-benzoylpyridine N(4)-cyclohexylthiosemicarbazone (HL<sup>1</sup>)**

The thiosemicarbazone was prepared by adopting a reported procedure of Klayman [1].

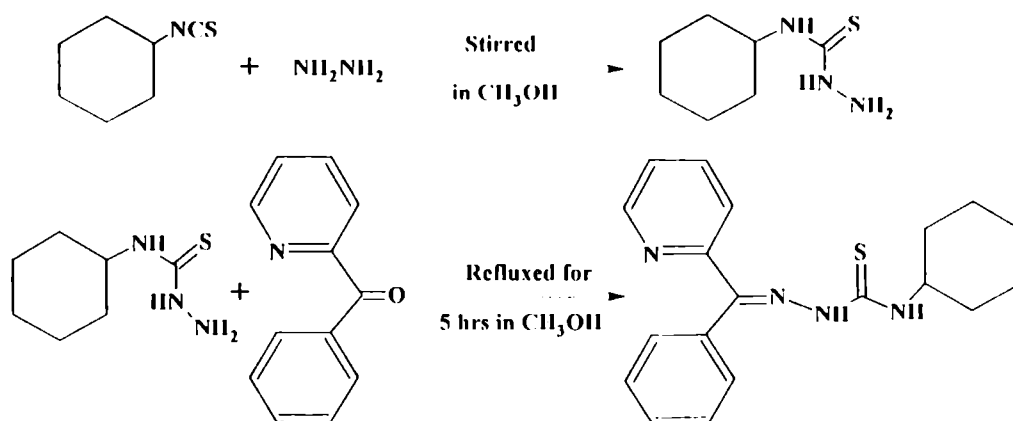
#### *Chemicals used*

Cyclohexyl isothiocyanate (Fluka), hydrazine hydrate (Lancaster), 2-benzoylpyridine (Lancaster), methanol, acetic acid.

#### *Method*

**Step 1:** Cyclohexyl isothiocyanate 7.1 ml (50 mmol, 7.062 g) in 50 ml methanol and hydrazine hydrate 2.4 ml (50 mmol) in 50 ml methanol were mixed with constant stirring. The resulting solution was kept in stirred condition for 0.5 hr. The white product, *N*-cyclohexylthiosemicarbazide formed was washed with methanol and dried. m.p. 140 °C.

**Step 2:** *N*-Cyclohexylthiosemicarbazide (50 mmol, 8.65 g) was dissolved in 100 ml methanol. To this solution, a methanolic solution of 2-benzoylpyridine (50 mmol, 9.16 g) was added. 2 or 3 drops of acetic acid were added and refluxed for 5 hrs. The volume of the solution was reduced to half. The pale yellow crystals, separated on cooling, were filtered, washed with methanol, recrystallised from ethanol and dried over P<sub>4</sub>O<sub>10</sub> *in vacuo*. m.p. 170 °C.



Scheme for the synthesis of III.1

### 2.2.2. Synthesis of 2-benzoylpyridine *N*(4)-phenylthiosemicarbazone (III<sup>2</sup>)

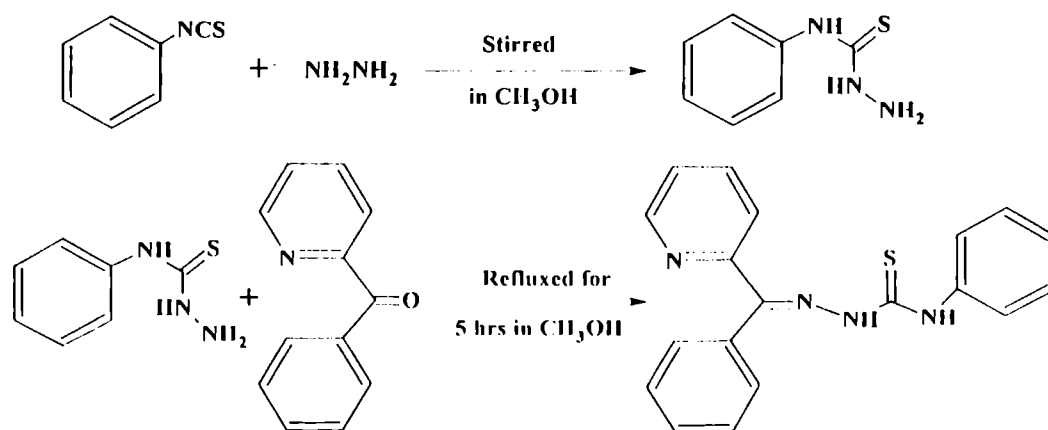
#### Chemicals used

Phenyl isothiocyanate (Fluka), hydrazine hydrate (Lancaster), 2-benzoylpyridine (Lancaster), methanol, acetic acid.

#### Method

**Step 1:** Phenyl isothiocyanate 5.9 ml (50 mmol, 6.759 g) in 50 ml methanol and hydrazine hydrate 2.4 ml (50 mmol) in 50 ml methanol were mixed with constant stirring. The resulting solution was kept in stirred condition for 0.5 hr. The white product, *N*-phenylthiosemicarbazide formed was washed with methanol, and dried. m.p. 125 °C.

**Step 2:** *N*-Phenyl thiosemicarbazide (50 mmol, 8.35 g) was dissolved in 100 ml methanol. To this solution, a methanolic solution of 2-benzoylpyridine (50 mmol, 9.16 g) and 2 or 3 drops of acetic acid were added and refluxed for 5 hrs. The volume of the solution was reduced to half. The dark brown crystals, separated on cooling, were washed with methanol, recrystallised from ethanol and dried over P<sub>4</sub>O<sub>10</sub> *in vacuo*. m.p. 135 °C.

Scheme for the synthesis of HL<sup>2</sup>

### 2.3. Physical measurements

Details regarding the analytical measurements and various spectral techniques are given in Chapter 1.

#### 2.3.1. X-Ray crystallography

Slow evaporation of the ligand in methanol yielded single crystals suitable for X-ray analysis. A pale yellow crystal of HL<sup>1</sup> was mounted on a glass fiber with epoxy cement for the crystallographic study. The crystallographic data and structure refinement parameters for the compound at 293 K are given in Table 1. The data were collected using a SMART CCD diffractometer equipped with graphite-monochromated Mo K<sub>α</sub> radiation, with a detector distance of 5 cm and swing angle of -35°. A hemisphere of the reciprocal space was covered by

combination of three sets of exposures. Each set had a difference of angle (0, 88°, 180°) and each exposure of 10s covered 0.3° in  $\omega$ .

## 2.4. Results and discussion

### 2.4.1. Synthesis

The empirical formulas, melting points and partial elemental analyses of the ligands are listed in Table 2.1. The two thiosemicarbazones HL<sup>1</sup> and HL<sup>2</sup> are pale yellow and brown colored crystals respectively. Crystals of HL<sup>1</sup> suitable for X-ray diffraction studies were obtained by slow evaporation from methanol.

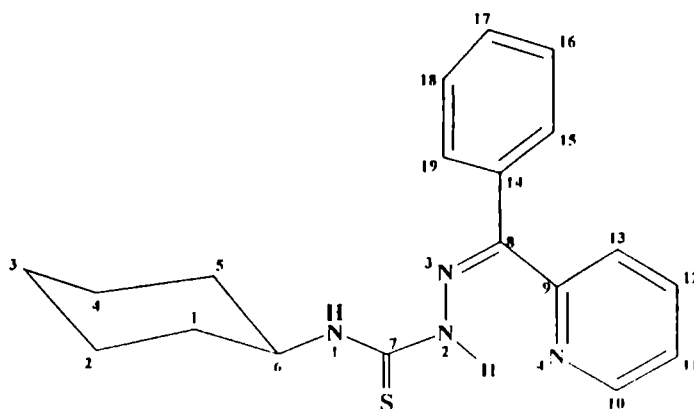
Table 2.1 Analytical data

Compound	Empirical formula	Melting point (°C)	Analytical data Found (Calculated) %		
			C	H	N
HL <sup>1</sup>	C <sub>19</sub> N <sub>4</sub> H <sub>22</sub> S	170	67.63	6.70	16.54
			(67.45)	(6.50)	(16.57)
HL <sup>2</sup>	C <sub>19</sub> N <sub>4</sub> H <sub>16</sub> S	135	68.25	4.77	16.48
			(68.67)	(4.82)	(16.86)

### 2.4.2. Crystal structure of HL<sup>1</sup>

The molecular structure of HL<sup>1</sup> along with the atomic numbering scheme is given in Fig. 2.2. The compound crystallizes as monoclinic lattice with space group  $P2_1/n$  and the molecule shows an *Z* configuration with respect to the C8 = N3 bond. A torsion angle value of  $-174.31^\circ$  corresponding to the S1–C7–N2–N3 moiety confirms the trans configuration of the thiocarbonyl S1 atom with respect to the hydrazine nitrogen atom N3. This is in accordance with the data available for the unprotonated thiosemicarbazones [8].

The C7–S1 bond distance ( $1.675 \text{ \AA}$ ) is close to that expected for a C=S double bond ( $1.60 \text{ \AA}$ ) and the C8–N3 bond length ( $1.290 \text{ \AA}$ ) is nearly the same as that of the C=N double bond length, ( $1.28 \text{ \AA}$ ). Similarly, the N2–N3 bond length ( $1.367 \text{ \AA}$ ) is closer to that of single bond length ( $1.45 \text{ \AA}$ ) than to double bond length ( $1.25 \text{ \AA}$ ) [9]. These data are in strong support of the existence of 2-benzoylpyridine *N*(4)-cyclohexyl thiosemicarbazone, in the thione form in the solid state. The mean plane deviation calculations show that the pyridyl ring Cg(1) is planar with a max deviation of  $-0.0096 \text{ \AA}$ . The thiosemicarbazone moiety also is planar with a maximum mean plane deviation value of  $-0.0596 \text{ \AA}$  and a torsion angle value of  $3.65^\circ$  for N2–N3–C8–C9 confirms that the C8–C9 bond is in the same plane as the thiosemicarbazone moiety. Also, the atoms C9, N4, C10, C11, C12, C13 and C8 are coplanar as evidenced from the maximum deviation value of  $0.0205 \text{ \AA}$  from the plane. The dihedral angle formed by the two least square planes Cg(3) and Cg(1) is equal to  $67^\circ$ , which confirms the non-planarity of the two rings. {Cg(1) is the plane consisting of atoms N(4), C(9), C(10), C(11), C(12), C(13) and Cg(3) is the plane consisting of atoms C(14), C(15), C(16), C(17), C(18), C(19) respectively}.

Fig.2.2. Structure of 11L.<sup>1</sup>

The intramolecular hydrogen bonding interaction N(1) – H(1)N(1)---N(3) leads to the formation of a five membered ring comprising of N(1), H(1)N(1), C(7), N(2) and N(3). A similar six membered ring involving N(2), H(1)N(2), N(3), C(8), C(9) and N(4) is also developed by the N(2) – H(1)N(2) --- N(4) intramolecular hydrogen bonding interaction in the compound. The axial substitution of the cyclohexyl ring at the N1 nitrogen of the thiosemicarbazone is confirmed by a torsion angle value of  $-178.26^\circ$  for the N2 – C7 – N1 – C6 bond. Ring Puckering Analysis and least square planes calculations show that the cyclohexyl ring, Cg(2) adopts a chair conformation ( $Q_T = 0.5701 \text{ \AA}$ ). Atoms C1, C2, C4 and C5 constitute the best fitting plane of the cyclohexyl ring, and atoms C3 and C6 deviate by 1.2462 and 1.2358  $\text{\AA}$  respectively, on either side of this plane.

The packing of the molecule in a unit cell is shown in Fig. 2.4. The unit cell is viewed down the 'a' axis and four molecules of the compound are arranged in the unit cell. It is evident from the figure that the unit cell, as a whole, is packed in a centrosymmetric manner. The self-assembly of molecules in the crystal lattice in this manner is effected by the  $\pi - \pi$  interaction between the two pyridyl rings, i.e., Cg(1) of the two neighbouring units are observed at a distance of 3.8582  $\text{\AA}$

whereas these are observed at an average distance  $5.7295\text{\AA}$  between the Cg(1) of one unit with the phenyl ring Cg(3) of the adjacent molecule.

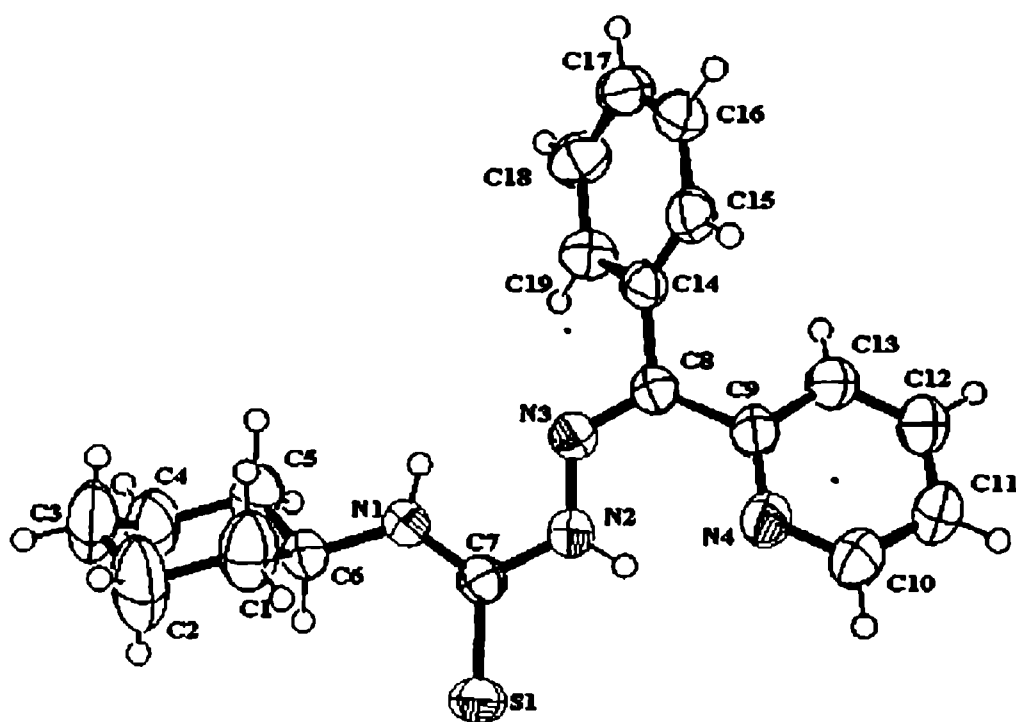


Fig. 2.3. ORTEP diagram for HL<sup>1</sup>, displacement ellipsoids are drawn at 50% probability level and hydrogen atoms are shown as small spheres of arbitrary radii.

Table 2.2 Summary of crystal data and structural refinement for III.<sup>1</sup>

Empirical Formula	C <sub>19</sub> H <sub>22</sub> N <sub>4</sub> S
Formula weight (M)	338.47
Temperature (T) K	293(2)
Wavelength (Mo K) (Å)	0.71073
Crystal system	Monoclinic
Space group	P2 <sub>1</sub> /n
Lattice constants	
<i>a</i> (Å)	6.1522(3)
<i>b</i> (Å)	17.9701(8)
<i>c</i> (Å)	16.9023(7)
$\alpha$ (°)	90.00
$\beta$ (°)	94.423(1)
$\gamma$ (°)	90.00
Volume <i>V</i> (Å <sup>3</sup> )	1863.08(15)
<i>Z</i>	4
Calculated density ( $\rho$ ) (Mg m <sup>-3</sup> )	1.207
Absorption coefficient ( $\mu$ ) (mm <sup>-1</sup> )	0.181
<i>F</i> (000)	720
Crystal size (mm)	0.86 x 0.38 x 0.32
$\theta$ Range for data collection	2.42- 28.30
Limiting Indices	-7 $\leq$ <i>h</i> $\leq$ 8, -19 $\leq$ <i>k</i> $\leq$ 23, -22 $\leq$ <i>l</i> $\leq$ 21
Reflections collected	4559
Unique Reflections	3581 [ <i>R</i> <sub>int</sub> = 0.0169]
Completeness to $\theta$	28.29 (91.1 %)
Max. and min. transmission	0.9444 and 0.8599
Refinement method	Full-matrix least-squares on <i>F</i> <sup>2</sup>
Data / restraints / parameters	4559/0/297
Goodness-of-fit on <i>F</i> <sup>2</sup>	1.047
Final <i>R</i> indices [ <i>I</i> > 2 $\sigma$ ( <i>I</i> )]	<i>R</i> <sub>1</sub> = 0.0452, <i>wR</i> <sub>2</sub> = 0.1228
<i>R</i> indices (all data)	<i>R</i> <sub>1</sub> = 0.0587, <i>wR</i> <sub>2</sub> = 0.1374
Largest difference peak and hole (e Å <sup>-3</sup> )	0.298 and -0.233



Table 2.3 Selected bond lengths (Å) and bond angles (°) of III.<sup>1</sup>

C(1) – C(6)	1.499(3)	N(1) – C(6) – C(5)	109.43(14)
C(5) – C(6)	1.525(2)	N(1) – C(6) – C(1)	111.57(15)
C(6) – N(1)	1.452(19)	C(6) – N(1) – C(7)	125.92(13)
C(7) – N(1)	1.328(19)	N(1) – C(7) – S(1)	125.62(11)
C(7) – S(1)	1.675(15)	N(2) – C(7) – S(1)	118.87(11)
C(7) – N(2)	1.364(18)	N(1) – C(7) – N(2)	115.51(13)
N(2) – N(3)	1.367(17)	N(2) – N(3) – C(8)	120.14(12)
C(8) – N(3)	1.290(18)	N(3) – C(8) – C(9)	126.94(13)
C(8) – C(14)	1.489(2)	C(9) – C(8) – C(14)	118.95(12)
C(8) – C(9)	1.488(2)	N(4) – C(9) – C(8)	118.25(13)
C(9) – N(4)	1.345(2)	C(8) – C(9) – C(13)	120.04(14)
C(10) – N(4)	1.337(2)	N(4) – C(9) – C(13)	121.62(14)
C(9) – C(13)	1.391(2)	C(8) – C(14) – C(19)	119.82(13)
C(14) – C(15)	1.393(2)	C(8) – C(14) – C(15)	121.17(14)
C(14) – C(19)	1.384(2)	C(15) – C(14) – C(19)	118.99(14)

Table 2.4. H bonding,  $\pi$ --- $\pi$  and  $CH$ --- $\pi$  interactions of III.<sup>1</sup>

<b>H bonding (<math>\text{\AA}</math>, <math>^\circ</math>)</b>				
D-H---A	D-H	H---A	D---A	D- H---A
N1-H1N1---N3	0.87	2.15	2.5905	117
N2-H1N2-N4	0.90	2.01	2.6853	131
<b><math>\Pi</math>---<math>\pi</math> interactions</b>				
Cg(I)-Res(I)---Cg(J)	Cg-Cg( $\text{\AA}$ )	$\alpha$ ( $^\circ$ )	$\beta$ ( $^\circ$ )	
Cg(1)-[ 1]---Cg(1) <sup>a</sup>	3.8582	0.00	13.64	
Cg(1)-[ 1]---Cg(3) <sup>b</sup>	5.4642	67.00	53.66	
Cg(3)-[ 1]---Cg(1) <sup>c</sup>	5.9949	69.28	48.82	
Equivalent position codes: a=-x, 1-y, -z		Cg(1)=N(4),C(9), C(10), C(11),		
b=-1+x, y, z		C(12),C(13)		
c= 1/2 +x, 1/2-y, 1/2 +z		Cg(2)=C(1), C(2), C(3), C(4), C(5), C(6)		
		Cg(3)=C(14), C(15), C(16), C(17), C(18),		
		C(19)		
<b>CH---<math>\pi</math> interactions</b>				
X-H(1)---Cg(J)	H..Cg( $\text{\AA}$ )	X-H..Cg ( $^\circ$ )	X..Cg( $\text{\AA}$ )	
C(3)-H(3B)---Cg(3) <sup>d</sup>	2.8680	139.71	3.6608	
Equivalent position code: d = -x, 1-y, 1-z				
D=Donor, A=acceptor, Cg=Centroid. $\alpha$ =dihedral angles between planes I & J, $\beta$ = angle Cg(I)-Cg(J)				

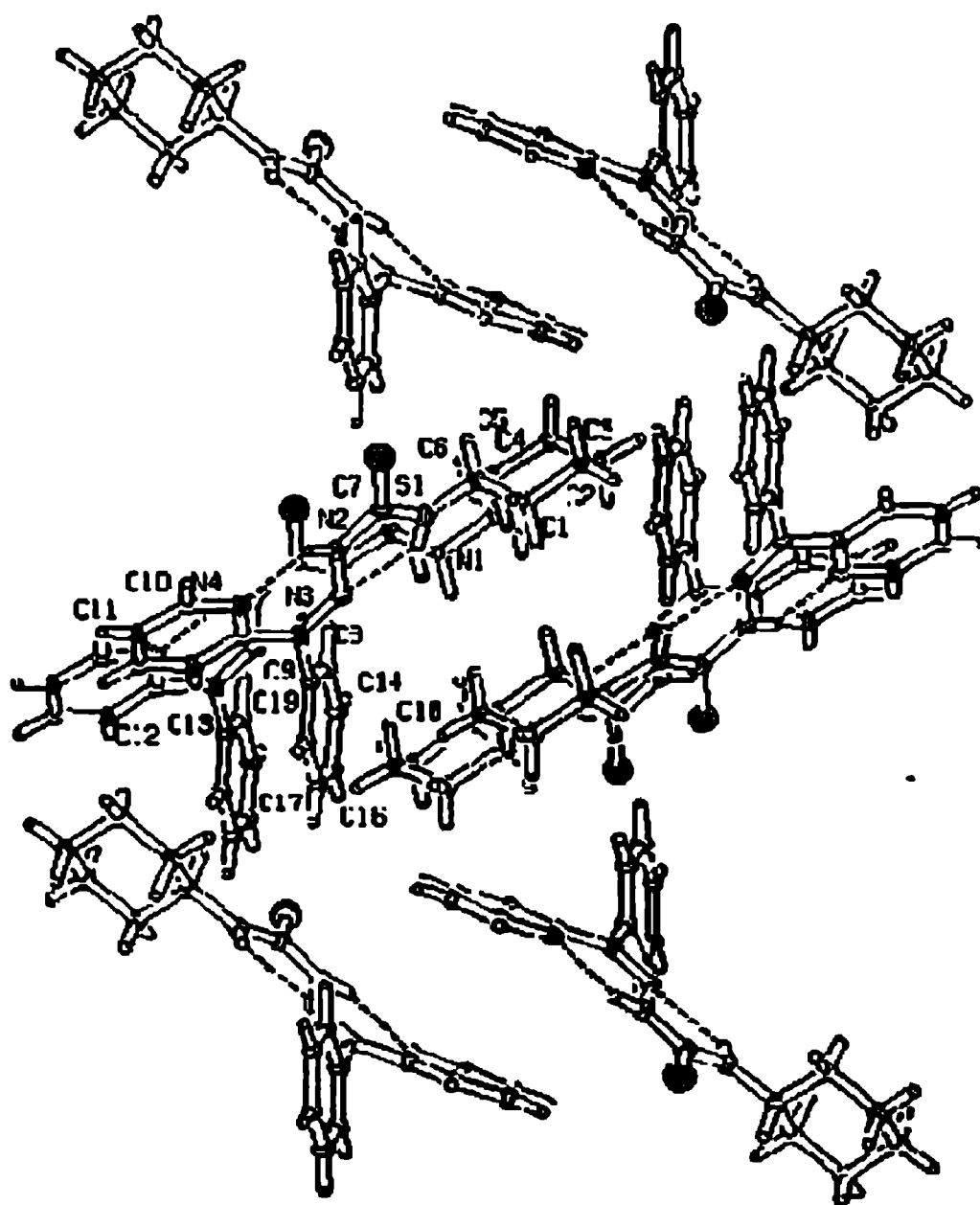


Fig. 2.4. Unit cell packing diagram of HL<sup>1</sup>, viewed along the 'a' axis

### 2.4.3. Infrared spectra

The IR spectral bands are assigned based on the positions of the atoms as shown in Fig. 2.1. The IR spectra of the two ligands HL<sup>1</sup> and HL<sup>2</sup> contain strong broad bands at 3334 and 3423 cm<sup>-1</sup> due to  $\nu(\text{NH})$  [10].

The bands at 833 and 835 cm<sup>-1</sup> in the spectra of ligands HL<sup>1</sup> and HL<sup>2</sup> are due to the  $\nu(\text{C}=\text{S})$  band. The presence of the  $\nu(\text{C}=\text{S})$  band and the absence of the  $\nu(\text{S-H})$  band, which should be in the range 2600-2550 cm<sup>-1</sup> suggest that the two ligands remain in the thione form in the solid state [11].

Schiff bases contain C=N stretching band in the range 1471-1689 cm<sup>-1</sup>. The two thiosemicarbazones HL<sup>1</sup> and HL<sup>2</sup> contain strong bands at 1582 and 1591 cm<sup>-1</sup> which are due to the  $\nu(\text{C}=\text{N})$  band. The IR spectral bands of HL<sup>1</sup> and HL<sup>2</sup> observed at 1118 and 1102 cm<sup>-1</sup> correspond to  $\nu(\text{N-N})$  [12,13].

The spectrum of the ligand HL<sup>1</sup> which is 2-benzoylpyridine *N*(4)-cyclohexylthiosemicarbazone contains a strong band at 1447 cm<sup>-1</sup> which corresponds to cyclohexyl ring [11].

Aromatic and heteroaromatic compounds display strong out-of-plane C-H bending and ring bending absorption bands in the 900-650 cm<sup>-1</sup> region. The bands at 607 and 622 cm<sup>-1</sup> in the spectra of HL<sup>1</sup> and HL<sup>2</sup> can be assigned as due to the in-plane ring deformation band of the pyridine ring [14].

### 2.4.4. Electronic spectra

In the solid-state reflectance spectra of HL<sup>1</sup> and HL<sup>2</sup>, the bands observed at *ca.* 341 and 288 nm are assigned to the  $n \rightarrow \pi^*$  transitions of the thioamide group and pyridine nitrogen respectively [15]. The bands observed at 259 and 261 nm in the spectra of HL<sup>1</sup> and HL<sup>2</sup> respectively are assigned to the  $\pi \rightarrow \pi^*$  transition. In the

spectra from the DMF solution, these bands are blue shifted to 332, 280 and 255 nm having log $\epsilon$  values 4.13, 3.38 and 4.20 and respectively.

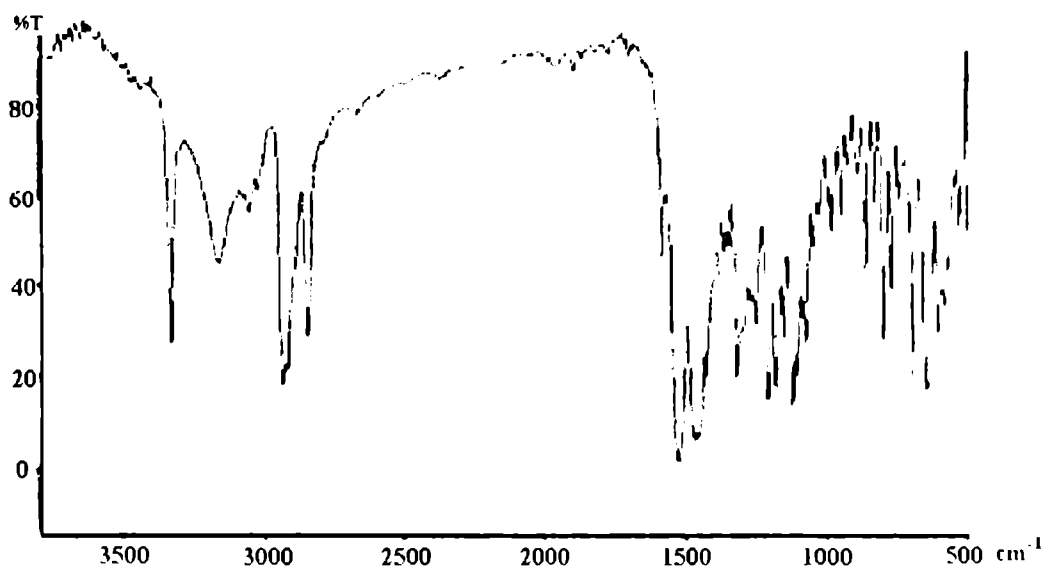


Fig 2.5. IR spectrum of III.<sup>1</sup>

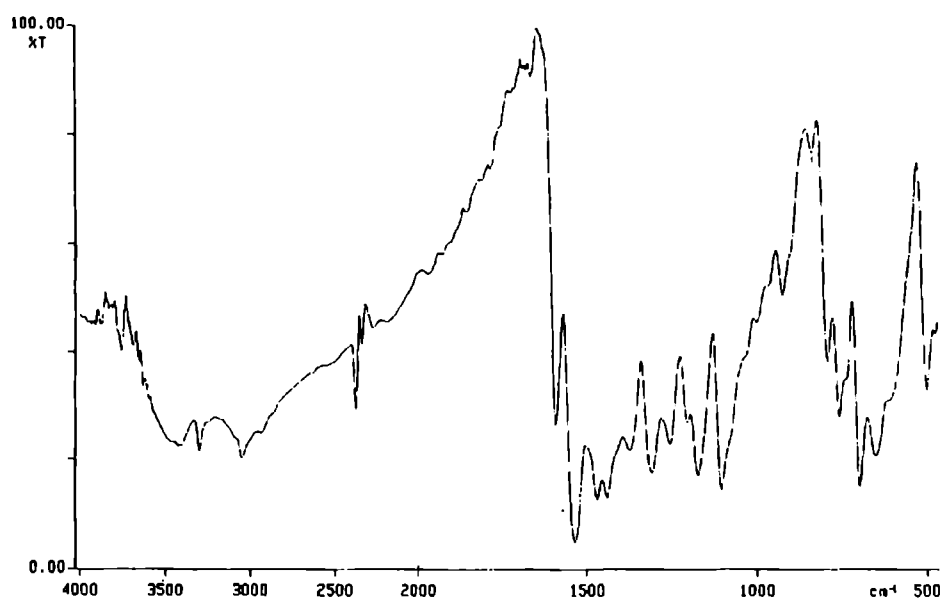


Fig 2.6. IR spectrum of III.<sup>2</sup>

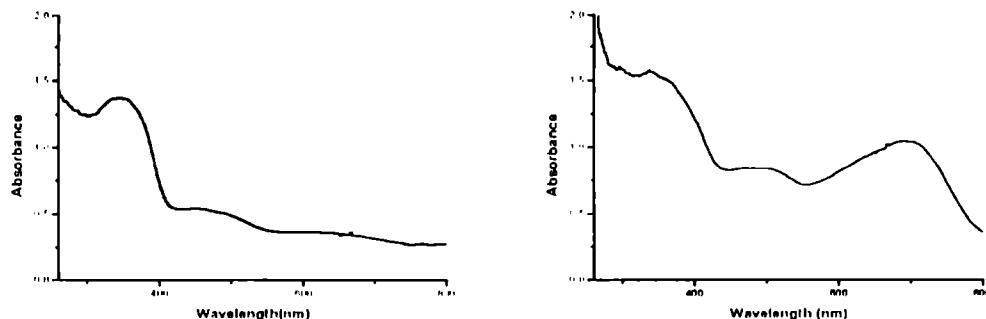


Fig. 2.7. Electronic spectra of HL<sup>1</sup> and HL<sup>2</sup>

#### 2.4.5. NMR spectrum of HL<sup>1</sup>

<sup>1</sup>H NMR spectrum of the ligand HL<sup>1</sup> is recorded in CDCl<sub>3</sub>. The one-dimensional and two dimensional nuclear magnetic resonance spectra are used in resolving the carbon and hydrogen atoms of HL<sup>1</sup> and the assignments are based on the structure shown in Fig 2.8. The <sup>1</sup>H resonances are assigned on the basis of the chemical shift values, multiplicities and coupling constants and connectivity from <sup>1</sup>H and <sup>1</sup>H-<sup>1</sup>H correlation experiments [11,16]. These give insight into the average effective magnetic fields present, interaction of the nuclear spin with the adjacent atoms and the number of equivalent protons.

The NMR spectral assignments are based on the positions of the atoms given in Fig. 2.8, which is based on the X-ray diffraction studies of HL<sup>1</sup> which has been already mentioned in section 2.4.2. The <sup>1</sup>H NMR spectrum reveals four signals for the pyridyl moiety, multiplet for the phenyl moiety and seven well-resolved peaks for the cyclohexyl moiety. The signals at  $\delta = 13.48$  and 7.63 ppm are assigned to the <sup>2</sup>NH and <sup>1</sup>NH protons respectively [17]. The intensity of these peaks decreases on the addition of D<sub>2</sub>O, which suggests that they are easily exchangeable. These protons are shifted downfield because they are attached to

heteroatoms and so are easily subjected to hydrogen bonding and are decoupled by the electrical quadrupole effects. The proton attached to  $^2N$  appears as singlet as expected since the NH protons are decoupled from the nitrogen atoms and the protons from the adjacent atoms. But contrary to this,  $^1NH$  shows coupling with the adjacent hydrogen H6 and hence gives a doublet. This coupling is clear in COSY (correlation spectroscopy), which can be attributed to the low NH exchange rate. The peak at 8.80 ppm is due to the H10 proton.

This proton is very sensitive to the electron densities as it is close to the pyridyl nitrogen and is observed to be deshielded due to the electronic effect of the phenyl ring. The phenyl moiety appears as a multiplet at about 7.45 ppm where the chemical shift values are very close and hence it is very difficult to be resolved. The complexity of the COSY predicts that the spectrum is not strictly of the first order. The peaks (7.3 ppm) corresponding to the solvent ( $CDCl_3$ ) appear to be superimposed with that of the phenyl protons. The cyclohexyl moiety forms a chair conformation and hence puts the hydrogen in two different electronic environments, *viz.* axial and equatorial and hence gives seven well-resolved peaks. The equatorial protons (H5e - 2.08 ppm) are found to resonate at a slightly higher frequency than that of the axial protons (H5a - 1.27 ppm). A multiplet present at 4.32 ppm is attributed to the H6, which is deshielded by the adjacent electronegative nitrogen.

Fig. 2.10. shows the  $^1H$ - $^1H$ -correlation spectral assignments of the compound. The COSY separates out the interactions among the protons and establishes the proton-proton couplings. The proton spectrum is plotted along the X and Y-axes and can be seen as contours in diagonal. In the proton NMR spectrum we have already identified a doublet at 8.80 ppm as of pyridyl proton H10.

In the proton NMR spectrum we have already identified a doublet at 8.80 ppm as of pyridyl proton H10.

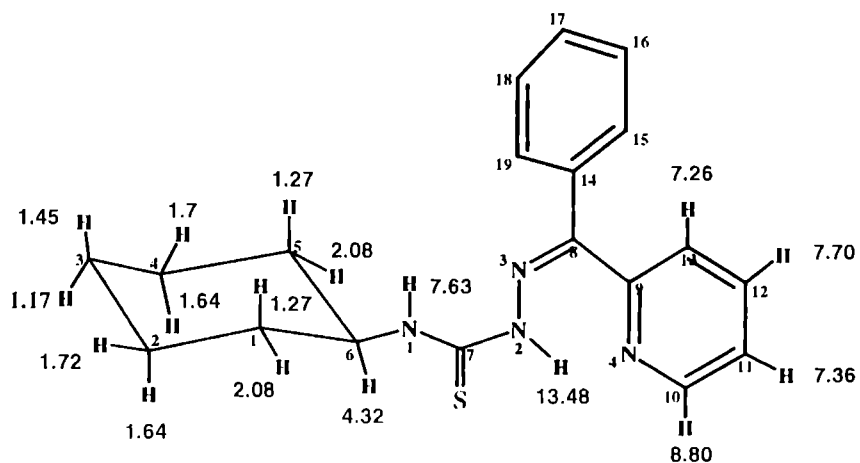


Fig 2.8. <sup>1</sup>H NMR spectral assignments of HL<sup>1</sup>

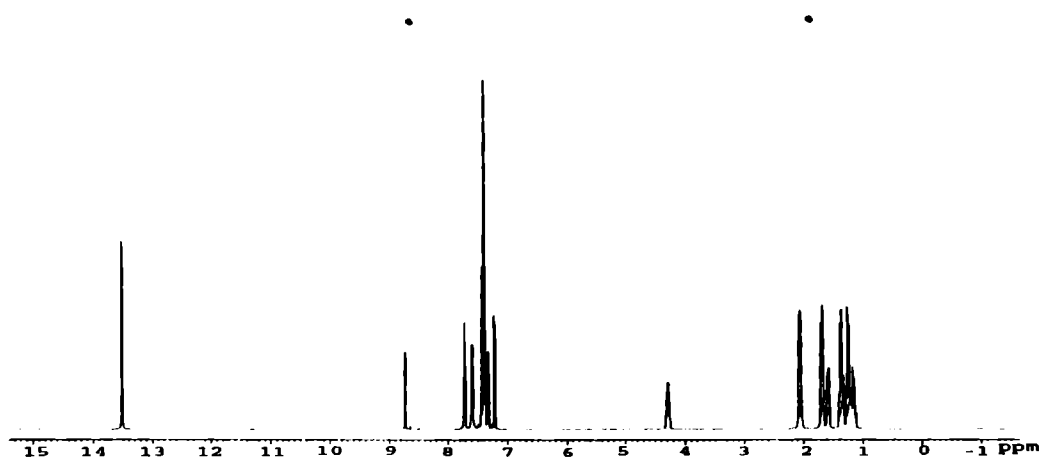


Fig. 2.9. <sup>1</sup>H NMR spectrum of HL<sup>1</sup>



off diagonal spots at 8.86 ppm (H10) and 7.70 ppm (H12). The multiplet at 7.36 ppm is related to the number of possible orientations these neighboring protons can adopt. The H12 proton is also split by H13 proton and vice versa. In the spectrum around  $\delta = 7.40$  ppm, the contours are seen ambiguous and the multiplet is assigned to the protons of the phenyl moiety. The chemical shifts are very close, so this spectrum is not strictly first order. The peak at 2.08 ppm is assigned to the equatorial proton on the carbon atom C5. From the COSY, it is shown to interact with three other protons H6, H5a and H4e. The couplings are of diequatorial and axial/equatorial type. The coupling constants agree well with those corresponding to the chair conformation of cyclohexane. Similarly the H5e and H4e protons split the peak of the axial proton H5a. In the  $^1\text{H}$  NMR the multiplet at 1.72 ppm is assigned to the H4e proton, which interacts with five other protons H5a, H5e, H4a, H3e and H3a, where interaction with H3a is very weak. All these couplings are of vicinal type.

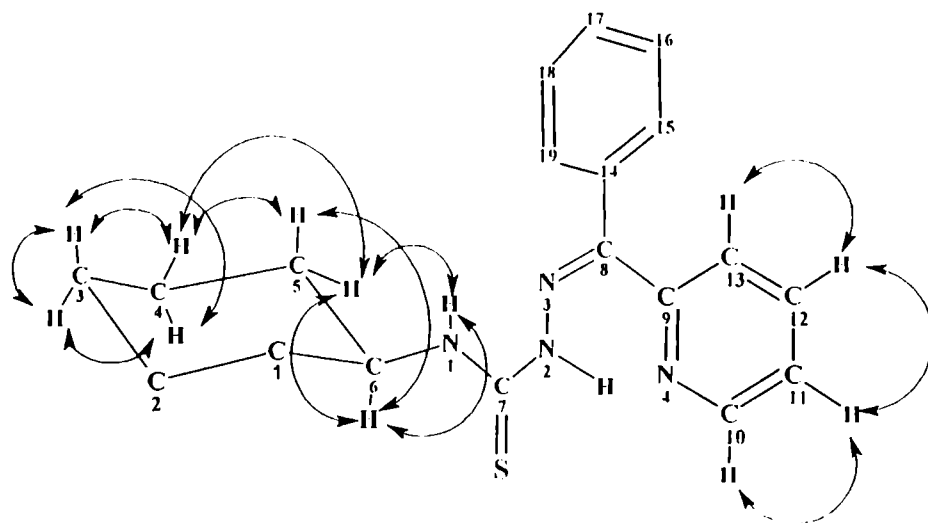
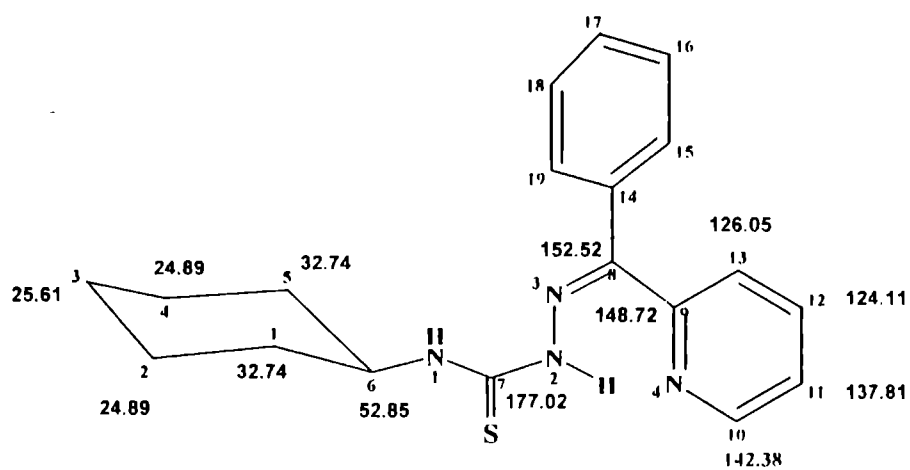
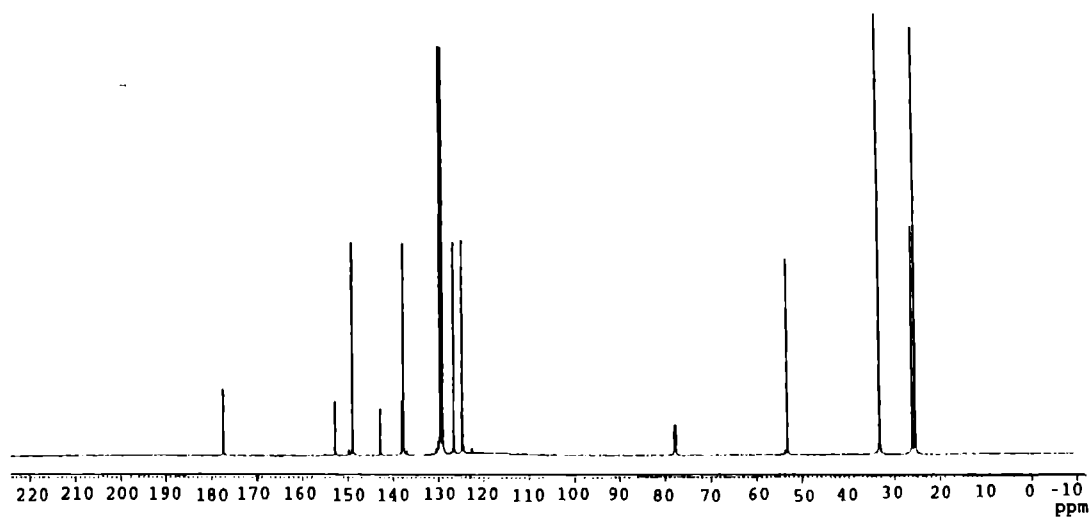


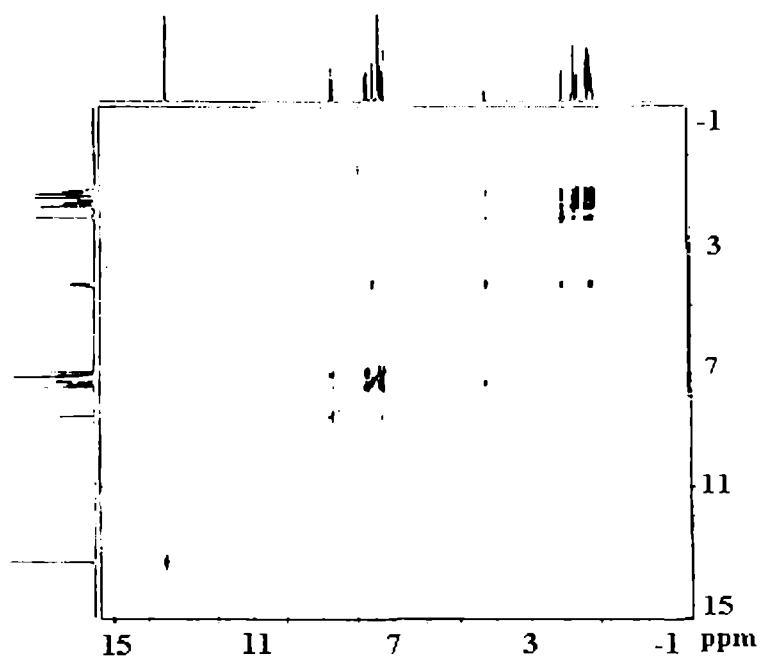
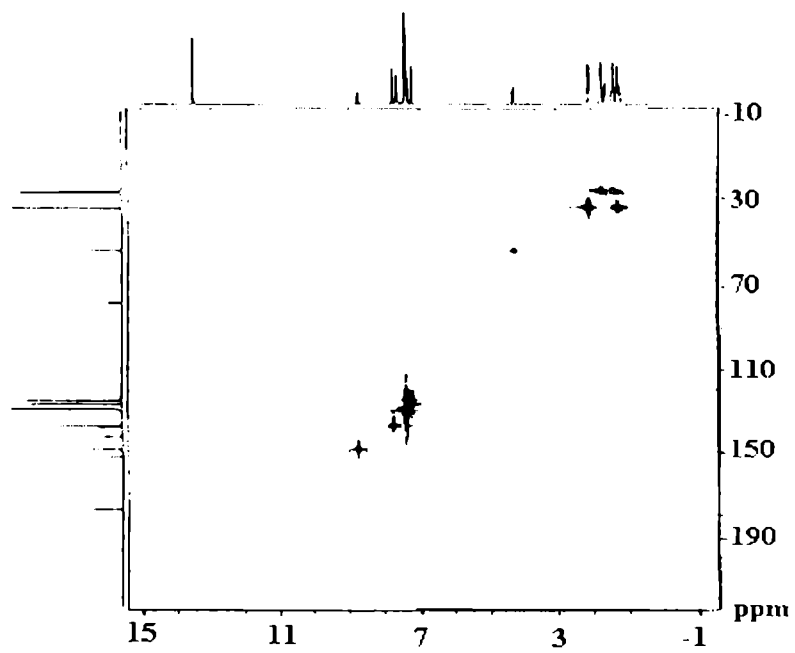
Fig. 2.10.  $^1\text{H}$  -  $^1\text{H}$  COSY assignments of HL<sup>1</sup>

The coupling of the H4a proton with the neighboring H4e, H3a and H3e protons forms the multiplet at 1.64 ppm. This proton shows no coupling with the

H5e and H5a protons. The coupling between the H3a and H4a protons gives J value around 11 Hz, which is consistent with diaxial type coupling constants. Even though the coupling in the region 1.5 ppm is difficult to resolve, as the chemical shift values of H3a, H3e and H5a are very close, it is clearly evident from the spectrum that the H3a proton couples with the H4a and H3e protons. Similarly the H3e is coupled with H3a, H4e and H4a protons. The same coupling is observed for the protons at C1 and C2, which are magnetically equivalent to the C5 and C4 protons. The H6 proton interacts with the  $^1\text{NH}$  and also with two protons of C1 and C5.

The  $^{13}\text{C}$  NMR spectrum was assigned on the basis of the proton-decoupled  $^{13}\text{C}$  spectrum and the HMQC (heteronuclear multiple quantum coherence). The HMQC experiment provides the correlation between the protons and their attached heteronuclei through the heteronuclear scalar coupling. The decoupled  $^{13}\text{C}$  spectrum of the compound contains 15 peaks corresponding to fifteen magnetically unique atoms. The signal from the  $^{13}\text{C}$  spectrum is much weaker than that of the corresponding proton NMR. From the HMQC, it is evident that the peaks at 177.02, 152.52 and 148.72 ppm are of the non-protonated carbons and they correspond to the S=C7, N=C8 and C9 carbon atoms respectively. The carbon atom closest to the electronegative atom is farthest downfield. The carbon atoms on the pyridyl ring can be assigned as C10 142.38, C11 137.81, C12 124.11, C13 126.05. Aromatic carbons of the phenyl ring appear around 129 ppm and it is very difficult to be resolved. The peaks at 32.74, 24.89, 25.61 and 52.85 ppm are assigned to the C1, C2, C3 and C6 carbons respectively. The C4 and C5 are chemically equivalent with the C2 and C1 carbons and hence have the values 24.89 and 32.74 ppm respectively.

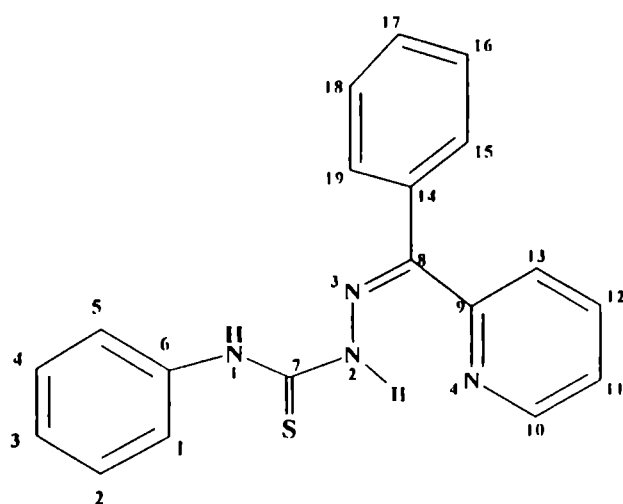
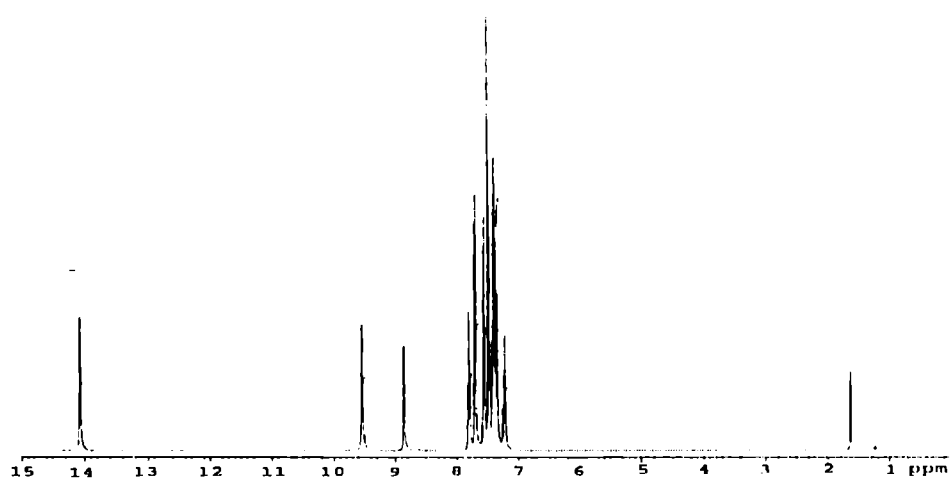
Fig. 2.11.  $^{13}\text{C}$  NMR spectral assignments of HL<sup>1</sup>Fig. 2.12.  $^{13}\text{C}$  NMR spectrum of HL<sup>1</sup>

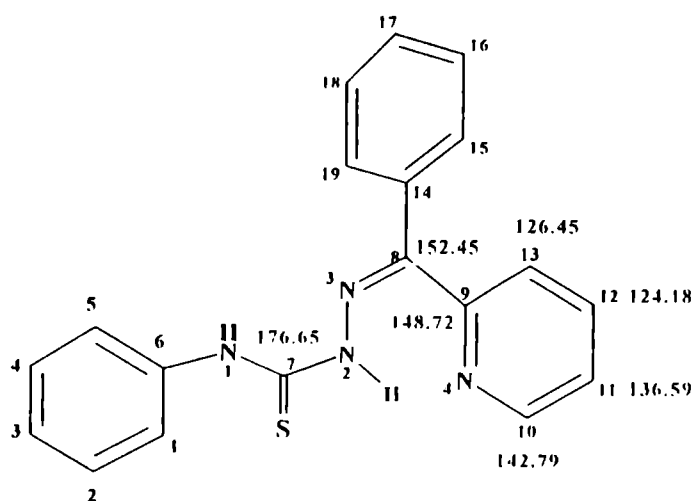
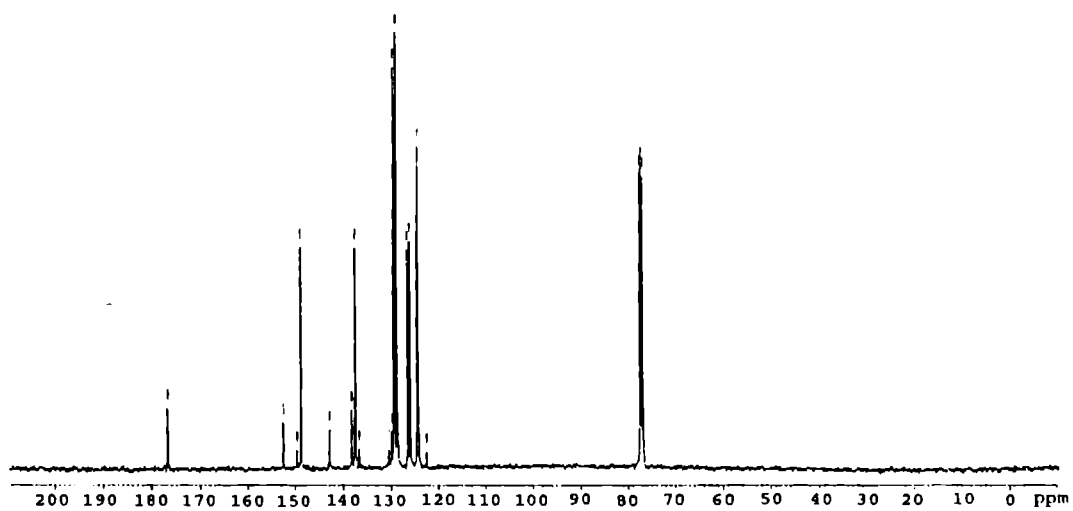
Fig. 2.13.  $^1\text{H}$ - $^1\text{H}$  COSY spectrum of HL1Fig. 2.14.  $^{13}\text{C}$ - $^1\text{H}$  HMQC spectrum of HL1

#### 2.4.6. NMR spectrum of HL<sup>2</sup>

<sup>1</sup>H and C<sup>13</sup> NMR spectra of the compound were recorded in CDCl<sub>3</sub> and the assignments are based on earlier works [17,18]. <sup>1</sup>H NMR spectrum of HL<sup>2</sup> shows signals at  $\delta = 14.06$  (s, 1H), 8.83 (d, 1H) and 9.53 (s, 1H) which correspond to the <sup>2</sup>N-H, C(10)-H, and <sup>1</sup>N-H respectively. The downfield value of <sup>1</sup>N-H proton is due to the deshielding effect of the phenyl group. The aromatic protons of the two phenyl groups and the three protons of the pyridine ring appear at  $\delta$  values in the range 7.2 -7.8. The signals are at  $\delta = 7.79$  (m, 1H), 7.69 (d, 2H), 7.56 (m, 2H), 7.48 (m, 3H), 7.38 (m, 4H), 7.22 (m, 1H). The absence of peaks corresponding to the S-H proton in the spectrum supports the fact that in solution, the predominant tautomer is in the thione form.

The <sup>13</sup>C NMR spectrum was assigned on the basis of the proton-decoupled <sup>13</sup>C spectrum. The decoupled <sup>13</sup>C spectrum of the compound contains 15 peaks corresponding to the fifteen magnetically unique atoms. Pair of carbon atoms C1-C5, C2-C4, C15-C19, C16-C18 are magnetically equivalent. In the <sup>13</sup>C NMR spectrum of HL<sup>2</sup>, the signals observed were assigned values based on earlier works. The peaks at 176.65, 152.45 and 148.72 ppm correspond to S=C7, N=C8 and C9 carbon atoms. The carbon atoms on the pyridyl ring can be assigned as C10 142.79, C11 136.59, C12 124.18, and C13 126.45. Aromatic carbons of the two phenyl rings appear around 129 ppm and it is very difficult to be resolved.

Fig.2.15. Structure of HL<sup>2</sup>2.16. <sup>1</sup>H NMR spectrum of HL<sup>2</sup>

Fig.2.17. <sup>13</sup>C NMR spectral assignments of HL<sup>2</sup>2.18. <sup>13</sup>C NMR spectrum of HL<sup>2</sup>

## References

1. D.L. Klayman, J.F. Bartosevich, T.S. Griffin, C.J. Mason, J.P. Scovill, *J. Med. Chem.* 22 (1979) 855.
2. P. Bindu, M.R.P. Kurup, T.R. Satyakcerty, *Polyhedron* 18 (1999) 321.
3. R.P. John, A. Sreekanth, M.R.P. Kurup, S.M. Mobin, *Polyhedron* 21 (2002) 2515.
4. M.R.P. Kurup, M. Joseph, *Synth. React. Inorg. Met-Org Chem.* 33 (2003) 1275.
5. D.X. West, G.A. Bain, R.J. Butcher, J.P. Jainski, Y. Li, R.Y. Pozdniakiv, J. Vades-Martinez, R.A. Toscano, S. Hernandez-Ortega, *Polyhedron* 15 (1996) 665.
6. A. Usman, I.A. Razak, S. Chantrapromma, H.K. Fun, V. Philip, A. Sreekanth, M.R.P. Kurup, *Acta Crystallogr. C* 58 (2002) 652.
7. M.B. Ferrari, G. Fava, C. Pelizzi, P. Tarasani, *J. Chem.Soc., Dalton Trans.* (1992) 2153.
8. D. Chattopadhyay, T. Banerjee, S.K. Mazumdar, S. Ghosh, R. Kuroda, *Acta Crystallogr., Sect.C.* 43 (1987) 974.
9. J.March, *Advanced Organic Chemistry, Reactions, Mechanisms and structure*, 4<sup>th</sup> ed., Wiley, New York, 1992.
10. D.X. West, N.M. Kozub, G.A. Bain, *Transition Met. Chem.* 21(1996) 52.
11. R.M. Silverstein, G.C. Bassler, T.C. Morrill, *Spectrometric Identification of Organic Compounds*, 4<sup>th</sup> ed., Wiley, New York, 1981.
12. D.X. West, A.M. Stark, G.A. Bain, A.E. Liberta, *Transition Met. Chem.* 21 (1996) 289.
13. H. Beraldo, A.M. Barreto, R.P. Vicira, A.P. Rebolledo, N.L. Speziali, C.B. Pinheiro, G. Chapuis, *J.Mol. Struct.* 645 (2003) 213.



14. D.X. West, I.S. Billeh, J.P. Jesinski, J.M. Jcsinski, R.J. Butcher, *Transition Met. Chem.* 23 (1998) 209.
15. V.Philip, V.Suni, M.R.P. Kurup, M.Nethaji, *Polyhedron* 23 (2004) 1225.
16. W.Kemp. *Organic spectroscopy*, 3<sup>rd</sup>ed., Macmillan Press Ltd.,Hampshire, 1996.
17. D.X. West, H. Gebremedhin, T.J. Romack, *Transition Met. Chem.*19 (1994) 426.
18. D.X. West, J.S. Ives, J. Krejct, M.M. Salberg, T.L. Zumbahlen, G.A. Bain, A.E. Liberta, *Polyhedron* 14 (1995) 2189.

## **CHAPTER 3**

**SYNTHESIS, SPECTRAL CHARACTERIZATION AND  
ANTIMICROBIAL ACTIVITIES OF COPPER(II) COMPLEXES  
OF 2-BENZOYLPYRIDINE *N*(4)-CYCLOHEXYL  
THIOSEMICARBAZONE**

### 3.1. Introduction

Copper is widely distributed in nature as metal, in sulphides, arsenides, chlorides, carbonates and so on [1]. The name *copper* and the symbol Cu are derived from *aes cyprum* (later cuprum), since it was from Cyprus that the Romans first obtained their copper metal [2]. Copper is one of the transition elements frequently found at the active site of proteins. The copper containing enzymes and proteins constitute an important class of biologically active compounds [3]. The biological functions of copper proteins/enzymes include electron transfer, dioxygen transport, oxygenation, oxidation, reduction, and disproportionation [4,5].

The common oxidation states of copper are I ( $d^{10}$ ), II ( $d^9$ ), and III ( $d^8$ ). Cu(I) has mononuclear and polynuclear complexes having linear, planar, tetrahedral and distorted planar geometries. The most common oxidation state of Cu is (II), and Cu(II) complexes have been extensively studied. These complexes have trigonal planar, tetrahedral, octahedral, distorted octahedral, square planar and pentagonal bipyramidal geometries [1]. Cu(III) complexes, which include high spin paramagnetic complexes and low spin diamagnetic square planar complexes, are not common, thiosemicarbazones and their copper complexes have been extensively studied owing to their pharmacological interest [6]. These compounds present a great variety of biological activity ranging from antitumoral [7,8],

fungicide [9], bactericide [10] and anti-inflammatory [11]. Copper(II) complexes are interesting due to their biological applications and interesting stereochemistries. There have been reports dealing with *N*(4)-aryl thiosemicarbazones derived from 2-formyl, 2-acetyl and 2-benzoylpyridine [12,13].

This Chapter deals with the synthesis, magnetic studies, spectral characterization, X ray diffraction studies and antimicrobial activities of Cu(II) complexes of 2-benzoylpyridine *N*(4)-cyclohexylthiosemicarbazone (HL<sup>1</sup>).

### 3.2. Experimental

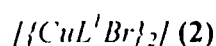
#### 3.2.1. Materials

Details regarding the synthesis of HL<sup>1</sup> are described in Chapter 2. Various copper(II) salts (GR.) were used as obtained.

#### 3.2.2. Synthesis of complexes



A solution of CuCl<sub>2</sub>·2H<sub>2</sub>O (2 mmol, 0.340 g) in 25 ml ethanol and a solution of HL<sup>1</sup> (2 mmol, 0.676 g) in 40 ml hot ethanol were mixed and refluxed for 4 hrs. On cooling, the blue solids separated were filtered, washed with hot water, hot ethanol and ether and dried *in vacuo* over P<sub>4</sub>O<sub>10</sub>.



CuBr<sub>2</sub> (2 mmol, 0.446 g) dissolved in a mixture of hot methanol and ethanol (40 ml) and HL<sup>1</sup> (2 mmol, 0.676 g) dissolved in 40 ml hot methanol were mixed and refluxed for 4 hrs. The blue colored solids, separated on cooling, were filtered,

and washed with hot water, hot ethanol and ether. The compound was dried over  $P_4O_{10}$  *in vacuo*.

#### $[CuL^1NO_3]$ (3)

A solution of  $Cu(NO_3)_2 \cdot 3H_2O$  (2 mmol, 0.482 g) in 20 ml ethanol and a solution of  $HL^1$  (2 mmol, 0.676 g) in 40 ml hot ethanol were mixed and refluxed for 5 hrs. The green solids separated on keeping overnight, were filtered and washed with hot water, hot ethanol and ether and dried over  $P_4O_{10}$  *in vacuo*.

#### $[CuL^1NCS]$ (4)

A mixture of  $Cu(CH_3COO)_2 \cdot H_2O$  (2 mmol, 0.399 g) in 20 ml methanol and  $HL^1$  (2 mmol, 0.676 g) in 40 ml methanol were refluxed for 2 hrs. To the refluxing solution, a solution of potassium thiocyanate (2 mmol, 0.198 g) in 20 ml ethanol was added and again refluxed for 4 hrs. The green colored crystals, separated on keeping for a few days, were filtered and washed with hot ethanol, hot water and ether and then dried over  $P_4O_{10}$  *in vacuo*.

#### $[CuL^1N_3] \cdot 3H_2O$ (5)

Solutions of  $Cu(CH_3COO)_2 \cdot H_2O$  (2 mmol, 0.398 g) in 20 ml methanol and  $HL^1$  (2 mmol, 0.676 g) in 40 ml methanol were mixed and refluxed for 2 hrs. Then a solution of sodium azide (2 mmol, 0.13 g) was added to the refluxing solution and again refluxed for 2 hrs. The blue solids separated, were filtered, washed with hot water, hot ethanol, and ether and dried over  $P_4O_{10}$  *in vacuo*.

#### $[Cu_2(L^1)_2SO_4] \cdot 2H_2O$ (6)

$CuSO_4 \cdot 5H_2O$  (2 mmol, 0.499 g) dissolved in a hot mixture of 20 ml methanol and 10 ml water and a solution of  $HL^1$  (2 mmol, 0.676 g) in 40 ml

methanol were mixed and refluxed for 7 hrs. The dark green colored shining crystals, separated on keeping the solution overnight, were collected by filtration and washed with hot water, hot methanol, and ether and dried over  $P_4O_{10}$  *in vacuo*.

### 3.2.3. Analytical methods

Details regarding the various analytical methods are discussed in the previous Chapter.

### 3.2.4. X-Ray crystallography

Single crystals of compound **1** for X-ray analysis were grown by slow evaporation of the complex in a chloroform methanol mixture. A deep blue monoclinic crystal of compound  $[CuL^1Cl]$  (**1**) was mounted on a glass fiber using epoxy cement. The X-ray diffraction data were measured in frames with increasing  $\theta$  (width of  $0.3^\circ$ /frame) at room temperature (293 K) using a Bruker SMART APEX CCD diffractometer, equipped with a fine focus sealed tube X-ray source. The SMART software was used for data acquisition and the SAINT software for data extraction [14]. Empirical absorption corrections were made on the intensity data [15]. The structure was solved by the heavy atom method and refined by full-matrix least squares using the SHELX system of programs [16] and the graphics tool was PLATON for windows [17]. All the non-hydrogen atoms of the complex cations were refined anisotropically. A few hydrogen atoms were located from the difference Fourier map and the rest were generated, assigned isotropic thermal parameters, and refined using a riding model. The hydrogen atoms were used for structure factor calculation only. Similarly, a dark blue crystal of  $[CuL^1Br]_2$  (**2**) and a light green colored crystal of  $[CuL^1NCS]$  (**4**) were analysed in a similar way

and the crystallographic data along with the structural refinements are given in Table 3.2.

### **3.2.5. Antimicrobial activity**

For antimicrobial activity, two Gram positive and three Gram negative bacteria were used as test organisms. Disc diffusion method was used for screening the antimicrobial property and determining the MIC (minimum inhibitory concentration) of the compounds.

## **3.3. Results and discussion**

### **3.3.1. Analytical measurements**

The colors, stoichiometries, elemental analyses, and magnetic moments of the Cu(II) complexes are given in Table 3.1. All the Cu(II) complexes prepared are either blue or green in color. They are insoluble in polar solvents and soluble in dimethylformamide, dimethylsulphoxide and in chloroform. The elemental analyses data of all the compounds suggest a formula  $[ML^1X]$  where X is Cl,  $NO_3$ , NCS,  $N_3$  and L is the deprotonated ligand. The bromo complex has the formula  $\{[CuL^1Br]_2\}$ , while the sulfato complex formed is  $[Cu_2(L^1)_2SO_4] \cdot 2H_2O$ . The compounds **5** and **6** contain water molecules and the IR data suggests that the water molecules are not coordinated, but exist as lattice water [18].

Molar conductances of the complexes were measured using a  $10^{-3}$  M solution in DMF. The values are found below  $20 \text{ ohm}^{-1}\text{mol}^{-1}\text{cm}^{-1}$ , which show that all the complexes are nonconductors [19]. This fact indicates that the anion and the deprotonated ligand are coordinated to the central Cu(II).

Magnetic moments of the complexes are calculated from magnetic susceptibility measurements and the values of all the Cu(II) complexes at room temperature are found to be in the range 1.5-1.9 B.M. The values of the magnetic moments, which are close to the spin only value of 1.7 B.M., indicate the presence of one unpaired electron as expected for  $d^9$  configuration [20].

Table 3.1 Colors, partial elemental analyses data and magnetic moment of the complexes

Compound	Empirical formula	Color	Found (Calculated) (%)			$\mu$ (BM) at 300 K
			C	H	N	
[CuL <sup>I</sup> Cl] (1)	C <sub>19</sub> H <sub>21</sub> N <sub>4</sub> SClCu	Blue	52.62 (52.29)	4.94 (4.82)	12.72 (12.84)	1.52
[(CuL <sup>I</sup> Br) <sub>2</sub> ] (2)	C <sub>19</sub> H <sub>21</sub> N <sub>4</sub> SBrCu	Blue	47.16 (47.45)	4.55 (4.37)	11.70 (11.65)	1.81
[CuL <sup>I</sup> NO <sub>3</sub> ] (3)	C <sub>19</sub> H <sub>21</sub> N <sub>5</sub> SO <sub>3</sub> Cu	Green	49.35 (49.29)	4.54 (4.76)	14.73 (15.13)	1.75
[CuL <sup>I</sup> NCS] (4)	C <sub>20</sub> H <sub>21</sub> N <sub>5</sub> S <sub>2</sub> Cu	Green	52.40 (52.34)	4.70 (4.58)	15.03 (15.26)	1.94
[CuL <sup>I</sup> N <sub>3</sub> ].3H <sub>2</sub> O (5)	C <sub>19</sub> H <sub>27</sub> N <sub>7</sub> O <sub>3</sub> Cu	Blue	45.46 (45.96)	4.94 (5.43)	20.14 (19.74)	1.97
[Cu <sub>2</sub> (L <sup>I</sup> ) <sub>2</sub> SO <sub>4</sub> ].2H <sub>2</sub> O (6)	C <sub>38</sub> H <sub>46</sub> N <sub>8</sub> S <sub>2</sub> O <sub>6</sub> Cu	Dark green	48.81 (48.87)	5.03 (4.93)	11.99 (12.00)	1.80



### 3.3.2. Crystal structures of $[\text{CuL}^1\text{Cl}]$ , $[\{\text{CuL}^1\text{Br}\}_2]$ and $[\text{CuL}^1\text{NCS}]$

The structures of  $[\text{CuL}^1\text{Cl}]$  (**1**),  $[\{\text{CuL}^1\text{Br}\}_2]$  (**2**) and  $[\text{CuL}^1\text{NCS}]$  (**4**) along with the atomic labeling are shown in Figs. 3.1, 3.3 and 3.5 respectively. The crystal data is given in Table 3.2 and the comparison of selected bond lengths and bond angles of  $\text{HL}^1$ , with compounds **1**, **2** and **4** are summarized in Table 3.3. Compound **1** crystallized into a monoclinic lattice, with space group symmetry  $P2_1/n$  with two molecules per asymmetric unit. The compounds **2** and **4** crystallized into triclinic lattices with space group  $P-1$ .

#### 3.3.2.1. $[\text{CuL}^1\text{Cl}]$ (**1**)

The compound  $[\text{CuL}^1\text{Cl}]$  (**1**) crystallizes into a monoclinic lattice with a  $P2_1/n$  space group symmetry. There are two crystallographically independent molecules, A and B, in the asymmetric unit of the compound, with bond lengths and angles that agree with each other and are within normal ranges. The experimental refinement parameters of the compound are illustrated in Table 3.2 and the molecular structure along with the atomic numbering scheme is presented in Fig. 1. Selected bond length and angles are presented in Table 3.3. The compound shows a square planar geometry with the Cu atom lying in an approximate plane with the N1, N3, S1 and Cl1 atoms. Due to coordination, the C13 – S1 bond length of the thiosemicarbazone moiety approaches the value corresponding to a C – S single bond, as evident from the increased value of 1.746(3) Å in the complex, compared to 1.675(15) Å in the ligand. The C13 – S1 distance in **1** compares well with those reported for the related thiosemicarbazone complexes, in which the coordination by the thiolate tautomer has been definitely established by X-ray structural determinations [21, 22]. The square planar nature



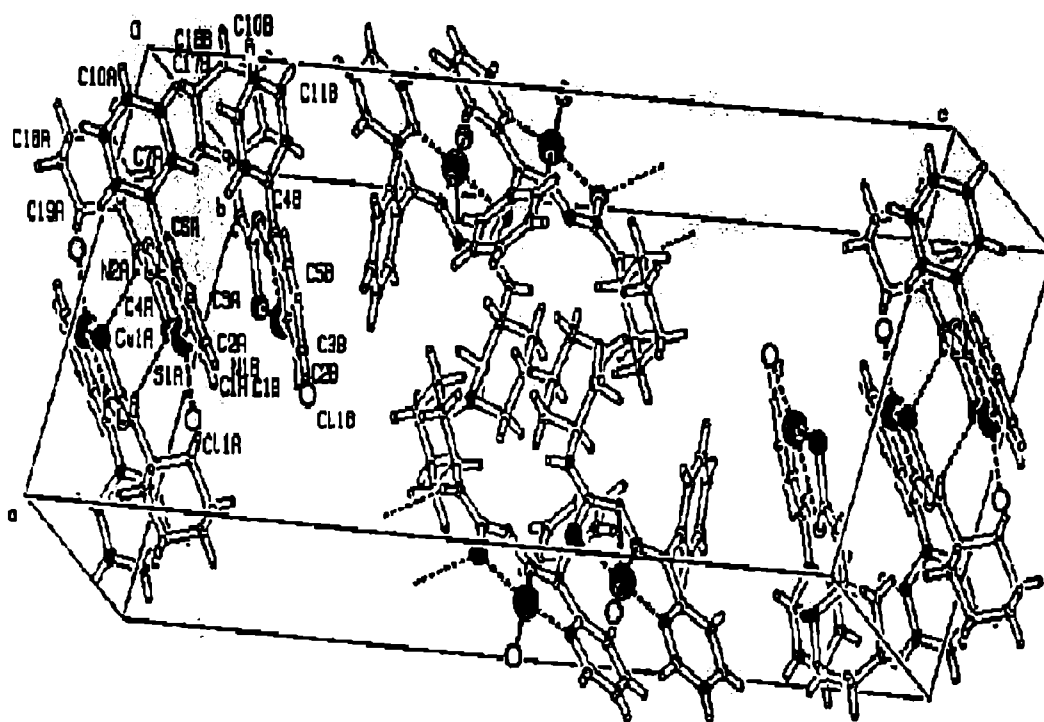


Fig.3.2. Close packing of compound 1

A slight distortion from the square planar geometry is evidenced by the bond angles. The bonding parameters reveal that the Cu1 – N1 (2.036(2) Å) and Cu1 – N2 (1.966(2) Å) bond lengths are much smaller than the Cu1 – Cl1 (2.2099(10) Å) bond length. This implies stronger Cu–N bonds compared to the Cu–Cl bond indicating the domination of the thiosemicarbazone moiety in the bonding. The repeating unit in the crystal packing consists of three molecules where two of them, set in an offset fashion, are self-assembled by the intermolecular (N2H – S1) hydrogen bonding interactions, while the third molecule is arranged in a face to face manner with the neighbouring molecule. The repeating

units are packed in an offset fashion and a three dimensional packing is effected by the  $\pi - \pi$  stacking, ring – metal and CH –  $\pi$  interactions.

### 3.3.2.2. $[\{CuL^1Br\}_2]$ (2)

Compound 2 is a thiolato bridged copper(II) dimer complex of 2-benzoylpyridine *N*(4)-cyclohexylthiosemicarbazone crystallised into a triclinic lattice with P1 symmetry. Thiolato bridging by sulfur ligands are well reported [23-25], and recently, the metal complexes of Schiff bases [26, 27] and thiosemicarbazone [28] involving the phenolate oxygen bridging are reported. Each  $CuL^1Br$  unit in the molecule assembles into a symmetric binuclear complex by bridging through the thiolato sulfur atom of the adjacent thiosemicarbazone *via* axial ligation. Thus, the Cu(II) ions reveal a distorted pentacoordinated *viz.* (4 + 1) (N1N2S1Br + S') square-based pyramidal geometry in the complex. The thiolate sulfur, azomethine nitrogen, pyridyl nitrogen, and the bromine atom occupy the basal plane. The bond lengths CuI – S1 (2.289(2) Å), CuI – N2 (1.978(4) Å), CuI – N1 (2.028(5) Å) and CuI – Br1 (2.371(12) Å) are consistent with the other similar bond distances of square pyramidal copper complexes [29]. The apical position of the square pyramid is occupied by the thiolate sulfur of the second unit, with a Cu–Cu distance of 3.523 Å with the CuI – S1 – Cu1A or CuI – S1A – Cu1A angle being *ca.* 84.47°. In the equatorial plane, the CuI – S1 or Cu1A – S1A and CuI – S1A or Cu1A – S1 bond lengths are 2.266 and 2.937 Å respectively and the non-equivalent bonds give rise to the asymmetric binuclear thiolate double bridged structure. The basal planes around CuI and Cu1A are essentially planar with mean deviations being 0.1905 Å and 0.1891 Å respectively. The significantly longer Cu – S axial bond length of *ca.* 2.937 Å is likely to reduce the spin – spin coupling

between Cu1 and Cu1A centres. The  $\text{Cu}_2\text{S}_2$  unit in the complex is planar with a mean deviation of 0.0073 Å.

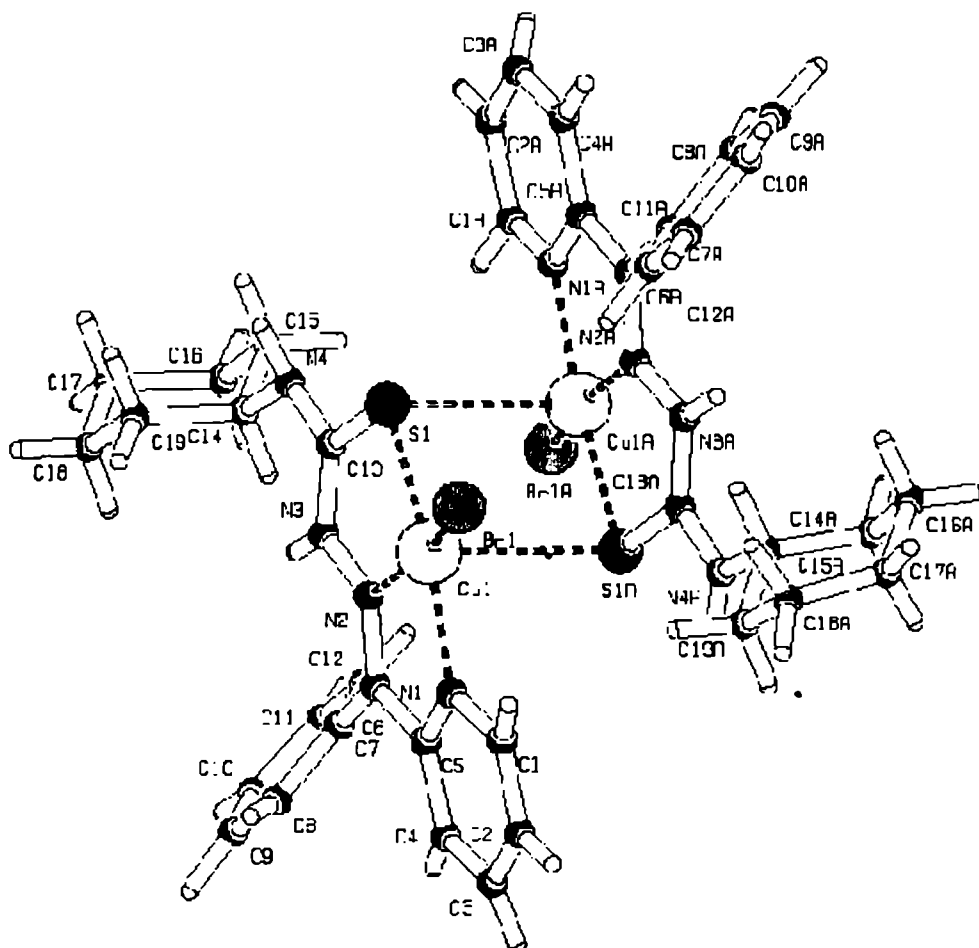


Fig. 3.3. PLATON diagram for  $[\{\text{CuL}^1\text{Br}\}_2] (2)$

The  $\text{Cu}_2\text{S}_2$  plane is observed at angles  $81.76^\circ$  and  $80.60^\circ$  respectively with the basal planes around Cu1 and Cu1A. The wide network of CH  $\pi$  interactions and the  $\pi - \pi$  stacking interactions involving the phenyl, pyridyl and metal chelate rings effects the crystal packing. The thiolate bridging structure is further stabilized by the comparatively stronger  $\pi - \pi$  interactions between the centroids Cg(3) and Cg(9) consisting of Cu(1), S(1), Cu(1A), S(1A) and Cu(1A), N(1A), C(5A), C(6A),

N(2A) respectively, which is observed at a remarkably shorter distance of 2.7632 Å.

### 3.3.2.3. [CuL<sup>1</sup>NCS] (4)

A perspective view for CuL<sup>1</sup>NCS (4) with the atomic numbering scheme is given in Fig. 3.5. The crystal is developed into a triclinic lattice with P-1 symmetry and it reveals a distorted square planar N<sub>3</sub>S coordination sphere with the copper centre. The thiosemicarbazone ligand occupies three positions and the thiocyanate nitrogen, the fourth position of an approximate square plane. The C13 – S1 bond length of 1.675(15) Å in the ligand HL<sup>1</sup> is an evidence for the thione form in the solid state, which is shifted to 1.746(2) Å in the complex, which confirms the coordination *via* the thiolate sulfur in compound 4. The N2 – N3 bond length of 1.367(17) Å in the, uncomplexed thiosemicarbazone is found to remain unchanged in the complex whereas, the C13 – N3 bond length of 1.364(18) Å in HL<sup>1</sup> is shifted to 1.325(3) Å in compound 4. This is in support of the shifting of the thione form of the thiosemicarbazone to the thiol form during complexation. The ligand is deprotonated at N3 and the complex carries two five-membered chelate rings. The two planes through Cu1, N1, C5, C6, N2 and Cu1, N2, N3, C13, S1 show that the sets of atoms are almost coplanar, with a dihedral angle of 9.52°. This small deviation from coplanarity would certainly not hinder the delocalisation of electrons in the coordination sphere, and the stability of the complex is sustained. The distorted square planar structure is evidenced by the acute value displayed by the thiosemicarbazone bite angles, *viz.* N1 – Cu1 – N2 (80.40(7) Å) and N2 – Cu1 – S1 (84.43(6) Å) [30].

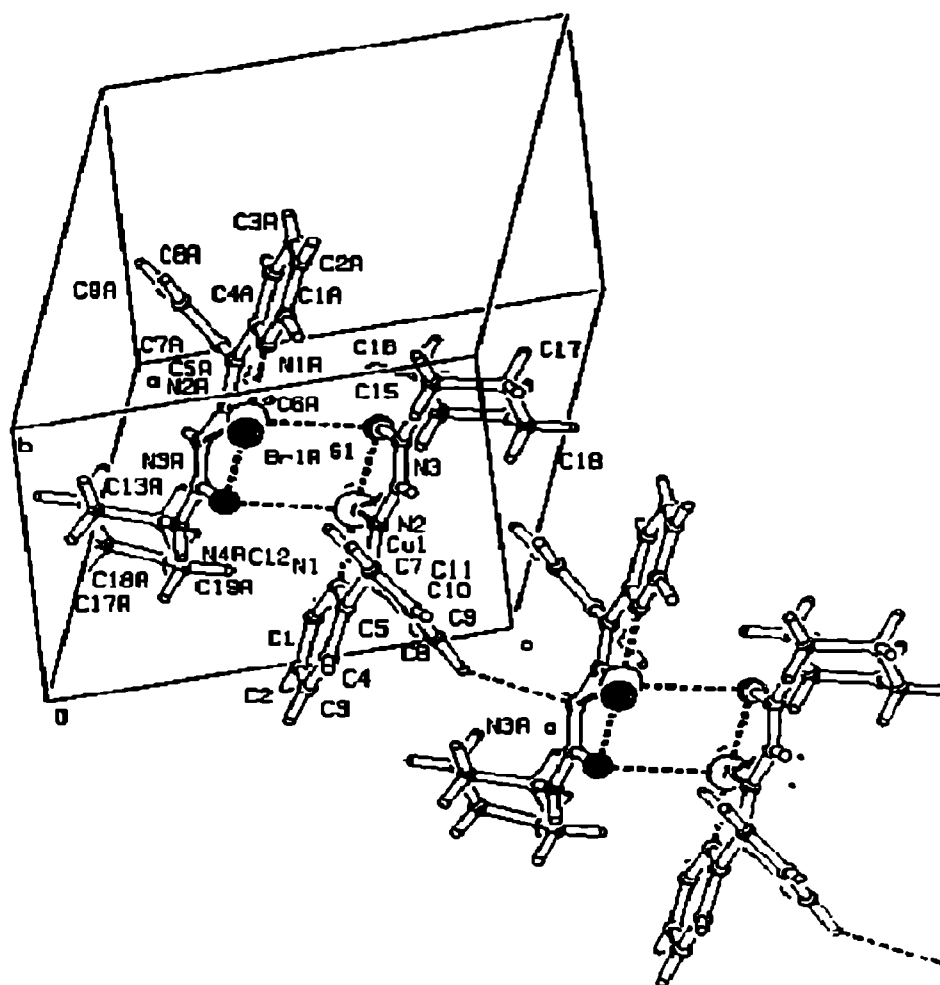


Fig 3.4. Close packing in compound 2

The bond angles of the trans donor atoms i.e., N1 – Cu1 – S1 ( $160.36^\circ$ ) and N5 – Cu1 – N2 ( $176.88(8)^\circ$ ) are  $\geq 160^\circ$  in **4**, which is consistent with the work on the copper(II) complexes of 2-benzoylpyridine *N*(4)-substituted thiosemicarbazones by West *et al* [31]. In the crystal lattice, the unit cell volume contains 2 molecules and is viewed down the 'a' axis. The adjacent molecules are packed in a zig-zag manner facilitated by the  $\pi$ - $\pi$ , CH –  $\pi$  and ring-metal interactions.

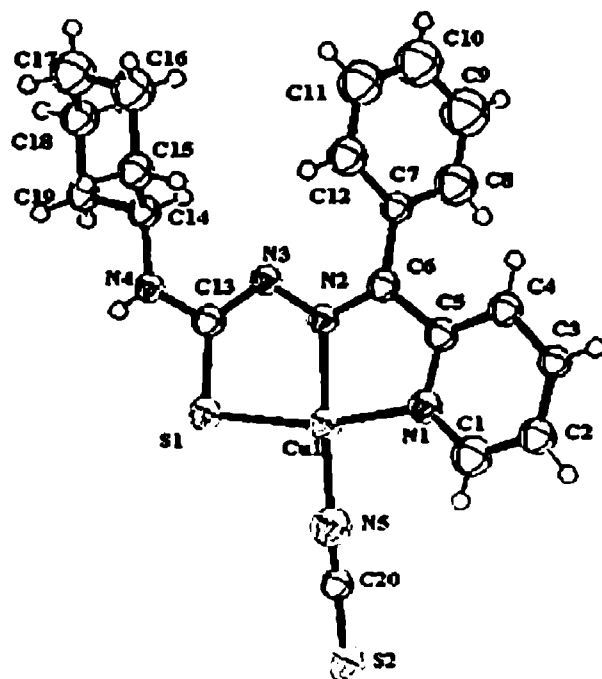


Fig.3.5. ORTEP diagram for  $\text{CuL}^1\text{NCS}$  (4), displacement ellipsoids are drawn at 50% probability level and hydrogen atoms are shown as small spheres of arbitrary radii.

It is also interesting to note that in all the three crystals, the torsion angle values and ring puckering analyses show that the cyclohexyl ring adopts a chair conformation. Atoms C14, C16, C17 and C19 constitute the best-fitting plane of the cyclohexyl ring, while the atoms C15 and C18 deviate by  $-0.6868$  and  $0.6475$  Å respectively, on either side of the plane.



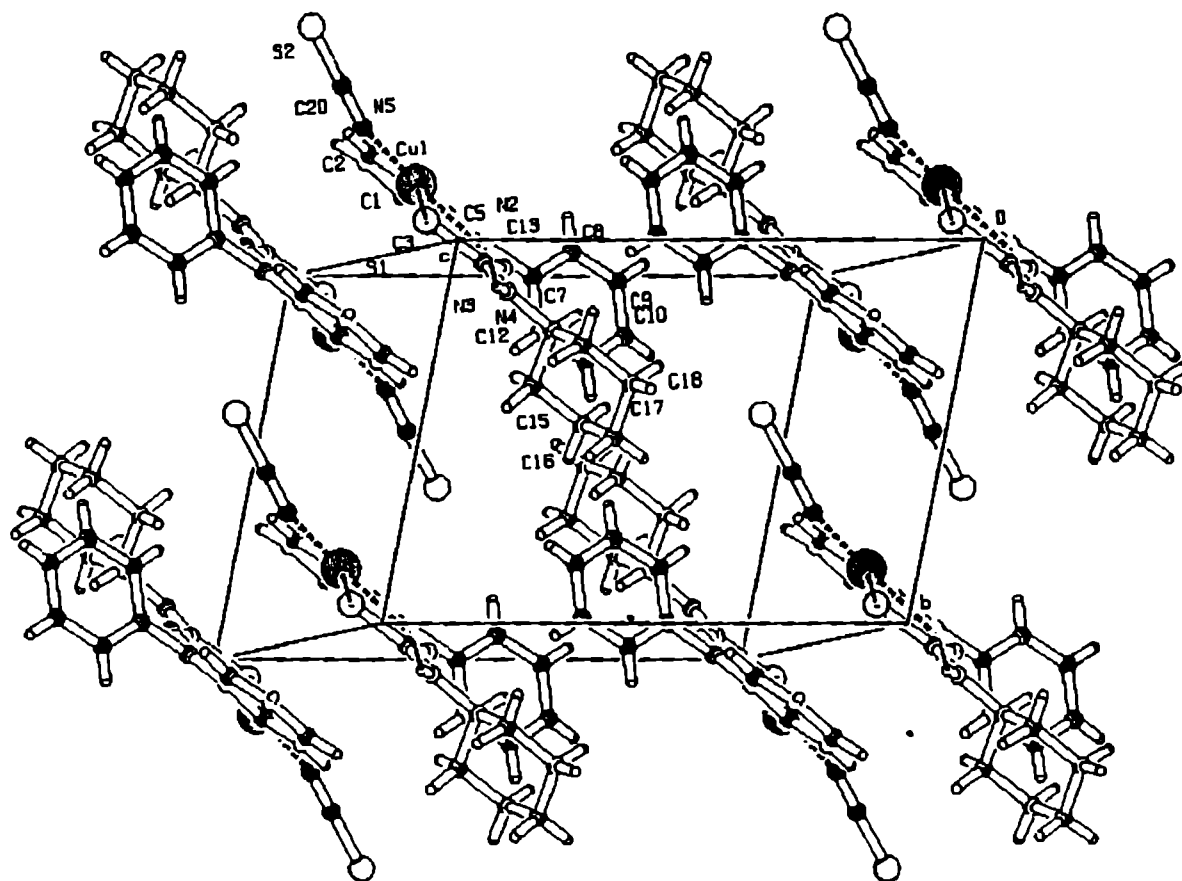


Fig.3.6. Close packing arrangement of [CuL<sup>1</sup>NCS]

Table 3.2 Crystal data and structural refinement for the complexes

Parameters	[CuL <sup>1</sup> Cl] (1)	[{CuL <sup>1</sup> Br} <sub>2</sub> ] (2)	[CuL <sup>1</sup> NCS] (4)
Empirical Formula	C <sub>19</sub> H <sub>21</sub> ClCuN <sub>4</sub> S	C <sub>19</sub> H <sub>21</sub> BrCuN <sub>4</sub> S	C <sub>20</sub> H <sub>21</sub> CuN <sub>5</sub> S <sub>2</sub>
Formula weight, M	436.45	481.92	459.08
Temperature, T (K)	293(2)	293(2)	293(2)
Crystal system	Monoclinic	Triclinic	Triclinic
Space group	P2 <sub>1</sub> /n	P1	P-1
a (Å)	13.170(3)	9.642(5)	8.679(5)
b (Å)	8.670(2)	10.714(6)	9.376(5)
c (Å)	35.445(9)	10.899(6)	13.280(7)
α (°)	90.00	72.746(9)	80.761(9)
β (°)	98.00	76.413(9)	81.187(9)
γ (°)	90.00	70.887(8)	76.876(9)
Volume V (Å <sup>3</sup> )	4008.1(18)	1004.1(9)	1031.1(10)
Calculated density, ρ (Mg m <sup>-3</sup> )	1.446	1.5940	13.4787
Absorption coefficient, μ(mm <sup>-1</sup> )	1.337	3.191	1.277
F(000)	1800	488	474
Crystal size (mm)	0.40x0.35x0.30	0.40x0.35x0.20	0.45x0.40x0.35
θ Range for data collection	2.82 - 26	2.5 - 29.59	2.43 - 28.08
Limiting Indices	-16 ≤ h ≤ 16, -10 ≤ k ≤ 10, -43 ≤ l ≤ 43	-13 ≤ h ≤ 13, -14 ≤ k ≤ 14, -14 ≤ l ≤ 14	-11 ≤ h ≤ 11, -12 ≤ k ≤ 12, -17 ≤ l ≤ 17
Reflections collected	29574	12475	12440
Unique Reflections	7862	9644	4951
	[R <sub>int</sub> = 0.0498]	[R <sub>int</sub> = 0.0227]	[R <sub>int</sub> = 0.0220]
Completeness to θ	26.00 (99.6 %)	29.59 (91.1 %)	28.08 (98.5 %)
Absorption correction	None	None	None
Max. and min. transmission	0.6898 and 0.6168	0.5678 and 0.3617	None
Data / restraints / parameters	7862/0/ 637	9644/ 3/ 529	4951/0/ 337
Goodness-of-fit on F <sup>2</sup>	1.091	0.955	1.050
Final R indices	R <sub>1</sub> = 0.0555,	R <sub>1</sub> = 0.0362,	R <sub>1</sub> = 0.0406,
[I > 2σ (I)]	wR <sub>2</sub> = 0.1041	wR <sub>2</sub> = 0.0899	wR <sub>2</sub> = 0.0926

Table 3.3 Comparison of selected bond lengths (Å) and bond angles (°) of HL<sup>1</sup>, [CuL<sup>1</sup>Cl],  
[CuL<sup>1</sup>Br]<sub>2</sub>, and [CuL<sup>1</sup>NCS].

	HL <sup>1</sup>	[CuL <sup>1</sup> Cl]	[CuL <sup>1</sup> Br] <sub>2</sub>	[CuL <sup>1</sup> NCS]
C(6)-N(2)	1.290 (18)	1.309 (3)	1.306 (7)	1.299 (3)
N(2)-N(3)	1.367(17)	1.365 (3)	1.377 (7)	1.366 (2)
N(3)-C(13)	1.364(18)	1.323 (14)	1.327 (7)	1.325 (3)
S(1)-C(13)	1.675(15)	1.746 (3)	1.719 (6)	1.746 (2)
C(13)-N(4)	1.328(19)	1.334 (4)	1.348 (8)	1.339 (3)
Cu(1)-S(1)		2.245 (10)	2.289 (2)	2.261 (12)
Cu(1)-N(1)		2.036 (2)	2.028 (5)	2.016 (2)
Cu(1)-N(2)		1.966 (2)	1.978 (4)	1.962 (19)
Cu(1)-Cl(1)		2.2099 (10)		
Cu(1)-N(5)				1.924 (2)
Cu(1)-Br(1)			2.371 (12)	
Cu(1A)-S(1A)			2.266	
Cu(1A)-S(1)			2.937	
N(1)-C(5)-C(6)	118.25(13)	115.0 (2)	114.70 (19)	114.60 (5)
N(2)-N(3)-C(13)	118.46(12)	111.6 (2)	111.45 (17)	112.20 (4)
N(3)-C(13)-S(1)	118.87(11)	124.9 (2)	125.62 (16)	126.20 (5)
N(1)-Cu(1)-Cl(1)		98.15 (7)		
N(1)-Cu(1)-N(2)		80.31 (9)	79.7 (2)	80.40 (7)
N(2)-Cu(1)-S(1)		84.21 (7)	84.55 (16)	84.43 (6)
S(1)-Cu(1)-Cl(1)		97.22 (4)		
N(2)-Cu(1)-Cl(1)		164.00 (8)		
N(1)-Cu(1)-Br(1)			99.11 (13)	
S(1)-Cu(1)-Br(1)			96.24 (6)	
N(2)-Cu(1)-Br(1)			164.20 (12)	
Cu(1)-S(1)-Cu(1A)			84.11	
Cu(1A)-S(1A)-Cu(1)			84.47	
S(1)-Cu(1A)-S(1A)			95.56	
S(1A)-Cu(1)-S(1)			95.89	
N(1)-Cu(1)-N(5)				97.44 (9)

Table 3.4 Interaction parameters of compound I

$\pi$ ---- $\pi$ interactions			
Cg(I)-Res(I)----Cg(J)	Cg-Cg(Å)	$\alpha$ (°)	$\beta$ (°)
Cg(2)-[2]----Cg(4) <sup>a</sup>	3.4400	13.87	10.39
Cg(2)-[2]----Cg(8) <sup>a</sup>	4.0394	18.57	24.52
Cg(4)-[1]----Cg(2) <sup>a</sup>	3.4400	13.87	16.73
Cg(4)-[1]----Cg(5) <sup>a</sup>	3.4689	12.57	16.13
Cg(5)-[2]----Cg(4) <sup>a</sup>	3.4689	12.57	12.94
Cg(5)-[2]----Cg(8) <sup>a</sup>	3.9143	17.03	22.56
Cg(6)-[2]----Cg(8) <sup>a</sup>	3.5211	12.73	3.09
Cg(8)-[1]----Cg(6) <sup>a</sup>	3.5211	12.73	12.69
Equivalent position codes: a = x, y, z		Cg(2)=Cu(1B),S(1B), C(13B), N(3B), Cg(4)=Cu(1A), N(1A), C(5A), C(6A), N(2A) Cg(5)=Cu(1B), S(1B), C(13B), N(3B), N(2B) Cg(6)=Cu(1B), N(1B), C(5B), C(6B), N(2B) Cg(8)=N(1A), C(1A), C(2A), C(3A), C(4A),C(5A)	
<i>CH</i> ---- $\pi$ interactions			
X-H(I)----Cg(J)	H.Cg(Å)	X-H.Cg (°)	X.Cg (Å)
C(18A)-H(9)[1]----Cg(8) <sup>b</sup>	2.9077	138.95	3.6433
C(19A)-H(12)[1]----Cg(4) <sup>b</sup>	3.1561	112.93	3.6846
C(8A)-H(1)[1]----Cg(17) <sup>c</sup>	3.1890	141.19	3.9619
C(2A)- H(14)[1]----Cg(9) <sup>c</sup>	3.3292	97.35	3.5457
N(4B)- H(22)[2]----Cg(3) <sup>c</sup>	3.2012	101.26	3.5639
Equivalent position code: <sup>b</sup> = 1-x, -y, -z; <sup>c</sup> = x, y, z			
Cg=Centroid, $\alpha$ =dihedral angles between planes I & J, $\beta$ = angle Cg(I)-Cg(J)			

Table 3.5 Interaction parameters of compound 2

$\pi$ --- $\pi$ interactions			
Cg(I)-Res(I)---Cg(J)	Cg-Cg(Å)	$\alpha$ (°)	$\beta$ (°)
Cg(3)-[1]---Cg(7) <sup>a</sup>	2.7784	88.94	59.71
Cg(3)-[1]---Cg(9) <sup>a</sup>	2.7841	88.54	59.52
Cg(4)-[1]---Cg(5) <sup>a</sup>	3.8763	0.26	41.39
Cg(4)-[1]---Cg(8) <sup>a</sup>	3.9070	1.44	42.37
Cg(5)-[1]---Cg(4) <sup>a</sup>	3.8763	0.26	41.13
Cg(6)-[1]---Cg(5) <sup>a</sup>	3.9053	1.36	41.97
Cg(6)-[1]---Cg(8) <sup>a</sup>	3.9613	0.28	43.10
Equivalent position codes: a = x, y, z		Cg(3)=Cu(1), S(5), Cu(3), S(6) Cg(4)=Cu(1), S(6), C(6), N(5) Cg(5)=Cu(3), S(5), C(8), N(7) Cg(6)=Cu(1), S(6), C(6), N(5), N(2) Cg(7)=Cu(1), N(1), C(12), C(9), N(2) Cg(8)=Cu(3), S(5), C(8), N(7), N(4) Cg(9)=Cu(3), N(3), C(11), C(13), N(4)	
$C/H$ --- $\pi$ interactions			
X-H(I)---Cg(J)	H..Cg(Å)	X-H..Cg (°)	X..Cg(Å)
C(8)-H(8)[1]---Cg(17) <sup>b</sup>	3.2529	120.46	3.6855
C(15)H(15)[1]---Cg(4) <sup>c</sup>	3.3790	125.51	4.0206
C(16)-H(6)[1]---Cg(14) <sup>c</sup>	3.3580	96.24	3.5951
C(18A)- H(18C)[1]---Cg(15) <sup>d</sup>	3.0601	119.70	3.6395
C(18A)- H(18D)[1]---Cg(9) <sup>d</sup>	3.3762	138.60	4.1532
Equivalent position code: <sup>b</sup> = -1+x, y, 1+z; <sup>c</sup> = x, y, -1+z; <sup>d</sup> = x, -1+y, z			
Cg=Centroid, $\alpha$ = dihedral angles between planes I & J, $\beta$ = angle Cg(I)-Cg(J)			

Table 3.6 Interaction parameters of compound 4

$\pi$ --- $\pi$ interactions			
Cg(I)-Res(I)---Cg(J)	Cg-Cg(Å)	$\alpha$ (°)	$\beta$ (°)
Cg(2)-[1]---Cg(4) <sup>a</sup>	4.1225	12.24	33.79
Cg(3)-[1]---Cg(2) <sup>a</sup>	4.3860	2.78	32.52
Cg(3)-[1]---Cg(4) <sup>a</sup>	4.24	9.52	34.7
Cg(4)-[1]---Cg(2) <sup>a</sup>	4.1225	12.24	26.48
Equivalent position codes: a = -1-x, -y, 2-z		Cg(2)=Cu(1), S(2), C(2), N(5) Cg(3)=Cu(1), S(2), C(2), N(5), N(3) Cg(4)=Cu(1), N(1), C(7), C(3), N(3)	
$CH$ --- $\pi$ interactions			
X-H(I)---Cg(J)	H..Cg(Å)	X-H..Cg (°)	X..Cg(Å)
C(17)-H(4)[1]---Cg(6) <sup>b</sup>	2.9584	149.15	3.8027
C(17)-H(20)[1]---Cg(2) <sup>c</sup>	3.2439	118.38	3.7250
C(16)-H(20)[1]---Cg(3) <sup>c</sup>	3.3120	123.76	3.8511
Equivalent position code: <sup>b</sup> = -1+x, 1+y, z; <sup>c</sup> = 1+x, y, z			
Cg=Centroid, $\alpha$ =dihedral angles between planes I & J, $\beta$ = angle Cg(I)-Cg(J)			

### 3.3.3. IR spectra

The tentative assignments of the significant IR spectral bands of III<sup>1</sup> and its copper(II) complexes are presented in Table 3. 7. The  $\nu(C=N)$  band of the thiosemicarbazone at  $1582\text{ cm}^{-1}$  is found to be shifted to lower energies in the

spectra of the complexes indicating coordination *via* the azomethine nitrogen [31]. This is confirmed by the bands in the range 440 - 465  $\text{cm}^{-1}$ , which have been assigned to the  $\nu(\text{Cu-N})$  band [32]. The  $\nu(\text{N-N})$  of the thiosemicarbazone is found at 1118  $\text{cm}^{-1}$ . The increase in the frequency of this band in the spectra of the complexes, due to the increase in the bond strength, again confirms the coordination *via* the azomethine nitrogen. In all the complexes another strong band is found at *ca.* 1592  $\text{cm}^{-1}$  which may be due to the newly formed C=N bond.

Spectra of compounds in which C=S group is attached to a nitrogen atom contains several bands in the region 1563-700  $\text{cm}^{-1}$  which are due to the vibrations involving interaction between C=S and C-N stretching [33]. In the spectrum of III<sup>1</sup>, a strong band at 833  $\text{cm}^{-1}$  is assigned to  $\nu(\text{C=S})$ , whereas in the complexes, this band is found to be shifted to lower frequencies in the range 783-795  $\text{cm}^{-1}$ . Another band observed in the spectrum of III<sup>1</sup> at 1370  $\text{cm}^{-1}$  is found to be shifted to lower frequencies in the range 1279-1339  $\text{cm}^{-1}$  in the spectra of complexes. This negative shift of the  $\nu(\text{C=S})$  bands in the complexes is indicated by the coordination *via* the thiolate sulfur atom. The strong bands observed in the region 340 - 353  $\text{cm}^{-1}$  have been assigned to the  $\nu(\text{Cu-S})$  bond. In all the copper complexes a strong band is observed in the region 265 -282  $\text{cm}^{-1}$ , which is consistent with the  $\nu(\text{Cu-N})$  of pyridine as suggested by Clark and Williams [34]. Based on the above spectral evidences, it is confirmed that the ligand is coordinated to the Cu(II) ion as a tridentate anion, coordinating *via* the azomethine nitrogen, pyridyl nitrogen and thiolate sulfur.

In the chloro complex, a strong band observed at 324  $\text{cm}^{-1}$  has been assigned to the  $\nu(\text{Cu-Cl})$  band. The  $\nu(\text{Cu-Br})$  frequency is observed at 222  $\text{cm}^{-1}$  in the bromo complex [35]. The  $\nu(\text{Cu-Br})$  and  $\nu(\text{Cu-Cl})$  frequencies are consistent with the terminal chloro and bromo ligands [18].

In the IR spectrum of the complex containing nitrate as gegenion, the bands observed at  $268\text{ cm}^{-1}$  can be assigned to  $\nu(\text{Cu-ONO}_2)$  in consistence with the bands at  $253\text{-}280\text{ cm}^{-1}$  reported earlier for  $\text{Cu-ONO}_2$  in metal complexes [36]. Moreover, in the nitrate complex of III, the two strong bands at  $1280$  and  $1410\text{ cm}^{-1}$  corresponding to the  $\nu_1$  and  $\nu_4$  modes of the nitrate group with a separation of  $130\text{ cm}^{-1}$  indicate the presence of a terminally bonded monodentate nitrate group [18]. In the azido complex, the strong band observed at  $2037\text{ cm}^{-1}$  is assigned to  $\nu_1$  of the azide group indicative of azide coordination [37]. In the thiocyanato complex, the very strong bands observed at  $2093\text{ cm}^{-1}$  correspond to  $\nu(\text{C}\equiv\text{N})$ . The bands observed at  $783$ ,  $481$ , and  $461\text{ cm}^{-1}$  are assigned to  $\nu(\text{C}=\text{S})$ ,  $\delta(\text{NCS})$  and  $\nu(\text{Cu-N})$  respectively. These facts indicate that the thiocyanate group is N-coordinated to copper [38].

In the sulfato complex, the fourth coordinate position is occupied by the oxygen atom of the sulfate ion that belongs to the high symmetry point group  $T_d$ . The symmetry of the sulfate is reduced to the  $C_{2v}$  point group, when it functions as a bidentate ligand in the complex. The IR spectrum of compound **6** contains strong bands at  $1002$ ,  $1117$ ,  $1204\text{ cm}^{-1}$  due to  $\nu_3$ ,  $960\text{ cm}^{-1}$  due to  $\nu_1$ ,  $465\text{ cm}^{-1}$  due to  $\nu_2$  and these can be assigned to the bridging bidentate sulfato group [18]. This type of bidentate bridging by the sulfato group is proved by an earlier single crystal X-ray diffraction study for a copper(II) complex of a substituted thiosemicarbazone derived from di-2-pyridyl ketone [39]. According to Stefov et al [40] coordinated water should exhibit frequencies at  $825$ ,  $575$  and  $500\text{ cm}^{-1}$ . The absence of spectral bands in these regions in the spectra of complexes **5** and **6** indicates that the water molecules in these complexes are not coordinated but are present as lattice water.



Table 3.7 IR spectral assignments ( $\text{cm}^{-1}$ ) of HL<sup>1</sup> and the Cu(II) complexes

Compound	$\nu(\text{C}=\text{N})$	$\nu(\text{N}-\text{N})$	$\nu(\text{C}-\text{S})$	$\rho$ (py)	$\nu(\text{Cu}-\text{N})$	$\nu(\text{Cu}-\text{Npy})$	$\nu(\text{Cu}-\text{S})$	$\nu(\text{Cu}-\text{X})$
HL <sup>1</sup>	1582m	1118s	1370m, 833s	607w	----	----	----	----
[CuL <sup>1</sup> Cl] (1)	1488s	1150m	1337m, 785m	642w	460m	280 s	349m	324s
[(CuL <sup>1</sup> Br) <sub>2</sub> ] (2)	1544s	1150m	1336s, 794m	644m	443s	282s	353s	222s
[CuL <sup>1</sup> NO <sub>3</sub> ] (3)	1543w	1138m	1279s, 786w	646m	459m	275s	352s	268s
[CuL <sup>1</sup> NCS] (4)	1542s	1138s	1331s, 783w	642m	461s	266m	350s	350s
[CuL <sup>1</sup> N <sub>3</sub> ].3H <sub>2</sub> O (5)	1540m	1131	1324m, 788s	644s	464s	278m	351 w	--
[Cu <sub>2</sub> (L <sup>1</sup> ) <sub>2</sub> SO <sub>4</sub> ].2H <sub>2</sub> O (6)	1544m	1130s	1332m, 789m	641m	463s	280s	352s	397s

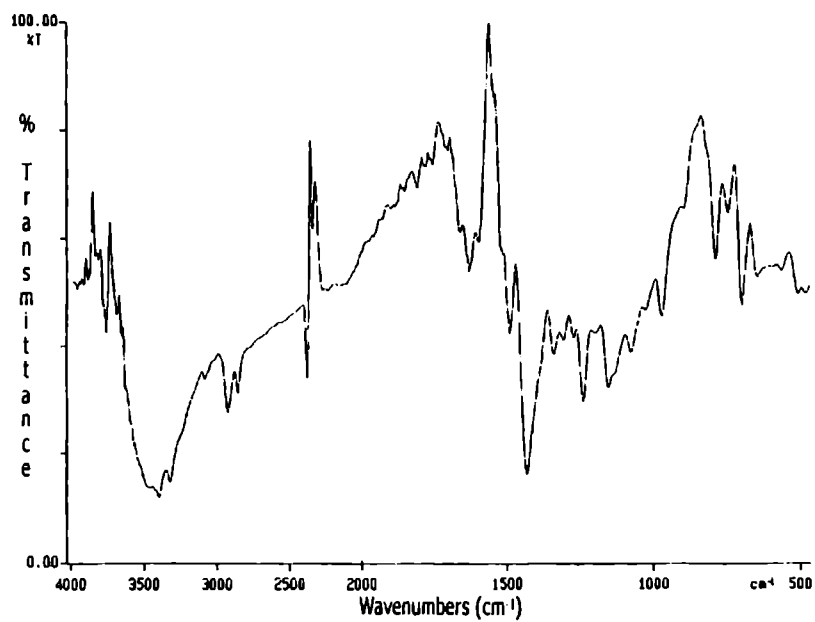


Fig.3.7. IR spectrum of [CuL'Cl]

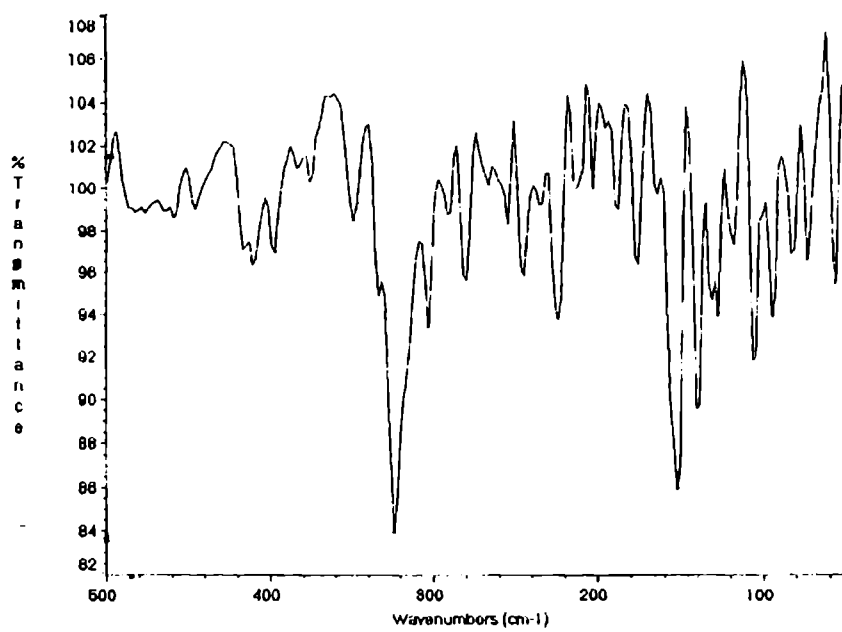
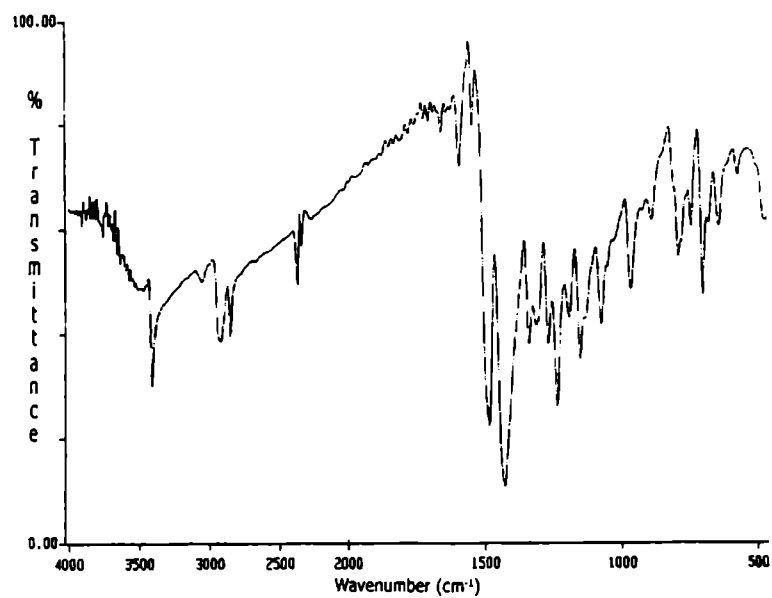
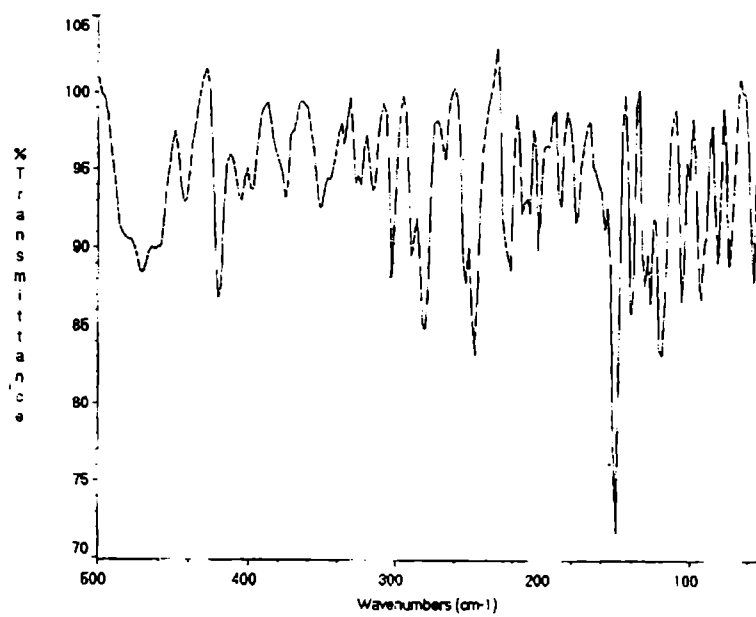
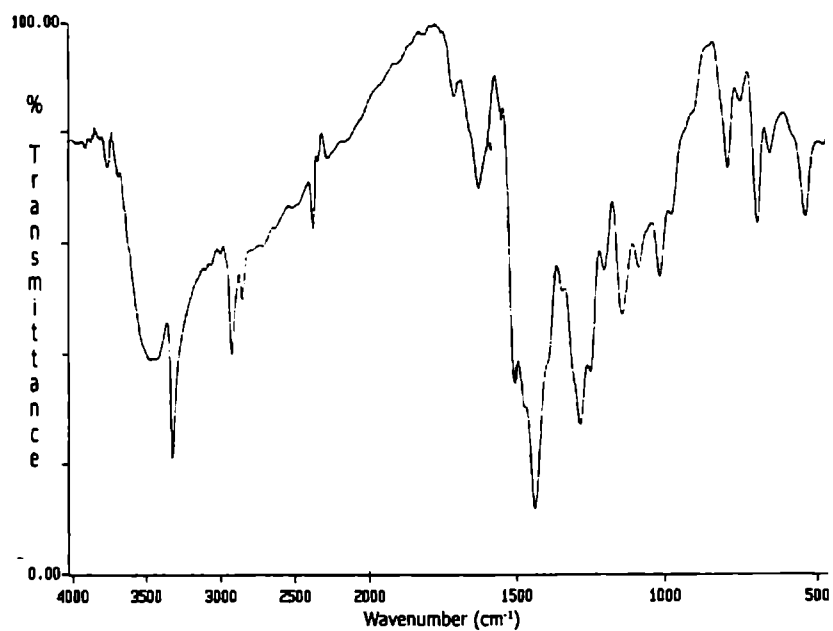
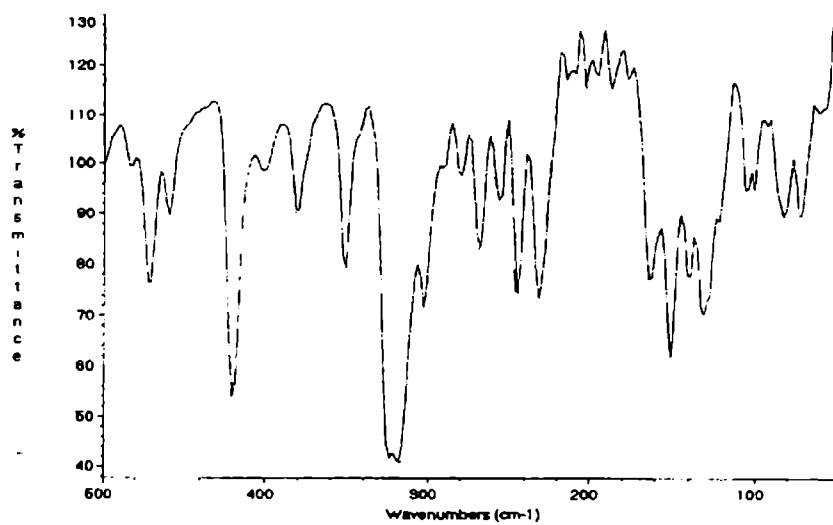
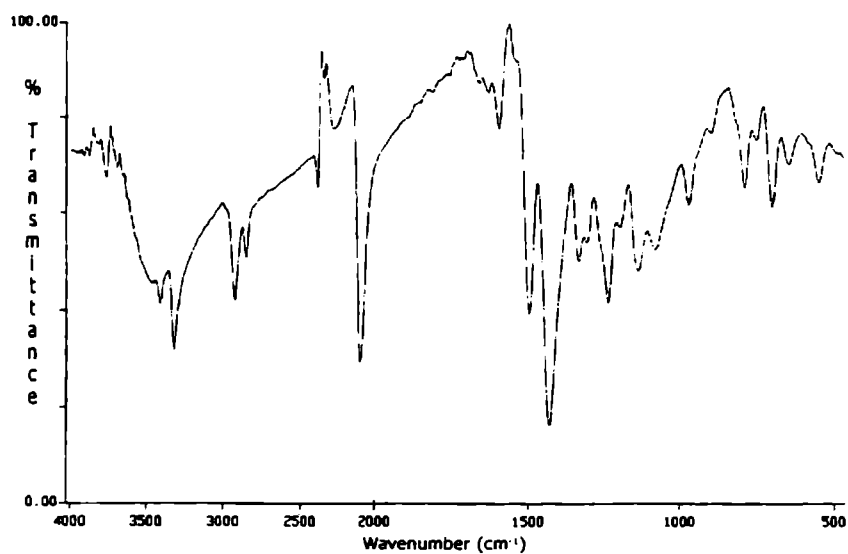
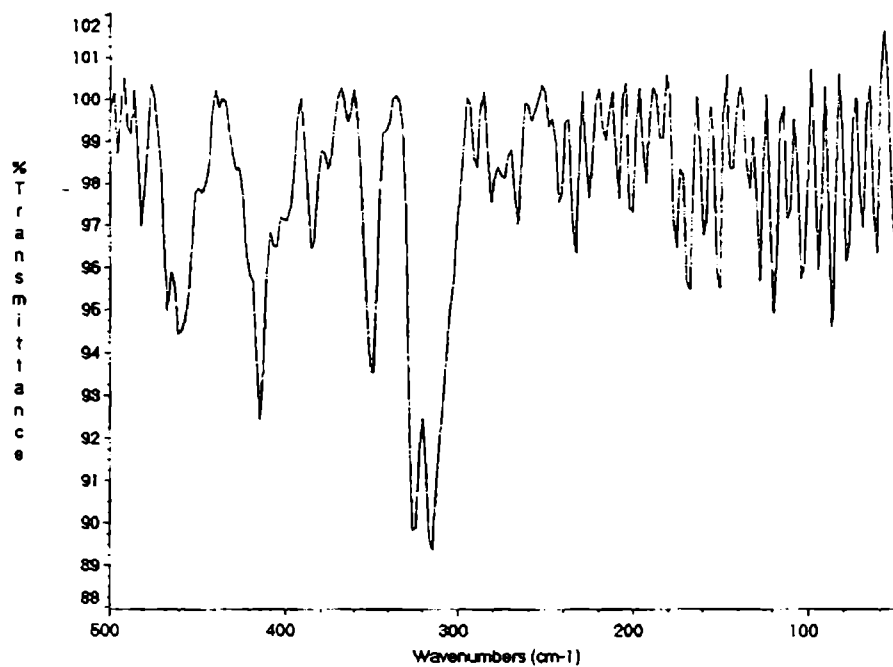
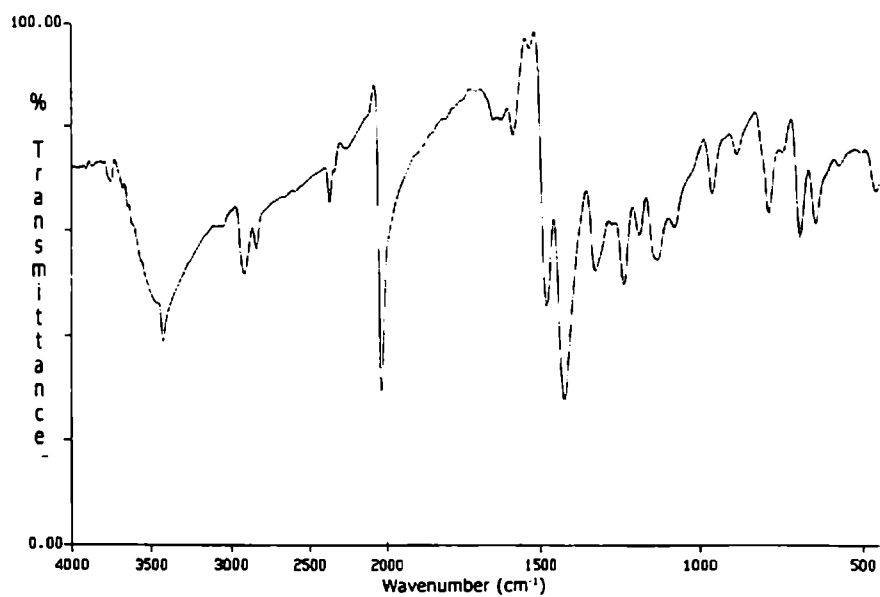
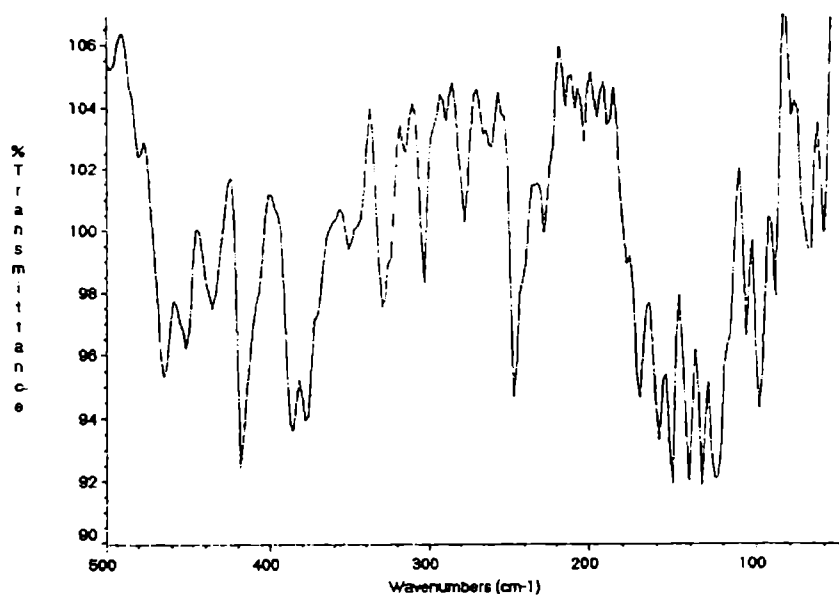


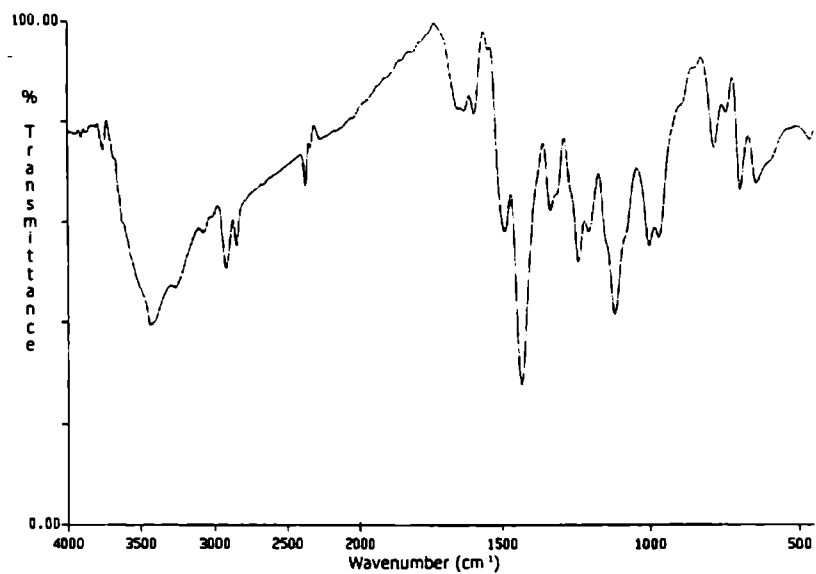
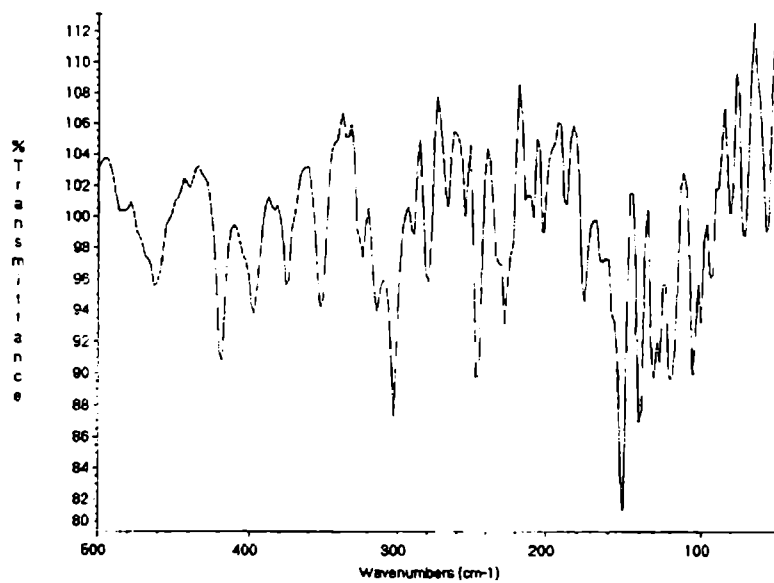
Fig.3.8. Far IR spectrum of [CuL'Cl]

Fig.3.9. IR spectrum of  $[CuLBr_2]$ Fig.3.10. Far IR spectrum of  $[CuLBr_2]$

Fig.3.11. IR spectrum of  $[\text{CuL}^1\text{NO}_3]$ Fig.3.12. Far IR spectrum of  $[\text{CuL}^1\text{NO}_3]$

Fig.3.13. IR spectrum of [CuL<sup>1</sup>NCS]Fig.3.14. Far IR spectrum of [CuL<sup>1</sup>NCS]

Fig.3.15.IR spectrum of  $[\text{CuL}^1\text{N}_3 \cdot 3\text{H}_2\text{O}]$ Fig.3.16. Far IR spectrum of  $[\text{CuL}^1\text{N}_3 \cdot 3\text{H}_2\text{O}]$

Fig.3.17. IR spectrum of  $[\text{Cu}^2(\text{L}^1)_2\text{SO}_4 \cdot 2\text{H}_2\text{O}]$ Fig.3.18. Far IR spectrum of  $[\text{Cu}^2(\text{L}^1)_2\text{SO}_4 \cdot 2\text{H}_2\text{O}]$

### 3.3.4. Electronic spectra

The variety of colors among transition metal complexes arises from the electronic transition between energy levels whose spacing corresponds to the wavelengths available in visible light. In complexes, these transitions are frequently referred to as *d-d* transitions because they involve the molecular orbitals that are mainly metal *d* in character [41]. Since this spacing depends on factors such as the geometry of the complex, the nature of the ligands present, and the oxidation state of the central metal atom, the electronic spectra of complexes can provide valuable information relating to bonding and structure [42].

Obviously, the colors produced are related to the magnitude of the spacing between the energy levels. Charge transfer transitions are transitions in which an electron is transferred from one atom or group in the molecule to another atom or group. Such transitions are of high intensity and usually occur at the ultraviolet or the near ultraviolet i.e. at the high-energy end of the visible spectrum. Since a charge transfer transition originates from the redox character of the metal ion and the ligand, it is of two distinct types, namely ligand to metal and metal to ligand [43].

Virtually all the Cu(II) complexes are blue or green. The blue or green colors are due to the absorption of radiations in the 600 to 900 nm region of the spectrum. The energies of the electronic transitions for the thiosemicarbazones and their Cu(II) complexes (solid state and DMF solution) are listed in Table 3.8. The solid-state electronic spectrum of the thiosemicarbazone HL<sup>1</sup> consists of a broad band at 348 nm which is the  $n \rightarrow \pi^*$  band of thioamide function. Another  $n \rightarrow \pi^*$  band of the pyridine ring is present at 288 nm region [13]. The band observed at 259 nm in the spectrum of HL<sup>1</sup> is assigned to  $\pi \rightarrow \pi^*$  transition. The  $n \rightarrow \pi^*$  transition observed at 348 nm in the solid state spectra of the thiosemicarbazone



moiety is shifted in energy, in solution, which is probably due to the hydrogen bonding taking place between the thiosemicarbazone moiety and the solvent molecules.

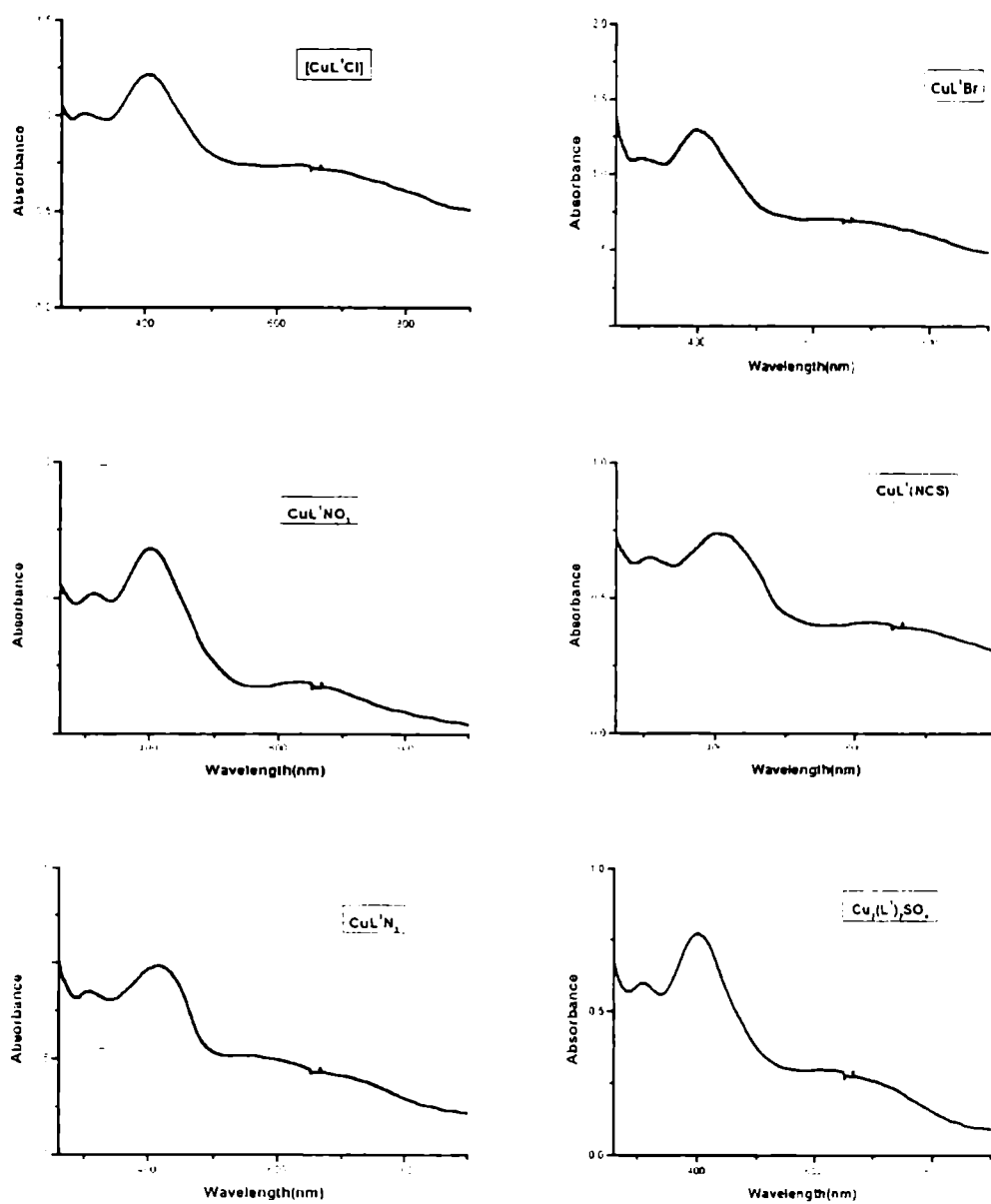


Fig.3.19. Electronic spectra of copper(II) complexes of HL<sup>3</sup>

Table 3.8 Electronic spectral assignments (nm) of Cu(II) complexes of HL<sup>1</sup>

Compound	Mode	$d \rightarrow d$	$L \rightarrow M$	$n \rightarrow \pi^*$	$\pi \rightarrow \pi^*$
HL <sup>1</sup>	Solid	---	---	348, 288sh	259
	DMF	---	---	340 (4.13), 280 (3.32)	256 (4.20)
[CuL <sup>1</sup> Cl] (1)	Solid	585	406.325sh	333,325sh	256
	DMF	573 (2.602)	438 (4.14)	362(3.83)	256 (4.41)
[CuL <sup>1</sup> Br] <sub>2</sub> (2)	Solid	582sh	410	310	267sh
	DMF	544 (2.51)	402 (3.21)	316 (4.12)	266sh (4.25)
[CuL <sup>1</sup> NO <sub>3</sub> ] (3)	Solid	590	402	314	260
	DMF	544 (2.51)	425(4.13)	309 (4.10)	271 (4.61)
[CuL <sup>1</sup> NCS] (4)	Solid	575	408	306	255sh
	DMF	569sh (2.61)	438 (3.81)	350 (4.34)	263 (4.06)
[CuL <sup>1</sup> N <sub>3</sub> ].3H <sub>2</sub> O (5)	Solid	577sh,	417	309	260sh
	DMF	584sh (2.34)	440 (4.35)	352 (4.21)	270sh (4.01)
[Cu <sub>2</sub> (L <sup>1</sup> ) <sub>2</sub> SO <sub>4</sub> ].2H <sub>2</sub> O (6)	Solid	565sh,	402	313	267sh
	DMF	580 (2.5)	415 (4.30)	308 (4.43)	265 (4.21)

log $\epsilon$  in parentheses (Lmol<sup>-1</sup>cm<sup>-1</sup>)

The molar absorptivities for  $n \rightarrow \pi^*$  transition are  $>10^4$ , which is consistent with the values of previously studied heterocyclic thiosemicarbazones [44].

In the solid state electronic spectra of the Cu(II) complexes, the  $n \rightarrow \pi^*$  band of the thiosemicarbazone is found to be blue shifted and appears as broad bands in

the range 302 to 333 nm. The  $\pi \rightarrow \pi^*$  band of the ligand is found to be remain unshifted in all the complexes. Another broad band observed in the range 400 – 418 nm are assigned as the S $\rightarrow$ Cu and Py $\rightarrow$ Cu charge –transfer bands [45]. In the compound **1**, the shoulder observed at 325 nm is assigned to the Cl $\rightarrow$ Cu charge-transfer transitions [46].

The solid-state spectra of all the Cu(II) complexes have a broad band in the region 600-565 nm. This is consistent with the broad structured band for square planar complexes in the range 769-500 nm [47].

### 3.3.5. *Electron paramagnetic resonance spectra*

The EPR spectra of the complexes in the polycrystalline state at 298 K and in different solutions at 298 and 77 K were recorded in the X band, using the 100 KHz field modulation;  $g$  factors were quoted relative to the standard marker TCNE ( $g = 2.0277$ ). The EPR parameters of the Cu(II) complexes are presented in Table 3.9. The EPR spectra of CuL<sup>1</sup>Cl and Cu<sub>2</sub>(L<sup>1</sup>)<sub>2</sub>SO<sub>4</sub> in the polycrystalline state at 298 K show only one broad signal each at  $g = 2.13$  and 2.07 respectively. Such isotropic spectra, consisting of a broad signal, and hence only one  $g$  value, arise from the extensive exchange coupling through misalignment of the local molecular axes between the different molecules in the unit cell (dipolar broadening) and enhanced spin lattice relaxation. These types of spectra unfortunately give no information on the electronic ground state of the Cu(II) ion present in the complexes. The spectra of [ $\{\text{CuL}^1\text{Br}\}_2$ ] and [CuL<sup>1</sup>NCS] are rhombic with three  $g$  values. The spectra of the other compounds show typical axial spectra with well-defined  $g_{\parallel}$  and  $g_{\perp}$  values. The spectra are often broad because of the broadening resulting from the fast spin-lattice relaxation time and exchange coupling. The geometric parameter  $G$ , which is a measure of the exchange interaction between the

copper centres in the polycrystalline compound, is calculated and the value of  $G$  is found to be in the range 2.3-3.9. In all the copper(II) complexes  $g_{\parallel} > g_{\perp} > 2.0023$  and  $G$  value less than 4.1 is consistent with a  $d_{x^2-y^2}$  ground state. EPR spectral studies are in agreement with the X-ray diffraction studies for the complexes **1**, **2** and **4** [48, 49].

EPR spectra of all the complexes in DMF solution,  $\text{CHCl}_3$  and in a 1:1 mixture of  $\text{CHCl}_3$  and toluene at 298 K were recorded. However we did not get clearly resolved spectra in any of the instances. The EPR spectra of the complexes in glassy state at 77 K were also recorded in different solvents. Spectra of all the compounds in chloroform-toluene mixture show well resolved four hyperfine lines which arises from the coupling of the Cu nuclei with ( $I=3/2$ ) with the odd electron. In the spectra of compounds **1** and **2**, three of the four hyperfine lines are clearly resolved in the parallel region. The fourth hyperfine line overlaps with the perpendicular component  $g_{\perp}$  and five superhyperfine lines are observed in the perpendicular component. The superhyperfine splitting in the high field arises from the coupling of the electron spin with the nuclear spin of the coordinating nitrogen atoms. The spectrum of compound **5**,  $[\text{CuL}^1\text{N}_3]$  show well resolved four hyperfine lines with seven superhyperfine lines. The seven superhyperfine lines in the perpendicular region arises from the coupling of the electron spin with the nuclear spin of the three nitrogen atoms i.e. one azomethine nitrogen, one nitrogen atom of the pyridine ring and one nitrogen from the azido anion coordinated to the copper(II).

The  $g_{\parallel}$  values of all the compounds are found to be almost the same, which indicate that the bonding is dominated by the thiosemicarbazone moiety. Kivelson and Nieman [50] have reported that  $g_{\parallel}$  values less than 2.3 indicate considerable covalent character to M-L bonds, while values greater than 2.3 indicate ionic character. The  $g_{\perp}$  values of all the compounds are found to be less than 2.3, which

indicate considerable covalent character to the M-L bond. The computer simulation of the frozen solution EPR spectra of the complexes have been performed and obtained a set of magnetic parameters. The EPR parameters  $g_{\parallel}$ ,  $g_{\perp}$ ,  $g_{av}$ ,  $A_{\parallel}(\text{Cu})$  and  $A_{\perp}(\text{Cu})$  and the energy values of the  $d-d$  transition were used to evaluate the bonding parameters  $\alpha^2$ ,  $\beta^2$  and  $\gamma^2$  which may be regarded as measures of the covalency of the in-plane  $\sigma$  bonds, in-plane  $\pi$  bonds, and out-of-plane  $\pi$  bonds respectively [51]. The value of in-plane sigma bonding parameter  $\alpha^2$  was calculated [43] using the expression:

$$\alpha^2 = -A_{\parallel} / 0.036 + (g_{\parallel} - 2.0023) + 3/7(g_{\perp} - 2.0023) + 0.04$$

The orbital reduction factors,  $K_{\parallel} = \alpha^2 \beta^2$  and  $K_{\perp} = \alpha^2 \gamma^2$  were calculated using the following expressions:

$$K_{\parallel}^2 = (g_{\parallel} - 2.0023) E_{d-d} / 8\lambda_0$$

$$K_{\perp}^2 = (g_{\perp} - 2.0023) E_{d-d} / 2\lambda_0$$

where  $\lambda_0$  is the spin-orbit coupling constant with a value of  $-828 \text{ cm}^{-1}$  for copper(II)  $d^9$  system. According to Hathaway [48], for pure  $\sigma$ -bonding,  $K_{\parallel} \approx K_{\perp} \approx 0.77$ , and for in-plane  $\pi$  bonding,  $K_{\parallel} < K_{\perp}$ ; while for out-of-plane  $\pi$  bonding,  $K_{\perp} < K_{\parallel}$ . In all the complexes, it is observed that  $K_{\parallel} < K_{\perp}$  which indicates the presence of significant in-plane  $\pi$  bonding. This is further confirmed by the bonding parameters  $\alpha^2$ ,  $\beta^2$  and  $\gamma^2$ , which are less than 1.0 expected of the purely ionic character of the bonds, and decreases with the increasing covalent nature of the bonding.

Table 3.9 EPR parameters of the Cu(II) complexes of HL<sup>1</sup>

Compound	Solid (298 K)		DMF solution (298 K)		CHCl <sub>3</sub> /toluene (77 K)			
	$g_1/g_2/g_3$	$g_{  }$	$g_{iso}$	$A_{iso}$	$g_1/g_2/g_3$	$g_{av}$	$A_{  }^a$	G
[CuL <sup>1</sup> Cl]	$g_{iso}$ 2.1257		2.0828	84.13	$g_{  }$ 2.1630 $g_{\perp}$ 2.0466	2.0854	166.39	3.63
[(CuL <sup>1</sup> Br) <sub>2</sub> ]	$g_1$ 2.0649 $g_2$ 2.0710 $g_3$ 2.1559	2.097	2.1330	79.0	$g_{  }$ 2.1270 $g_{\perp}$ 2.0340	2.065	176.17	3.93
[CuL <sup>1</sup> NO <sub>3</sub> ]	$g_{  }$ 2.1840 $g_{\perp}$ 2.0510	2.095	2.0807	79.46	$g_{  }$ 2.1923 $g_{\perp}$ 2.0532	2.0995	180.7	3.73
[CuL <sup>1</sup> NCS]	$g_1$ 2.0370 $g_2$ 2.054 $g_3$ 2.169	2.086	2.1200	88.80	$g_1$ 2.0367 $g_2$ 2.053 $g_3$ 2.1764	2.0887	168.26	4.14
[CuL <sup>1</sup> N <sub>3</sub> ].3H <sub>2</sub> O	$g_{  }$ 2.2064 $g_{\perp}$ 2.0993	2.152	2.1456	82.26	$g_{  }$ 2.1276 $g_{\perp}$ 2.0338	2.064	171.1	3.97
[Cu <sub>2</sub> (L <sup>1</sup> ) <sub>2</sub> SO <sub>4</sub> ].2H <sub>2</sub> O	$g_{iso}$ 2.063		2.1152	81.32	$g_{  }$ 2.1826 $g_{\perp}$ 2.0498	2.0940	169.8	3.84

<sup>a</sup>- A values are given in \*10<sup>-4</sup> cm<sup>-1</sup>

Therefore the evaluated values of  $\alpha^2$ ,  $\beta^2$  and  $\gamma^2$  are consistent with both the in-plane  $\sigma$  and in-plane  $\pi$  bonding [52].

The empirical factor  $f = g_{\parallel} / A_{\parallel} \text{ cm}^{-1}$  is an index of tetragonal distortion and its value may vary from 105 to 135 for small to extreme distortion in square planar complexes and that depends on the nature of the coordinated atom [53]. Recent studies have shown that biological activity is related to the geometry at the metal sites. Complexes with more tetrahedral distortion are reported to display higher activity [54].

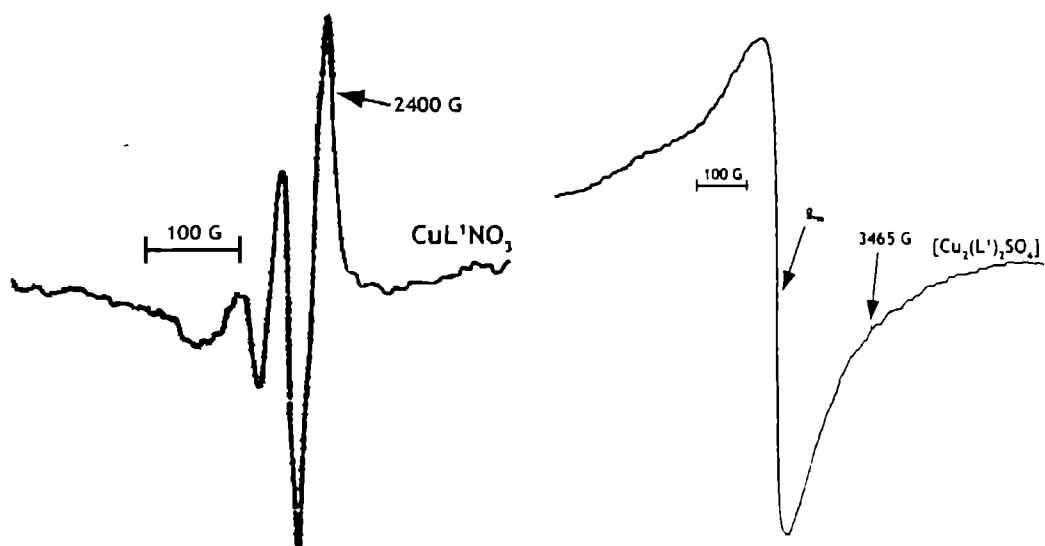


Fig. 3.20. EPR spectra of compounds 3 and 6 in DMF solution (298 K)

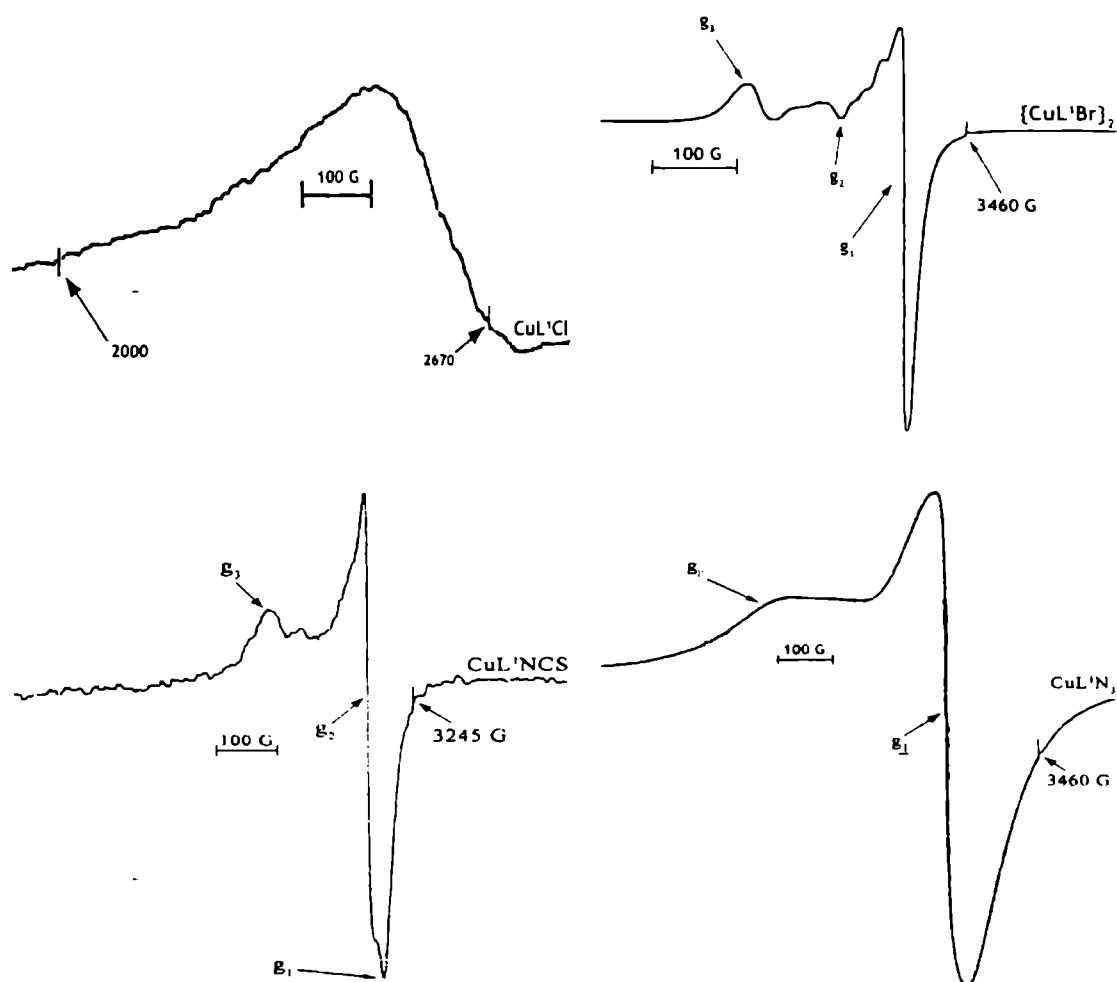


Fig. 3.21. EPR spectra of compounds 1, 2, 4 and 5 in polycrystalline state at 298 K.



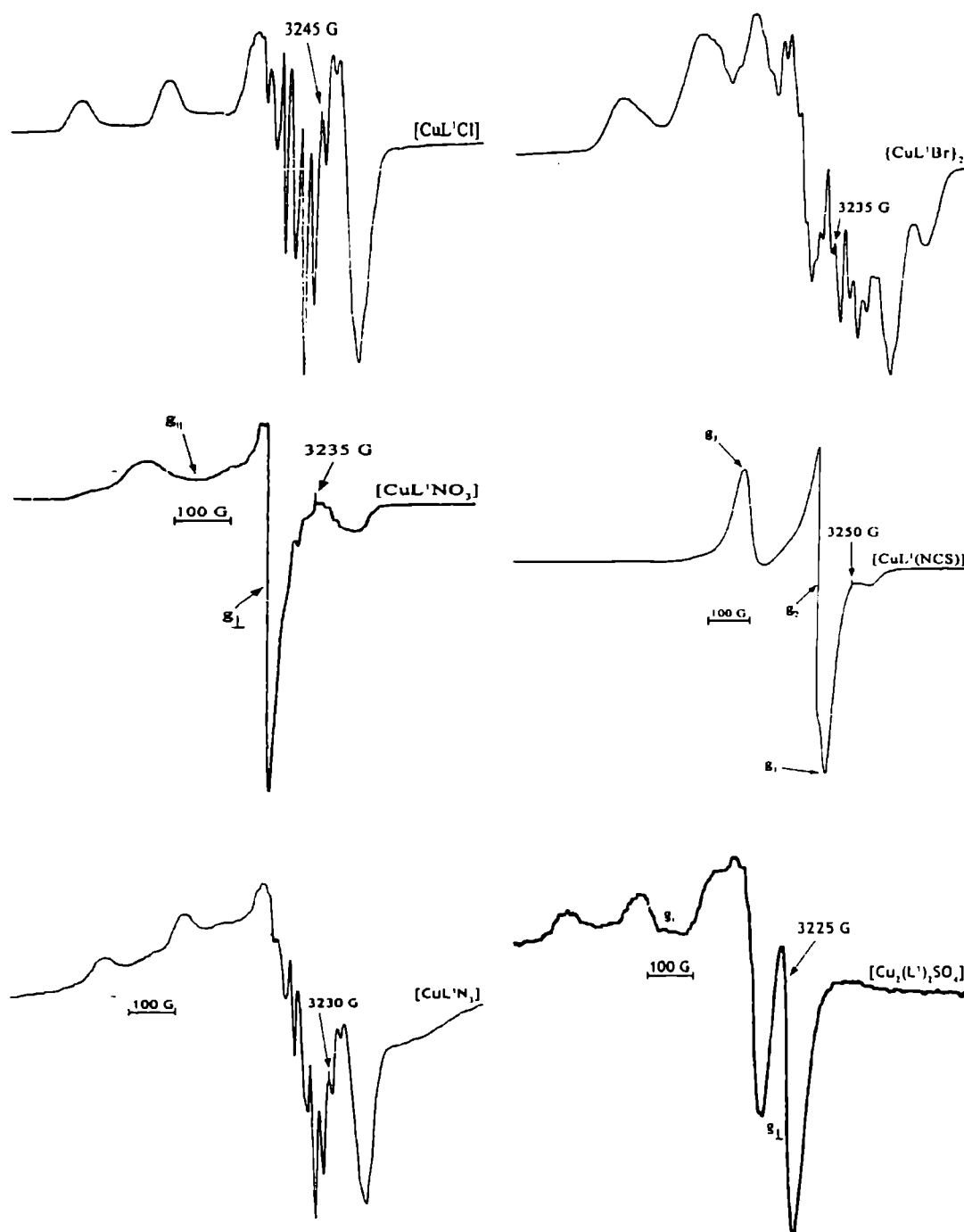


Fig.3.22. EPR spectra of compounds 1, 2, 3, 4, 5 and 6 in DMF (77 K)

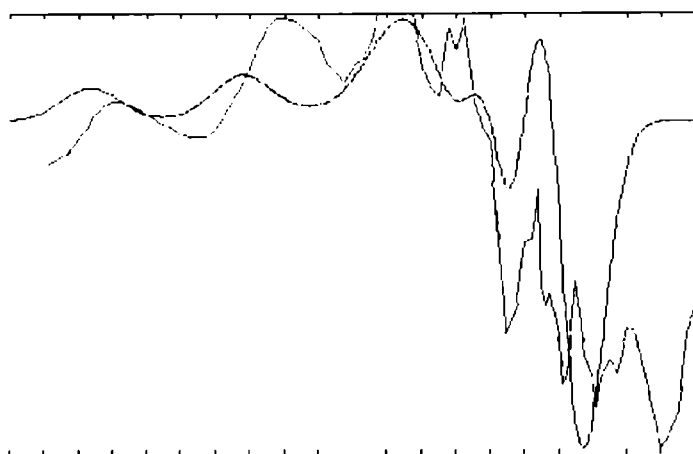


Fig. 3.23. Simulated best fits superimposed over the experimental spectra for compound 2  
Experimental -- (green) and simulated -- (pink)

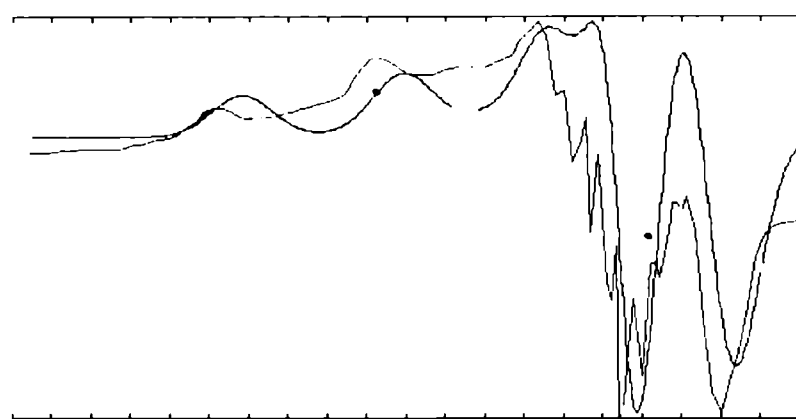


Fig. 3.24. . Simulated best fits superimposed over the experimental spectra for compound 5  
Experimental -- (green) and simulated -- (pink)

Table 3.10 Bonding parameters and orbital reduction parameters of the Cu(II) complexes of HL<sup>1</sup>

Compound	$\alpha^2$	$\beta^2$	$\gamma^2$	$K_{\parallel}$	$K_{\perp}$	$K_2$	$f$
[CuL <sup>1</sup> Cl] (1)	0.6810	0.9455	0.9862	0.6439	0.6716	0.3283	129.99
[{CuL <sup>1</sup> Br} <sub>2</sub> ] (2)	0.66676	0.8518	0.8590	0.5687	0.5735	0.3312	121.32
[CuL <sup>1</sup> NO <sub>3</sub> ] (3)	0.75371	0.9250	0.9575	0.6972	0.7217	0.3440	121.32
[CuL <sup>1</sup> NCS] (4)	0.7062	0.9226	0.9643	0.6516	0.6810	0.3581	129.30
[CuL <sup>1</sup> N <sub>3</sub> ].3H <sub>2</sub> O (5)	0.6538	0.8750	0.8782	0.5720	0.5742	0.2997	124.42
[Cu <sub>2</sub> (L <sup>1</sup> ) <sub>2</sub> SO <sub>4</sub> ].2H <sub>2</sub> O (6)	0.7165	0.9355	0.960	0.6658	0.6834	0.3394	128.54

### 3.4. Antimicrobial studies

The synthesized chemical ligands and the complexes were tested for their antimicrobial activity. Antimicrobial activity is the ability of a compound to inhibit the growth of a given microorganism. The antimicrobial agent may be either bacteriostatic or bactericidal.

The effectiveness of an antimicrobial agent in sensitivity testing is based on the size of the zones of inhibition. When the test substances are introduced on to a lawn of bacterial culture by disc diffusion method, if the bacteria are sensitive, there develops a zone of no growth around the disc, which is referred to as the zone of inhibition [54]. The diameter of the zone is measured to the nearest millimeter. Test substances which produce zones of inhibition of diameters 9 mm or more are regarded as positive, i.e. having antimicrobial activity; while those cases where the

diameter is below 9 mm, the bacteria are resistant to the sample tested and the sample is said to have no antimicrobial activity.

The microorganisms used as test organisms were bacteria isolated from clinical samples. Based on stain test microbial organisms can be divided into two types, Gram-positive and Gram-negative. The following five bacteria are used for our studies.

1. *Staphylococcus aureus*, 2. *Bacillus* sp (Gram Positive), 3. *Escherichia coli*
4. *Salmonella paratyphi* and 5. *Vibrio cholerae O1* (Gram Negative).

#### **3.4.1. Disc diffusion method**

The disc diffusion method was used for screening the antimicrobial property of the test samples. The compounds were dissolved in DMF to get a 1% solution and then diluted with the same solvent so that the concentration per disc would be 0.5 µg. Discs of 4 mm diameter were cut out of Whatman No.1 filter paper and autoclaved at 15 psi for 15 minutes. 5 µL each of the test chemical samples were dispensed on to the discs under aseptic conditions. The discs were dried at 30 °C and stored in sterile vials until further use.

In the disc diffusion method, a loopful of an overnight slant culture of the test organism was inoculated to 5 ml of sterile physiological saline to make a uniform suspension. This suspension culture was surface spread on a nutrient agar plate by swabbing it with a sterile cotton swab so as to get a uniform lawn culture. The discs with the test complexes prepared as mentioned above, were placed on the swabbed surfaces of the plates (4 discs per plate) using sterile forceps. The plates were incubated at 37 °C for 24 hours and then checked for zones of inhibition around the discs. The zone diameters were measured in millimeters.

Table 3.11 The antimicrobial activity of the complexes using the disc diffusion method

Compound	Microbial activity inhibition zone				
	<i>Bacillus</i> <i>sp</i>	<i>Staphylococcus</i> <i>aureus</i>	<i>Vibrio</i> <i>cholera</i> O1	<i>Escherichia</i> <i>coli</i>	<i>Salmonella</i> <i>paratyphi</i>
HL <sup>1</sup>	--	--	--	--	--
[CuL <sup>1</sup> Cl] (1)	+9 mm	+ 9 mm	+ 11 mm	--	--
[{CuL <sup>1</sup> Br} <sub>2</sub> ] (2)	--	--	+ 10 mm	--	--
[CuL <sup>1</sup> NO <sub>3</sub> ] (3)	+11 mm	+10 mm	+11 mm	--	--
[CuL <sup>1</sup> (NCS)] (4)	--	--	+10 mm	--	--
[CuL <sup>1</sup> N <sub>3</sub> ].3H <sub>2</sub> O (5)	--	--	+10 mm	--	+9 mm
[Cu <sub>2</sub> (L <sup>1</sup> ) <sub>2</sub> SO <sub>4</sub> ].2H <sub>2</sub> O (6)	+10 mm	--	+14 mm	--	+9 mm

The ligand HL<sup>1</sup> and the six copper(II) complexes were screened against the five types of bacteria. The ligand HL<sup>1</sup> was found to be inactive, but all the copper(II) complexes were found to be active. The copper(II) complexes 1 and 4 were found to be active against *Bacillus* sp., *Vibrio cholerae* O1 and *Staphylococcus aureus*. Compound 6 was found to be active against *Bacillus* sp. *Vibrio cholerae* O1 and *Salmonella paratyphi*. Compound 5 was found to be active against *Vibrio cholerae* O1 and *Salmonella paratyphi* and compounds 2 and 4 were found to be active against *Vibrio cholerae* O1.

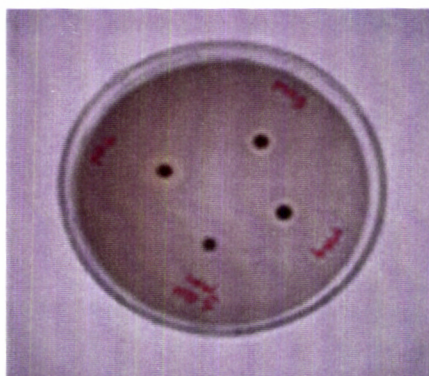


Fig 3.25. Zone of inhibition of compounds against *Staphylococcus aureus*

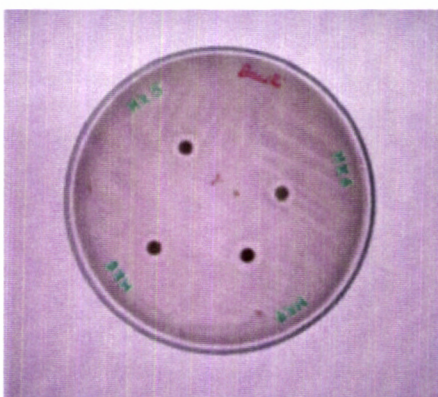


Fig.3.26. Zone of inhibition of compounds against *Bacillus sp*

### 3.4.2. Minimum inhibitory concentration (MIC)

The antimicrobial activities of compounds are expressed in terms of MIC. Minimum inhibitory concentration is that minimum concentration of the antimicrobial agent at which it can inhibit the growth of the test microorganism. The MIC of the test samples that showed a positive antimicrobial property was determined by the disc diffusion method.

Nutrient agar plates were prepared as before. Discs of 4 mm diameter were prepared with different concentrations of each of the test samples (4  $\mu$ l, 3  $\mu$ l, 2  $\mu$ l and 1  $\mu$ l). The plates were incubated at 37 °C for 24 hours and then checked for zones of inhibition around the wells (Table 3.11). The MIC for each sample was recorded and are given in Table 3.12.

Table 3.12 MIC of Cu(II) complexes

Compound	MIC in $\mu$ l			
	<i>Bacillus</i> <i>sp</i>	<i>Vibrio</i> <i>cholerae</i> O1	<i>Salmonella</i> <i>paratyphi</i>	<i>Staphylococcus</i> <i>aureus</i>
[CuL <sup>1</sup> Cl] (1)	5	5	--	4
{[CuL <sup>1</sup> Br] <sub>2</sub> } (2)	--	5	--	--
[CuL <sup>1</sup> NO <sub>3</sub> ] (3)	5	5	--	5
[CuL <sup>1</sup> NCS] (4)	--	5	--	--
[CuL <sup>1</sup> N <sub>3</sub> ].3H <sub>2</sub> O (5)	--	5	4	--
[Cu <sub>2</sub> (L <sup>1</sup> ) <sub>2</sub> SO <sub>4</sub> ].2H <sub>2</sub> O (6)	5	5	5	--

## References

1. F.A. Cotton, G. Wilkinson, C.A. Murillo, M. Bochmann, *Advanced Inorganic Chemistry*, 6<sup>th</sup> ed., Wiley, New York, 1999.
2. N.N. Greenwood, A. Earnshaw, *Chemistry of the elements*, 2<sup>nd</sup> ed., Reed Educational and Professional Publishing Ltd. Great Britain, 1997.
3. R.N. Mukherjee, *Indian J. Chem.* 42A (2003) 2175.
4. R.N. Mukherjee, *Comprehensive Coordination Chemistry-II: From Biology to Nanotechnology*, 5 (2003).
5. R.H. Holm, P. Kennepohl, E.I. Solomon, *Chem. Rev.* 96 (1996) and references therein.
6. A. Diaz, R. Pogni, R. Cao, R. Basosi, *Inorg. Chim. Acta* 275 (1998) 552.
7. I.H. Hall, K.G. Rajendran, D.X. West, A.E. Liberta, *Anticancer Drugs*. 4 (1993) 231.
8. O.E. Offiong, S. Martelli, *Farmaco*, 48 (1993) 777.
9. S.P. Mittal, R.K. Sharma, R.V. Singh, J.P. Tandon, *Curr. Sc.* 50 (1981) 483.
10. A.S. Dobeck, D.I. Klayman, E.J. Dickson, J.P. Scovill, E.C. Tramont, *Antimicrob agents Chemother.* 18 (1980) 27.
11. K. Raman, H.K. Singh, S.K. Salman, S.S. Parmar, *J. Pharm. Sci.* 82 (1993) 167.
12. D.X. West, J.S. Ives, M.M. Salberg, T.L. Zumbahlen, G.A. Bain, A.E. Liberta, *Polyhedron* 14 (1995) 2189.
13. D.X. West, N.M. Kozub, G.A. Bain, *Transition Met. Chem.* 21 (1996) 52.
14. Siemens, SMART and SAINT, Area Detector Control and Integration Software. Siemens Analytical X-ray Instruments Inc., Madison, Wisconsin, USA. 1996.
15. R.H. Blessing, *Acta Crystallogr. Sect. A* 51(1995) 33.



16. G.M. Sheldrick, SHELXS 97. University of Göttingen, Germany. 1997.
17. A.L. Spek, PLATON. A Multipurpose Crystallographic Tool. Utrecht University, Utrecht, Netherlands. 1999.
18. K. Nakamoto, Infrared and Raman spectra of Inorganic and Coordination compounds, 5<sup>th</sup> ed., Wiley, New York. 1997.
19. W.J. Geary, Coord. Chem. Rev. 7 (1971) 81.
20. B.N. Figgis, Introduction to Ligand fields, Wiley, New Delhi. 1976.
21. E.W. Ainscough, A.M. Bordie. E.N. Bake. R.J. Cresswell. J. Ranford, J.M. Waters, Inorg. Chim. Acta 172 (1990) 185.
22. C.F. Bell, C.R. Theocharis, Acta Crystallogr. C 43 (1987) 26.
23. J.G. Anton. J. Pons, X. Solans. M.F. Bardia, L. Ros, Inorg. Chim. Acta 355 (2003) 87.
24. V.E. Kaasjager, J. van den Broeke, R.K. Henderson, W.J. Smeets. A.L. Spek, W.L. Driessen. E. Bouwman. J. Reedijk. Inorg. Chim. Acta 316 (2001) 99.
25. M. Cha, J. Sletten, S. Critchlow, J.A. Kovacs, Inorg. Chim. Acta 263 (1997) 153.
26. K.S. Anjali, Yung-Lin Pui, V. Wing-Wah Yam, J.J. Vittal, Inorg. Chim. Acta 319 (2001) 57.
27. N. Ancin, S.G. Ozta, M. Tuzun. J. Mol. Struct. 606 (2002) 45.
28. E. Labisbal, K.D. Haslow. A. Sousa-Pedrares. J. Valdes-Martinez. S. Hernandez-Ortega. D.X. West, Polyhedron 22 (2003) 2831.
29. G.J. Palenik, D.F. Rendle. W.S. Carter. Acta Crystallogr. Sect. B 30 (1974) 2390.
30. M.E. Hossain, M.N. Alam. J. Begum, M.A. Ali, M. Nazimuddin. F.E. Smith. R.C. Hynes, Inorg. Chim. Acta 249 (1996) 207.

31. D.X. West, H. Gebremedhin, T.J. Romack, *Transition Met. Chem.* 19 (1994) 426.
32. D.X. West, I.S. Billeh, J.P. Jesinski, J.M. Jesinski, R.J. Butcher, *Transition Met. Chem.* 23 (1998) 209.
33. D.X. West, A.M. Stark, G.A. Bain, A.E. Liberta, *Transition Met. Chem.* 21 (1996) 289.
34. R.J. Clark, C.S. Williams, *Inorg. Chem.* 4 (1965) 350.
35. A.E. Martell, *Coordination Chemistry Vol.1*, Van Nostrand Reinhold, New York, 1971, p.167.
36. S.K. Jain, B.S. Garg, Y.K. Bhoon, *Spectrochim. Acta* 42 (1986) 701.
37. D.X. West, G. Ertem, R.M. Makeever, *Transition Met. Chem.* 10 (1985) 41.
38. A. Sreekanth, M.R.P. Kurup, *Polyhedron*, 22 (2003) 3321.
39. V. Philip, V. Suni, M.R.P. Kurup, M. Nethaji, Unpublished results.
40. V. Stefov, V.M. Petrusevski, B. Soptrajanov, *J. Mol. Struct.* 293 (1993) 97.
41. J.E. Huheey, E.A. Keiter, R.L. Keiter, *Inorganic Chemistry*, 4<sup>th</sup> ed., Addison-Wesley Publishing Company, India, 1993.
42. R.S. Drago, *Physical Methods in Inorganic Chemistry*. Reinhold Publishing Corporation, New York.
43. R.L. Dutta, A. Syamal, *Elements of Magnetochemistry*, 2<sup>nd</sup> ed., East-west press, New Delhi, 1993.
44. D.X. West, S.I. Dietrich, I. Thientanavanich, C.A. Brown, *Transition Met. Chem.* 19 (1994) 195.
45. E. Ainscough, A.M. Brodie, N.G. Larsen, *Inorg. Chim. Acta.* 60 (1982) 25.
46. D.X. West, C.S. Carlson, C.P. Galloway, A.E. Liberta, C.R. Daniel, *Transition Met. Chem.* 15 (1990) 91.

47. A.B.P. Lever, *Inorganic Electronic Spectroscopy*, 2<sup>nd</sup> ed., Elsevier, Amsterdam, 1984.
48. B.J. Hathaway, G. Wilkinson, R.D. Gillard, J.A. McCleverty, *Comprehensive Coordination Chemistry II*, vol. 5, Pergamon, Oxford, 1987.
49. A.H. Maki, B.R. McGrahey, *J. Chem. Phys.* 28 (1958) 35.
50. D. Kivelson, R. Neiman, *J. Chem. Phys.* 35 (1961) 149.
51. P. Bindu, M.R.P. Kurup, T.R. Satyakeerty, *Polyhedron* 18 (1999) 321.
52. R-P. John, A. Sreekanth, M.R.P. Kurup, S.M. Mobin, *Polyhedron*, 21 (2002) 2515.
53. R. Pogni, M.C. Bartto, A. Diaz, R. Basosi. *J. Inorg. Biochem.*, 79 (2000) 333.
54. J.S. Wolfson, D.C. Hooper, M.N. Swartz. J.S. Walfson, D.C. Hooper, *American Society for Microbiology*, Washington, D.C. 21 (1989) 655.

## SYNTHESIS AND SPECTRAL CHARACTERIZATION OF COPPER(II) COMPLEXES OF 2- BENZOYLPYRIDINE N(4)--PHENYLTHIOSEMICARBAZONE

### 4.1. Introduction

Copper is the third most abundant transition element in biological systems. It is bound to proteins in the body either as metalloproteins or as enzymes. The +II oxidation state is the most stable and the most important state for copper [1]. The  $d^9$  configuration makes Cu(II) subject to Jahn-Teller distortion if placed in an environment of cubic i.e. regular octahedral or tetrahedral symmetry and this has a profound effect on all its stereochemistry [2]. Generally copper(II) forms octahedral complexes, with the weakening of two axial bonds or square planar complexes. Cu(II) also forms five coordinated complexes having square pyramidal or trigonal bipyramidal structures.

Spectral and structural investigations of a series of biologically active copper(II) complexes of thiosemicarbazones have been reported earlier. Thiosemicarbazones belong to a large group of thiourea derivatives, the biological activities - of which are functions of the parent aldehyde or ketone [3, 4]. Thiosemicarbazones are compounds with versatile structural features [5, 6] and they can coordinate to the metal either as a neutral ligand or as a deprotonated anion through the N, N, S or O, N, S donor atoms [7]. There were numerous reports on the structural and biological studies of copper(II) complexes of 2-formyl, and 2-acetylpyridine thiosemicarbazones [8, 9, 10]. D. X. West reported the structural and antifungal activities of copper(II) complexes of 2-benzoylpyridine N(4)-substituted thiosemicarbazones [11]. Recently there are reports on the

antifungal and antibacterial activities of the metal complexes of *N*(4)-phenyl 2-benzoylpyridine thiosemicarbazone [12]. Structural studies and spectral characteristics of 4-benzoylpyridine thiosemicarbazone and *N*(4)-phenyl 4-benzoylpyridine thiosemicarbazone are also reported [13]. In a review of the coordination chemistry of copper [14], there are reports on the copper(II) complexes of pyridine 2-carbaldehyde thiosemicarbazone [15], 6-methylpyridine-2-aldehyde thiosemicarbazone [16] and methyl-2-pyridyl ketone thiosemicarbazone [17].

This Chapter describes the synthesis, conductance, magnetic and spectral studies and antimicrobial activities of copper(II) complexes of 2-benzoylpyridine *N*(4)-phenylthiosemicarbazone ( $HL^2$ ).

## 4.2. Experimental

### 4.2.1. Materials

Details regarding the synthesis of  $HL^2$  is described in Chapter 2. Various copper(II) salts (GR) were used as obtained. Copper perchlorate hexahydrate was prepared by treating copper carbonate with perchloric acid, followed by evaporation and crystallization.

### 4.2.2. Synthesis of complexes

#### $[CuL^2Cl] \cdot CH_3OH$ (7)

$CuCl_2 \cdot 2H_2O$  (2 mmol, 0.341 g) in 20 ml ethanol and  $HL^2$  (2 mmol, 0.664 g) in 20 ml hot ethanol were mixed and refluxed for 5 hrs. On cooling, blue colored solids separated, which were filtered, washed with hot water, hot ethanol and ether and dried over  $P_4O_{10}$  *in vacuo*.

$[CuL^2Br] \cdot 2H_2O$  (8)

CuBr<sub>2</sub> (2 mmol, 0.446 g) dissolved in a mixture of hot methanol and ethanol (40 ml) and HL<sup>2</sup> (2 mmol, 0.664 g) dissolved in 40 ml hot methanol were mixed and refluxed for 4 hrs. The blue solids separated were filtered, washed with hot water, hot ethanol and ether and dried over P<sub>4</sub>O<sub>10</sub> *in vacuo*.

 $[CuL^2NO_3] \cdot H_2O$  (9)

To a hot solution of HL<sup>2</sup> (2 mmol, 0.664 g) in 40 ml methanol, Cu(NO<sub>3</sub>)<sub>2</sub>·3H<sub>2</sub>O (2 mmol, 0.482 g) in 20 ml methanol was added and refluxed for 5 hrs. The blue colored solids formed were filtered, washed with hot water, hot ethanol and ether and then dried over P<sub>4</sub>O<sub>10</sub> *in vacuo*.

 $[CuL^2NCS] \cdot 2H_2O$  (10)

A mixture of Cu(CH<sub>3</sub>COO)<sub>2</sub>·H<sub>2</sub>O (2 mmol, 0.398 g) in 20 ml methanol and HL<sup>2</sup> (2 mmol, 0.664 g) in 40 ml methanol were refluxed for 2 hrs. To the refluxing solution, a solution of potassium thiocyanate (2 mmol, 0.198 g) in 10 ml methanol was added and again refluxed for 4 hrs. The blue colored crystals, separated on keeping for a few days, were filtered, washed with hot ethanol, hot water and ether and then dried over P<sub>4</sub>O<sub>10</sub> *in vacuo*.

 $[CuL^2N_3]$  (11)

Solutions of Cu(CH<sub>3</sub>COO)<sub>2</sub>·H<sub>2</sub>O (2 mmol, 0.3998 g) in 20 ml methanol and HL<sup>2</sup> (2 mmol, 0.664 g) in 40 ml methanol were mixed and refluxed for 2 hrs. Then a solution of sodium azide (2 mmol, 0.130 g) was added to the refluxing solution and again refluxed for 2 hrs. The green solids, which separated, were filtered, washed with hot water, hot ethanol, and ether and dried over P<sub>4</sub>O<sub>10</sub> *in vacuo*.

### $[CuL^2(HL^2)](ClO_4)$ (12)

Copper perchlorate (2 mmol, 0.414 g) in 20 ml methanol and  $HL^2$  (2 mmol, 0.664 g) in 40 ml methanol were refluxed for 5 hrs. The dark blue solids, which separated, were filtered, washed with water, hot methanol, ether and dried over  $P_4O_{10}$  *in vacuo*.

#### 4.2.3. Analytical methods

The details regarding the various analytical methods were discussed in the previous Chapter.

### 4.3. Results and discussion

#### 4.3.1. Analytical measurements

The colors, stoichiometries, elemental analyses, and magnetic moments of the Cu(II) complexes are given in Table 4.1. All the Cu(II) complexes prepared are either blue or green in color. They are insoluble in polar solvents and soluble in dimethyl formamide and chloroform.

The molar conductances of the complexes were measured using  $10^{-3}$  M solution in DMF. The molar conductance values of the compounds 1, 2, 3, 4 and 5 are found to be less than  $20 \text{ ohm}^{-1}\text{mol}^{-1}\text{cm}^{-1}$ , showing that they are nonconductors [18] which indicate that the anion and the ligand are coordinated to the central Cu(II). But the molar conductance value of compound 12 is  $72 \text{ ohm}^{-1}\text{mol}^{-1}\text{cm}^{-1}$  and this is consistent with the value of 1:1 electrolyte as suggested by the formula.

The magnetic moments of the complexes are calculated from the magnetic susceptibility measurements and the values are found to be in the range 1.5-1.9 B.M. The values of magnetic moment close to the spin only value of 1.7

B.M.. indicate the presence of one unpaired electron as expected for Cu(II) complexes.

Table 4.1 Analytical data

Compound	Empirical formula	Color	Found (Calculated) (%)			$\mu$ (B.M.) at 300K
			C	H	N	
[CuL <sup>2</sup> Cl]·CH <sub>3</sub> OH (7)	C <sub>20</sub> H <sub>19</sub> N <sub>4</sub> SOClCu	Blue	51.45 (51.95)	4.01 (4.12)	12.16 (12.12)	1.54
[CuL <sup>2</sup> Br]·2H <sub>2</sub> O (8)	C <sub>19</sub> H <sub>19</sub> N <sub>4</sub> SBrO <sub>2</sub> Cu	Blue	44.79 (44.66)	3.42 (3.72)	10.60 (10.97)	1.67
[CuL <sup>2</sup> NO <sub>3</sub> ]·H <sub>2</sub> O (9)	C <sub>19</sub> H <sub>17</sub> N <sub>5</sub> SO <sub>2</sub> Cu	Blue	48.61 (48.04)	3.31 (3.58)	14.87 (14.75)	1.84
[CuL <sup>2</sup> NCS]·2H <sub>2</sub> O (10)	C <sub>20</sub> H <sub>19</sub> N <sub>5</sub> S <sub>2</sub> O <sub>2</sub> Cu	Blue	49.72 (49.12)	3.22 (3.88)	14.57 (14.32)	1.85
[CuL <sup>2</sup> N <sub>3</sub> ] (11)	C <sub>19</sub> H <sub>15</sub> N <sub>7</sub> SCu	Green	51.23 (51.06)	3.44 (3.36)	22.41 (21.94)	1.47
[Cu(HL <sup>2</sup> )L <sup>2</sup> ](ClO <sub>4</sub> ) (12)	C <sub>38</sub> H <sub>31</sub> N <sub>8</sub> S <sub>2</sub> OCICu	Dark blue	54.80 (55.20)	3.38 (3.75)	13.94 (13.55)	1.91



### 4.3.2 IR spectra

The tentative assignments of the significant IR spectral bands of HL<sup>2</sup>, and their copper(II) complexes are presented in Table 4.2. The  $\nu(\text{C}=\text{N})$  band of the thiosemicarbazone at  $1591\text{ cm}^{-1}$  is found to be shifted in energy in the spectra of the complexes indicating coordination *via* the azomethine nitrogen. This is confirmed by the bands in the range  $440\text{-}475\text{ cm}^{-1}$  which have been assigned to the  $\nu(\text{Cu}-\text{N})$  band [19]. In all the complexes a strong band is found at *ca.*  $1596\text{ cm}^{-1}$  which may be due to the formation of the newly formed  $^2\text{N}=\text{C}$  bond. This indicates that the ligand enolizes and coordinates in the thiolate form. A strong band found at  $1102\text{ cm}^{-1}$  in the spectrum of HL<sup>2</sup> is assigned to the  $\nu(\text{N}-\text{N})$  band of the thiosemicarbazone. The increase in the frequency of this band in the spectra of the complexes, due to the increase in the bond strength, again confirms the coordination *via* the azomethine nitrogen.

In the uncomplexed thiosemicarbazone, the two bands, which appear at frequencies  $1369$  and  $835\text{ cm}^{-1}$ , have been assigned to  $\nu(\text{C}=\text{S})$ . In the complexes these two bands are found to be shifted to lower frequencies in the ranges  $1280\text{-}1335\text{ cm}^{-1}$  and  $745\text{-}788\text{ cm}^{-1}$  respectively. This negative shift of the  $\nu(\text{C}=\text{S})$  band in the complexes indicates the coordination *via* the thiolate sulfur atom. Strong bands observed in the region  $340\text{-}355\text{ cm}^{-1}$  have been assigned to the  $\nu(\text{Cu}-\text{S})$  band [20].

In all the copper complexes a strong band is observed in the region  $266\text{-}280\text{ cm}^{-1}$ . This is consistent with the  $\nu(\text{Cu}-\text{N}$  of pyridine) as suggested by Clark and Williams [21].

Based on the above spectral evidences, it is confirmed that the ligand HL<sup>2</sup> like HL<sup>1</sup> is tridentate, coordinating *via* the azomethine nitrogen, pyridyl nitrogen and thione / thiolate sulfur.

In the chloro complex the strong band observed at  $349\text{ cm}^{-1}$  has been assigned to the  $\nu(\text{Cu-Cl})$  bond. The  $\nu(\text{Cu-Br})$  frequency is observed at  $255\text{ cm}^{-1}$  in the bromo complex. The  $\nu(\text{Cu-Cl})$  and  $\nu(\text{Cu-Br})$  bands are consistent with the terminal chloro and bromo ligands. The ratio of  $\nu(\text{Cu-Br})/\nu(\text{Cu-Cl})$  is 0.73 and is consistent with the usual values obtained for the complexes of the first row transition metals [19,22].

The structures and vibrational spectra of a large number of nitrate complexes have been reviewed by Addison *et al.* [23,24]. X-ray analyses show that the  $\text{NO}_3^-$  ion coordinates to a metal as a unidentate, chelating bidentate and bridging bidentate ligand of various structures. It is rather difficult to differentiate these structures by vibrational spectroscopy since the symmetry of the nitrate ion differs very little among them. Even so, vibrational spectroscopy is still useful in distinguishing unidentate and bidentate ligands.

In the nitrate complex, of  $\text{HL}^2$ , the three bands observed at 1431, 1302 and  $1014\text{ cm}^{-1}$  correspond to the  $\nu_a(\text{NO}_2)$ ,  $\nu_s(\text{NO}_2)$  and  $\nu(\text{NO})$  modes of the nitrate group. The separation of the two highest frequency bands is  $129\text{ cm}^{-1}$ , which indicate the presence of a terminally bonded monodentate nitrate group [19]. Besides, in the far IR spectrum of the complex, the band observed at  $271\text{ cm}^{-1}$  can be assigned to  $\nu(\text{Cu-ONO}_2)$  in consistence with the bands at  $253\text{-}280\text{ cm}^{-1}$ , reported earlier for  $\text{Cu-ONO}_2$  in metal complexes [25].

In the azido complex **11**, the strong band observed at  $2046\text{ cm}^{-1}$  is assigned to  $\nu_a$  of the azide group indicative of azide coordination [26]. In thiocyanato complex **10**, a very strong band at  $2098\text{ cm}^{-1}$ , a medium band at  $869\text{ cm}^{-1}$  and a strong band at  $480\text{ cm}^{-1}$  are assigned to  $\nu(\text{CN})$ ,  $\nu(\text{CS})$ , and  $\nu(\text{NCS})$  modes of the NCS group respectively. The intensity and position of these bands indicate the unidentate coordination of the thiocyanate group through the nitrogen. [27,28].

Table 4.2. IR spectral assignments of Cu(II) complexes of HL<sup>2</sup>

Compound	$\nu(\text{C}=\text{N})$	$\nu(\text{N}-\text{N})$	$\nu(\text{C}-\text{S})$	$\rho(\text{py})$	$\nu(\text{Cu}-\text{N})$	$\nu(\text{Cu}-\text{Npy})$	$\nu(\text{Cu}-\text{S})$	(Cu-X)
HL <sup>2</sup>	1591s	1102s	1369s, 835s	622m	--	--	--	--
[CuL <sup>2</sup> Cl]·CH <sub>3</sub> O	1554s	1123s	1318s, 784s	632w	460m	272s	349s	349s
[CuL <sup>2</sup> Br]·2H <sub>2</sub> O	1536s	1128s	1316s, 754s	640m	451s	296s	344s	255s
[CuL <sup>2</sup> NO <sub>3</sub> ]·H <sub>2</sub> O	1545s	1128m	1280s, 788s	644s	446s	272s	345s	271s
[CuL <sup>2</sup> NCS]2H <sub>2</sub> O	1534s	1124m	1314m, 748s	629s	452m	276s	346m	--
[CuL <sup>2</sup> N <sub>3</sub> ]	1529s	1123s	1322s, 788s	647m	463s	274s	352m	--
[CuL <sup>2</sup> (HL <sup>2</sup> )](ClO <sub>4</sub> )	1554s 1601s	1123s	1318s, 785s	644m	455s	278s	351s	--

For the perchlorate complex **12**, the bonding of the neutral ligand needs to be considered because the perchlorate group is not coordinated to the metal ion. The perchlorate complex contains a single broad band at  $1123\text{ cm}^{-1}$  and an unsplit band at  $644\text{ cm}^{-1}$ , indicating the presence of ionic perchlorate. The bands at  $1123$  and  $644\text{ cm}^{-1}$  can be assigned to  $\nu_3(\text{ClO}_4)$  and  $\nu_4(\text{ClO}_4)$ . The presence of these bands and the absence of a band near  $930\text{ cm}^{-1}$  assignable to  $\nu_1(\text{ClO}_4)$  suggest ionic perchlorate [29]. The IR spectrum of the compound **12** contains a strong band at  $785\text{ cm}^{-1}$  which has been assigned to  $\nu(\text{C-S})$  indicating coordination *via* the thiolate sulfur. In addition to this band, the spectrum also contains a band at  $830\text{ cm}^{-1}$  indicating the presence of the ligand in the thione form.

According to Stefov *et al* [30] coordinated water should exhibit frequencies at  $825$ ,  $575$  and  $500\text{ cm}^{-1}$ . The absence of spectral bands in these regions in the spectra of compounds **8**, **9** and **10** indicate that the water molecules in these complexes are not coordinated but are present as lattice water.

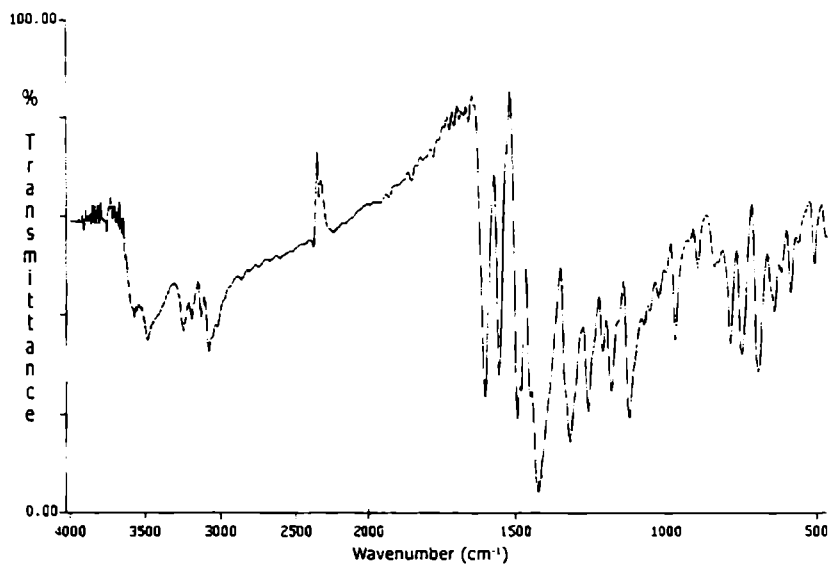


Fig.4.1. IR spectrum of  $[\text{CuL}_2\text{Cl}]\cdot\text{CH}_3\text{OH}$

546.3  
MAR

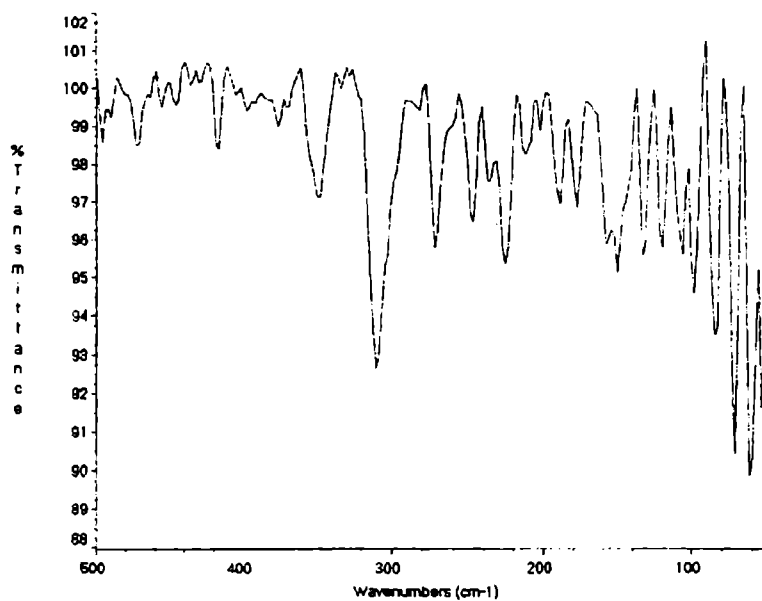


Fig.4.2. Far IR spectrum of  $[\text{CuL}^2\text{Cl}]\cdot\text{CH}_3\text{OH}$

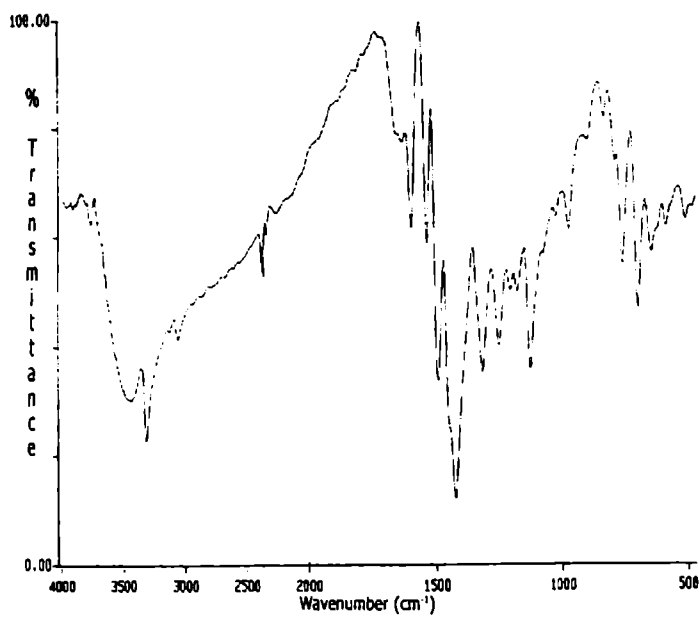
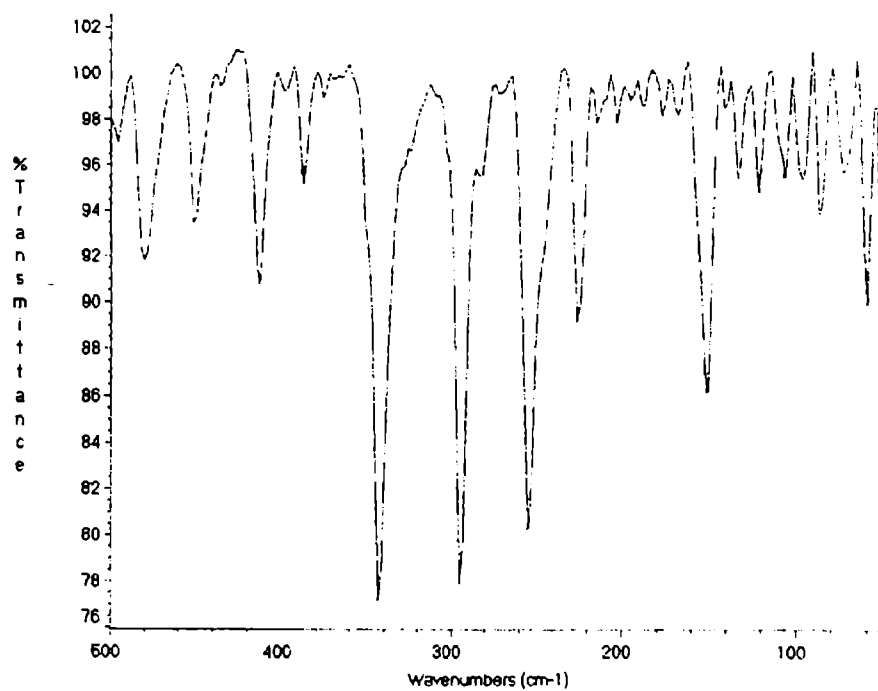
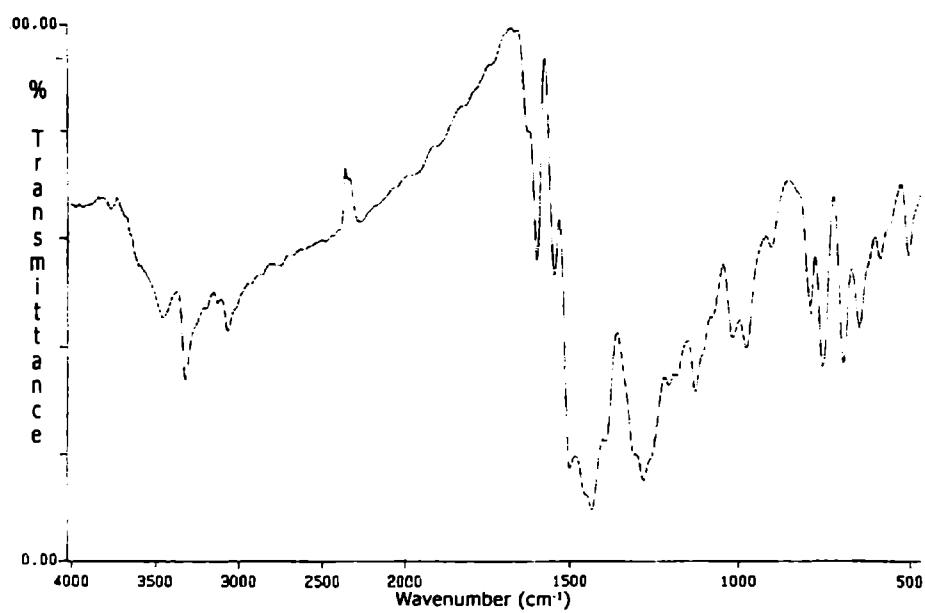
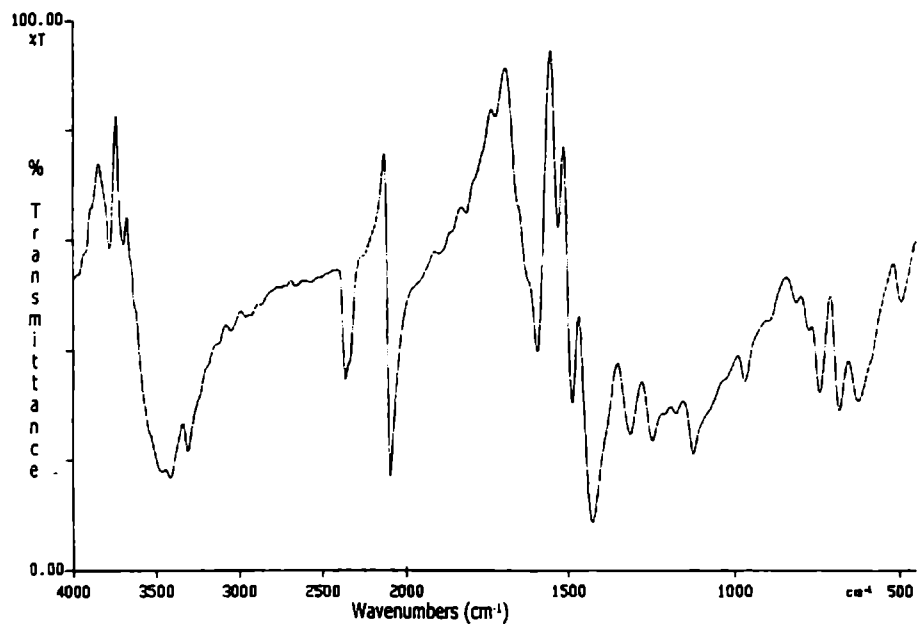
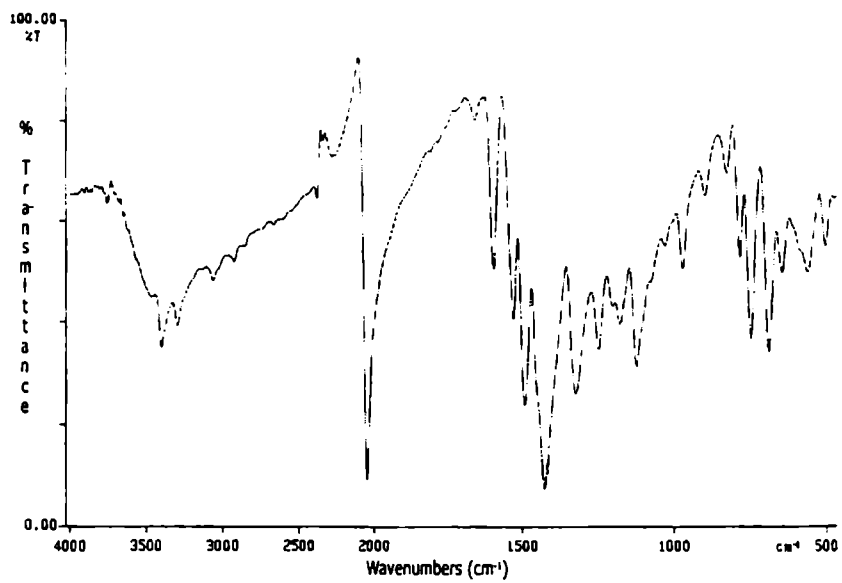


Fig.4.3. IR spectrum of  $[\text{CuL}^2\text{Br}]\cdot 2\text{H}_2\text{O}$

Fig.4.4. Far IR spectrum of  $[\text{CuL}^2\text{Br}] \cdot 2\text{H}_2\text{O}$ Fig.4.5. IR spectrum of  $[\text{CuL}^2\text{NO}_3] \cdot \text{H}_2\text{O}$

Fig.4.6. IR spectrum of  $[\text{CuL}^2\text{NCS}] \cdot 2\text{H}_2\text{O}$ Fig.4.7. IR spectrum of  $[\text{CuL}^2\text{N}_3]$

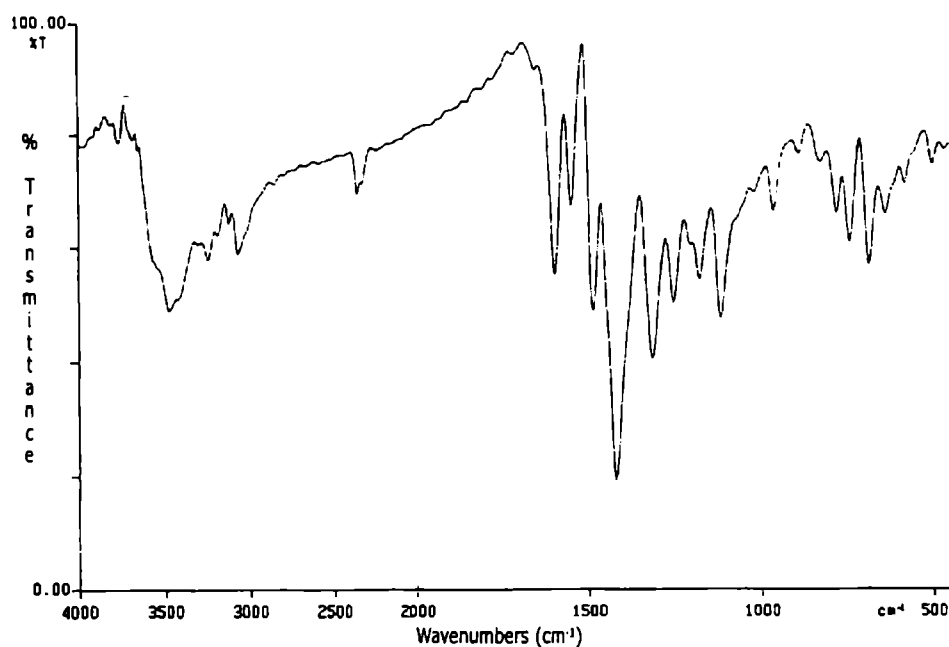


Fig.4.8. IR spectrum of  $[\text{Cu}(\text{HL}^2)\text{L}^2]\text{ClO}_4$

### 4.3.3. Electronic spectra

The blue or green color of all the Cu(II) complexes is due to the absorption of energy in the 600 to 900 nm region of the spectrum. The energies of the electronic transitions for the thiosemicarbazone  $\text{HL}^2$  and its Cu(II) complexes (solid state and DMF solution) are listed in Table 4.3. The solid-state electronic spectrum of the thiosemicarbazone  $\text{HL}^2$  consists of a broad band at *ca.* 345 nm which is the  $n \rightarrow \pi^*$  band of the thioamide function. Another  $n \rightarrow \pi^*$  band of the pyridine ring is present at 286 nm [31]. The  $n \rightarrow \pi^*$  transition of the ligand at 345 nm is shifted in energy in solution which is probably due to the hydrogen bonding taking place between the thiosemicarbazone moiety and the solvent molecules. The molar absorptivities for  $n \rightarrow \pi^*$  transition are  $>10^4$ , which is



consistent with the values of the previously studied heterocyclic thiosemicarbazones [32].

In the solid state electronic spectra of the Cu(II) complexes, an absorption band due to the  $n \rightarrow \pi^*$  transition of the thiosemicarbazone appears in the range 307-330 nm. The broad bands observed in the range 410-425 nm are assigned to the S $\rightarrow$ Cu and Py $\rightarrow$ Cu charge -transfer bands. In the chloro complex the shoulder observed at 318 nm is assigned to the Cl $\rightarrow$ Cu charge-transfer transition [31,33].

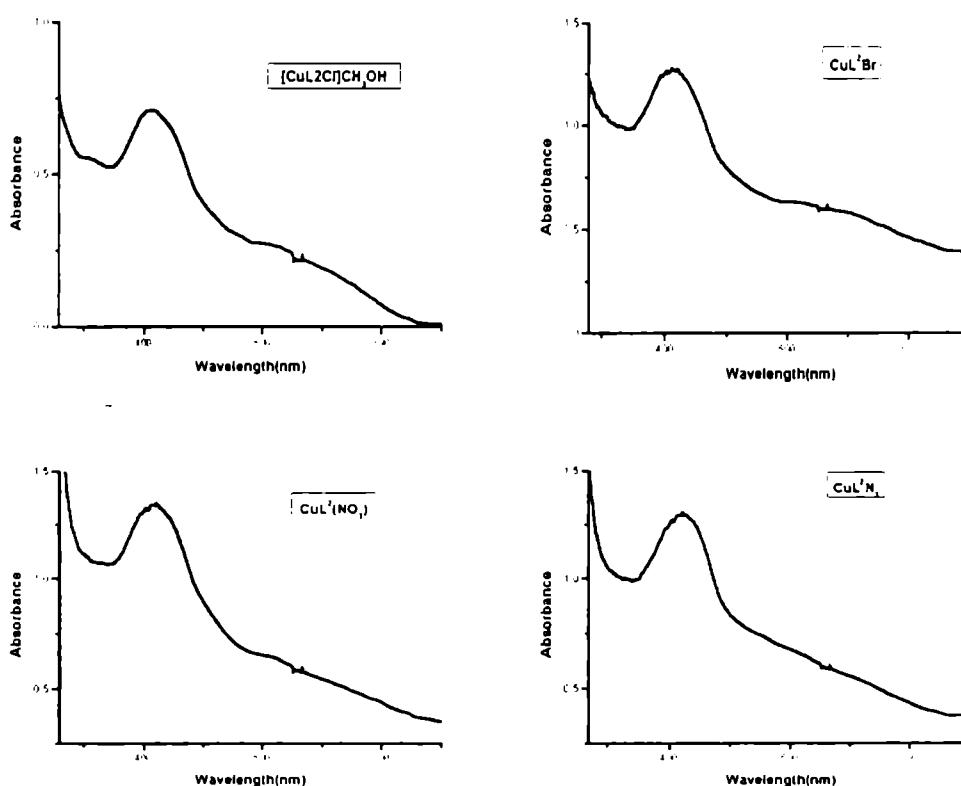
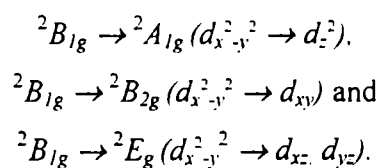


Fig.4.9. Electronic spectra of compounds 7, 8, 9 and 11

The solid-state spectra of all the Cu(II) complexes have a broad band in the region 526-610 nm. This is consistent with the broad structured band for the square planar complexes in the range 500-770 nm [34]. All the complexes exhibit a  $d \rightarrow d$  band, whose maximum of absorption lie in the visible region  $\approx$  590 nm, as weak shoulders. Such a feature is expected for a square planar complex in accordance with the earlier reports [35]. For the square planar complexes with  $d_{x^2-y^2}^2$  ground state, three spin allowed transitions are possible *viz.*,



It is difficult to resolve it into three bands [36]. The four lower orbitals are often so close in energy that individual transfer from there to the upper d level cannot be distinguished and hence the appearance of a single absorption band. It is observed that the spectra of the complexes are dominated by intense intraligand and charge transfer bands. These intense bands cause the low energy bands to appear as weak shoulders.

Table 4.3 Electronic spectral assignments (nm) of HL<sup>2</sup> and its Cu(II) complexes loge in parentheses (Lmol<sup>-1</sup>cm<sup>-1</sup>)

Compound	Mode	<i>d</i> → <i>d</i>	L→M	<i>n</i> → <i>π</i> *	<i>π</i> → <i>π</i> *
HL <sup>2</sup>	Solid DMF	--	--	340, 335 (4.13),	268 262
[CuL <sup>2</sup> Cl]·CH <sub>3</sub> OH (7)	Solid DMF	610 573 (2.60)	414, 318sh 437 (4.14)	313 362 (3.83)	255 256 (4.41)
[CuL <sup>2</sup> Br]·2H <sub>2</sub> O (8)	Solid DMF	591 553 (2.41)	413 453 (4.27)	330 353 (4.61)	271sh 274sh(4.15)
[CuL <sup>2</sup> NO <sub>3</sub> ]·H <sub>2</sub> O (9)	Solid DMF	607 624 (2.43)	417 407 (4.27)	326 311 (4.32)	282 260sh(4.25)
[CuL <sup>2</sup> NCS]·2H <sub>2</sub> O (10)	Solid DMF	561sh 625 (2.5)	423 443 (4.33)	307 311 (4.25)	279 277 (4.16)
[CuL <sup>2</sup> N <sub>3</sub> ] (11)	Solid DMF	590sh 528 (2.41)	422 442 (3.81)	323 352 (4.71)	277 280sh(4.15)
[CuL <sup>2</sup> (HL <sup>2</sup> )](ClO <sub>4</sub> ) (12)	Solid DMF	535sh 584sh(2.34)	413 440 (4.35)	309 352 (4.21)	267sh 270sh(4.01)

#### 4.3.4. Electron paramagnetic resonance spectra

The EPR spectra of the complexes in the polycrystalline sample at 298 K in solution at 298 and 77 K were recorded in the X band, using 100 KHz field modulation and the *g* factors were quoted relative to the standard marker TCNE (*g* = 2.0277). The EPR parameters of the copper(II) complexes obtained for the polycrystalline state at 298 K and in DMF at 298 and 77 K are presented in Table 4.4.

The copper(II) ion with a  $d^9$  configuration, has an effective spin of  $S = 1/2$  and is associated with a spin angular momentum  $m_s = \pm 1/2$ , leading to a doubly degenerate spin state in the absence of a magnetic field. In a magnetic field, this degeneracy is lifted and the energy difference between these states is given by  $E = h\nu = g\beta H$  where  $h$  is Planck's constant,  $\nu$  is the frequency,  $g$  is the Lande splitting factor (equal to 2.0023 for the free electron),  $\beta$  is the Bohr Magneton and  $H$  is the magnetic field. In the case of a  $3d^9$  copper(II) ion the appropriate spin Hamiltonian assuming a  $B_{1g}$  ground state is given by [37].

$$\hat{H} = \beta [ g_{\parallel} H_z S_z + g_{\perp} (H_x S_x + H_y S_y) ] + A I_z S_z + B (I_x S_x + I_y S_y)$$

The EPR spectra of compound **11** in the polycrystalline state (298 K) show only one broad signal at  $g = 2.07$ . The spectra of the compounds **8**, **9** and **10** show typical axial spectra with well-defined  $g_{\parallel}$  and  $g_{\perp}$  values at  $\approx 2.21$  and 2.05 respectively. The spectra are often broad because of the broadening resulting from the fast spin-lattice relaxation time and exchange coupling. The spectra of compounds **7** and **12** give three  $g$  values *viz*  $g_1$ ,  $g_2$  and  $g_3$ , which indicate rhombic distortions in their geometry.

The geometric parameter  $G$ , which is a measure of the exchange interaction between the copper centres in the polycrystalline compound, is calculated using the equation:

$$G = (g_{\parallel} - 2.0023) / (g_{\perp} - 2.0023), \text{ for rhombic spectra, } g_{\perp} = (g_1 + g_2) / 2$$

If  $G > 4$ , exchange interaction is negligible and if it is less than 4, considerable exchange interaction is indicated in the solid complex [38,39]. In all the copper(II) complexes  $g_{\parallel} > g_{\perp} > 2.0023$  and  $G$  value within the range 2.5-3.5 is consistent with a  $d_{x^2-y^2}$  ground state.

The solution spectra of all the complexes were recorded in DMF at 298 and 77 K. In the EPR spectra of the complexes in DMF, at 298 K, four hyperfine lines are observed which arises from the coupling of copper nuclei ( $^{65}\text{Cu}$ ,  $I=3/2$ ) with the

odd electron. The spectrum of compound **7** at 77 K is a typical axial spectrum with well-resolved four hyperfine lines, no superhyperfine lines are observed in the spectrum. The spectrum of compound **8**, is isotropic without any hyperfine lines due to poor glass formation. The spectrum of compound **12** is a typical rhombic spectrum without any hyperfine and superhyperfine lines.

It was reported that the  $g_{\parallel}$  values less than 2.3 indicate considerable covalent character to the M-L bond and greater than 2.3 indicate ionic character. The  $g_{\parallel}$  values of the complexes are found to be less than 2.3, which indicate considerable covalent character to the M-L bond [40,41].

The EPR parameters  $g_{\parallel}$ ,  $g_{\perp}$ ,  $g_{av}$ ,  $A_{\parallel}(\text{Cu})$  and  $A_{\perp}(\text{Cu})$  and the energies of  $d-d$  transition were used to evaluate the bonding parameters  $\alpha^2$ ,  $\beta^2$  and  $\gamma^2$ , which may be regarded as measures of the covalency of the in-plane  $\sigma$  bonds, in-plane  $\pi$  bonds, and out-of-plane  $\pi$  bonds respectively (the mathematical expressions are given in Chapter 3.).

In all the copper(II) complexes, it is observed that  $K_{\parallel} < K_{\perp}$  which indicates the presence of significant in-plane  $\pi$  bonding. This is further confirmed by the bonding parameters  $\alpha^2$ ,  $\beta^2$ , and  $\gamma^2$  which are less than 1.0, expected for 100% ionic character of the bonds, and decrease on increasing the covalent character of the bonding. This observation supports the argument that there is significant in-plane  $\pi$  bonding and in-plane  $\sigma$  bonding in the copper(II) complexes of HL<sup>2</sup>.

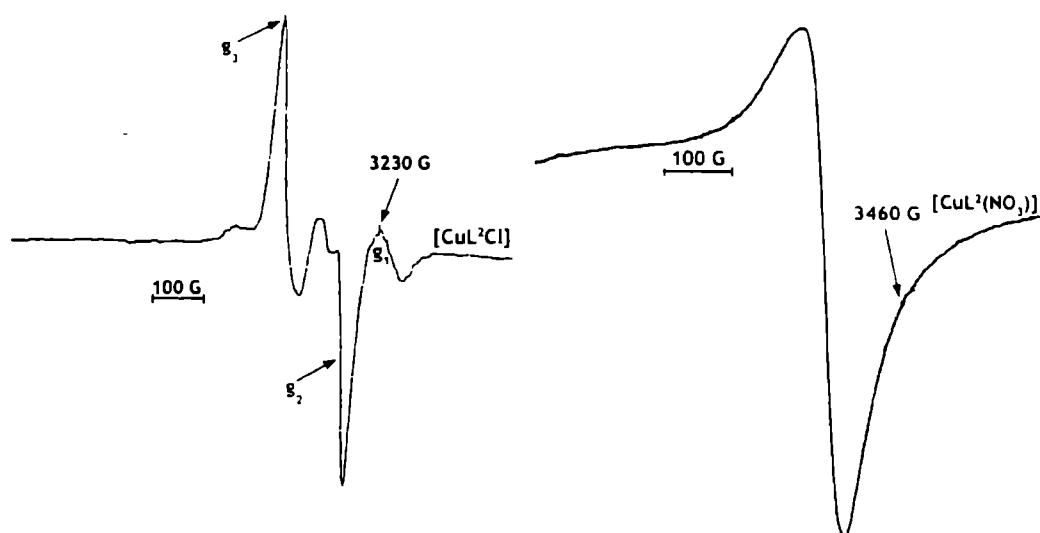


Fig.4.10. EPR spectra of compounds 7 and 9 in the polycrystalline at 298 K

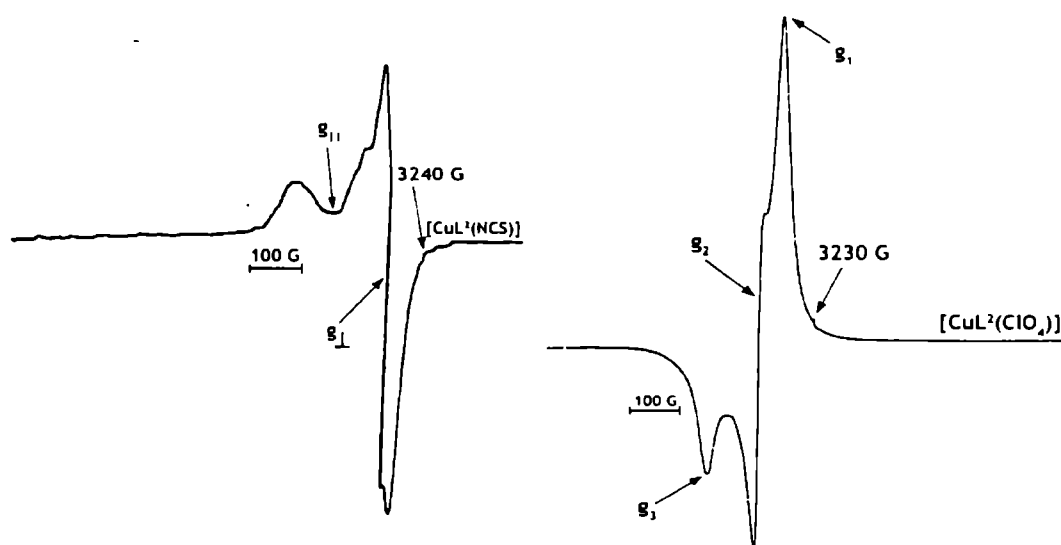


Fig. 4.11. EPR spectra of compounds 10 and 12 in the polycrystalline state at 298 K

Table 4.4 EPR parameters of the Cu(II) complexes of HL<sup>2-</sup>

Compound	Solid (298 K)		DMF solution (298 K)		DMF solution (77 K)			
	$g_1/g_2/g_3$	$g_{av}$	$g_{iso}$	$A_{iso}$	$g_1/g_2/g_3$	$g_{av}$	$A_{  }$	$G_{av}$
[CuL <sup>2-</sup> Cl]·CH <sub>3</sub> OH (7)	$g_1$ 1.9991 $g_2$ 2.0434 $g_3$ 2.1230	2.0552	2.0698	84.13	$g_1$ 2.1500 -- $g_L$ 2.0510	2.0840	158.91	3.03
[CuL <sup>2-</sup> Br]·2H <sub>2</sub> O (8)	$g_{  }$ 2.2348 $g_L$ 2.0898	2.1381	2.0749	112.13	$g_{iso}$ 2.072	--	--	--
[CuL <sup>2-</sup> NO <sub>3</sub> ]·2H <sub>2</sub> O (9)	$g_{  }$ 2.213 -- $g_L$ 2.0960	2.135	2.0560	84.00	$g_1$ 1.971 $g_2$ 2.0498 $g_3$ 2.1274	2.0494	154.23	2.457
[CuL <sup>2-</sup> NCS]·H <sub>2</sub> O (10)	$g_{  }$ 2.1168 -- $g_L$ 2.0433	2.0678	2.1618	85.10	$g_1$ 2.0593 $g_2$ 2.169 $g_3$ 2.2913	2.1732	175.73	2.685
[CuL <sup>2-</sup> N <sub>3</sub> ] (11)	$g_{iso}$ 2.0720		2.0750	102.90	$g_1$ 1.972 $g_2$ 2.065 $g_3$ 2.2052	2.0809	163.58	3.20
[CuL <sup>2-</sup> (HL <sup>2-</sup> )]ClO <sub>4</sub> (12)	$g_1$ 2.0306 $g_2$ 2.0649 $g_3$ 2.1274	2.0743	2.0886	79.45	$g_1$ 2.0301 $g_2$ 2.0498 $g_3$ 2.1274	2.0691	168.26	2.69

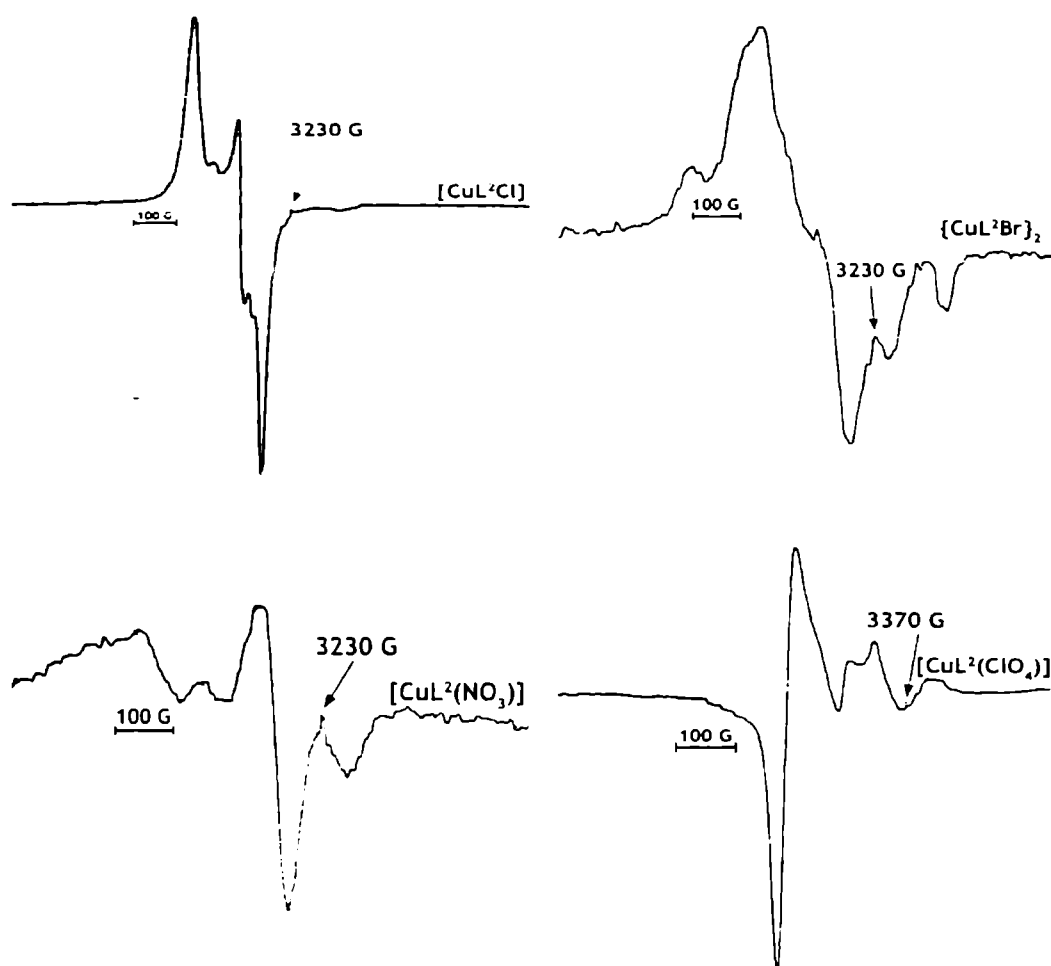


Fig.4.12. EPR spectra of compounds 7, 8, 9 and 12 in DMF at 298 K



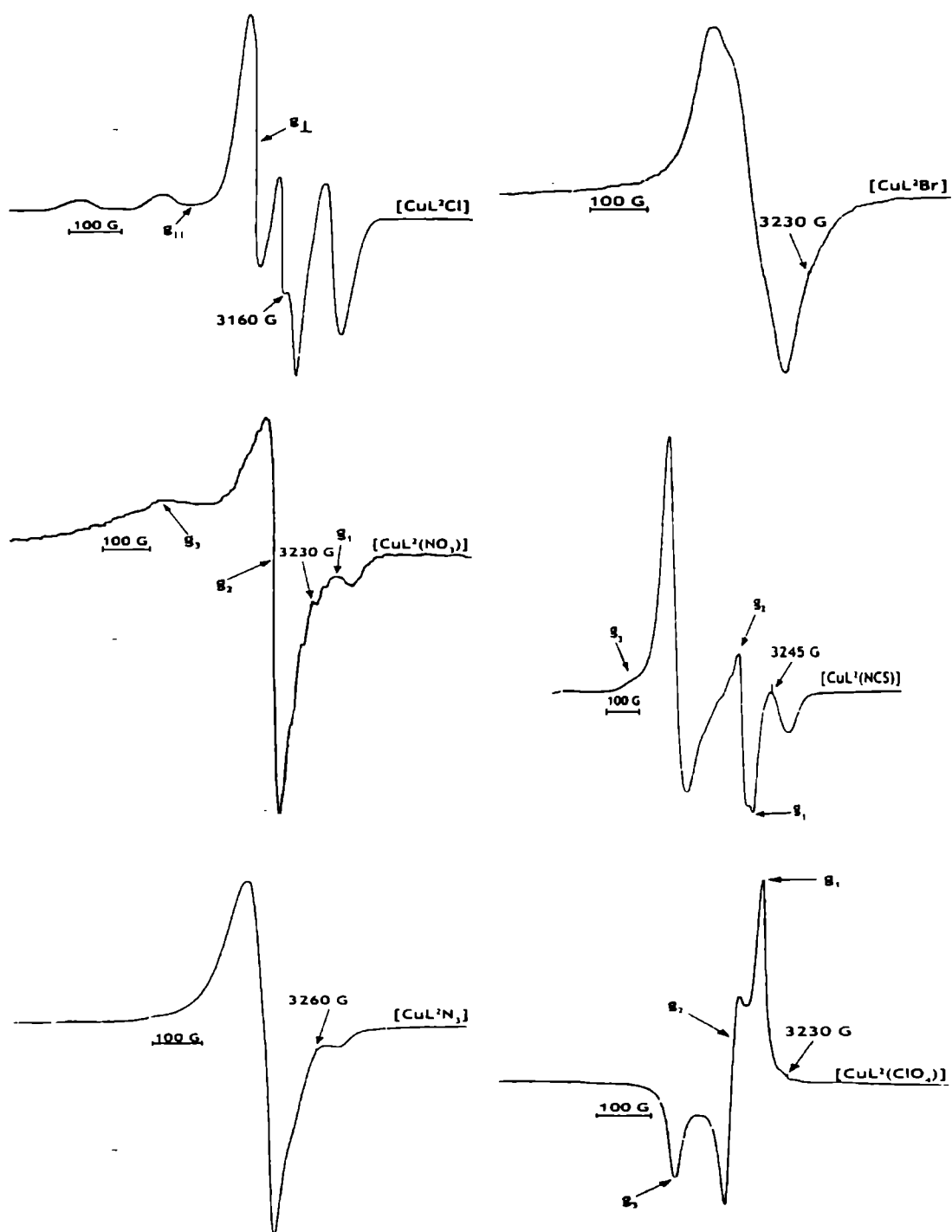


Fig. 4.13 EPR spectra of compounds 7, 8, 9, 10, 11 and 12 in DMF at 77 K.

Table.4.5 Bonding parameters and orbital reduction parameters of Cu(II) complexes of HL<sup>2</sup>

Compound	$\alpha^2$	$\beta^2$	$\gamma^2$	$K_{\parallel}$	$K_{\perp}$	$K_c$	$f$
[CuL <sup>2</sup> Cl]·CH <sub>3</sub> OH	0.6392	0.9877	0.9976	0.6315	0.6333	0.3168	133.4
[CuL <sup>2</sup> Br]·2H <sub>2</sub> O	0.6423	0.9505	0.9582	0.6105	0.6155	0.4359	134.19
[CuL <sup>2</sup> NO <sub>3</sub> ]·H <sub>2</sub> O	0.6479	0.9101	0.9793	0.5897	0.6345	0.3025	126.4
[CuL <sup>2</sup> NCS]·H <sub>2</sub> O	0.660	0.8440	0.9224	0.5570	0.608	0.3532	130.38
[CuL <sup>2</sup> N <sub>3</sub> ]	0.6741	0.9980	0.9877	0.6741	0.6677	0.3526	132.16
[CuL <sup>2</sup> (HL <sup>2</sup> )](ClO <sub>4</sub> )	0.6484	0.9162	1.005	0.5941	0.65190	0.3132	126.44

#### 4.4. Antimicrobial activity

The ligand HL<sup>2</sup> and its five Cu(II) complexes were tested for their antimicrobial activity. The effectiveness of an antimicrobial agent in sensitivity testing is based on the size of the zones of inhibition. The diameter of the zone is measured to the nearest millimeter. Test substances which produce the zone of inhibition with diameters 9 mm or more are regarded as positive. i.e. having antimicrobial activity; while those cases where the diameter is below 9 mm, the bacteria are resistant to the sample tested and the sample is said to have no antimicrobial activity. Two Gram positive bacteria and three Gram negative bacteria were used as test organisms.

1. *Staphylococcus aureus* (Gram positive)
2. *Bacillus sp* (Gram positive)
3. *Escherichia coli* (Gram negative)
4. *Salmonella paratyphi* (Gram negative)
5. *Vibrio cholerae O1* (Gram negative)

The MIC (minimum inhibitory concentration), expressed in micro litres, of the compounds was also determined using the disc diffusion method and is given in

Table 4.6 The antimicrobial activity of the complexes using the disc diffusion method

Compound	Conc. (Conc/Disc in $\mu\text{g}$ )	Activity Inhibition zone.				
		<i>Bacillus</i> sp	<i>Vibrio</i> <i>cholerae</i> 01	<i>Escherichia</i> <i>coli</i>	<i>Staphylococcus</i> <i>aureus</i>	<i>Salmonella</i> <i>paratyphi</i>
$\text{HL}^2$	50 $\mu\text{g}$	--	--	--	+ 12mm	--
$[\text{CuL}^2\text{Cl}]\cdot\text{CH}_3\text{OH}$ (7)	50 $\mu\text{g}$	--	+ 9 mm	--	--	--
$[\text{CuL}^2\text{Br}]\cdot 2\text{H}_2\text{O}$ (8)	50 $\mu\text{g}$	--	+ 10mm	--	--	--
$[\text{CuL}^2\text{NCS}]\cdot\text{H}_2\text{O}$ (10)	50 $\mu\text{g}$	--	+ 10 mm	--	--	--
$[\text{CuL}^2\text{N}_3]$ (11)	50 $\mu\text{g}$	--	+ 10 mm	--	--	+ 9 mm
$[\text{CuL}^2(\text{HL}^2)](\text{ClO}_4)$ (12)	50 $\mu\text{g}$	--	+ 9 mm	--	--	--

Table 4.6. Fig 4.14. shows the study of antimicrobial property by the disc diffusion method.

It is observed that the ligand  $HL^2$  was active against *Staphylococcus aureus* while it was inactive against the other four test organisms. But all its Cu(II) complexes are found to be inactive against this particular bacteria. Out of the five Cu(II) complexes, four complexes are found to be active against only one type of microorganism under study, i.e. *Vibrio cholerae O1*. The complex  $[CuL^2N_3]$  was found to be active against *Vibrio cholerae* and *Salmonella paratyphi*. The ligand and the Cu(II) complexes are found to be inactive against *Bacillus sp* and *Escherichia coli*.

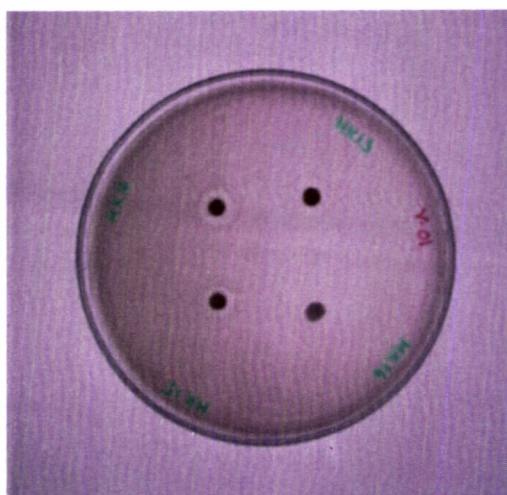


Fig.4.14. Zone of inhibition of compounds 7, 8, 9 and 10 against *Vibrio cholerae O1*

Table 4.7 MIC of HL<sup>2</sup> and its Cu(II) complexes

Compound	MIC in $\mu\text{l}$			
	<i>Bacillus</i> <i>sp</i>	<i>Vibrio</i> <i>cholerae</i> <i>O1</i>	<i>Salmonella</i> <i>paratyphi</i>	<i>Staphylococcus</i> <i>aureus</i>
HL <sup>2</sup>	--	--	--	4
[CuL <sup>2</sup> Cl]CH <sub>3</sub> OH (7)	--	5	--	--
[CuL <sup>2</sup> Br]·2H <sub>2</sub> O (8)	--	5	--	--
[CuL <sup>2</sup> NCS]·H <sub>2</sub> O (10)	--	5	--	--
[CuL <sup>2</sup> N <sub>3</sub> ] (11)	--	5	4	--
[CuL <sup>2</sup> (HL <sup>2</sup> )](ClO <sub>4</sub> ) (12)	--	5	--	--

## References

1. J.D. Lee. Concise Inorganic Chemistry, 4<sup>th</sup>ed., Oxford University Press 1991.
2. F.A. Cotton, G. Wilkinson, C.A. Murillo, Advanced Inorganic Chemistry, 6<sup>th</sup> ed., Wiley, New York, 1999.
3. S. Padhye, G.B. Kauffman, Coord. Chem. Rev. 63 (1985) 127.
4. E. Lukevics, D. Jansone, K. Rubina, E. Abele, S. Germane, L. Leite, M. Shymanska, J. Popelis, Eur.J.Med.Chem. 30 (1995) 983.
5. A. Usman, I.A. Razak, S. Chantrapromma, H.K. Fun, V. Philip, A. Sreekanth, M.R.P. Kurup, Acta Crystallogr, C 58 (2002) 652.
6. D.X. West, G.A. Bain, R.J. Butcher, J.P. Jainski, Y. Li, R.Y. Pozdniakiv, J. Valdes-Martinez, R.A. Toscano, Polyhedron 15 (1996) 665.
7. M.B. Ferrari, G. Fava, C. Pelizzi, P. Tarasani, J. Chem. Soc., Dalton Trans. (1992) 2153.
8. M.E. Hossain, M.N. Alam, J. Begum, M. Akbar Ali, M. Nazimuddin, F.E. Smith, R.C. Hynes, Inorg. Chim. Acta 249 (1996) 207.
9. A.E. Liberta, D.X. West, Biometals 5 (1992) 121.
10. D.X. West, A.M. Stark, G.A. Bain, A.E. Liberta, Transition Met. Chem. 21 (1996) 289.
11. D.X. West, J.S. Ives, J. Krejci, M.M. Salberg, T.L. Zumbahlen, G.A. Bain, A.E. Liberta, Polyhedron 14 (1995) 2189.
12. H. Beraldo, W. Nacif, A. Rebolledo, R. Costa, J.D. Ardisson, XI<sup>th</sup> Brazilian Meeting on Inorg. Chem. (2002).
13. H. Beraldo, A.M. Barreto, R.P. Vieira, A.P. Rebolledo, N.L. Speziali, C.B. Piheiro, G. Chapuis, J. Mol. Struct. 645 (2003) 213.
14. D.R. Smith, Coord. Chem. Rev. 172 (1998) 457.

15. J. Garcia-Tojal, J. Garcia-Jaca, R. Cortes, T. Rojo, M.K. Urriaga, M.I. Arriortua, *Inorg. Chim. Acta* 249 (1996) 25.
16. M.A. Ali, K.K. Dey, M. Nazimuddin, F.E. Smith. R.J. Butcher, J.P. Jasinski, J.M. Jasinski, *Polyhedron* 15 (1996) 3331.
17. P. Souza, A.I. Matesanz, V. Fernandez, *J.Chem. soc.. Dalton Trans.* (1996) 3011.
18. W.J. Geary, *Coord. Chem. Rev.* 7 (1971) 81.
19. K. Nakamoto, *Infrared and Raman spectra of Inorganic and Coordination Compounds*, 5<sup>th</sup> ed. Wiley, New York, 1997.
20. D.X. West, N.M. Kozub, G.A. Bain, *Transition Met. Chem.* 21 (1996) 52.
21. R.J. Clark, C.S. Williams. *Inorg. Chem.* 4 (1965) 350.
22. S.K. Jain, B.S. Garg, Y.K. Bhoon, *Spectrochim. Acta* 42A (1986) 959.
23. M.R. Rosenthal, *J. Chem. Edu.* 50 (1973) 331.
24. C.C. Addison, N. Logan, S.C. Wallwork, D. Barner, *Rev. Chem. Soc.* 25 (1971) 289.
25. S.K. Jain, B.S. Garg, Y.K. Bhoon, *Spectrochim. Acta* 42 (1986) 701.
26. D.X. West, G. Ertem, R.M. Makeever. *Transition Met. Chem.* 10 (1985) 41.
27. A. Sreekanth, M.R.P. Kurup, *Polyhedron* 22 (2003) 3321.
28. R.A. Bailey, S.L. Kozak, T.W. Michelson, W.N. Mills. *Coord. Chem. Rev.* 6 (1971) 407.
29. B.S. Garg, M.R.P. Kurup, S.K. Jain, Y.K. Bhoon, *Transition Met. Chem.* 13 (1988) 309.
30. V. Stefov, V.M. Petrusevski, B. Soptrajanov, *J. Mol. Struct.* 293 (1993) 97.
31. D.X. West, N.M. Kozub, G.A. Bain, *Transition Met. Chem.* 21 (1996) 52.
32. D.X. West, S.I. Dietrich, I. Thientanavanich, C.A. Brown, *Transition Met. Chem.* 19 (1994) 195.
33. D.X. West, C.S. Carlson, C.P. Galloway, A.E. Liberta, C.R. Daniel, *Transition Met. Chem.* 15 (1990) 91.

34. A.B.P. Lever, *Inorganic Electronic Spectroscopy*, 2<sup>nd</sup> ed., Elsevier Science, New York, 1984.
35. B. Harikumar, M.R.P. Kurup, T.N. Jayaprakash, *Transition Met. Chem.* 22 (1997) 507.
36. D.N Sathyanarayana, *Electronic Absorption Spectroscopy and Related Techniques*, Universities Press, Hyderabad, 2001.
37. D. Kivelson, R. Neiman, *J. Chem. Phys.* 35 (1961) 149.
38. I.M. Proctor, B.J. Hathaway, P. Nicholis, *J. Chem. Soc.*(1968) 1678.
39. B.J. Hathaway, D.E. Billing, *Coord. Chem. Rev.* 5 (1970) 1949.
40. A.H. Maki, B.R. McGrahey, *J. Chem. Phys.* 28 (1958) 35.
41. P. Bindu, M.R.P. Kurup, T.R. Satyakeerty, *Polyhedron* 18 (1998) 321.



## SYNTHESIS, SPECTRAL AND BIOLOGICAL STUDIES OF IRON(III) COMPLEXES

### 5.1. Introduction

Iron is the second most abundant metal after Al and the fourth most abundant element in the earth's crust. The name 'iron' is Anglo-Saxon in origin (*iren*) and the symbol Fe and words such as ferrous and ferric are derived from the Latin *ferrum*, *iron*. Iron is the most important transition element involved in living systems, being vital to both plants and animals. Iron plays crucial role in the transport and storage of oxygen and also in electron transport [1].

The main oxidation states of iron are II ( $d^6$ ) and III ( $d^5$ ). Most iron(II) complexes are octahedral, tetrahedral, square planar and trigonal bipyramidal, though dodecahedral iron(II) complexes also are known to exist. Iron(III) complexes may be high spin or low spin, and an octahedral stereochemistry is most common. A number of other geometries also are found.

There have been several reports on iron(III) complexes of 2-acetylpyridine thiosemicarbazone, 2-formylpyridine thiosemicarbazone, substituted 2-acetylpyridine thiosemicarbazones etc [2, 3, 4]. Spingam and Sartorelli [5] have synthesized several thiosemicarbazones of 2-pyrazine carboxaldehyde thiosemicarbazone and related compounds to remove iron from the model systems designed to mimic particular aspects of chronic transfusional iron overload. The 2-pyrazine carboxaldehyde thiosemicarbazone has been found to be more effective in reducing tissue iron levels than the deferoxamine, which is used for removing the excess iron accumulated in the tissues of patients with Cooley's anemia [6, 7]. This Chapter contains the synthesis of four iron(III) complexes using the ligands HL<sup>1</sup> and HL<sup>2</sup> and their spectral, magnetic and biological studies.

## 5.2. Experimental

### 5.2.1. Materials

The details regarding the synthesis and characterization of HL<sup>1</sup> and HL<sup>2</sup> are given in Chapter 2. All the iron(III) salts were used as received. The solvents were purified by the usual methods.

### 5.2.2. Synthesis of complexes

#### $[Fe(L^1)_2NO_3] \cdot C_2H_5OH$ (13)

Ferric nitrate  $Fe(NO_3)_3 \cdot 9H_2O$  (1 mmol, 0.404 g) in 20 ml ethanol and HL<sup>1</sup> (2 mmol, 0.676 g) in 50 ml hot ethanol were mixed and refluxed for 8 hrs. On keeping for 2 days the brown shining solids that separated, were filtered, washed with hot water, hot ethanol and ether and dried over  $P_4O_{10}$  *in vacuo*.

#### $[Fe(L^2)_2NO_3] \cdot 2H_2O$ (14)

Ferric nitrate  $Fe(NO_3)_3 \cdot 9H_2O$  (1 mmol, 0.404 g) in 20 ml methanol and HL<sup>2</sup> (2 mmol, 0.664 g) in 40 ml hot methanol were mixed and refluxed for 6 hrs. On cooling, the brown shining solids that separated, were filtered, washed with hot water, hot ethanol and ether and dried over  $P_4O_{10}$  *in vacuo*.

#### $[Fe(L^2)_2Cl]$ (15)

Ferric chloride anhydrous  $FeCl_3$  (1 mmol, 0.162 g) dissolved in 20 ml hot methanol and HL<sup>2</sup> (2 mmol, 0.664 g) dissolved in 40 ml hot methanol were mixed and refluxed for 6 hrs. The blue colored solids that separated while heating, were filtered, washed with hot water, hot methanol and ether. The compound was dried over  $P_4O_{10}$  *in vacuo*.

***[Fe(L<sup>2</sup>)<sub>2</sub>NCS] (16)***

Ferric chloride, FeCl<sub>3</sub> (1 mmol, 0.162 g) dissolved in 20 ml hot methanol and HL<sup>2</sup> (2 mmol, 0.664 g) dissolved in 40 ml hot methanol were refluxed for 2 hrs. To the refluxing solution, potassium thiocyanate (1 mmol, 0.097 g) in 10 ml methanol was added and again refluxed for 4 hrs. The black crystals that separated, on keeping overnight, were filtered, washed with hot water, hot methanol and ether and dried over P<sub>4</sub>O<sub>10</sub> *in vacuo*.

***5.2.3. Analytical methods***

Details regarding the various analytical methods such as elemental analysis, magnetic susceptibility measurements, molar conductivity measurements, electronic, infrared, and EPR spectral analyses were discussed in Chapter 2.

**5.3. Results and discussion*****5.3.1. Analytical measurements***

The colors, stoichiometries, elemental analyses, and magnetic moments of the Fe(III) complexes are given in Table 5.1. The analytical data calculated for the four iron(III) complexes reveal the 1:2:1 stoichiometry for iron, thiosemicarbazone and gegenion. All the iron(III) complexes are found to be insoluble in methanol, ethanol, acetone and chloroform, but soluble in dimethylformamide and in dimethyl sulphoxide.

The molar conductivity measurements of all the complexes in DMF (10<sup>-3</sup> M solution) have values in the range 30-50 ohm<sup>-1</sup>cm<sup>2</sup> mole<sup>-1</sup>, which are consistent with their non-electrolytic nature [8]. This indicates that the anions are associated in the first coordination sphere of Fe(III).

Table 5.1 Analytical data, color and magnetic moments of Fe(III) complexes

Compound	Empirical formula	Color	Analytical data. Found (Calculated)%			$\mu$ (B.M.) at 300K	$\Lambda^*_M$ (in DMF)
			C	H	N		
[Fe(L <sup>1</sup> ) <sub>2</sub> NO <sub>3</sub> ].C <sub>2</sub> H <sub>5</sub> OH (13)	C <sub>40</sub> H <sub>48</sub> N <sub>9</sub> S <sub>2</sub> O <sub>4</sub> Fe	Brown	56.95 (57.29)	5.62 (5.73)	15.16 (15.04)	2.0	49.9
[Fe(L <sup>2</sup> ) <sub>2</sub> NO <sub>3</sub> ].2H <sub>2</sub> O (14)	C <sub>38</sub> H <sub>34</sub> N <sub>9</sub> S <sub>2</sub> O <sub>5</sub> Fe	Brown	56.57 (55.89)	4.41 (4.16)	15.07 (15.44)	2.2	35.6
[Fe(L <sup>3</sup> ) <sub>2</sub> Cl]	(15) C <sub>38</sub> H <sub>30</sub> N <sub>8</sub> S <sub>2</sub> ClFe	Blue	60.91 (60.53)	4.11 (3.98)	14.60 (14.86)	2.49	31.2
[Fe(L <sup>2</sup> ) <sub>2</sub> NCS]	(16) C <sub>39</sub> H <sub>30</sub> N <sub>9</sub> S <sub>3</sub> Fe	Black	60.01 (60.32)	4.09 (3.87)	16.04 (16.24)	1.98	42.6

\*Molar conductivity in ohm<sup>-1</sup>cm<sup>2</sup>mol<sup>-1</sup> at 298 K using 10<sup>-3</sup> M solution

### 5.3.2. Magnetic susceptibilities

High spin Fe(III) complexes in general, have magnetic moments at room temperature very close to the spin only value of 5.9 B.M. because the ground state (derived from the  ${}^6S$  state of free ion) has no orbital angular momentum and there is no effective mechanism for introducing any coupling with the excited state. The low-spin complexes with  $t_{2g}^5$  configurations, usually have considerable orbital contribution to their magnetic moments and at room temperature the magnetic moment value is  $\sim 2.3$  B.M. [9]. The magnetic moments of the synthesized iron(III) complexes in the polycrystalline state at room temperature are found to be in the range of 1.95-2.46. These  $\mu_{eff}$  values fall in the range of those of low-spin iron(III) complexes [4].

### 5.3.3. Infrared spectra

The tentative infrared spectral assignments of the ligands HL<sup>1</sup> and HL<sup>2</sup> and their Fe(III) complexes are given in Table 5.2. The  $\nu(C=N)$  bands of the thiosemicarbazones are found at 1582 and 1591  $\text{cm}^{-1}$  respectively. These strong bands are shifted after coordination towards lower energies by *ca.* 30  $\text{cm}^{-1}$ , indicating coordination *via* azomethine nitrogen [10]. The  $\nu(N-N)$  bands of the thiosemicarbazones are found at 1118 and 1102  $\text{cm}^{-1}$ . The increase in the frequency of this band in the spectra of the complexes is an evidence for the enolisation of the ligand and the coordination *via* the azomethine nitrogen.

The bands observed at 833 and 835  $\text{cm}^{-1}$  for HL<sup>1</sup> and HL<sup>2</sup> respectively are assigned to  $\nu(C=S)$ . These bands are found to be shifted to low energy in the spectra of the complexes, indicating coordination *via* the thiolate sulfur. The out-of-plane pyridine ring deformation modes of the free ligands at 607 and 622  $\text{cm}^{-1}$

are found to be shifted to higher energies in the spectra of the complexes indicating coordination *via* the nitrogen atom of the pyridine ring [11].

The coordination positions of the thiosemicarbazones in the iron(III) complexes are confirmed by assigning the strong bands observed in the far IR spectra of the complexes as suggested by Nakamoto [12]. The strong bands observed at 363-370  $\text{cm}^{-1}$  are assigned to  $\nu(\text{Fe-N})$  of the pyridine ring. Another  $\nu(\text{Fe-N})$  band is observed at 482-495 in the spectra of the Fe(III) complexes indicating  $\nu(\text{Fe-N})$  of the azomethine group. Again the strong bands observed in the region 442-455 are assigned to the  $\nu(\text{Fe-S})$  bond. The iron-chlorine stretching band is normally observed between 300-200  $\text{cm}^{-1}$  [13]. A strong band at 255  $\text{cm}^{-1}$  in the chloro complex confirms the coordination of the chloride ion to Fe(III).

The IR spectrum of  $[\text{Fe}(\text{L}^1)_2\text{NO}_3]\cdot\text{C}_2\text{H}_5\text{OH}$  which exhibits two bands at 1492 and 1384  $\text{cm}^{-1}$  corresponds to the NO stretching bands of the nitrate ion. The separation of these bands by 108  $\text{cm}^{-1}$  indicates the unidentate nature of the nitrate ion in the complex [14].

Similarly the bands at 1439 and 1319  $\text{cm}^{-1}$  in the spectrum of  $[\text{Fe}(\text{L}^2)_2\text{NO}_3]\cdot 2\text{H}_2\text{O}$  confirm the terminal unidentate coordination of the nitrate ion to Fe(III) in the complex. According to Stefov et al [15] coordinated water should exhibit frequencies at 825, 575 and 500  $\text{cm}^{-1}$ . The absence of spectral bands in these regions in the spectrum of this complex indicates that the water molecules in  $[\text{Fe}(\text{L}^2)_2\text{NO}_3]\cdot 2\text{H}_2\text{O}$  are not coordinated, but exist as lattice water.

Table 5.2 I.R. spectral assignments ( $\text{cm}^{-1}$ ) of  $\text{HL}^1$  and  $\text{HL}^2$  and its Fe(III) complexes

Compound	$\nu(\text{C}=\text{N})$	$\nu(\text{N}-\text{N})$	$\nu(\text{C}-\text{S})$	$\rho(\text{py})$	$\nu(\text{Fe}-\text{N})$	$\nu(\text{Fe}-\text{N})_{\text{py}}$	$\nu(\text{Fe}-\text{S})$	$\nu(\text{Fe}-\text{X})$
$\text{HL}^1$	1582w	1118s	833m	607m	--	--	--	--
$[\text{Fe}(\text{L}^1)_2\text{NO}_3] \cdot \text{C}_2\text{H}_5\text{OH}^{\text{a}}$ (13)	1546s	1153m	744m	641w	482s	368s	454s	--
$\text{HL}^2$	1591s	1102s	835	622m	--	--	--	--
$[\text{Fe}(\text{L}^2)_2\text{NO}_3] \cdot 2\text{H}_2\text{O}^{\text{b}}$ (14)	1546s	1125m	752m	665m	492s	363s	442s	--
$[\text{Fe}(\text{L}^2)_2\text{Cl}]$ (15)	1566s	1123s	756s	659m	491s	368s	455s	255s
$[\text{Fe}(\text{L}^2)_2\text{NCS}]$ (16)	1562 s	1118m	766s	638w	495s	370s	451s	--

<sup>a</sup>  $\nu(\text{NO}_3)$ -1492  $\text{cm}^{-1}$ , 1384  $\text{cm}^{-1}$ ; <sup>b</sup>  $\nu(\text{NO}_3)$ -1439  $\text{cm}^{-1}$ , 1319  $\text{cm}^{-1}$

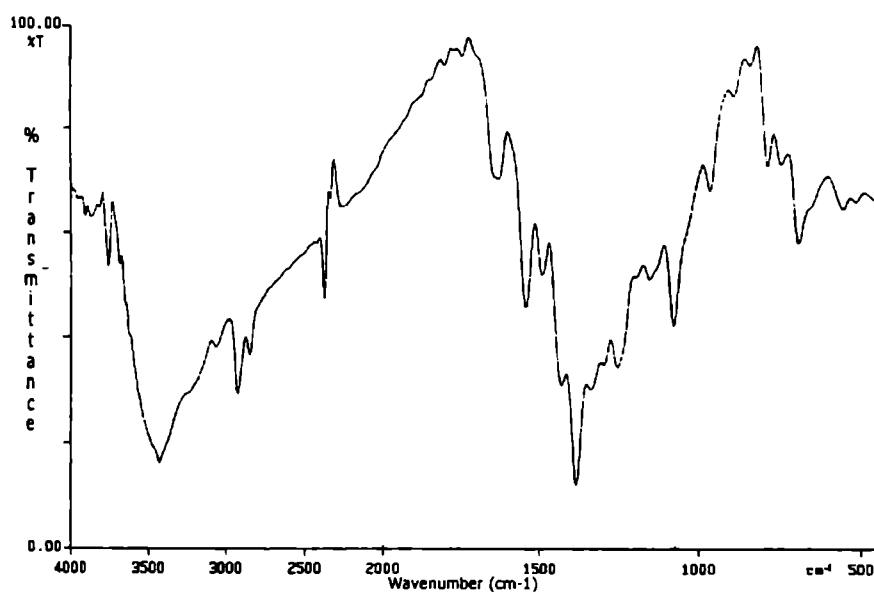


Fig.5.1. IR Spectrum of compound 13

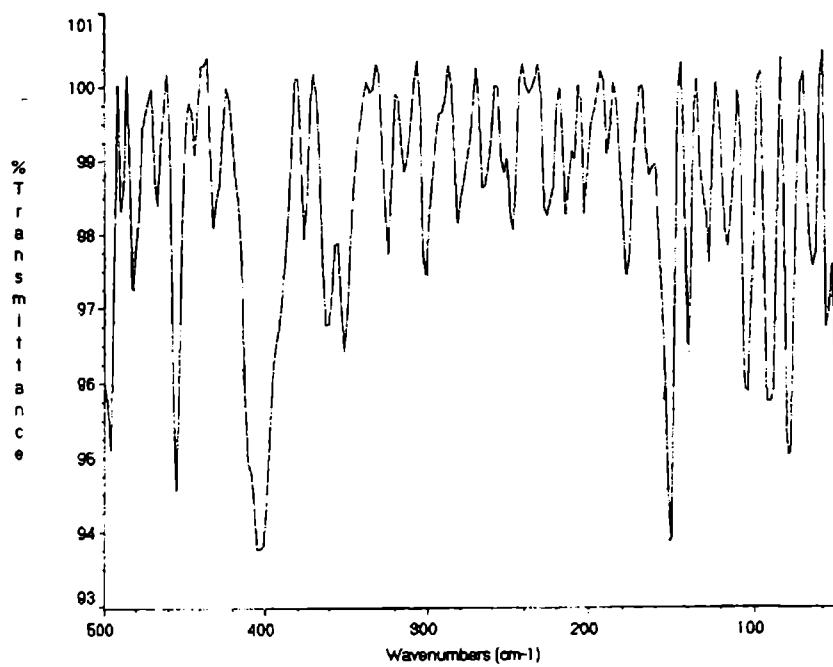


Fig. 5.2. Far IR spectrum of compound 13



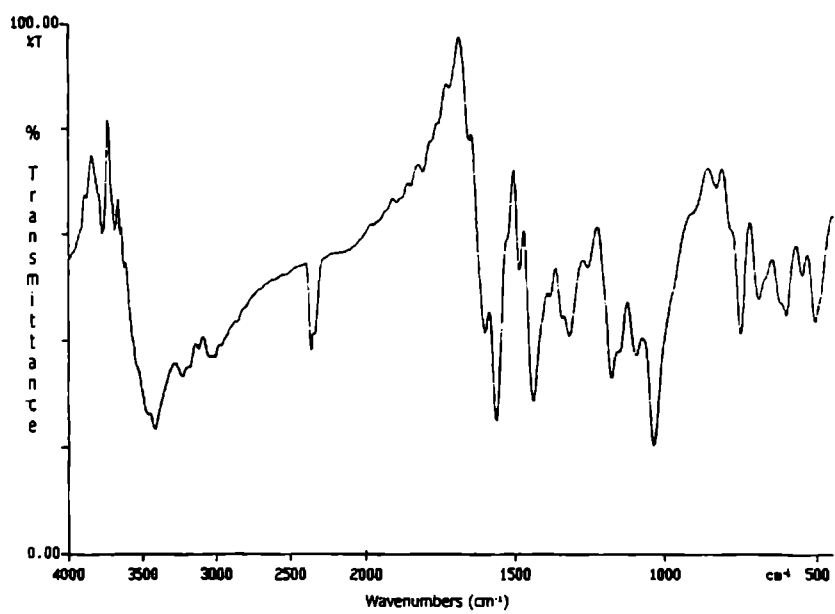


Fig.5.3. IR Spectrum of compound 14

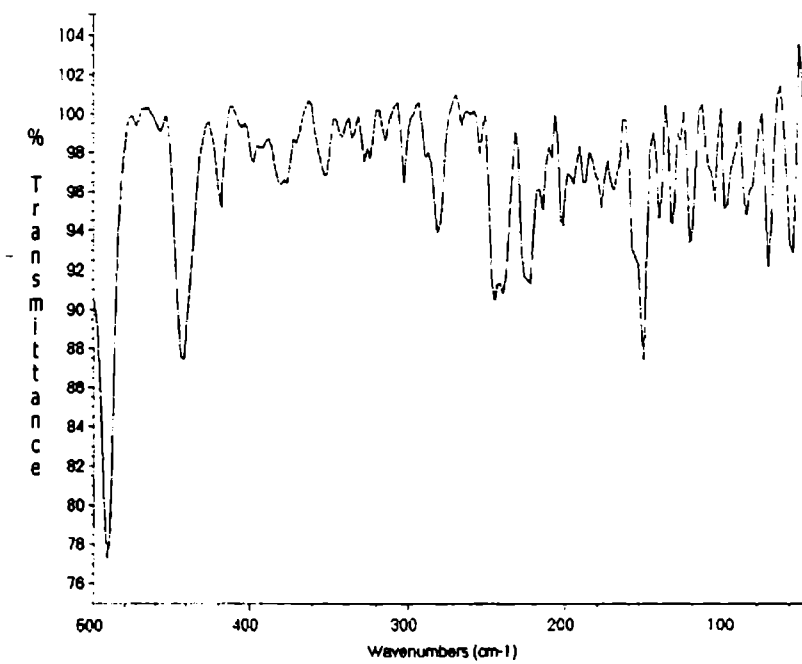


Fig. 5.4. Far IR spectrum of compound 14

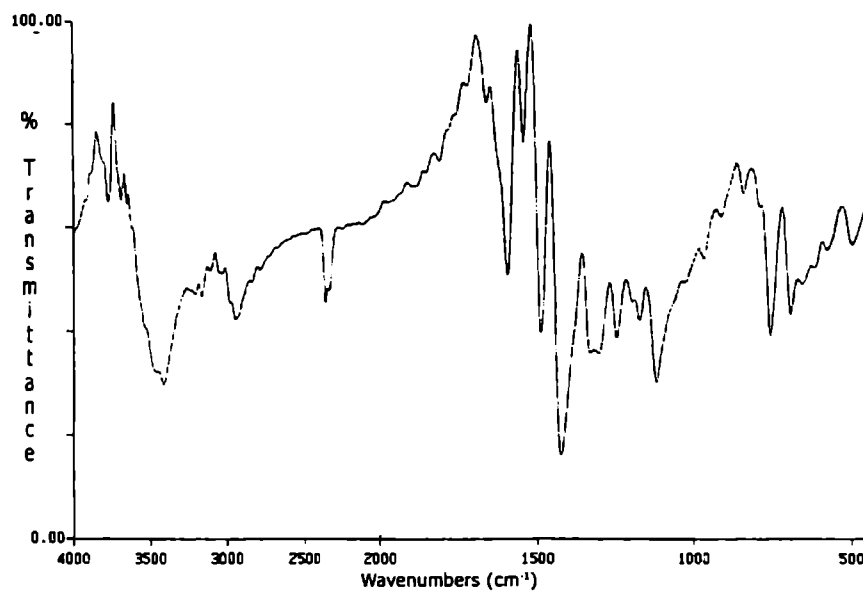


Fig.5.5. IR spectrum of compound 15

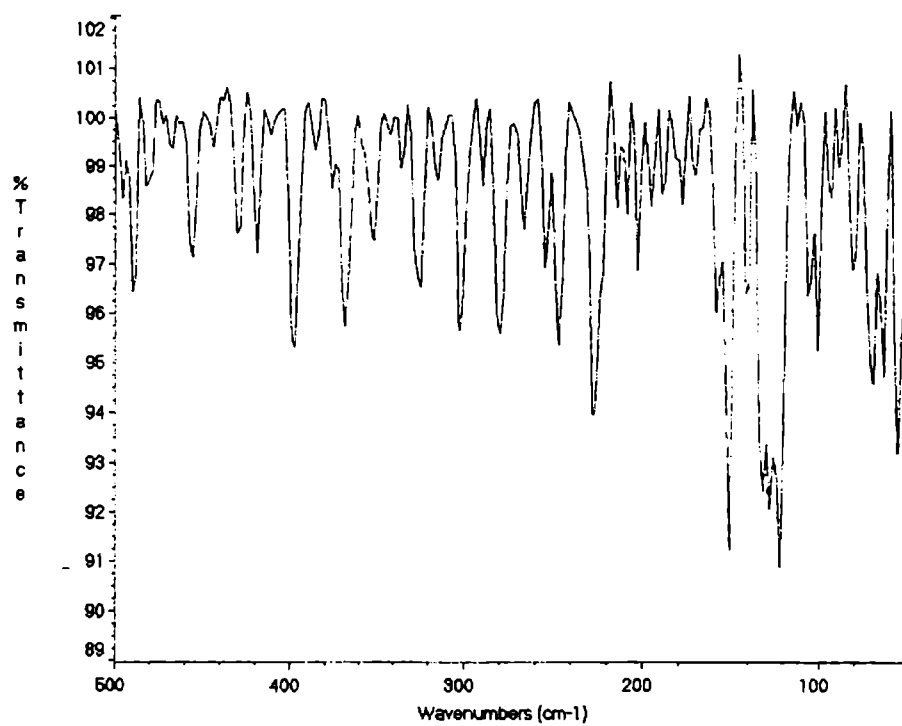


Fig.5.6. Far IR spectrum of compound 15

### 5.3.4. Electronic spectra

The electronic absorption bands recorded in the polycrystalline state of the iron(III) complexes are given in Table 5.3. The bands observed at *ca.* 277 and 335 nm can be assigned to the  $\pi \rightarrow \pi^*$  and  $n \rightarrow \pi^*$  transitions of the ligand. Usually  $n \rightarrow \pi^*$  transitions occur at a lower energy than  $\pi \rightarrow \pi^*$  transitions. Two broad absorption bands are present in the region 656–400 nm. They are charge transfer transitions [16] due to  $d \rightarrow \pi^*$  metal-to-ligand and  $S \rightarrow Fe(III)$  electronic transitions [17].

Because of the greater oxidizing power of Fe(III), ligand to metal charge transfer bands often obscure the very low intensity, spin forbidden,  $d-d$  absorption bands [18]. In the spectra of iron(III) complexes, the shoulders that appeared at *ca.* 890 nm are due to  $d \rightarrow d$  transitions [11].

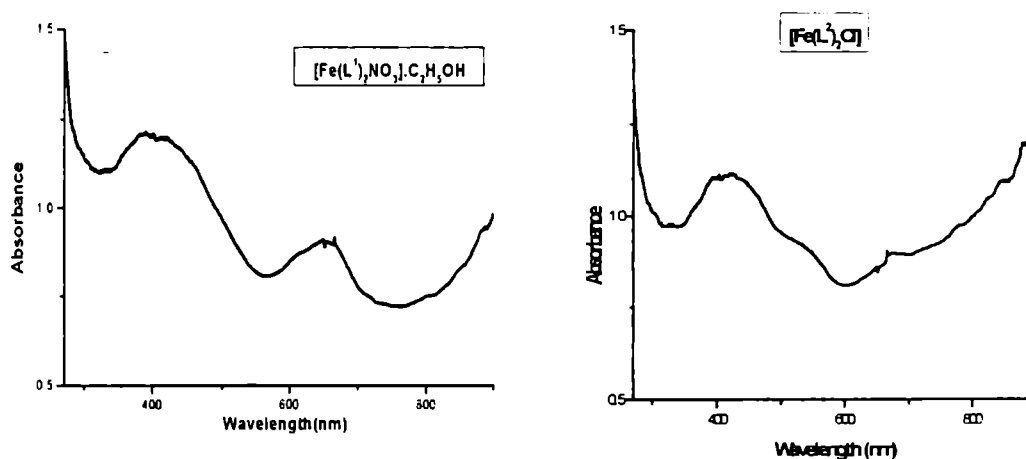


Fig.5.7. Electronic spectra of compounds 13 and 14

Table 5.3 Electronic spectral data (nm) of Iron(III) complexes

Compound	<i>d-d</i>	Charge transfer	<i>n</i> → <i>π</i> *	<i>π</i> → <i>π</i> *
Fe(L <sup>1</sup> ) <sub>2</sub> NO <sub>3</sub> ·C <sub>2</sub> H <sub>5</sub> OH (13)	890sh	650, 402	335	276
[Fe(L <sup>2</sup> ) <sub>2</sub> NO <sub>3</sub> ]·2H <sub>2</sub> O (14)	875sh	656, 419	332	278
[Fe(L <sup>2</sup> ) <sub>2</sub> Cl] (15)	887sh	655, 417	337	278
[Fe(L <sup>2</sup> ) <sub>2</sub> NCS (16)	884sh	652, 408	330	280

### 5.3.5. Electron paramagnetic resonance spectra

The EPR spectra of the iron(III) complexes in the polycrystalline state were recorded at 298 and 110 K and in DMF solution at 110 and 77 K and the EPR parameters are given in Table 5.4. The EPR spectrum of the *d*<sup>5</sup> iron(III) is expressed by the spin Hamiltonian [19, 20]:

$$\hat{H} = \beta[g_x H_x \cdot S_x + g_y H_y \cdot S_y + g_z H_z \cdot S_z] \quad \text{with } S = 1/2 \text{ and } g = 2.00$$

The spectra of all the complexes in the polycrystalline state and in DMF solution at different temperatures, show three *g* values, indicating that these complexes have rhombic distortion. There is little difference in the spectra obtained in frozen DMF and in the solid state indicating that the iron(III) centres do not undergo alteration in solution.

The observed anisotropic character with three *g* values due to rhombic distortion is common for spin-paired iron(III) complexes [21]. The *g* values confirm the low-spin character of iron(III) as obtained from the magnetic moment. The anisotropic character with the three *g* values due to rhombic distortion is not uncommon for spin paired iron(III) since this behavior has been reported for Schiff base as well as porphyrin Fe(III) complexes. The small deviation of the anisotropic

$g$  value from 2.0 suggests that the electronic structure of the ground state is  $(d_{xz})^2$ ,  $(d_{yz})^2$ ,  $(d_{xy})^1$  [22,23].

At 77 and 110 K, all the iron(III) complexes in DMF solution have similar anisotropic spectra with almost the same  $g_{av}$  values, indicating that the bonding in all the complexes is similar and is unaffected by the coordination of the anion.

Based on the physicochemical studies, the iron(III) complexes with nitrate, chloro, thiocyanato as counter-ions are assigned either a capped octahedral or a pentagonal bipyramidal geometry [24]. EPR data also suggest that the iron(III) complexes are low spin with the association of anions in the first coordination sphere of iron(III) in the solid state. In the capped octahedral structure two molecules of the ligand  $L^2$  or  $L^1$  can occupy the six corners of an octahedron and an additional position is occupied by an anion at one triangular face of this octahedron. In an alternate pentagonal bipyramidal structure [25], two molecules of the  $L^2$  or  $L^1$  can occupy two axial positions and four positions in the equatorial position plane, an additional fifth position in the equatorial plane being occupied by the anion. The structure suggested for the complexes is shown in Fig. 5.18.

Table 5.4 EPR spectral parameters of iron(III) complexes

Compound	State	Temperature (K)	$g_1$	$g_2$	$g_3$
[Fe(L <sup>1</sup> ) <sub>2</sub> NO <sub>3</sub> ]-C <sub>2</sub> H <sub>5</sub> OH (13)	Powder	298	2.080	2.2940	2.3344
	Powder	110	2.0176	2.1731	2.2098
	DMF	110	2.0199	2.1594	2.2046
	DMF	77	2.0695	2.1484	2.1809
[Fe(L <sup>2</sup> ) <sub>2</sub> NO <sub>3</sub> ]-2H <sub>2</sub> O (14)	Powder	298	2.0446	2.1282	2.1796
	Powder	110	2.0270	2.1414	2.1837
	DMF	110	2.0218	2.1564	2.2029
	DMF	77	2.0042	2.1292	2.1796
[Fe(L <sup>3</sup> ) <sub>2</sub> Cl (15)	Powder	298	2.0085	2.1301	2.1547
	Powder	110	2.0228	2.1496	2.1838
	DMF	110	2.0254	2.1472	2.1847
	DMF	77	2.1128	2.1266	2.1584
[Fe(L <sup>3</sup> ) <sub>2</sub> NCS (16)	Powder	298	2.0084	2.1340	2.1697
	DMF	77	2.0053	2.1272	2.1663

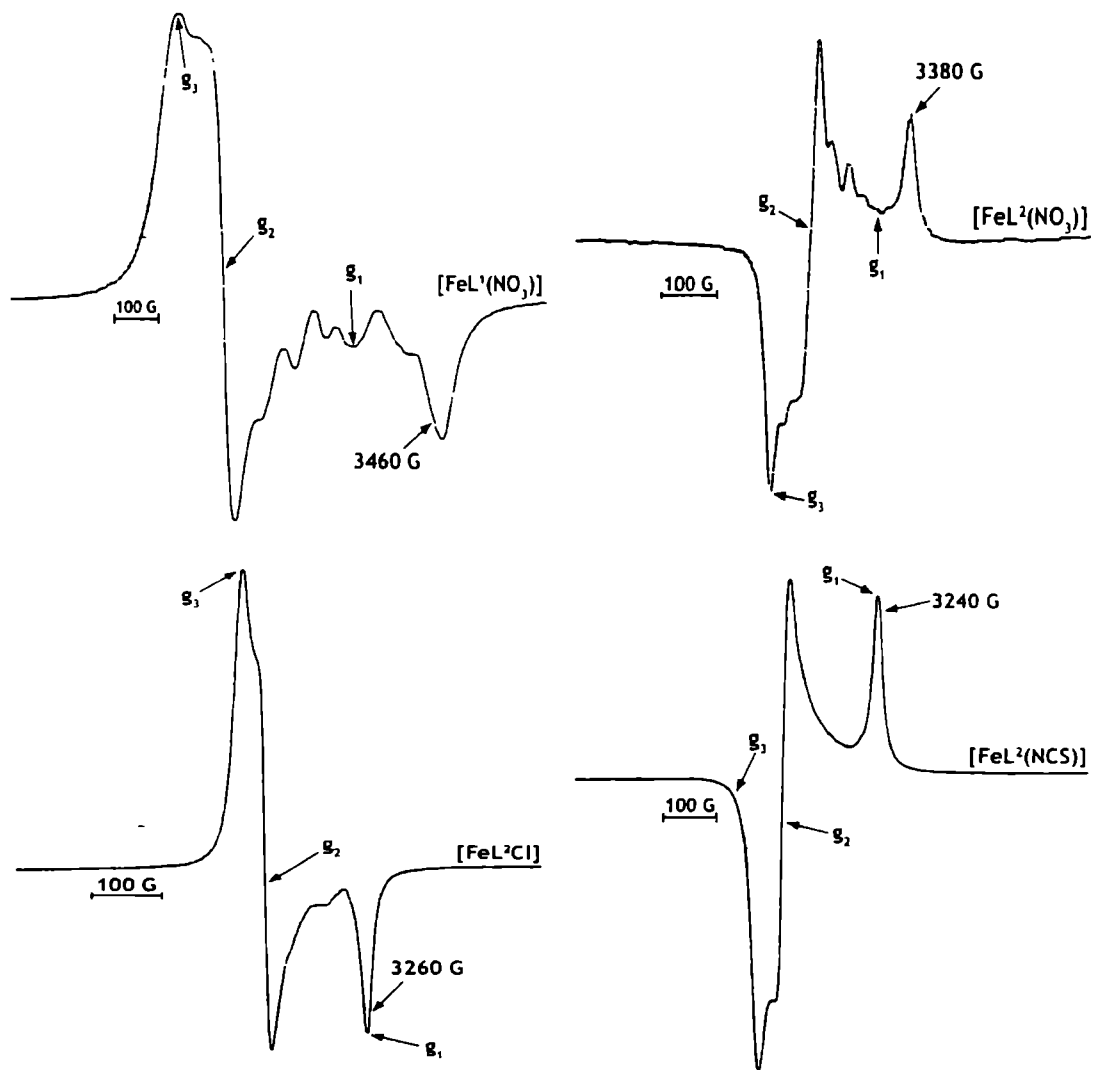


Fig 5.8. EPR spectra of compounds 13, 14, 15 and 16 in the polycrystalline state at 298 K

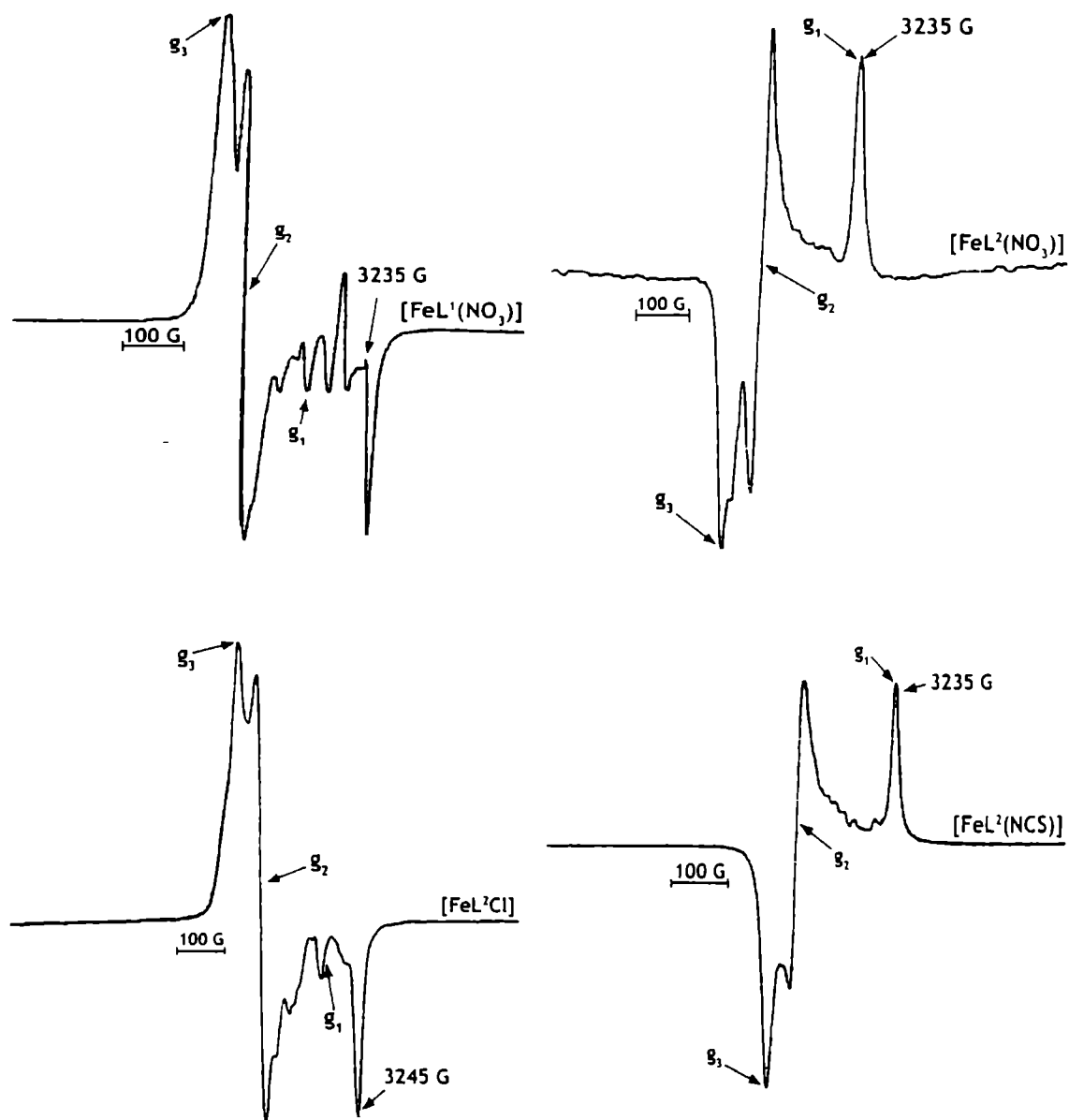


Fig 5.9. EPR spectra of compounds 13, 14, 15 and 16 in DMF at 77 K

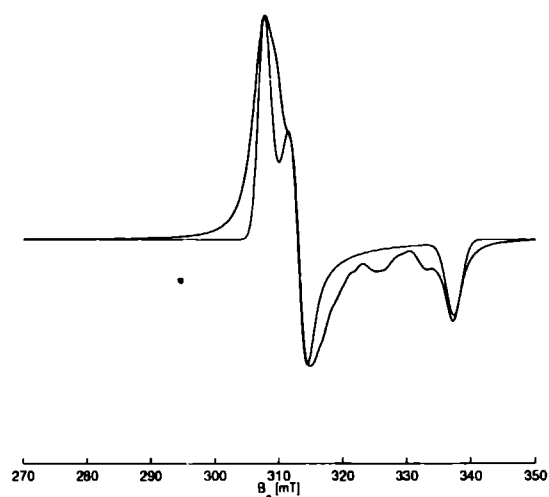


Fig.5.10. EPR spectrum of compound 13 in the polycrystalline state at 298 K

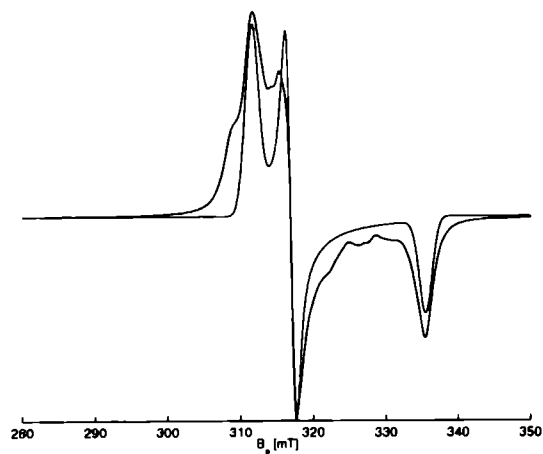


Fig.5.11. EPR spectrum of compound 14 in the polycrystalline state at 298 K

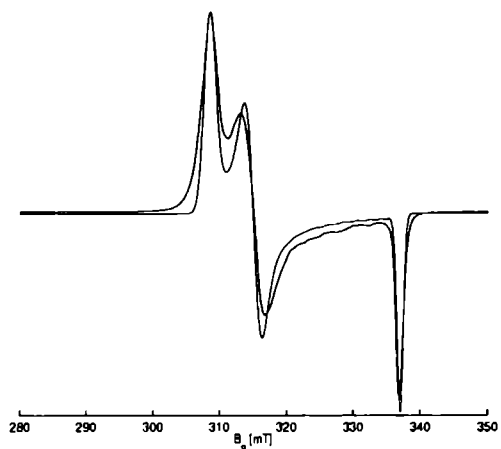


Fig.5.12. EPR spectrum of compound 13 in DMF at 110 K

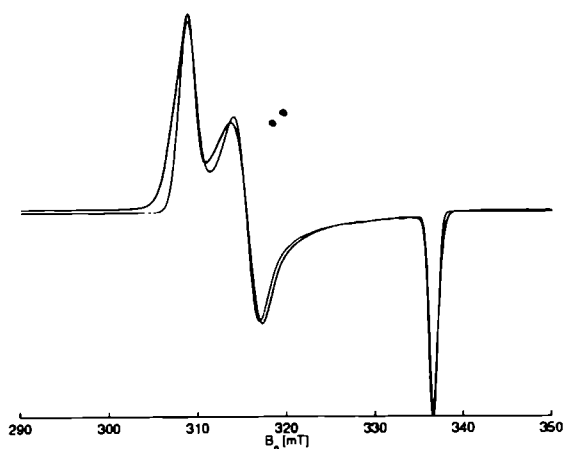


Fig.5.13. EPR spectrum of compound 14 in DMF at 110 K

Red-simulated; Blue-experimental



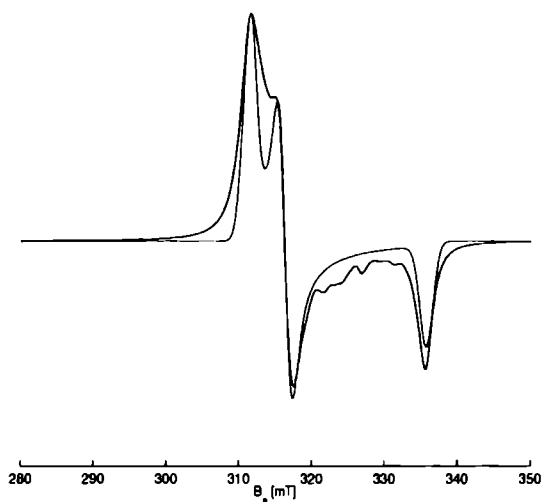


Fig.5.14. EPR spectrum of compound 15 in the polycrystalline state at 298 K

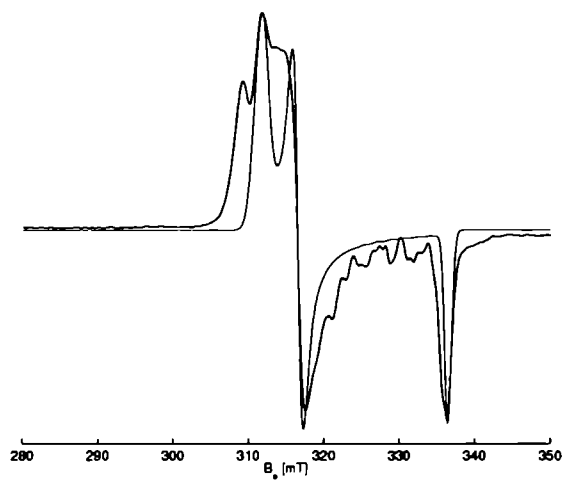


Fig.5.15. EPR spectrum of compound 15 in DMF at 110 K

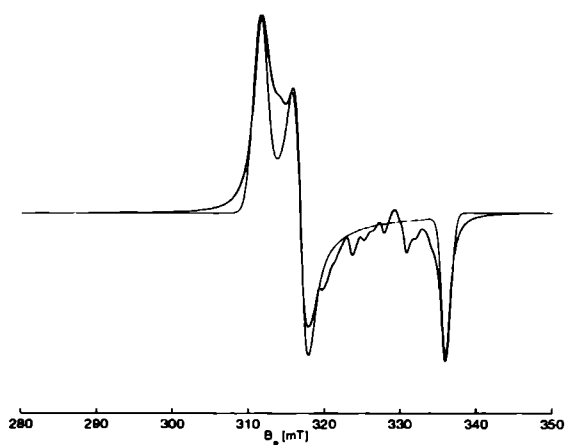


Fig.5.16. EPR spectrum of compound 13 in the polycrystalline state at 110 K

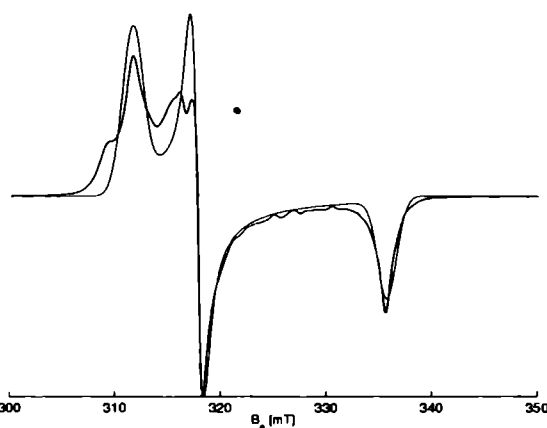


Fig.5.17. EPR spectrum of compound 14 in the polycrystalline state at 110 K

Red-simulated; Blue- experimental

#### 5.4. Antimicrobial activity

The four Fe(III) complexes are screened for antimicrobial activity using the Disc diffusion method against the five types of bacteria: 1. *Staphylococcus aureus*, 2. *Bacillus* sp (Gram Positive) 3. *Escherichia coli* 4. *Salmonella paratyphi* 5. *Vibrio cholerae* O1 (Gram Negative). All the complexes are found to be microbial inactive.

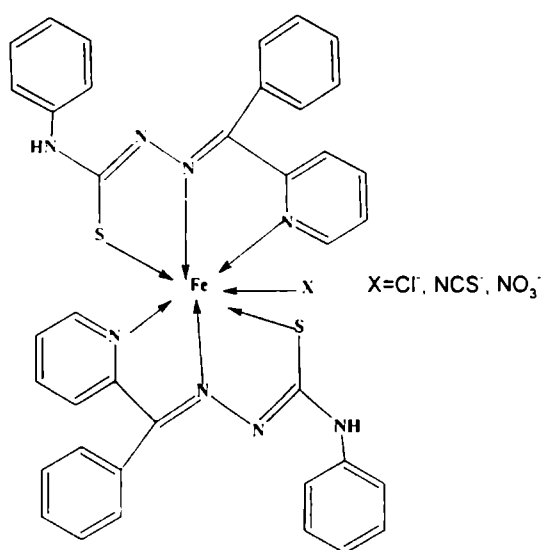


Fig.5.18. Tentative structure for  $[\text{Fe}(\text{L}^2)_2\text{X}]$

## References

1. N.N. Greenwood, A. Earnshaw, Chemistry of the Elements, 2<sup>nd</sup> ed., Reed Educational and Professional Publishing Ltd, 1997.
2. R. Raina, T.S. Srivastava, Inorg. Chim. Acta 91 (1984) 137.
3. B.S. Garg, M.R.P. Kurup, S.K. Jain, Y.K. Bhoon, Synth. React. Inorg. Met. Org. Chem. 28 (1998) 1415.
4. R. Raina, T.S. Srivastava, Indian J. Chem. 22A (1983) 701.
5. N.E. Spingarn, A.C. Sartorelli, J. Med. Chem. 22 (1979) 1314.
6. H.S. Waxman, E.B. Brown, Prog. Hematol 6 (1969) 338
7. A.W. Nienhius, J. Am. Med. Assos. 237 (1977) 1926.
8. W.J. Geary, Coord. Chem. Rev. 7 (1971) 81.
9. R.L. Dutta, A. Syamal, Elements of Magnetochemistry, 2<sup>nd</sup> ed., East-West Press, New Delhi, 1993.
10. V.M Leovac, L.S. Jovanovic, L.J. Bjelica, V.I. Cesljevic, Polyhedron 8 (1989) 135.
11. D.X. West, G. Ertem, M. Patricia, J.P. Scovill, D.L. Klayman, L. Judith. F. Anderson, R. Gillardi, C. George, L.K. Pannel, Transition Met. Chem. 10 (1985) 264.
12. K. Nakamoto. Infrared and Raman spectra of Inorganic and Coordination compounds, 5<sup>th</sup> ed., Wiley, New York, 1997.
13. R. Raina, T.S. Srivastava, Inorg. Chim. Acta 67 (1982) 83 .
14. S.K. Jain, B.S. Garg, Y.K. Bhoon, Transition Met.Chem.11 (1986) 89.
15. V. Stefov, V.M. Petrusevski, B. Soptrajanov, J.Mol.Struct. 293 (1993) 97.
16. S. Burman, D.N. Sathyanarayana, Indian J. Chem. 20A (1981) 57.
17. B.S. Garg, M.R.P. Kurup, S.K. Jain, Y.K. Bhoon, Transition Met. Chem. 13 (1988) 247.

18. A.B.P. Lever, *Inorganic Electronic Spectroscopy*, 2<sup>nd</sup> ed., Elsevier Science Publishing Company, Amsterdam, (1984).
19. B. Bleaney, M.C.M. Obrein. *Proc.Phys.Soc, London Sect. B* 69 (1956) 1216.
20. J.S. Griffith, *The Theory of Transition Metal ions*, Cambridge University Press, London, 1961.
21. Y. Nishida, A. Sumitha, K. Hayashida, H. Ohsima, S. Kida, Y. Maeda, *J.Coord.Chem.* 9 (1979) 161.
22. K. Nishida, O. Oshio, S. Kadia, *Inorg. Chim. Acta* 23 (1977) 59.
23. A. Sreekanth, M.R.P. Kurup, *Polyhedron* 23 (2004) 969.
24. B.S. Garg, M.R.P. Kurup, S.K. Jain, *Transition Met.Chem.*13 (1988) 247.
25. J.E. Huheey, *Inorganic Chemistry*, Harper and Row, Singapore, 1983.

## SPECTRAL CHARACTERIZATION OF MANGANESE(II) COMPLEXES

### 6.1. Introduction

Manganese is the twelfth most abundant element by weight in the earth's crust. Traces of manganese are found in many plants and bacteria, and a healthy human adult has about 10-20 mg of manganese in his body. It is an essential trace element, forming the active sites of a number of metalloproteins. In these metalloproteins, manganese can exist in any of the five oxidation states or in mixed valence states. For inorganic chemists, metalloproteins with two or even more manganese atoms per sub unit are particularly interesting. The most important natural role of manganese is in the oxidation of water in green plant photosynthesis where its presence in photosystem II is essential [1].

Manganese shows oxidation states ranging from (-III) to (+VII). The (+II) state is the most common and  $Mn^{2+}$  ions exist in the solid, in solution and as complexes. This Chapter deals with the synthesis, magnetic, spectral and biological studies of two Mn(II) complexes synthesized using the two ligands  $HL^1$  and  $HL^2$ .

### 6.2. Experimental

#### 6.2.1. Materials

The details regarding the synthesis of ligands  $HL^1$  and  $HL^2$  are discussed in Chapter 2. Manganese acetate and manganese sulphate are used for the synthesis of the complexes. The solvents are purified by standard methods of purification.

### 6.2.2. Synthesis of complexes

#### $[Mn(L^1)_2] \cdot H_2O$ (17)

Manganese acetate (1 mmol, 0.2449 g) dissolved in 20 ml ethanol and  $HL^1$  (2 mmol, 0.676 g) dissolved in 30 ml hot ethanol were mixed and stirred for 3 hrs. The yellow colored solids, which separated on cooling, were filtered, washed with hot ethanol and ether and dried over  $P_4O_{10}$  *in vacuo*.

#### $[Mn(L^2)_2]$ (18)

Manganese sulphate (1 mmol, 0.169 g) dissolved in a mixture of hot water and methanol and  $HL^2$  (2 mmol, 0.664 g) dissolved in 30 ml hot methanol were mixed and stirred for 3 hrs. The yellow colored solids, which separated, were filtered, washed with hot ethanol and ether and dried over  $P_4O_{10}$  *in vacuo*.

## 6.3. Results and discussion

### 6.3.1. Physical measurements

The two Mn(II) complexes are yellow powders, clearly soluble in chloroform, dimethylformamide and dimethylsulphoxide. The two complexes synthesised using the two ligands have the same stoichiometry  $MnL_2$  i.e. a structure in which two anionic ligands are coordinated to the Mn(II) ion. The details of the elemental analysis, physical characteristics and magnetic properties are given in Table 6.1.

Table 6.1 Analytical data

Compound	Empirical formula	Colour	Found (Calculated) %			$\Lambda_M^*$ (in DMF)	$\mu$ B.M.
			C	H	N		
$[\text{Mn}(\text{L}^1)_2] \cdot \text{H}_2\text{O}$ (17)	$\text{C}_{38}\text{H}_{44}\text{N}_8\text{S}_2\text{OMn}$	Yellow	61.78 (61.15)	5.96 (5.88)	14.92 (14.95)	1.8	5.94
$[\text{Mn}(\text{L}^2)_2]$ (18)	$\text{C}_{36}\text{H}_{30}\text{N}_8\text{S}_2\text{Mn}$	Yellow	63.27 (63.70)	4.30 (4.17)	15.46 (15.57)	5.02	5.79

\*Molar conductivity of  $10^{-3}\text{M}$  solution, in  $\text{ohm}^{-1}\text{cm}^2\text{mol}^{-2}$

### 6.3.2. Magnetic moments

Because of the additional stability of the half filled  $d$  shell, Mn(II) generally forms high spin complexes with an orbitally degenerate  ${}^6S$  ground state term and the spin only magnetic moment of 5.92 B.M., which will be independent of the temperature and stereochemistry, is expected [3]. The magnetic moments of the two Mn(II) complexes are calculated from the magnetic susceptibility measurements and using the diamagnetic corrections. The magnetic moments of the two complexes  $\text{Mn}(\text{L}^1)_2$  and  $\text{Mn}(\text{L}^2)_2$  are 5.94 and 5.79 B.M. respectively, indicating the presence of five unpaired electrons and hence these are high spin complexes [4].

### 6.3.3. IR spectra

The infrared spectral assignments ( $\text{cm}^{-1}$ ) of ligands  $\text{HL}^1$  and  $\text{HL}^2$  and their Mn(II) complexes are given in Table 6.2. The bonding sites of the thiosemicarbazone to the metal ion have been deduced by comparing the spectra of the complexes with the spectra of the ligands.

The  $\nu(\text{C}=\text{N})$  band of thiosemicarbazones are found to be shifted to higher frequencies in the spectra of the complexes suggesting the coordination of the

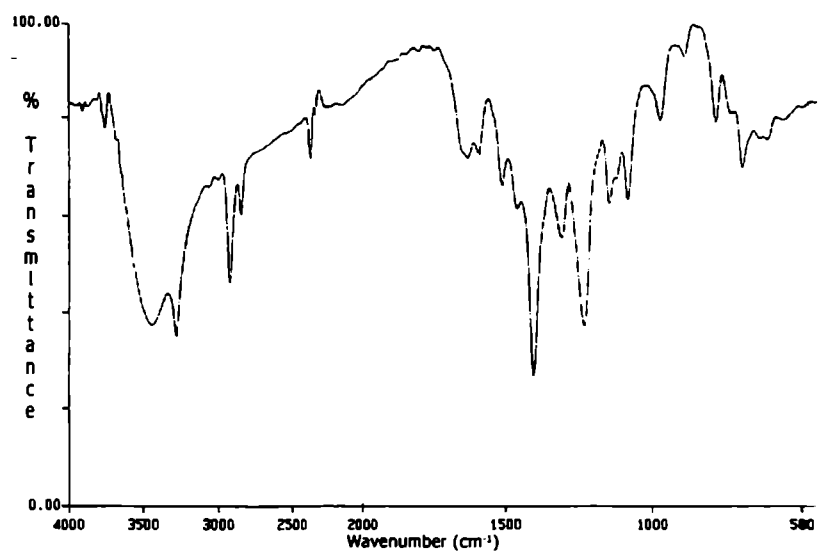


Fig.6.1. IR spectrum of compound 17

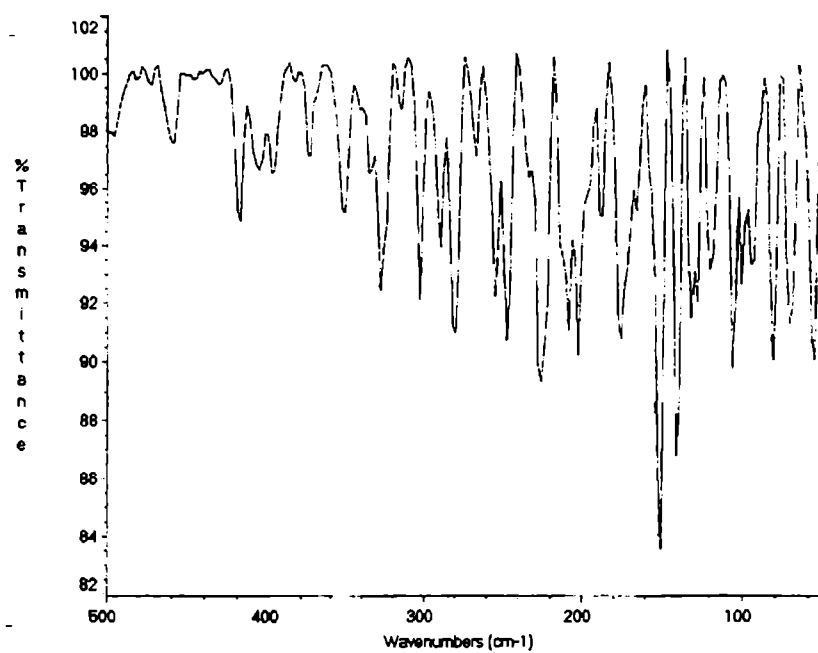


Fig.6.2. Far IR spectrum of compound 17



azomethine nitrogen to the Mn(II) ion. The involvement of this nitrogen in bonding is also supported by a shift in  $\nu(\text{N}-\text{N})$  to higher frequencies. The  $\nu(\text{C}=\text{S})$  bands in the ligands appear at *ca.* 1370 and 834  $\text{cm}^{-1}$ . These are found to be shifted to *ca.* 1319 and 784  $\text{cm}^{-1}$  in the complexes. This large negative shift of the  $\nu(\text{C}=\text{S})$  band indicates the coordination of the ligand via the thiolate sulfur to the manganese atom. The coordination of the nitrogen atom of the pyridine ring to the Mn(II) ion in the complexes is indicated by the shifting of the pyridine ring vibrations at 607 and 622  $\text{cm}^{-1}$  of HL<sup>1</sup> and HL<sup>2</sup>, respectively, to higher frequencies in their manganese complexes [5,6]. In the far IR spectra of the complexes, the bands at *ca.* 470, and 424  $\text{cm}^{-1}$  are assigned to the  $\nu(\text{Mn}-\text{N})$  and  $\nu(\text{Mn}-\text{S})$  modes [7] respectively.

#### 6.3.4. Electronic spectra

The electronic spectra of the two Mn(II) complexes are recorded in polycrystalline state and the spectral data are given in Table 6.3. The solid state electronic spectra of the two Mn(II) complexes contain a broad band at 435 nm which is a typical charge transfer transition as expected for an octahedral Mn(II) complex. The ground state term for high spin  $d^5$  configuration is  ${}^6S$ . Since there are no other terms of sextet spin multiplicity, all the  $d-d$  transitions in high spin  $d^5$  complexes are not only Laporte forbidden but also spin forbidden [8]. The ground state of the high spin octahedrally coordinated  $\text{Mn}^{2+}$  ion is  ${}^6A_{1g}$ . The ground state ( ${}^6A_{1g}$ ) is the only state with a multiplicity of 6. The  $d^5$  configuration gives rise to the  ${}^4G$ ,  ${}^4D$  and  ${}^4P$  excited states. The diffuse reflectance spectra of the Mn(II) complexes exhibit weak absorption bands at *ca.* 555, 435 and 385 nm. The three lowest energy bands are assigned to  ${}^6A_{1g} \rightarrow {}^4T_{1g}(G)$ ,  ${}^6A_{1g} \rightarrow {}^4T_{2g}(G)$  and  ${}^6A_{1g} \rightarrow {}^4E_g(G)$ ,  ${}^4A_{1g}(G)$  transitions. The pair of transitions  ${}^6A_{1g} \rightarrow {}^4E_g(G)$ ,  ${}^4A_{1g}(G)$  are degenerate in octahedral symmetry whose energies are given by  $10B+5C$ .

Table 6.2 IR spectral assignments of HL<sup>1</sup>, HL<sup>2</sup> and Mn(II) complexes

Compound	$\nu$ (C=N)	$\nu$ (N-N)	$\nu$ (C-S)	$\rho$ (py)	$\nu$ (Mn-N)	$\nu$ (Mn-S)	$\nu$ (Mn-N) py
HL <sup>1</sup>	1582m	1118s	1370s,833m	607m	--	--	--
[Mn(L <sup>1</sup> ) <sub>2</sub> ].H <sub>2</sub> O	1632m	1149m	1313s,786s	643w	459s	418s	303s
HL <sup>2</sup>	1591s	1102s	1369s,835m	622m	--	--	--
[Mn(L <sup>2</sup> ) <sub>2</sub> ]	1625m	1128s	1325s,782m	630s	489s	428m	316s

Table 6.3: Electronic spectral Data of Mn(II) complexes (nm)

Compound	${}^6A_{1g} \rightarrow {}^4T_{1g}(G)$	${}^6A_{1g} \rightarrow {}^4T_{2g}(G)$	${}^6A_{1g} \rightarrow {}^4E_g, {}^4A_{1g}(G)$	$n \rightarrow \pi^*$	$\pi \rightarrow \pi^*$	B	10Dq (cm <sup>-1</sup> )	C (cm <sup>-1</sup> )	$\beta = B/B_0$
[Mn(L <sup>1</sup> ) <sub>2</sub> ].H <sub>2</sub> O	550sh	437	386sh	334	271	692	8060	3058	0.8046
[Mn(L <sup>2</sup> ) <sub>2</sub> ]	546sh	433	389sh	329	277	667	8000	2948	0.775

These assignments are obtained by fitting the observed spectrum to the Tanabe Sugano diagram [9]. The energies corresponding to the above transitions and the values of Racah parameters B and C and Dq calculated are given in Table 6.3. The extent of covalence in the metal-ligand bond may be evaluated from the electronic spectrum by estimating  $\beta = B/B_0$ . The value of  $B_0$  for  $Mn^{2+}$  is  $860\text{ cm}^{-1}$  [10]. The absorption bands observed at  $\sim 350$  and  $270\text{ nm}$  are the  $n \rightarrow \pi^*$  and  $\pi \rightarrow \pi^*$  transitions of the ligand which remain unaltered in the complexes.

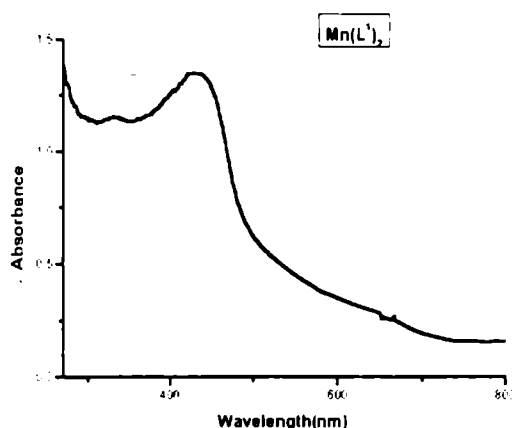


Fig.6.3. Electronic spectrum of compound 17

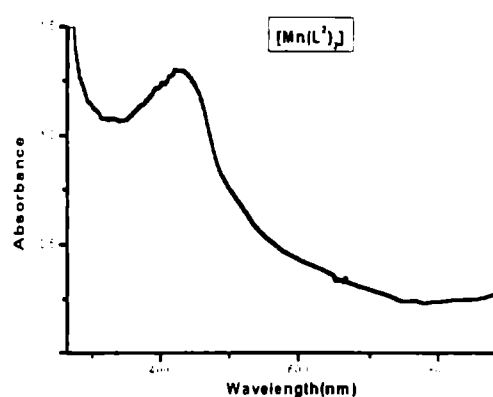


Fig.6.4. Electronic spectrum of compound 18

In the Tanabe-Sugano diagram for  $d^5$  octahedral complexes the ground state  ${}^6A_{1g}$  is taken as the abscissa, with the energies of the other states being plotted relative to it. Inter electronic repulsion is expressed in terms of the Racah parameters B and C, which are linear combinations of certain coulomb and exchange integrals pertaining to the uncomplexed ion. The parameter B is usually sufficient to evaluate the difference in energy between states of the same spin multiplicity; however, both the parameters are necessary for terms of different multiplicities [8].

### 6.3.5. EPR spectra

The high spin Mn(II) has  ${}^6S_{5/2}$  ground state term which should not interact with the electric field in the first order case. The spin-Hamiltonian ( $\hat{H}$ ) for Mn(II) can be defined as

$$\hat{H} = g\beta H_s + D[S_z^2 - S(S+1)/3] + E(S_x^2 - S_y^2)$$

where  $H$  is the magnetic field vector,  $g$  is the spectroscopic splitting factor,  $\beta$  the Bohr magneton,  $D$  is the axial zero field splitting term,  $E$  is rhombic zero field splitting parameter and  $S$  is the electron spin vector [11].

If  $D$  and  $E$  are very small, compared with  $g\beta H_s$ , five EPR transitions should be obtained with  $g$  value of  $\sim 2.0$  given by the Bra-Ket notations

$$|+5/2\rangle \leftrightarrow |+3/2\rangle, | +3/2\rangle \leftrightarrow | +1/2\rangle, | +1/2\rangle \leftrightarrow | -1/2\rangle, | -1/2\rangle \leftrightarrow | -3/2\rangle, \\ | -3/2\rangle \leftrightarrow | -5/2\rangle.$$

However, only if  $D$  is very large, the transition between  $|+1/2\rangle \leftrightarrow |-1/2\rangle$  will be observed. If  $D$  or  $E$  is very large, the lowest doublet has effective  $g$  value  $g_{\parallel} \sim 2.0$ ,  $g_{\perp} \sim 6.0$  for  $D \neq 0$  and  $E = 0$ , but for  $D = 0$  and  $E \neq 0$  middle Kramer's doublet has an isotropic  $g$  value of 4.29. Depending on the values of  $A$  and  $D$ , the number of lines appear in the spectra are 6, 24 or 30 [12].

For  $S = 5/2$  and noting the selection rule  $\Delta m_s = \pm 1$ , the allowed transitions should arise when field separations are dependent on  $\theta$ , the angle between the applied magnetic field and the symmetry axis. These transitions are:

$$\Delta m_s = \pm 5/2 \leftrightarrow 3/2; H = H_0 = 2D(3 \cos^2\theta - 1)$$

$$\Delta m_s = \pm 3/2 \leftrightarrow 1/2; H = H_0 = D(3 \cos^2\theta - 1)$$

$$\Delta m_s = \pm 1/2 \leftrightarrow -1/2; H = H_0$$

where  $H_0 = h\nu / g\beta$  and  $\theta$  is the angle between the applied magnetic field and the direction of the axial distortion. When the complex is very nearly octahedral only the central  $\Delta m_s = -1/2 \leftrightarrow +1/2$  transition will be observed since it

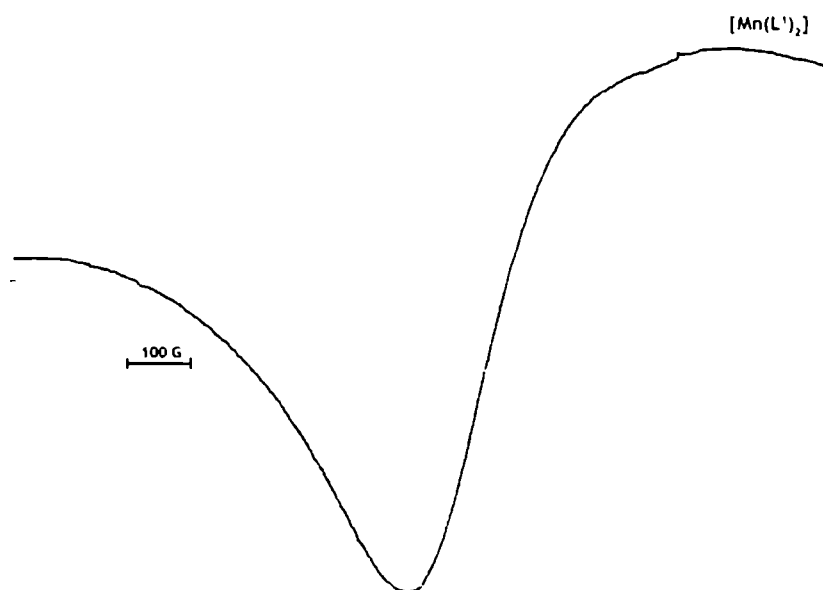


Fig.6.5. EPR spectrum of compound 17 in the polycrystalline state at 298 K

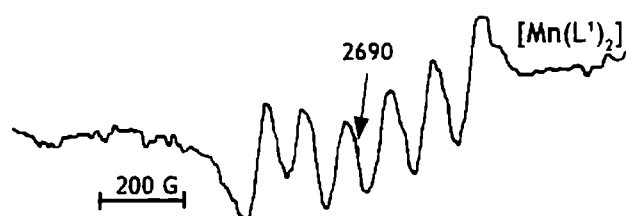


Fig. 6.6. EPR spectrum of compound 17 in DMF at 298 K

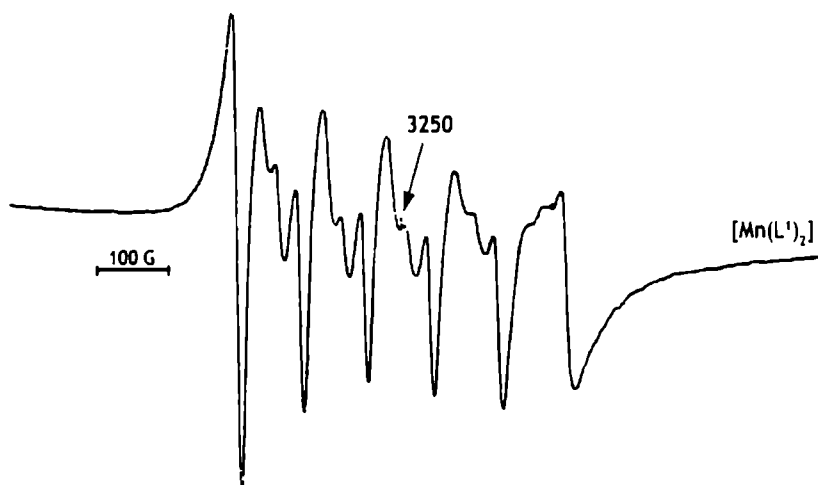


Fig.6.7. EPR spectrum of compound 17 in DMF at 77K

has only a second order dependence on  $D$ . This central line will of course be split into a sextet due to electron spin – nuclear spin hyperfine coupling ( $^{55}\text{Mn}$ ,  $I=5/2$ ). In addition to these allowed transitions the frozen solution spectra give low intensity pair of forbidden lines between each pair of hyperfine lines. These lines are due to the simultaneous change of both the electron and nuclear spin by  $\pm 1$ . The electron spin- nuclear spin hyperfine coupling constant  $A$  has been calculated by taking the average of all the observed lines [13].

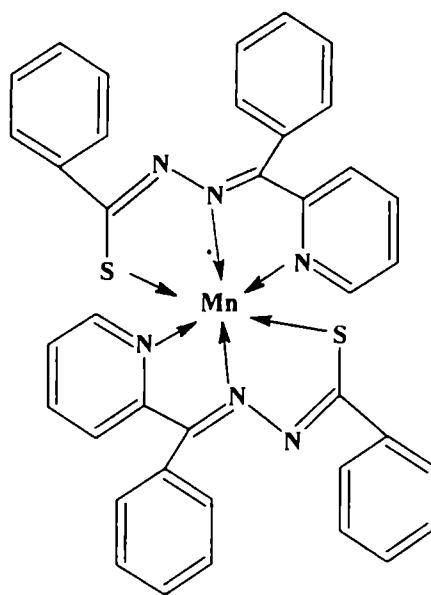
In the EPR spectra of the polycrystalline samples of two Mn(II) complexes at room temperature, a broad signal is observed with  $g$  value  $\sim 2.19$ . In polycrystalline samples, at room temperature, Mn(II) complexes give very broad signals, which are due to dipolar interactions and enhanced spin lattice relaxation [14].

The EPR spectra of the two compounds in DMF solution at RT are almost similar exhibiting a six line manganese hyperfine pattern centered at  $g = 1.993$  and  $2.008$  with hyperfine coupling constant  $A = 90$  and  $88$  G respectively. A sextet is

observed in the spectra of the compound **17** in DMF solution at room temperature due to electron spin nuclear spin coupling. This hyperfine spectrum of six lines corresponds to  $m_I = \pm 5/2, \pm 3/2, \pm 1/2$ , resulting from allowed transitions ( $\Delta m_S = \pm 1, \Delta m_I = 0$ ). This hyperfine lines are not clearly resolved in the spectrum of compound **18**, due to poor glass formation.

In addition to this axial field spectrum a pair of low intensity forbidden lines lying between each of the two main hyperfine lines is observed in the solution spectra of the complex **17** in DMF at 77 K, which is shown in figure 6.7. The forbidden lines in the spectrum arise due to the mixing of the nuclear hyperfine levels by the zero- field splitting factor of the Hamiltonian [15,16]. The  $g$  value is 2.005 and the  $A_{iso}$  value  $84.13 \times 10^{-4} \text{ cm}^{-1}$ . The average separation of the forbidden hyperfine lines in the spectrum is  $23.36 \times 10^{-4} \text{ cm}^{-1}$ .

The observed  $g$  values are very close to the free electron spin value of 2.0023 indicating the absence of spin-orbit coupling in the ground state,  ${}^6A_1$ . It is seen that the  $A$  values are somewhat lower than those of the pure ionic compounds. The  $A_{iso}$  values are consistent with the octahedral coordination [13] since  $A_{iso}$  in tetrahedral sites is 20-25% lower than those in octahedral sites. Based on the spectral studies an octahedral structure can be assigned to the Mn(II) complex as shown in Fig 6.8.

Fig.6.8. Tentative structure for  $[Mn(L^2)_2]$



## References

1. K. Wieghardt, *Angew.Chem. Int. Ed. Engl.* 28 (1989) 1153.
2. N.N. Greenwood, A. Earnshaw, *Chemistry of the Elements*, 2<sup>nd</sup> ed. Reed Educational and Professional, Great Britain, 1997.
3. B.N. Figgis, *Introduction to Ligand fields*, Wiley Eastern Limited, New Delhi. 1976.
4. B.N. Figgis, J. Lewis, *Prog.Inorg.Chem.* 6 (1964) 37.
5. R. Raina, T.S. Srivastava, *Indian J. Chem.* 22A (1983) 701.
6. M.A. Ali, M.T.H. Tarfdar, *J. Inorg. Nucl. Chem.* 39 (1977) 1785.
7. K. Nakamoto, *Infrared and Raman Spectra of Inorganic and Coordination Compounds*, 3<sup>rd</sup> ed., Wiley, New York. 1978.
8. J.E. Huheey, E.A. Keiter, R.L. Keiter, *Inorganic Chemistry* 4<sup>th</sup> ed., Addison-Wesley, New York, 1993.
9. A.B.P. Lever, *Inorganic Electronic Spectroscopy*. 2<sup>nd</sup> ed.. Elsevier Science Publishing Company, Amsterdam, 1984.
10. R.L. Dutta, A. Syamal, *Elements of Magnetochemistry*, 2<sup>nd</sup> ed., ISBN publication, 1993.
11. D.J.E. Ingram, *Spectroscopy at Radio and Microwave frequencies*. 2<sup>nd</sup> ed., Butterworth, London, 1967.
12. A. Sreekanth, Ph.D. Thesis, Cochin University of Science and Technology, 2003.
13. R. Singh, I.S. Ahuja, C.L. Yadava, *Polyhedron* 1 (1981) 327.
14. B.S. Garg, M.R.P. Kurup, S.K. Jain, Y.K. Bhoon, *Transition Met. Chem.* 13 (1988) 92.
15. B. Bleany, R.S. Rubins, *Proc. Phys. Soc. London*, 77 (1961) 103.
16. W. Linert, F. Renz, R. Boca, *J. Coord. Chem.* 40 (1996) 293.

## SYNTHESIS AND SPECTRAL CHARACTERIZATION OF NICKEL(II) COMPLEXES

### 7.1. Introduction

Nickel(II) ( $d^8$ ) forms a large number of complexes with coordination numbers 3 to 6. The coordination number of Ni(II) rarely exceeds 6 and its principal stereochemistries are octahedral and square planar with rather few examples of trigonal bipyramidal, square pyramidal and tetrahedral. Of the four coordinate complexes of Ni(II), those with the square planar stereochemistry are the most numerous. Although less numerous than the square planar complexes, tetrahedral complexes of nickel(II) also occur.

There are reports on the preparation and spectral characterization of Ni(II) complexes of 2-formylpyridine  $^4N$ -methyl,  $^4N$ -dimethyl,  $^4N$ -diethyl-and  $^4N$ -dipropyl thiosemicarbazones [1]. Further studies of Ni(II) complexes of 2-acetylpyridine thiosemicarbazones [2,3] as well as 2-acetylpyridine  $^4N$ -alkyl,  $^4N$ -dialkyl thiosemicarbazones [4,5] have also been reported.

We have prepared complexes of 2-benzoylpyridine  $N(4)$ -cyclohexyl thiosemicarbazone ( $HL^1$ ) and 2-benzoylpyridine  $N(4)$ -phenylthiosemicarbazone ( $HL^2$ ) using nickel chloride and nickel nitrate. This Chapter describes the synthesis and spectral characterization of the three Ni(II) complexes.

## 7.2. Experimental

### 7.2.1. Materials

All the nickel salts used were of analar grade and were used without further purification. The solvents were purified by standard methods. The methods used for the synthesis of HL<sup>1</sup> and HL<sup>2</sup> are given in Chapter 2.

### 7.2.2. Synthesis of Ni(II) complexes

#### $[NiL^1Cl]$ (19)

A methanolic solution of NiCl<sub>2</sub>·6H<sub>2</sub>O (2 mmol, 0.475 g) and a hot methanolic solution of HL<sup>1</sup> (2 mmol, 0.676 g) were mixed and refluxed for 5 hrs. The blue colored solids, which separated on keeping overnight, were filtered, washed with water, hot ethanol, then ether and dried *in vacuo* over P<sub>4</sub>O<sub>10</sub>.

#### $[Ni(HL^1)_2(NO_3)_2] \cdot 2H_2O$ (20)

Ni(NO<sub>3</sub>)<sub>2</sub>·6H<sub>2</sub>O (2 mmol, 0.457 g) dissolved in methanol and HL<sup>1</sup> (2 mmol, 0.676 g) dissolved in hot methanol were mixed and refluxed for 6 hrs. The brown colored solids, which separated on keeping overnight, were filtered, washed with water, hot ethanol, then ether and dried *in vacuo* over P<sub>4</sub>O<sub>10</sub>.

#### $[Ni(HL^2)(L^2)(NO_3)]$ (21)

A methanolic solution of Ni(NO<sub>3</sub>)<sub>2</sub>·6H<sub>2</sub>O (2 mmol, 0.457 g) and a hot methanolic solution of HL<sup>2</sup> (2 mmol, 0.664 g) were mixed and refluxed for 5 hrs. Brown colored solids separated on cooling. The crystals separated were filtered, washed with water, hot ethanol, then ether and dried *in vacuo* over P<sub>4</sub>O<sub>10</sub>.

### 7.3. Results and discussion

#### 7.3.1. Physical measurements

The colors, partial elemental analyses, stoichiometries, molar conductivities and magnetic moments of the complexes are presented in Table 7.1. The complex  $\text{NiL}^1\text{Cl}$  is blue crystal and the other two Ni(II) complexes are brown colored crystals. They are insoluble in methanol and ethanol and soluble in chloroform, dimethylformamide and dimethylsulphoxide.

In the complex,  $\text{NiL}^1\text{Cl}$ , the ligand coordinates as the deprotonated  $\text{L}^1$ , which is a tridentate ligand bonding *via* the pyridine nitrogen, the azomethine nitrogen and the sulfur atom. The non-electrolytic nature of the compound **19** in DMF shows that the chloride ion is coordinated to the Ni(II) ion. The molar conductivity measurements of the two Ni(II) complexes  $[\text{Ni}(\text{HL}^1)_2(\text{NO}_3)_2]\cdot 2\text{H}_2\text{O}$  and  $[\text{Ni}(\text{HL}^2)(\text{L}^2)(\text{NO}_3)]$  showed their non electrolytic nature which confirm that the nitrate ions are coordinated to the Ni(II) ion.

The stoichiometry  $[\text{Ni}(\text{HL}^1)_2(\text{NO}_3)_2]\cdot 2\text{H}_2\text{O}$  of the complex suggests the coordination of the neutral ligand *via* the pyridine and azomethine nitrogen atoms with octahedral coordination achieved with the two nitrate ions. In the complex  $[\text{Ni}(\text{HL}^2)(\text{L}^2)(\text{NO}_3)]$ , as the stoichiometry suggests the two ligand molecules are coordinated to the Ni(II) ion; one as the neutral molecule and the other as the anion. These proposed structures are supported by infrared spectral studies.

#### 7.3.2. Magnetic susceptibilities

For the vast majority of four-coordinate nickel(II) complexes, square planar geometry is preferred. The square planar geometry causes one of the *d* orbitals,  $d_{x^2-y^2}$  to be uniquely high in energy and the eight electrons can occupy the other

four  $d$  orbitals but leave this strongly antibonding  $d_{x^2-y^2}$  vacant. Almost all the planar complexes of Ni(II) are thus diamagnetic. However, weakly paramagnetic nickel (II) planar complexes have also been reported [6.7] but of low spin. Theoretical and experimental results have proved that these paramagnetic complexes have neither octahedral nor tetrahedral geometry. To explain this paramagnetic behaviour of the square planar complexes, equilibrium between spin free and spin-paired configuration is suggested [8].

In tetrahedral complexes ( $T_d$  symmetry) the  $d^8$  configuration gives rise to a  $^3T_1(F)$  ground state. Because the  $^3T_1(F)$  ground state has much inherent orbital angular momentum, the magnetic moment of truly tetrahedral Ni(II) should be  $\sim 4.2$  B.M. at room temperature [9]. The magnetic moment of a tetrahedral  $d^8$  complex ( $e^4 t_2^4$ ) should have contributions from spin-orbit coupling. In general, orbital contributions are expected in those complexes in which the ground state is triply degenerate ( $T$  term) and the values approximating the spin only value are obtained for non-degenerate and doubly degenerate ground states ( $A$  and  $E$  terms). However, even slight distortions reduce this markedly by splitting the orbital degeneracy. Thus fairly regular tetrahedral complexes have moments of 3.5 to 4.0 B.M. [10].

From both the  $d$  orbital splitting and the energy level diagram it is clear that, octahedral Ni(II) complexes have two unpaired electrons. An octahedral Ni(II) complex has the  $^3A_{2g}$  ground state term that has a considerable mixing with the  $^3T_{2g}$  excited state. The spin only magnetic moment is therefore modified by the spin-orbit coupling. Thus octahedral Ni(II) complexes have magnetic moments ranging from 2.9 to 3.4 BM.

The compound  $NiL^1Cl$  is found to be diamagnetic and so it is a square planar complex. The two Ni(II) complexes  $[Ni(HL^1)_2(NO_3)_2] \cdot 2H_2O$  and  $[Ni(HL^2)(L^2)(NO_3)]$  have magnetic moment values of 3.2 and 2.91 which is an evidence for the octahedral nature of these complexes.

### 7.3.3. Infrared spectra

The significant bands obtained in the vibrational spectra of the two ligands HL<sup>1</sup> and HL<sup>2</sup> and their Ni(II) complexes and their tentative assignments are presented in Table 7.2. Coordination of the azomethine nitrogen has been proposed for the majority of thiosemicarbazone ligands with the evidence for this coordination based on a shifting of the  $\nu(\text{C}=\text{N})$  band expected for both the neutral and anionic ligands. This shifting has been reported both to higher [11,12] and to lower energies [13,14]. It appears that both types of shifts can occur due to the differences in the energies of the bands with which  $\nu(\text{C}=\text{N})$  is in combination [15]. The  $\nu(\text{C}=\text{N})$  band of HL<sup>1</sup> at 1582 cm<sup>-1</sup> is found to be shifted to lower energies and appear at 1545 and 1553 cm<sup>-1</sup> respectively in compounds **19** and **20** which indicate the coordination *via* the azomethine nitrogen. Two other bands are found at 1649 and 1628 cm<sup>-1</sup> in the spectra of compounds **19** and **20** respectively, which are due to the newly formed  $\nu(\text{C}=\text{N})$  during the formation of the complex. *via* enolisation. The coordination of azomethine nitrogen to nickel can be confirmed by assigning the  $\nu(\text{Ni}-\text{N})$  band at *ca.* 465 cm<sup>-1</sup> in the far IR spectra of the complexes [16].

Coordination of pyridine nitrogen to the metal in the complexes is indicated by an increase in energy of the out of plane modes of the pyridine ring. The magnitude of the shift is somewhat higher in compound **21**, and this result is consistent with the previous reports on acetylpyridine thiosemicarbazones [15]. The strong bands observed in the far IR spectra of the Ni(II) complexes at *ca.* 280 cm<sup>-1</sup> can be assigned to  $\nu(\text{Ni}-\text{N})$  of the pyridine ring [17].

The coordination of the sulfur atom to the metal is indicated by the shifts of the two bands considered to have contributions from  $\nu(\text{C}-\text{S})$  to lower energies. The  $\nu(\text{C}-\text{S})$  bands of HL<sup>1</sup> at 1370 and 833 cm<sup>-1</sup> are found to be shifted to 1338 and 742 cm<sup>-1</sup> in NiL<sup>1</sup>Cl indicating the coordination of the sulfur atom to nickel(II). In

complex **20**, the  $\nu(\text{C}=\text{S})$  band of the ligand is found to be slightly shifted to higher energy compared to their position in the spectrum of the free ligand and the band at  $833\text{ cm}^{-1}$  suffers marginal shift to lower energy. This indicates non-coordination by the sulfur atom for the neutral ligands  $\text{HL}^1$ . In compound **21**, which contains both neutral and anionic ligands, the bands at  $823$  and  $762\text{ cm}^{-1}$  can be assigned to  $\nu(\text{C}-\text{S})$ . The coordination of sulfur to Ni(II) in complex **19** can be confirmed by a strong band corresponding to  $\nu(\text{Ni}-\text{S})$  at  $382\text{ cm}^{-1}$  in its far infrared spectrum.

A strong band observed in the spectrum of  $\text{NiL}^1\text{Cl}$  at  $302\text{ cm}^{-1}$  can be assigned to the  $\nu(\text{Ni}-\text{Cl})$  band. Compound **20** shows a broad band centered at  $3449\text{ cm}^{-1}$  in its spectrum indicating hydrate rather than coordinated water [18]. Strong bands at  $324$  and  $322\text{ cm}^{-1}$  in the far IR spectra of compounds **20** and **21** can be assigned to  $\nu(\text{Ni}-\text{O})$  for the nitrate ligands [19]. This is in support of the results from conductivity measurements, that the nitrate ion is coordinated to the nickel ion in compounds **20** and **21**.

Table 7.1. Analytical data

Compound	Empirical formula	Color	Found (Calculated) %			$\Lambda_M^*$ (in DMF)	$\mu$ (B.M.)
			C	H	N		
[Ni(L <sup>1</sup> )Cl] (19)	C <sub>10</sub> H <sub>21</sub> N <sub>4</sub> SClNi	Blue	52.94 (52.88)	5.15 (5.10)	12.72 (12.90)	1.8	Diamagnetic
[Ni(HL <sup>1</sup> ) <sub>2</sub> (NO <sub>3</sub> ) <sub>2</sub> ].2H <sub>2</sub> O (20)	C <sub>38</sub> H <sub>48</sub> N <sub>10</sub> SO <sub>8</sub> Ni	Brown	51.27 (50.96)	5.39 (5.36)	15.50 (15.64)	5.21	3.21
[Ni(HL <sup>2</sup> )(L <sup>2</sup> )(NO <sub>3</sub> )] (21)	C <sub>38</sub> H <sub>38</sub> N <sub>10</sub> SO <sub>6</sub> Ni	Brown	57.92 (58.11)	4.08 (3.95)	16.36 (16.07)	4.90	2.94

\*Molar conductivity of 10<sup>-3</sup>M solutions, in ohm<sup>-1</sup>cm<sup>2</sup> mol<sup>-2</sup>Table 7.2. IR spectral assignments (cm<sup>-1</sup>) of HL<sup>1</sup> and HL<sup>2</sup> and their Ni (II) complexes

Compound	$\nu$ (C=N)	$\nu$ (C-S)	$\nu$ (py)	$\nu$ (Ni-N)	$\nu$ (Ni-N py)	$\nu$ (Ni-S)	$\nu$ (Ni-X)
HL <sup>1</sup>	1582 m	1370w,833m	607w	--	--	--	--
NiL <sup>1</sup> Cl (19)	1545s 1649s	1338s,742m	647m	464s	261s	382s	302s
[Ni(HL <sup>1</sup> ) <sub>2</sub> (NO <sub>3</sub> ) <sub>2</sub> ].2H <sub>2</sub> O (20)	1553s 1628s	1384s,814w	635m	465s	281s	--	324s
HL <sup>2</sup>	1591s	1369s,835m	622m	--	--	--	--
[Ni(HL <sup>2</sup> )(L <sup>2</sup> )(NO <sub>3</sub> )] (21)	1527s 1596s	1307s,823s,	692m	469s	281s	--	322s



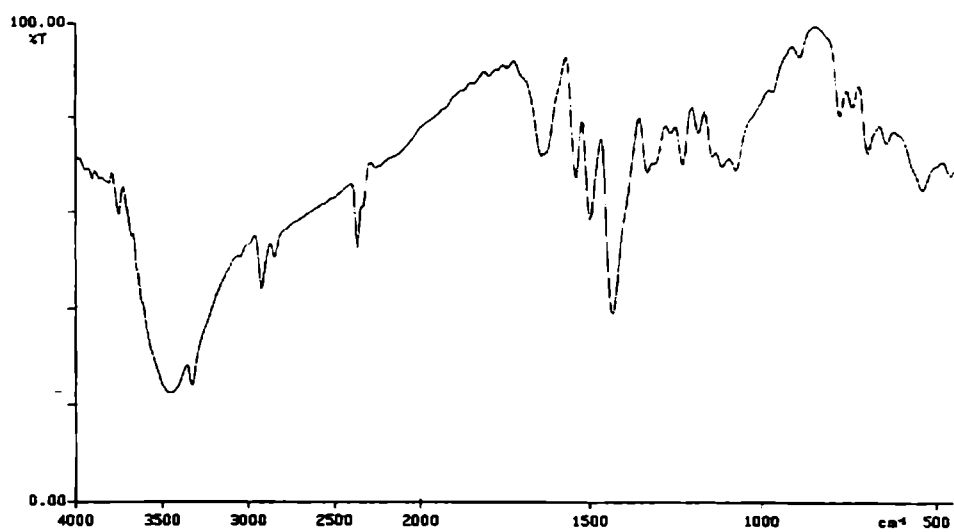


Fig.7.1. IR spectrum of compound 19

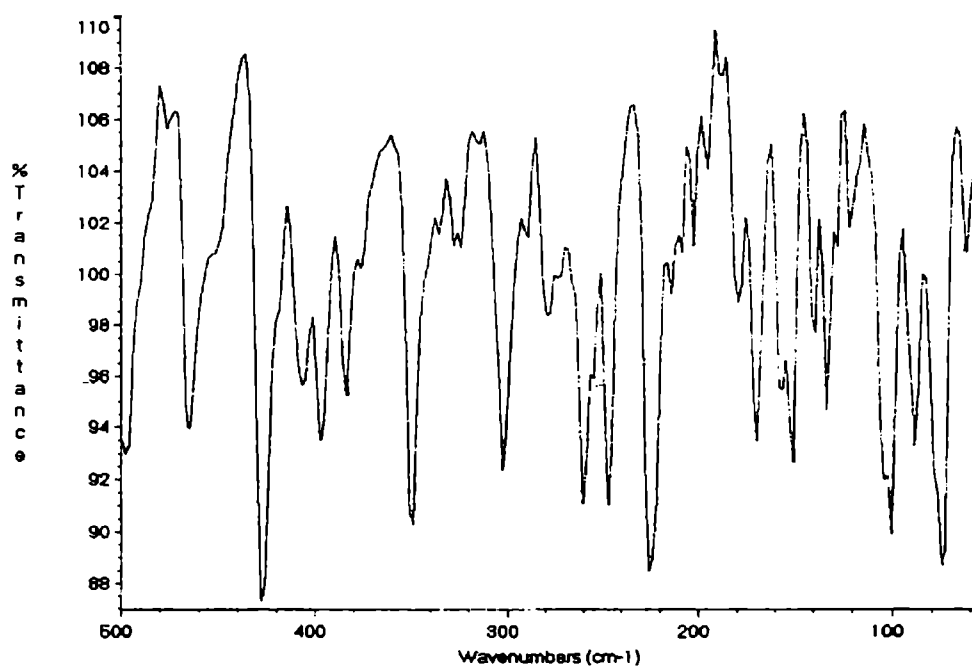


Fig.7.2. Far IR spectrum of compound 19

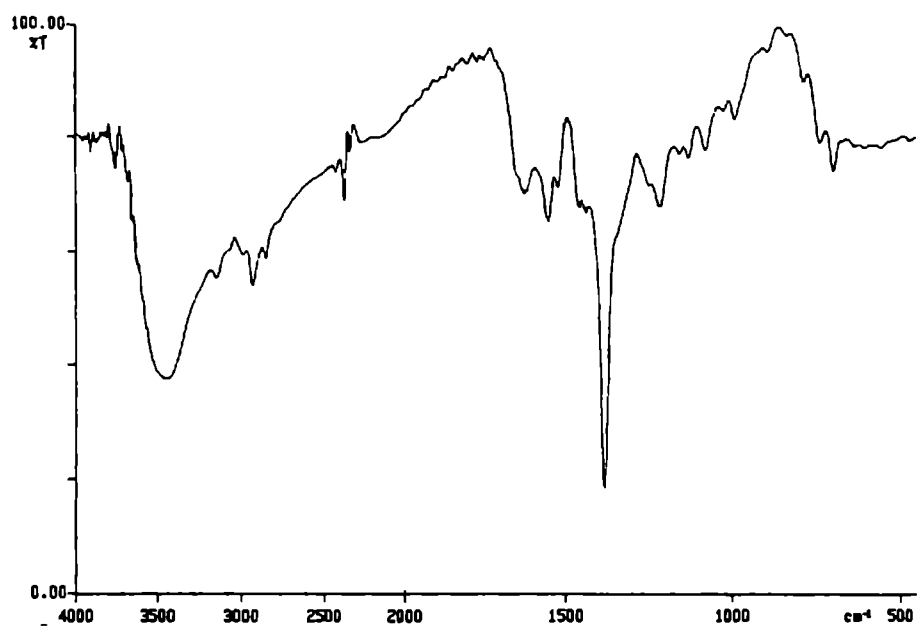


Fig 7.3. IR spectrum of compound 20

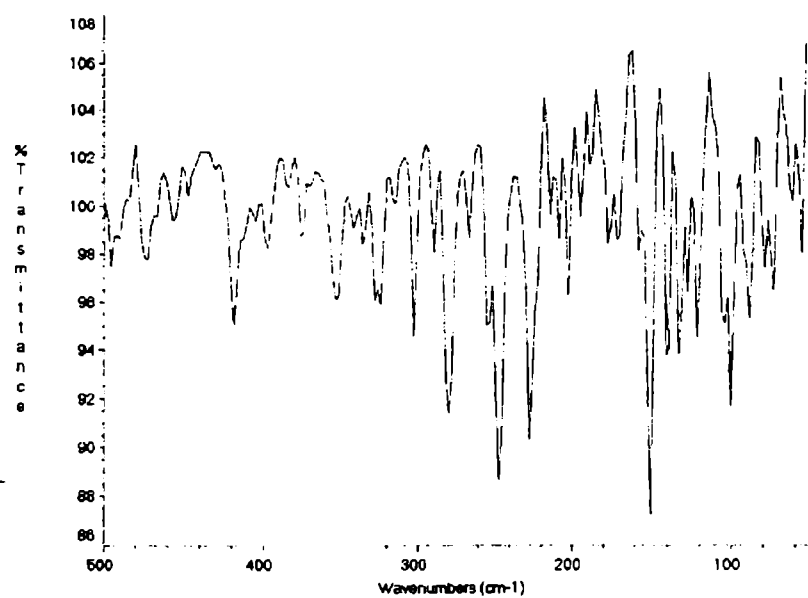


Fig.7.4. Far IR spectrum of compound 20

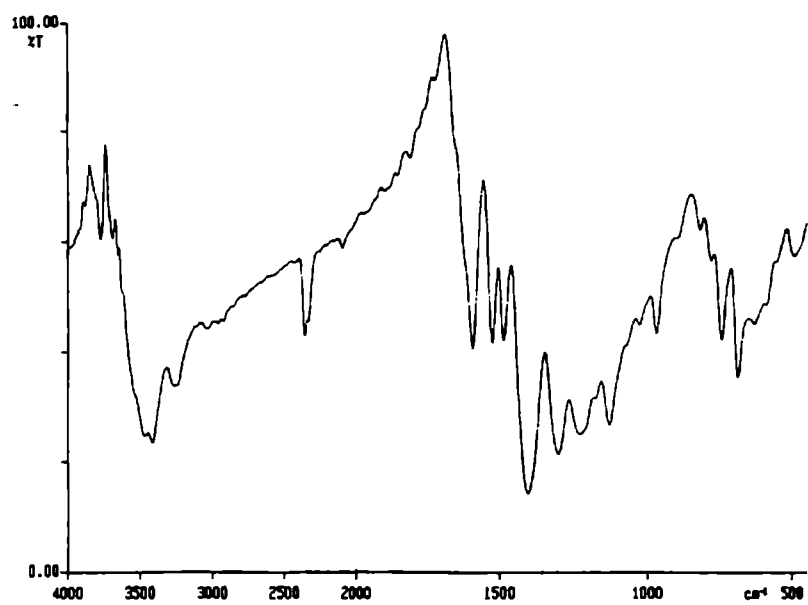


Fig. 7.5. IR spectrum of compound 21

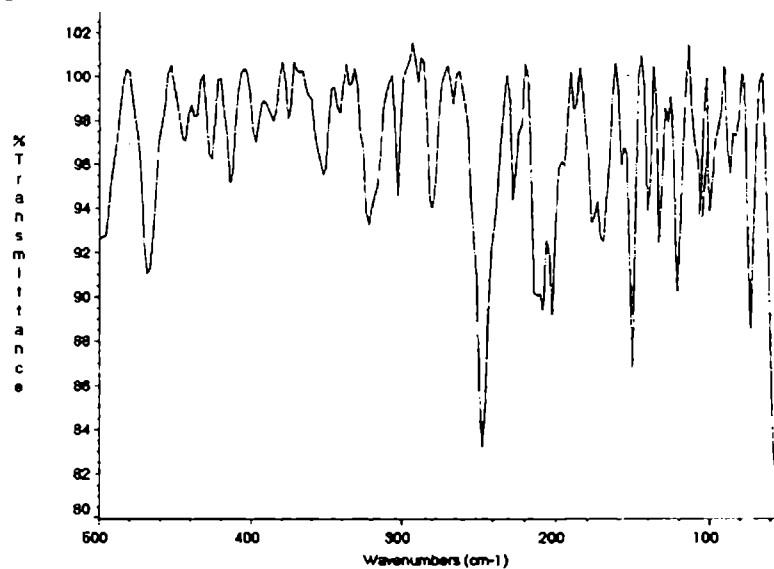


Fig.7.6. Far IR spectrum of compound 21

### 7.3.4. Electronic spectra

The significant electronic absorption bands recorded in the solid state and in DMF solution are presented in Table 7.3. The electronic spectra of the thiosemicarbazones HL<sup>1</sup> and HL<sup>2</sup> have absorption bands at *ca.* 340nm due to the  $n \rightarrow \pi^*$  transition of the thiosemicarbazone moiety and at *ca.* 259 nm due to  $\pi \rightarrow \pi^*$  transitions. These bands suffer marginal shifts on complexation. In the spectra of the three Ni(II) complexes, a high intense broad band is present at *ca.* 420 nm which may be due to the ligand  $\rightarrow$  metal charge transfer band. This high intensity charge transfer band may sometimes mask the  $d-d$  band [20].

From the magnetic and infrared spectral studies, NiL<sup>1</sup>Cl is considered as a square planar complex. The spectra of NiL<sup>1</sup>Cl, exhibit a strong broad band at 417 nm and shoulders at 593 and 662 nm. Assuming  $D_{4h}$  symmetry for this solid.

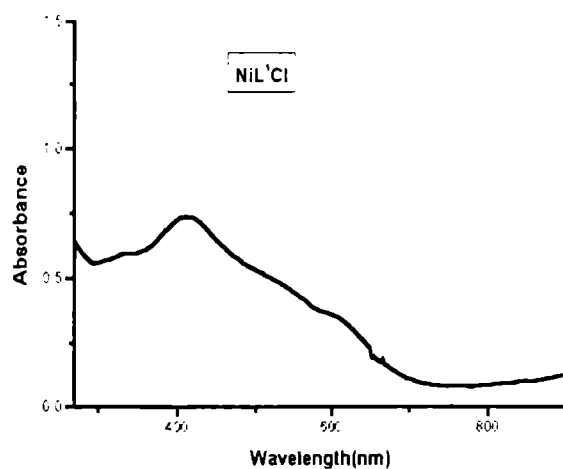


Fig. 7.7. Electronic spectrum of compound 19

Table 7.3 Electronic spectral data (nm) of Nickel (II) Complexes

Compound	State	Intraligand	C.T.	d→d
[NiL <sup>1</sup> Cl] (19)	Solid DMF	332sh, 275sh 330 (3.81), 274 (3.85)	417 416 (4.25)	593sh, 662sh 596 (1.68), 656 (1.71)
Ni(HL <sup>1</sup> ) <sub>2</sub> (NO <sub>3</sub> ) <sub>2</sub> ·2H <sub>2</sub> O (20)	Solid DMF	327sh, 272 330 (4.35), 271sh	439 430 (4.72)	513sh, 656sh, 824sh 518 (1.85), 674, 805 (1.5)
[Ni(HL <sup>2</sup> )(L <sup>2</sup> )(NO <sub>3</sub> )] (21)	Solid DMF	315sh, 292 302 (4.18)	413 415 (4.32)	537sh, 660sh, 762sh 521 (2.01), 640 (1.9)

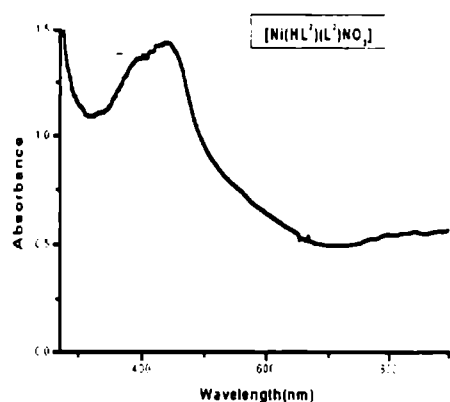


Fig.7.8. Electronic spectrum of compound 21

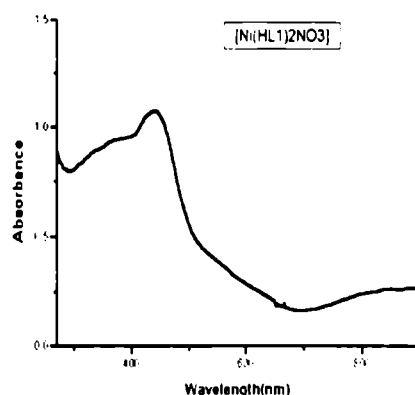


Fig.7.9. Electronic spectrum of compound 20

the three bands can be assigned to  ${}^1A_{1g} \rightarrow {}^1E_g$ ,  ${}^1A_{1g} \rightarrow {}^1A_{2g}$  and  ${}^1A_{1g} \rightarrow {}^1B_{2g}$  transitions respectively [21]. The absence of bands above 1000 nm confirms its square planar nature. In the spectrum of compound 19, a  $d-d$  band appearing as a weak shoulder centered around 500 nm is typical of square planar monoligated Ni(II) complexes [21].

For a  $d^8$  configuration in octahedral field, three spin-allowed transitions are expected, because of the splitting of the free-ion ground  ${}^3F$  term and the presence of the  ${}^3P$  term. The three transitions are  ${}^3A_{2g}(F) \rightarrow {}^3T_{2g}(F)$ ,  ${}^3A_{2g}(F) \rightarrow {}^3T_{1g}(F)$  and  ${}^3A_{2g}(F) \rightarrow {}^3T_{1g}(P)$ . In the spectra of the two complexes 20 and 21, the bands appearing at *ca.* 526, 657 and 800 nm can be assigned to  ${}^3A_{2g}(F) \rightarrow {}^3T_{1g}(P)$ ,  ${}^3A_{2g}(F) \rightarrow {}^3T_{1g}(F)$  and  ${}^3A_{2g}(F) \rightarrow {}^3T_{2g}(F)$  respectively [22].

### 7.3.5. ${}^1H$ NMR spectrum of $[NiL^1Cl]$

The signal observed in the spectrum of  $HL^1$  at  $\delta = 13.48$  (s, 1H) corresponding to the imino proton is found to be absent in the spectrum of  $[NiL^1Cl]$ , which indicates the deprotonation of the ligand on complexation. In the

spectrum of the complex a signal at 7.70 (s, 1H) corresponds to that of the  $^4\text{NH}$  proton. The doublet at 8.60 corresponding to the proton at position 6 ( $\alpha$  to pyridyl nitrogen) of the pyridine ring is found to be slightly shifted in the complex confirming the coordination *via* the pyridyl nitrogen. The signals corresponding to the other three protons of the pyridine are also found to be slightly shifted upfield, having  $\delta = 7.45$ , 7.34 and 7.28 respectively. The signals corresponding to the protons of the cyclohexane ring are found to be unshifted in the spectrum of  $[\text{NiL}^1\text{Cl}]$ . (The position of atoms are based on Fig.2.1)

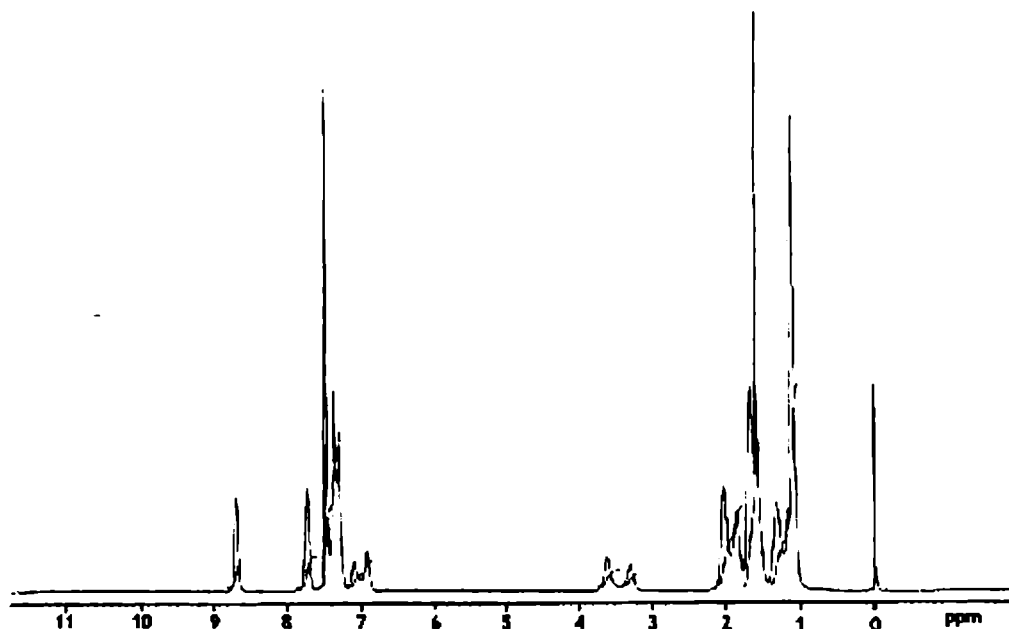


Fig. 7.10.  $^1\text{H}$  NMR spectrum of compound 19

## References

1. D.X. West, J.S. Saleda, A.E. Liberta, *Transition Met.Chem.*17 (1992) 568.
2. M.R.P. Kurup, B.S. Garg, S.K. Jain, *Transition Met.Chem.*16 (1991)111.
3. R. Raina, T.S. Srivastava, *Ind. J. Chem.* 22A (1983) 701.
4. D.X. West, C.S. Carlson, A.E. Liberta,, J.N. Albert, C.R. Daniel, *Transition Met. Chem.*15 (1990) 341.
5. B. Singh, U. Srivastava, *Transition Met. Chem.* 13 (1988) 205.
6. H.B. Gray, E.B. Billing, *J. Am. Chem. Soc.* 85 (1963) 2019.
7. M. Mathew, G.J. Palenik, G.R. Clark, *J. Inorg. Chem.* 12 (1973) 346.
8. M.R.P. Kurup, Ph.D. Thesis, Dept. of Chemistry, University of Delhi,1987.
9. F.A. Cotton, G. Wilkinson, C.A. Murillo, M. Bochmann, *Advanced Inorganic Chemistry*, 6<sup>th</sup> ed., Wiley, New York, 1999.
10. A. Earnshaw, *Introduction to Magnetochemistry*, Academic press, London, 1968.
11. R. Raina, T.S. Srivastava, *Inorg. Chim. Acta* 67 (1982) 83.
12. S. Chandra, B.B. Kaul, K.B. Pandeya, R.P. Singh, *J. Inorg. Nucl. Chem.* 30 (1977) 2079.
13. M. Mohan, Manmohan, *Synth. React. Inorg. Met-Org. Chem.* 12 (1982) 761.
14. B.B. Mahapatra, S.K. Pujari, *Ind. J. Chem.* 12 (1982) 761.
15. D.X. West, J.P. Scovill, J.V. Silverton, A. Bavoso, *Transition Met.Chem.*11 (1986) 123.
16. N.C. Mishra, B.B. Mohapatra, S. Guru, *J. Inorg. Nucl. Chem.* 41 (1979) 418.
17. V. Philip, V. Suni, M.R.P. Kurup, M. Nethaji, *Polyhedron* 23 (2004) 1225.
18. A.B.P. Lever, E. Mantovani, B.S. Ramaswamy, *Can. J. Chem.* 49 (1976) 1957.



19. I.S. Ahuja, R. Singh, B. Sriramulu, J. Inorg. Nucl. Chem. 42 (1980) 627.
20. A. Sreekanth, S. Sivakumar, M.R.P. Kurup, J. Mol. Struct. 655 (2003) 47.
21. D.N. Sathyanayarana, Electronic Absorption Spectroscopy and related Techniques, University Press India Limited, 2001.
22. A.B.P. Lever, Inorganic Electronic Spectroscopy, 2<sup>nd</sup> ed., Elsevier, New York, 1986.

## SYNTHESIS, SPECTRAL AND BIOLOGICAL STUDIES OF COMPLEXES OF ZINC(II), CADMIUM(II) AND MERCURY(II)

### 8.1. Introduction

Zinc is the second most abundant transition element in the human organism, following iron; the metal also plays an important role in many other living systems. Cadmium and mercury have no known beneficial biological role and are amongst the most toxic of elements. Today more than 200 different zinc proteins are known which include numerous essential enzymes [1]. Zn is present as enzyme in most body cells of human beings, but its concentration is very low. The two Zn enzymes which have received most attention are carboxypeptidase *A* and carbonic anhydrase. Metallothioneins, proteins containing zinc, remain unique in character but are encountered both in animals and microorganisms [2,3]. The wound healing effect of zinc containing ointment was already known in the ancient world and during the last decades, zinc has increasingly been used as a remedy for growth disorders due to malnutrition [4].

The elements Zn, Cd and Hg have a filled  $(n-1)d$  shell plus two  $ns$  electrons. In view of the stability of the filled  $d$  shell, these elements show few of the characteristic properties of transition metals despite their position in the  $d$  block of the periodic table. Zinc and cadmium resemble the transition elements in forming stable complexes not only with O-donor ligands but also with N and S donor ligands and with halides and  $CN^-$ . Hg has a preference for N, P and S donor ligands, with which Hg(II) forms complexes whose stability is rarely exceeded by those of any other divalent cation. Compounds of the M(II) ions of this group are characteristically diamagnetic [5].

Since the  $d^{10}$  configuration affords no crystal field stabilization, the stereochemistry of a particular compound depends on the size and polarizing power of the M(II) cation and the steric requirement of the ligands. The  $M^{2+}$  ion with their  $d^{10}$  configuration shows no stereochemical preferences arising from ligand field stabilization effects. Therefore they display a variety of coordination numbers and geometries based on the interplay of electrostatic forces, covalence and the size factor. Both Zn(II) and Cd(II) favour 4-coordinate tetrahedral complexes though Cd(II), being the larger one, forms 6-coordinate octahedral complexes more readily than does Zn(II). However, Hg(II) adopts a tetrahedral stereochemistry, an octahedral 6-coordination is less prevalent. Coordination numbers 4, 5 and 6 are the common ones for all the three elements, although linear 2-coordination is often seen for  $Hg^{2+}$  [4].

This Chapter describes the synthesis of three Zn(II) complexes, one Cd(II) complex and one Hg(II) complex and characterization of these complexes using electronic, infrared and  $^1H$  NMR spectral studies. Antimicrobial studies on Zn(II) complexes are also included in this Chapter.

## 8.2. Experimental

### 8.2.1. Materials

The method used for the synthesis of HL<sup>1</sup> and HL<sup>2</sup> are dealt with in Chapter 2. All the metal salts were used as received and the solvents were purified by the usual methods.

### 8.2.2. Synthesis of the complexes

#### $[ZnL^1OOCCH_3]$ (22)

An aqueous solution of  $Zn(CH_3COO)_2 \cdot 2H_2O$  (5 mmol, 1.09 g) and an ethanolic solution of  $HL^1$  (5 mmol, 1.69 g) were mixed and stirred for 2 hrs. The yellow colored solids, which separated, were filtered, washed with water, ethanol and ether and dried over  $P_4O_{10}$  *in vacuo*.

#### $[ZnL^1Cl] \cdot 2H_2O$ (23)

Methanolic solutions of  $ZnCl_2$  (5 mmol, 0.68 g) and  $HL^1$  (5 mmol, 1.69 g) were mixed and refluxed for 4 hrs. The pale yellow solids that separated were filtered, washed with methanol, water and ether and dried *in vacuo* over  $P_4O_{10}$ .

#### $[CdL^1NO_3]$ (24)

Solutions of  $Cd(NO_3)_2 \cdot 4H_2O$  (5 mmol, 1.54 g) and  $HL^1$  (5 mmol, 1.54 g) in methanol were mixed and refluxed for 4hrs. The yellow crystals separated on keeping over night, were filtered, washed with water, methanol and ether and dried over  $P_4O_{10}$  *in vacuo*.

#### $[Hg(HL^1)Cl_2]$ (25)

Methanolic solutions of  $HgCl_2$  (5 mmol, 1.36 g) and  $HL^1$  (5 mmol, 1.69 g) were mixed and stirred for 2 hrs. The colorless solids separated, were filtered washed with methanol and ether and dried over  $P_4O_{10}$  *in vacuo*.

#### $[ZnL^2OCOCH_3]$ (26)

Methanolic solutions of  $Zn(CH_3COO)_2 \cdot 2H_2O$  (5 mmol, 1.09 g) and  $HL^2$  (5 mmol, 1.66 g) were mixed and refluxed for 4 hrs. The yellow solids, which

Table 8.1. Analytical data

Compound	Empirical formula	Colour	Found(Calculated) %			$\Lambda_M^*$ (in DMF)	$\mu$ (B.M.)
			C	H	N		
[ZnL <sup>1</sup> OAc] (22)	C <sub>21</sub> H <sub>24</sub> N <sub>4</sub> SO <sub>2</sub> Zn	Yellow	54.75(54.62)	5.55(5.20)	12.05(12.13)	3.5	Diamagnetic
[ZnL <sup>1</sup> Cl]-2H <sub>2</sub> O (23)	C <sub>19</sub> H <sub>25</sub> N <sub>4</sub> SOCIZn	Yellow	49.63(49.79)	4.97(5.46)	11.91(12.23)	7.54	Diamagnetic
[CdL <sup>1</sup> NO <sub>3</sub> ] (24)	C <sub>19</sub> H <sub>21</sub> N <sub>5</sub> SO <sub>3</sub> Cd	Pale yellow	44.72(44.58)	4.75(4.11)	14.13(13.69)	7.6	Diamagnetic
[Hg(HL <sup>1</sup> )Cl <sub>2</sub> ] (25)	C <sub>19</sub> H <sub>22</sub> N <sub>4</sub> SCl <sub>2</sub> Hg	White	37.51(37.40)	3.80(3.61)	8.76(9.19)	20.5	Diamagnetic
[ZnL <sup>2</sup> OAc] (26)	C <sub>21</sub> H <sub>18</sub> N <sub>4</sub> SO <sub>3</sub> Zn	Yellow	53.15(53.45)	4.05(3.82)	12.30(11.88)	5.21	Diamagnetic

\*Molar conductivity of 10<sup>-4</sup>M solution, in ohm<sup>-1</sup>cm<sup>2</sup>mol<sup>-2</sup>

separated, were filtered, washed with water, methanol and ether and dried over  $P_4O_{10}$  *in vacuo*.

### 8.3. Results and discussion

#### 8.3.1. Physical measurements

The colors, partial elemental analyses, stoichiometries, molar conductivities and magnetic moments of the complexes are presented in Table 8.1. The five complexes are found to be diamagnetic as expected. Molar conductivity measurements of the solutions of the metal complexes in DMF solution indicate their non-conducting nature. This suggests the coordination of gegenions to the metal.

#### 8.3.2. Infrared spectra

The main IR spectral bands of  $HL^1$ ,  $HL^2$  and their Zn(II), Cd(II) and Hg(II) complexes are listed in Table 8.2. The strong bands observed in the spectra of  $HL^1$  and  $HL^2$  at 1582 and 1591  $cm^{-1}$  respectively can be assigned to the  $\nu(C=N)$  band. The  $\nu(C=N)$  band shifts to lower frequencies in the spectra of all the complexes suggesting the coordination of the azomethine nitrogen to the metal ions. The involvement of this nitrogen in bonding is also supported by a shift in the  $\nu(N-N)$  band of the thiosemicarbazones to higher frequencies. In the spectrum of compound **22**, a new band of medium intensity is found at 1588  $cm^{-1}$  which is due to the formation of a new C=N bond formed during the formation of the complex *via* enolisation. The coordination *via* the azomethine nitrogen is confirmed by the presence of the  $\nu(M-N)$  band at *ca.* 490  $cm^{-1}$  [6].

In the IR spectra of the complexes containing the deprotonated ligand  $L^1$ , the  $\nu(C-S)$  band is found to be shifted by 45-90  $cm^{-1}$  to lower frequencies, indicating the coordination *via* the sulfur atom [7]. The strong bands observed in the far IR spectra of the complexes at *ca.* 350  $cm^{-1}$  confirm the coordination *via* the S atom. In the Hg(II) complex containing the protonated ligand  $HL^1$ , the  $\nu(C-S)$  band remains slightly shifted to higher frequency.

Coordination *via* the pyridine nitrogen atom is indicated by a shift in the deformation band of the pyridine ring. In the complexes  $[ZnL^1OAc]$  and  $[ZnL^2OAc]$ , the strong bands observed at *ca.* 1590 and 1409  $cm^{-1}$ , when the acetate ion is bonded to the metal as a unidentate ligand [8], can be assigned to  $\nu_a(COO)$  and  $\nu_s(COO)$  of the acetate ion. In  $[CdL^1NO_3]$  the three bands observed at 1472, 1385 and 1078  $cm^{-1}$  can be assigned to  $\nu_a(NO_2)$ ,  $\nu_s(NO_2)$  and  $\nu(NO)$  of the nitrate group and this confirms the unidentate nature of the nitrate group. In the complexes  $[ZnL^1Cl] \cdot 2H_2O$  and  $[Hg(HL^1)Cl_2]$  the strong bands observed at 297 and 271  $cm^{-1}$  indicate the presence of M-Cl bond [9,10].

Table 8.2 IR spectral assignments ( $cm^{-1}$ ) of  $HL^1$  and  $HL^2$  and their Zn (II), Cd(II), Hg(II) complexes

Compound	$\nu(C=N)$	$\nu(C-S)$	$\nu(py)$	$\nu(N-N)$	$\nu(M-N)$	$\nu(M-S)$	$\nu(M-X)$
$HL^1$	1582m	833s	607s	1118m	--	--	--
$[ZnL^1OAc]$ (22)	1588s	787m	657m	1144m	487s	353s	--
$[ZnL^1Cl] \cdot 2H_2O$ (23)	1553s	748m	665m	1160m	490s	341s	297s
$[CdL^1NO_3]$ (24)	1563s	740s	638w	1161m	491s	375s	--
$[Hg(HL^1)Cl_2]$ (25)	1555s	840m	636w	1154m	491s	--	271s
$HL^2$	1591s	835m	622m	1102s	--	--	--
$[ZnL^2OAc]$ (26)	1567s	753s	657m	1128m	467s	334s	--

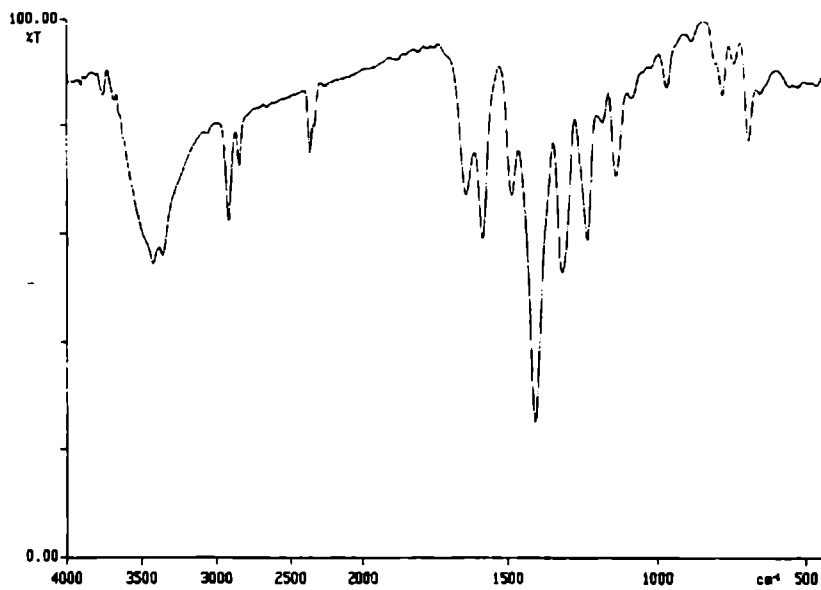


Fig. 8.1. IR spectrum of compound 22

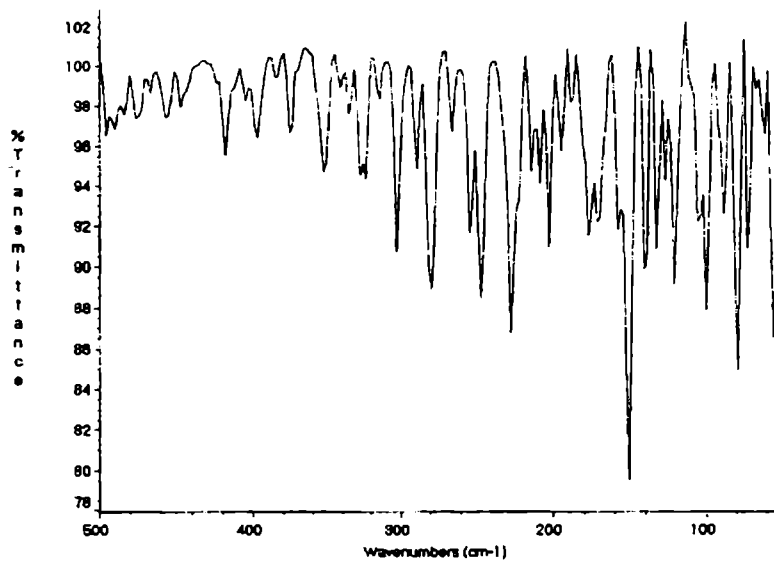


Fig. 8.2. Far IR spectrum of compound 22



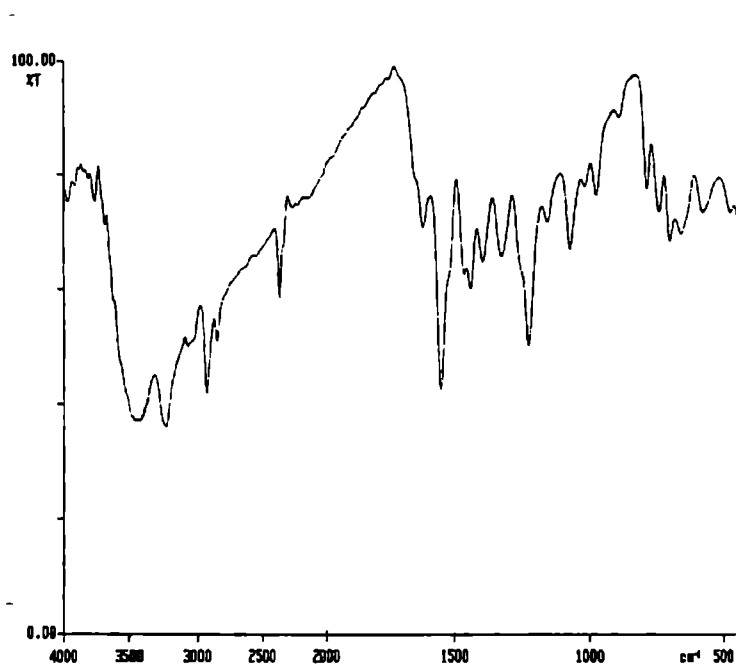


Fig. 8.3. IR spectrum of compound 23

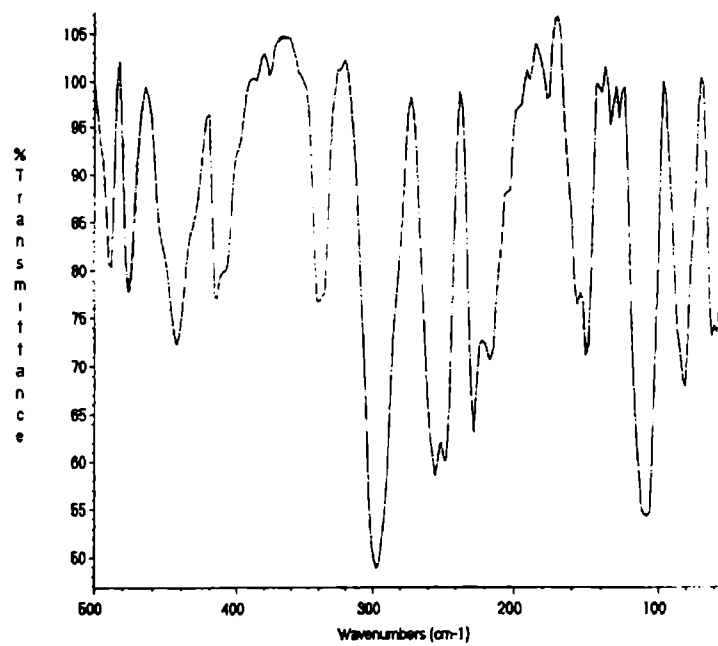


Fig. 8.4. Far IR spectrum of compound 23

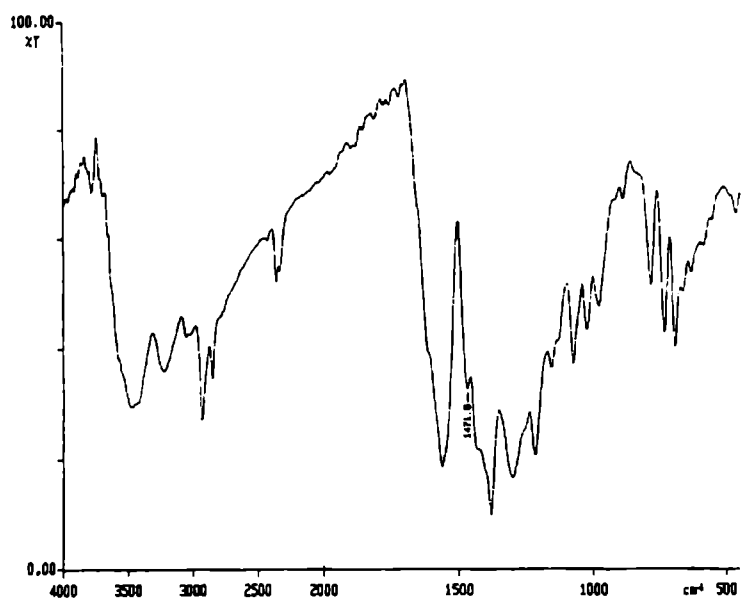


Fig. 8.5. IR spectrum of compound 24

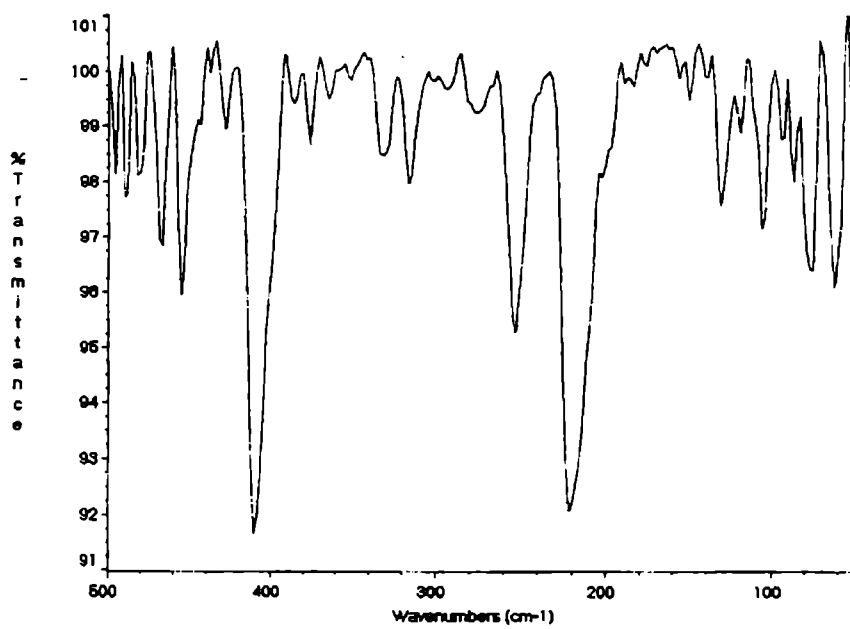


Fig. 8.6. Far IR spectrum of compound 24

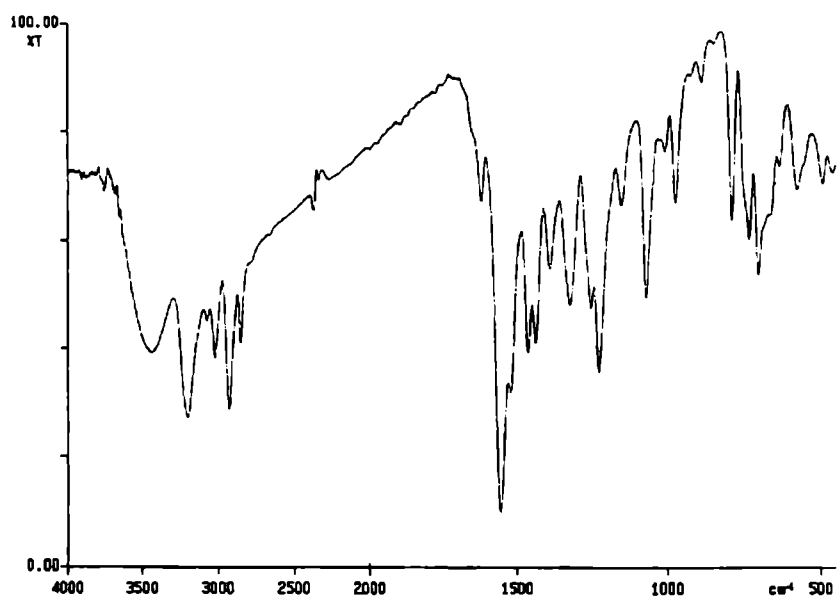


Fig. 8.7. IR spectrum of compound 25

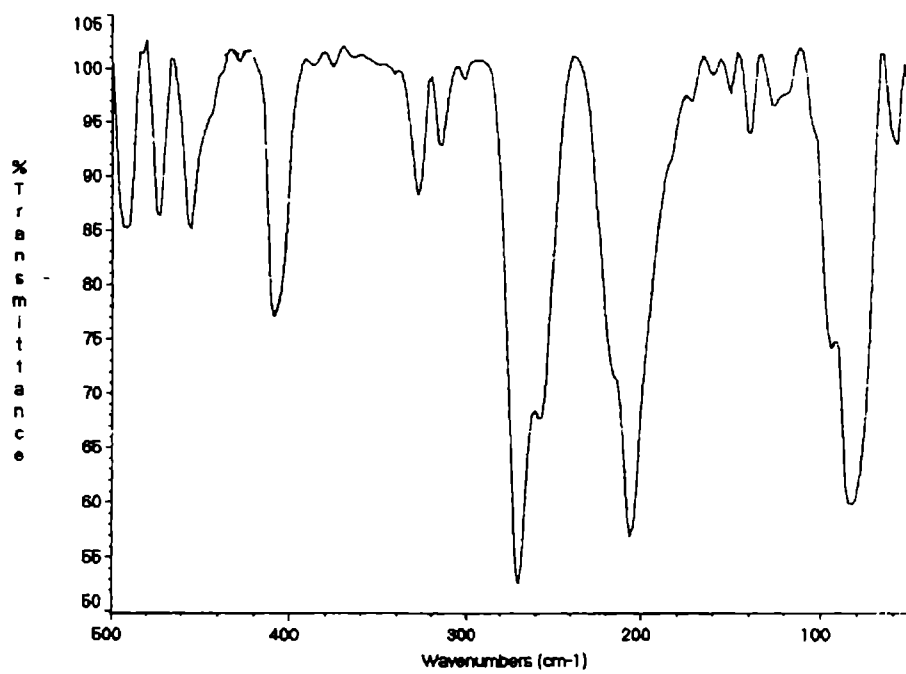


Fig. 8.8. Far IR spectrum of compound 25

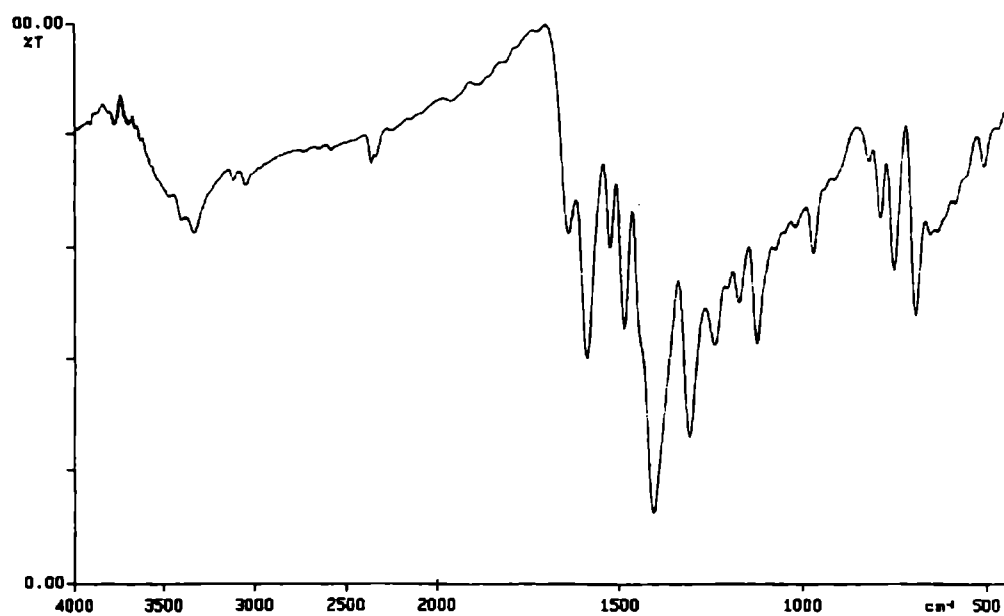


Fig.8.9. IR spectrum of compound 26

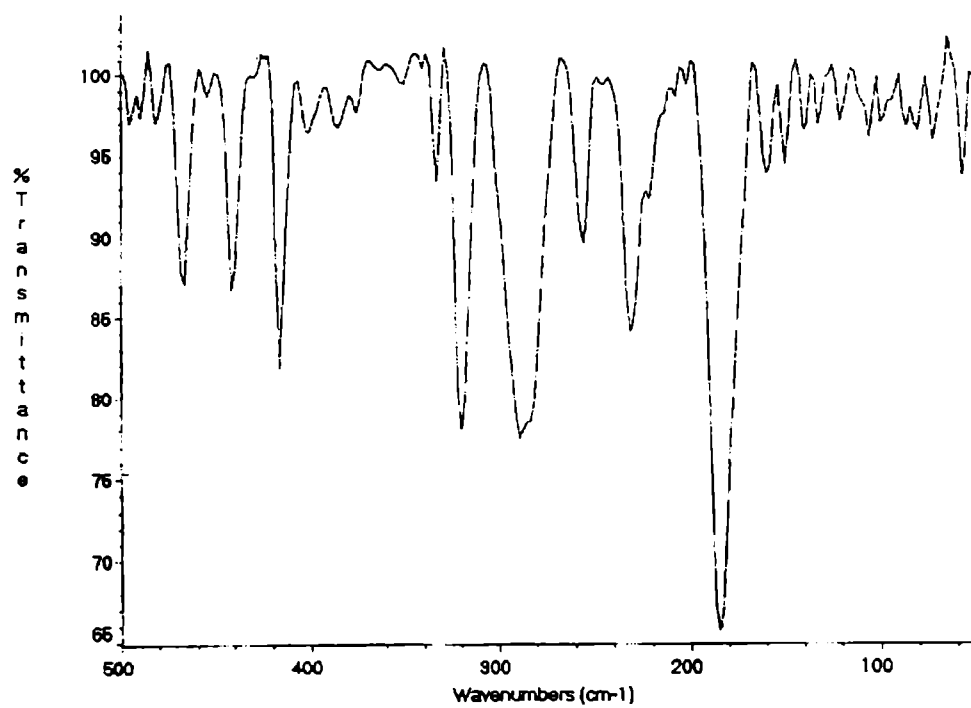


Fig.8.10. Far IR spectrum of compound 26

### 8.3.3. Electronic spectra

The ligand HL<sup>1</sup> has absorption bands at 270 and 348 nm due to the  $\pi \rightarrow \pi^*$  and  $n \rightarrow \pi^*$  transitions. The absorption due to  $\pi \rightarrow \pi^*$  transition remains almost unchanged in position in the spectra of the Zn(II) complexes. The absorption band due to the  $n \rightarrow \pi^*$  transitions at *ca.* 348 nm is found to be shifted to longer wavelength in the spectra of the Zn(II) complexes. This bathochromic shift may be due to the donation of a lone pair of electrons to the metal and hence the coordination of azomethine nitrogen [11,12]. A broad intense band observed at *ca.* 425 nm is assigned to the S  $\rightarrow$  Zn(II) charge transfer transitions. The complexes show no appreciable absorption in the region above 500 nm which is in accordance with the  $d^{10}$  electronic configuration of the Zn(II) ion [13].

Table 8.3. Electronic spectral assignments of HL<sup>1</sup> and HL<sup>2</sup> and their Zn(II), Cd(II), Hg(II) complexes.

Compound	$\pi \rightarrow \pi^*$	$n \rightarrow \pi^*$	LMCT
HL <sup>1</sup>	270	348	--
[ZnL <sup>1</sup> OAc] (22)	265	360	425
[ZnL <sup>1</sup> Cl]·2H <sub>2</sub> O (23)	266	372	430
[CdL <sup>1</sup> NO <sub>3</sub> ] (24)	273	351	420
[Hg(HL <sup>1</sup> )Cl <sub>2</sub> ] (25)	274	370	435
HL <sup>2</sup>	262	345	--
[ZnL <sup>2</sup> OAc] (26)	265	371	440

In the electronic spectrum of complex  $[\text{CdL}^1\text{NO}_3]$ , absorption bands appearing at 273 and 324 nm can be assigned to  $\pi \rightarrow \pi^*$  and  $n \rightarrow \pi^*$  respectively, of the thiosemicarbazone moiety and the intense band at 419 nm can be assigned to the  $\text{S} \rightarrow \text{Cd(II)}$  charge transfer transition. There are no absorption bands above 480 nm indicating the absence of  $d \rightarrow d$  bands in accordance with the  $d^{10}$  configuration. In the spectrum of Hg(II) complex, a broad band observed at 376 nm may be due to the  $n \rightarrow \pi^*$  transition of the thiosemicarbazone moiety.

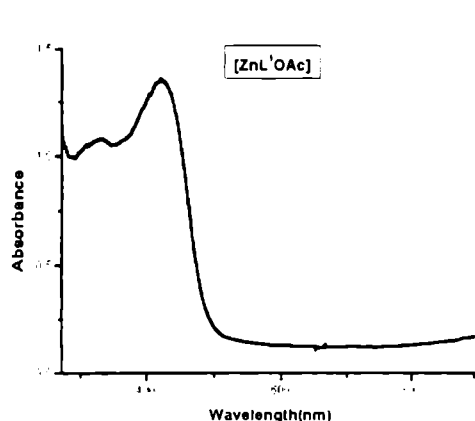


Fig. 8.11. Electronic spectrum of compound 22

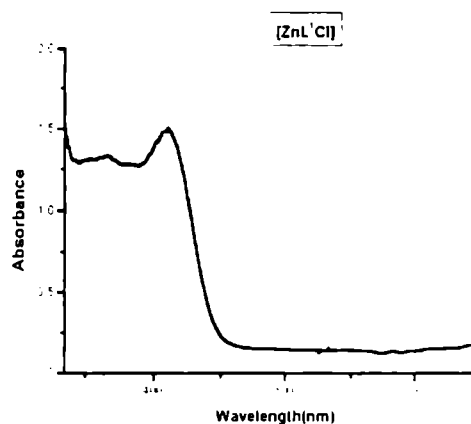


Fig. 8.12. Electronic spectrum of compound 23

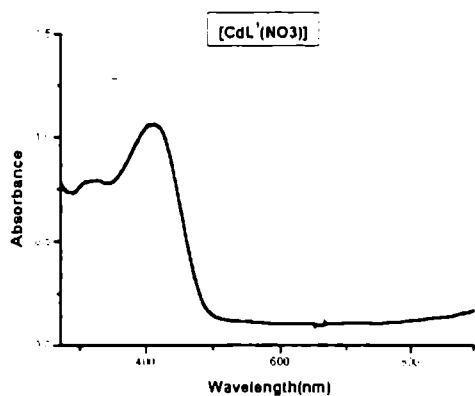


Fig. 8.13. Electronic spectrum of compound 24

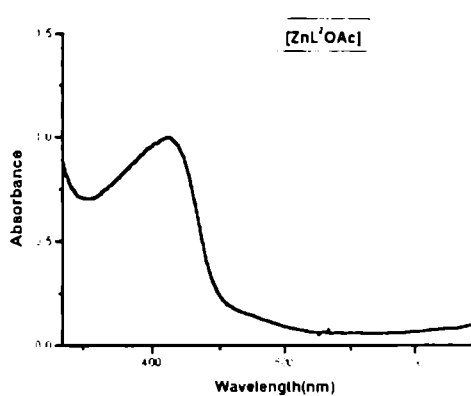


Fig. 8.14. Electronic spectrum of compound 26

### 8.3.4. $^1\text{H}$ NMR spectra

The  $^1\text{H}$  NMR signals of the two ligands  $\text{HL}^1$ ,  $\text{HL}^2$  and the complexes are listed in Table 8.3. (The positions of the atoms are as given in Fig.2.1.) The ligands  $\text{HL}^1$  and  $\text{HL}^2$  have signals at  $\delta = 13.48$  and  $14.06$  ppm respectively. These signals are due to the  $^2\text{NH}$  proton that disappears on  $\text{D}_2\text{O}$  exchange. This signal disappears in the three zinc(II) complexes as a consequence of the complete deprotonation of the ligand and coordination via the thiolate sulfur during complexation. In the spectrum of  $[\text{Hg}(\text{HL}^1)\text{Cl}_2]$ , the N-H proton signal appears at  $14.08$  ppm which supports the existence of the ligand in the neutral form in this complex. There is a slight shift in the signals corresponding to the protons of the pyridine ring, in all the complexes in support of the coordination *via* the pyridine nitrogen. In compound **24**, the downfield shift of the signals corresponding to all protons of the pyridyl ring and phenyl ring are remarkably high compared to that in other compounds.

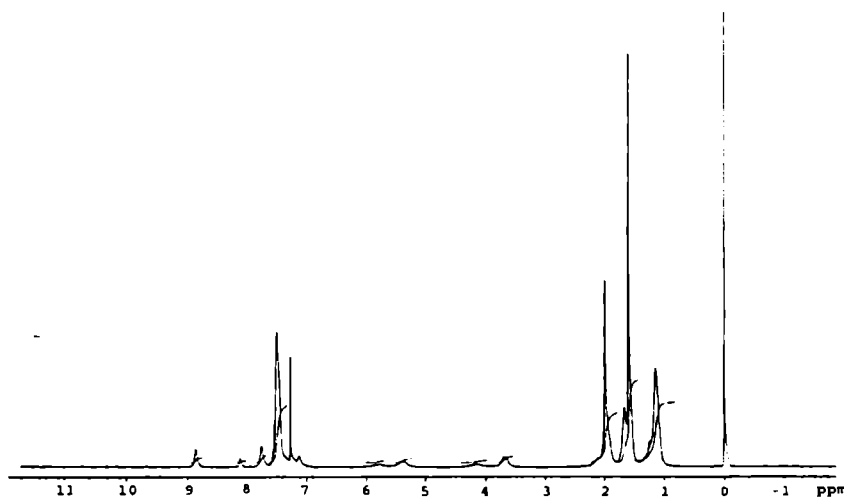


Fig. 8.15.  $^1\text{H}$  NMR spectrum of compound **22**

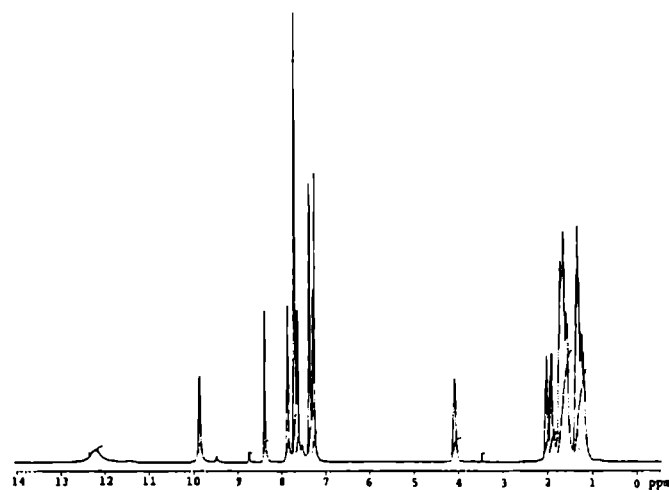


Fig. 8.16. <sup>1</sup>H NMR spectrum of compound 24

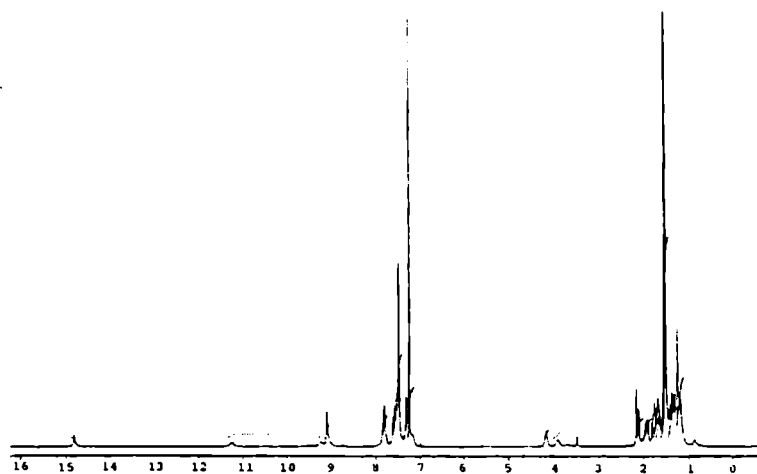


Fig. 8.17. <sup>1</sup>H NMR spectrum of compound 25



Table 8.4 <sup>1</sup>H NMR signals of HL<sup>1</sup>, HL<sup>2</sup> and their Zn(II), Cd(II).

Compound	Hg(II) complexes (δ, ppm)				
	<sup>2</sup> NH	<sup>4</sup> NH	<sup>6</sup> C	Aromatic protons	Aliphatic protons
HL <sup>1</sup>	13.48	7.63	8.81	7.26, 7.43, 7.63, 7.75	4.32, 2.12, 1.14-1.74
[ZnL <sup>1</sup> OAc] (22)	--	7.45	8.87	7.27, 7.48, 7.75, 8.11	3.8, 1.12, 1.59, 1.9
[ZnL <sup>1</sup> Cl].2H <sub>2</sub> O (23)	--	7.38	8.89	7.25, 7.46, 7.89	4.2, 1.15, 1.56, 1.78
[CdL <sup>1</sup> NO <sub>3</sub> ] (24)	--	7.4	9.85	7.25, 7.65, 7.97, 8.3,	4.16, 2.1, 1.9, 1.3
[Hg(HL <sup>1</sup> )Cl <sub>2</sub> ] (25)	14.82	7.38	9.10	7.25, 7.49, 7.81	4.16, 2.16, 1.53, 1.75
HL <sup>2</sup>	14.06	9.54	8.86	7.21, 7.40, 7.54, 7.77, 8.85	--
[ZnL <sup>2</sup> OAc] (26)	--	9.61	8.5	7.25, 7.42, 7.78, 8.82	--

#### 8.4. Antimicrobial studies

The three Zn(II) complexes are screened for antimicrobial activity using the Disc diffusion method against the five types of bacteria: 1. *Staphylococcus aureus*. 2. *Bacillus* sp (Gram Positive) 3. *Escherichia coli* 4. *Salmonella paratyphi* 5. *Vibrio cholerae* O1 (Gram Negative). All the Zn(II) complexes are found to be microbial inactive.

## References

- 1 W.Kaim, B.Schwiderski, Bioinorganic Chemistry, Inorganic Elements in the Chemistry of Life, Wiley, New York, 1991.
- 2 N.N. Greenwood, A. Eamshaw, Chemistry of the Elements. 2<sup>nd</sup> ed., Reed Educational and Professional Publishing Ltd. Great Britain, 1997.
- 3 D. Bryce-Smith, Chem.Brit.25 (1989) 783.
- 4 B.C.Cunningham, M.G.Mulkerrin, J.A.Wells, Dimerization of human growth hormone by zinc, Science, 253 (1991) 545.
- 5 J.D. Lee, Concise Inorganic Chemistry, 4<sup>th</sup> ed., ELBS, 1991.
- 6 E. Kumar, Prog, Inorg Chem. 41 (1994) 443.
- 7 E. Kimura, T. Koike, Adv. Inorg. Chem. 44 (1997) 229.
- 8 P.S.N. Reddy, B.V. Agarwala. Synth. React. Inorg. Met- Org. Chem. 17 (1987) 585.
- 9 A. Castineiras, A. Arquero. J.R. Masaguer, Transition Met. Chem. 9 (1984) 73.
- 10 K. Nakamoto, Infrared and Raman spectra of Inorganic and Coordination Compounds, Part B .5<sup>th</sup> ed., Wiley, New York, 1997.
- 11 E. Bermejo, R. Carbailo. A. Castifreiras, R. Domfnguez, A.E. Liberta, C. Maichle-Mossmer. M.M. Salberg, D.X. West, Eur. J. Inorg. Chem. (1999).
- 12 A. Sreekanth, S. Sivakumar. M.R.P. Kurup, J. Mol. struct., 655 (2003) 47.
- 13 J.S. Casas, A. Castineira. A. Sanchez, J. Sordo, A. Vazquel-Lopez. M.C. Rodriguez, Inorg. Chim. Acta. 224 (1994) 61.

## SUMMARY AND CONCLUSION

This thesis contains the synthesis and spectral characterization of two *N*(4)-substituted 2-benzoylpyridine thiosemicarbazones and their metal complexes. X-ray diffraction studies of some of the synthesised compounds and antimicrobial activities of the two ligands and their metal complexes.

Chapter 1 reviews the bonding, stereochemistry and biological activity of thiosemicarbazones and their metal complexes. The different analytical and spectroscopic techniques used for the analysis of the ligands and the metal complexes also are included in this Chapter.

Chapter 2 contains the synthesis of the two thiosemicarbazones 2-benzoylpyridine *N*(4)-cyclohexylthiosemicarbazone (HL<sup>1</sup>), and 2-benzoylpyridine *N*(4)-phenylthiosemicarbazone (HL<sup>2</sup>). They are characterized by electronic, infrared and NMR spectral studies. <sup>1</sup>H NMR, <sup>13</sup>C NMR, COSY and HMQC spectra are used in resolving the positions of the carbon and hydrogen atoms of HL<sup>1</sup>. From the spectral studies, the two ligands were found to exist in the thione form in the solid state. Single crystal X-ray diffraction studies of HL<sup>1</sup> revealed that the compound crystallised into a monoclinic lattice with four molecules in a unit cell and the molecule is in *Z* configuration. The bond lengths are in strong support of the existence of 2-benzoylpyridine *N*(4)-cyclohexylthiosemicarbazone in the thione form in the solid state. The Crystal structure reveals the existence of the cyclohexyl ring, in the compound, in chair conformation

Chapter 3 describes the synthesis, and characterization of six copper(II) complexes of 2-benzoylpyridine *N*(4)-cyclohexylthiosemicarbazone (HL<sup>1</sup>). The copper(II) complexes prepared are characterized by using magnetic studies, molar

conductance measurements, electronic, infrared and EPR spectral studies. The elemental analysis and molar conductance measurements reveal that in all the complexes, the anions are coordinated to the metal ion. The infrared spectra of the complexes prove that the deprotonated ligand coordinates to the metal via the azomethine nitrogen, pyridyl nitrogen and thiolate sulfur. From the EPR spectra of the complexes, the EPR parameters, bonding parameters and orbital reduction parameters of the complexes are calculated.

The single crystal X-ray diffraction studies show square planar geometry for  $[\text{CuL}^1\text{Cl}]$ , and  $[\text{CuL}^1\text{NCS}]$  and square pyramidal geometry for  $[\{\text{CuL}^1\text{Br}\}_2]$ . The compound  $[\text{CuL}^1\text{Cl}]$  crystallizes into a monoclinic lattice with two independent molecules in the asymmetric unit. The compound  $[\{\text{CuL}^1\text{Br}\}_2]$  is found to be a thiolato bridged dimer crystallised into a triclinic lattice. The compound  $[\text{CuL}^1\text{NCS}]$  crystallizes into a triclinic lattice and it reveals a distorted square planar  $\text{N}_3\text{S}$  coordination sphere with the copper centre.

Chapter 4 describes the synthesis, spectral characterization and antimicrobial activities of the ligand  $\text{HL}^2$  and its six copper(II) complexes. In all the copper(II) complexes, except in the perchlorate complex, the deprotonated ligand  $\text{L}^2$  and the anions are found to coordinate to the metal. In the perchlorate complex, one molecule each of the protonated and deprotonated ligand is found to coordinate to the metal. The absorption bands corresponding to the  $d-d$  transition, in the electronic spectra of the complexes, in the solid state and in solution are weak but those corresponding to the intraligand and charge transfer transitions are strong. From the EPR spectra of the complexes, the EPR parameters are calculated and they are used to evaluate the bonding parameters and orbital reduction parameters. From these values it is concluded that there is significant in-plane  $\pi$  bonding and in-plane  $\sigma$  bonding in the copper(II) complexes of  $\text{HL}^2$ .

The two ligands and their copper(II) complexes are screened for antimicrobial activity against five types of bacteria: 1.. *Staphylococcus aureus*. 2.

*Bacillus* sp (Gram Positive) 3. *Escherichia coli* 4. *Salmonella paratyphi* 5. *Vibrio cholerae* O1 (Gram Negative). The ligand 2-benzoylpyridine *N*(4)-phenylthiosemicarbazone is found to be active against *Staphylococcus aureus*, but the ligand, 2-benzoylpyridine *N*(4)-cyclohexylthiosemicarbazone is found to have no antimicrobial activity. But all the copper(II) complexes of these two ligands are found to have antimicrobial activity. While comparing the antimicrobial activities of the copper(II) complexes of the two ligands, the copper(II) complexes of 2-benzoylpyridine *N*(4)-cyclohexylthiosemicarbazone are found to be more active than those of the 2-benzoylpyridine *N*(4)-phenylthiosemicarbazone.

Chapter 5 contains the synthesis and characterization of four iron(III) complexes. The analytical data and the molar conductance measurements reveal that two molecules of the ligand and the anion are coordinated to the metal atom in the four complexes. The magnetic moments of the complexes suggest that they are low spin complexes. The spectra of the complexes in the polycrystalline state at 298 and 110 K and in DMF solution at 110 and 77 K are recorded and all the spectra show three *g* values indicating that these complexes have rhombic distortion. The similar electronic and EPR spectral data of the four Fe(III) complexes indicate that the bonding in all the complexes is similar and is unaffected by the coordination of the anion. The complexes are screened for antimicrobial activity and found to be inactive.

Chapter 6 describes the synthesis and spectral characterization of two manganese(II) complexes. The analytical data of the complexes suggest a structure in which two anionic ligands are coordinated to the Mn(II) ion. From the magnetic susceptibility measurements, they are found to be high spin complexes. The infrared spectral data of the complexes give insight into the coordination sites of the ligand around the metal atom. The EPR spectra of the complexes contain six hyperfine lines with a pair of forbidden lines between each of the hyperfine lines.

The electronic spectral data, together with the EPR data, suggest an octahedral geometry for the Mn(II) complexes. The Mn(II) complexes are found to have no antimicrobial activity.

Chapter 7 contains the spectral characterization of three nickel(II) complexes. The chloro complex of nickel is found to be diamagnetic, suggesting a square planar geometry and it is characterized by electronic, infrared and NMR spectral studies. The other two nickel(II) complexes are characterized by magnetic, electronic and infrared spectral studies.

Chapter 8 deals with the synthesis of zinc(II), cadmium(II) and mercury(II) complexes and their characterization by electronic, infrared and NMR spectral studies. The zinc(II) complexes are screened for antimicrobial activity against five types of bacteria and they are found to have no antimicrobial activity..

**Abbreviations**

HL <sup>1</sup>	-	2-Benzoylpyridine <i>N</i> (4)-cyclohexyl thiosemicarbazone
HL <sup>2</sup>	-	2-Benzoylpyridine <i>N</i> (4)-phenyl thiosemicarbazone
s	-	strong (Infrared spectrum)
m	-	medium (Infrared spectrum)
w	-	weak (Infrared spectrum)
nm	-	nanometer (Electronic spectrum)
sh	-	shoulder (Electronic spectrum)
$\delta$	-	chemical shift (NMR spectrum)
B.M.	-	Bohr Magneton
G	-	Gauss
COSY	-	Correlation spectroscopy
HMQC	-	Heteronuclear multiple quantum coherence

## RESUME

1. Name : Marthakutty Joseph
2. Sex : Female
3. Age And Date Of Birth : 43 Years, 22/07/1961
4. Nationality : Indian
5. Official Address : Selection Grade Lecturer  
Nirmala College, Muvattupuaha  
Ernakulam(Dt), Kerala.  
Affiliated to M.G. University.
6. Residential address : Aerathu House  
Avoly P.O.  
Muvattupuzha,Ernakulam(Dt)  
Kerala . 686677  
E-mail : marthavincent@rediffmail.com
7. Teaching Experience : 19 years
8. Academic Qualification : M.Sc. M.Phil.

### 10. List of Paper publications and Presentations

I., M.R. P. Kurup, Marthakutty Joseph, Transition Metal Complexes of Furan-2-aldehyde thiosemicarbazone: Synth. React. Inorg. Met-. Org. Chem. 33, 2003, pp 1275-1287.



2. Marthakutty Joseph, V.Suni, M.R. P. Kurup, K. Archana, Spectral characterization and antimicrobial activities of Cu(II) complexes of <sup>4</sup>N -phenyl -2- benzoylpyridine thiosemicarbazone. 10<sup>th</sup> symposium on modern trends in Inorganic chemistry, IIT Bombay, Dec 15-17,2003.
3. Marthakutty Joseph, M.R. P. Kurup, Synthesis and spectral characterization of Mn(II) complexes of <sup>4</sup>N -substituted -2- benzoylpyridine thiosemicarbazone. National Symposium on current trends in Inorganic Chemistry, Dept. Of Applied Chemistry, Cochin University, March 15-17- 2004.
4. Marthakutty Joseph, V.Suni. Chandini R.Nair, M.R.P. Kurup. H.K.Fun, Synthesis, spectral characterization and crystal structure of 2-benzoylpyridine N(4)-cyclohexylthiosemicarbazone J.Mol.Struct. in Press.
5. Marthakutty Joseph, V.Suni, M.R.P. Kurup, M.Nethaji, K.Archana, C.Jasmine, Structural, spectral and antimicrobial studies of copper(II) complexes of 2-benzoylpyridine N(4)-cyclohexylthiosemicarbazone Communicated.